UNCLASSIFIED

HW-54727
ADDENDUM (Rev.)

UNITED STATES ATOMIC ENERGY COMMISSION

AN ADDENDUM TO A PARAMETRIC STUDY OF THE GAS-COOLED REACTOR CONCEPT

Prepared by
The Staff of the
Process Design Operation

March 1, 1958

Irradiation Processing Department
Hanford Atomic Products Operation
General Electric Company

UNCLASSIFIED

metadc100571

LEGAL NOTICE

This report was prepared as an account of Government sponsored work. Neither the United States, nor the Commission, nor any person acting on behalf of the Commission:

A. Makes any warranty or representation, express or implied, with respect to the accuracy, completeness, or usefulness of the information contained in this report, or that the use of any information, apparatus, method, or process disclosed in this report may not infringe privately owned rights; or

B. Assumes any liabilities with respect to the use of, or for damages resulting from the use of any information, apparatus, method, or process disclosed in this report.

As used in the above, "person acting on behalf of the Commission" includes any employee or contractor of the Commission to the extent that such employee or contractor prepares, handles or distributes, or provides access to, any information pursuant to his employment or contract with the Commission.

This report has been reproduced directly from the best available copy.

AN ADDENDUM TO A PARAMETRIC STUDY OF THE GAS COOLED REACTOR CONCEPT

Prepared by

The Staff of the
Process Design Operation
IRRADIATION PROCESSING DEPARTMENT

March 1, 1958

TABLE OF CONTENTS

SECTION

I Introduction

II Fuel Element Studies

III Reactor Physics Study

IV Reactor Heat Transfer and Fluid Flow

V Coolant Gas Selection for a Gas Cooled Reactor

VI Reactor Core Arrangement and Vessel Studies

VII Direct Cycle Power Plant Studies

VIII Indirect Cycle Power Plant Studies

IX Fuel Cycle Cost Studies

X Cost Evaluation and Case Selection

ERRATA

Addendum to A Parametric Study of The Gas Cooled Reactor Concept

Section II - Page 3 - Table I

Fourth fuel column is Uranium Carbide.

Section III - Page 5 - Paragraph 1 - Line 15

Reference should read No. 6.

Section III - Page 7 - Paragraph 1 - Line 4

Should read - variation at enrichments of 1-2 w/o.

Section III - Figure III-9

This figure was omitted.

Section IV

Page 1 - Core Geometry - Line 3

change to: The ratio of core length to core diameter is $\sqrt{\pi}$:1 or approximately 1.77:1

Page 2 - Equation (5)

change to: $N_T \times \left(\frac{\ell^2}{144}\right) = \frac{\pi}{4} D^2$

Page 2 - Equation (7)

change to: $L = \frac{\ell}{6} N_T^{\frac{1}{2}} = 0.167 \ell N_T^{\frac{1}{2}}$

Page 3 - Equation (10)

change to: $W = \frac{\eta_{or}\ 3413L\ Q'\ MA}{C_p\ \Delta T_{bulk}}$

Page 4 - Equation (18)

change to: $A_f = 0.75 \ell^2 \frac{Nu}{Ng} \frac{\rho g}{\rho_{UO_2}} \times \frac{\text{Mol. Wt of } UO_2}{\text{Mol. Wt of graphite}}$

SECTION I

INTRODUCTION

This addendum to the report of parametric studies of the gas cooled reactor concept has been prepared to serve a twofold purpose: (1) To provide background information regarding the study results presented in the first volume of this report. (2) To provide additional information resulting from the studies made on the gas cooled reactor concept, which though not directly applicable to the cases studied may be of value in the evaluation of other studies of the gas cooled reactor concept.

The various sections of this addendum are individual topical reports on the various phases of work performed on this study. As a result there is considerable information contained in these topical reports that was not integrated into the final parametric study but does have value as reference material. Since certain amounts of this work were necessarily performed under different bases than that of the integrated study, portions of the individual reports should not be used for evaluation of other sections of this addendum without careful consideration of the bases used in preparation of the individual reports. This same consideration should be noted in use of these reports for evaluation of other gas cooled reactor concepts, since while individual topical items may seem to be quite significant they may be minor factors when integrated into an over-all reactor concept.

Reference should be made to the Table of Contents for a listing of the topical reports contained in this addendum. Where necessary, separate detailed Tables of Contents have been included in the various topical reports.

Section IV (Continued)

Page 4 - Equation (19)

add: where $\frac{Ng}{Nu} = 75$

$\rho_{UO_2} = 9.776$

$\rho_g = 1.6$

$M.W._{UO_2} = 270$

$MW_g = 12.01$

Page 4 - Equation (20)

change to: $r_i = \ell\left(\frac{.0368}{\pi n_r}\right)^{\frac{1}{2}}$

Pages 5 and 6 - Equations 26, 27, 28, 29, 30 and 31

change terms $\frac{12}{r_i h_i}$ and $\frac{12}{r_o h}$ to: $\frac{12}{2\pi r_1 h_1}$ and $\frac{12}{2\pi r_o h}$

Page 11 - Nomenclature - Line 10

change Cp units to BTU/lb-°F

Page 12 - Nomenclature

add: A_f cross sectional area of fuel, inches^2

C_1, C_2 constants for establishing linear functions for temperature change of C_p and μ

Constants are:

	C_p		μ	
	C_1	C_2	C_1	C_2
He	1.248	—	0.0465	0.000044
N_2	0.242	0.0000284	0.0506	0.0000341

g conversion constant, 4.17×10^8 ft lb $_{mass}$/hr^2 lb $_{force}$

G_2 mass flow rate in reflector region, lb/hr ft^2

ΔT max maximum power tube temperature increase across reactor, °F

Section IV - Page 12 (Continued)

Subscript

f fuel

j jacket

Section V - Page 9 - Table IV

Second jacket column is Be

Section VII - Figure VII-21 - Page 29

Curves are void. See Section V - Figure V-2 - Page 17 for correct curves.

Section X - Figure X-6 - Page 13

1500 MW data were not plotted because net power costs are above scale shown.

SECTION II

FUEL ELEMENTS STUDIES

by

L. F. Kusler
Engineering Operation
FUELS PREPARATION DEPARTMENT

FUEL ELEMENTS STUDIES

A preliminary survey of fuel systems of possible interest in a gas cooled reactor concept is presented in this report. The detail design of fuel elements and systems requires more detailed information on the operational requirements imposed by the reactor and a firmer basis as to reactor parameters. Thus the scope of this study was restricted primarily to the compatibility of fuel cores, cladding and coolants. Possible core materials investigated included uranium, uranium alloys, uranium dioxide, uranium monocarbide and uranium nitride. Cladding materials included aluminum, beryllium, magnesium, zirconium, stainless steel, iron, carbon, molybdenum and niobium. Coolants considered were carbon dioxide, carbon monoxide, nitrogen, hydrogen and the inert gases - helium, neon and argon.

Since coolant, core and jacket material are inter-related, several tables have been prepared to indicate the various combinations and limitations. From these tables and the assumption that the reactor is to be (1) graphite moderated, (2) gas cooled with temperatures varying between 300 and 700° C, (3) maximum fuel exposures of 15,000 MWD/T with minimum enrichments, and (4) financed by private industry, it is concluded that:

(1) Massive uranium will not be acceptable as a core material because of the distortion that would occur with long exposures.

(2) Helium or one of the other inert gases is the most desirable for cooling fuel elements.

(3) The only limitation, as to chemical reactivity, in using unclad fuel elements is the reaction of CO_2 with uranium dioxide at 500° C.

(4) From the limited data available uranium carbide appears to be limited at 1100° C due to the reaction with nitrogen.

(5) Uranium nitride appears to be stable at the high temperatures from the limited data presently available.

(6) Stainless steel, graphite and zirconium appear to be the most promising jacketing materials.

(7) The final selection of a fuel element will depend primarily on the environment in which it must operate.

Table I lists the maximum possible coolant temperatures for unclad fuel elements, as well as maximum core temperatures and thermal conductivities for the various materials. No data is given for the various uranium alloys, since these alloys represent a broad spectrum of physical properties. This category was included in order to indicate the possibility of operation at an 1100° C maximum core temperature. The possibility of a greater flexibility in the selection of a coolant for uranium alloys as compared to

uranium metal would require its verification for the particular alloy.

The gas, carbon monoxide, is included as a possible coolant because of some rather desirable properties. Very few data are available to evaluate this possibility, presumably because of the toxic nature of carbon monoxide; however, it is felt that the toxicity of the reactor coolant would be so great from the radiological composition that the additional chemical hazard would not be significant. We can feel reasonable confident of using bare uranium dioxide and uranium monocarbode fuels with carbon monoxide.

From Table I it is concluded that helium, argon, or neon with all of the oxygen removed is compatible with all the possible fuel materials. Since it is highly questionable if metallic uranium could be used at the required fuel exposures, uranium dioxide, uranium monocarbide and uranium nitride are the most likely candidates for unclad gas cooled fuel elements. However, it should be noted that ceramic fuels are highly susceptible to thermal fracture and allowances must be made for this weakness in the fuel element design.

Table II summarizes the compatibility of potential core and jacket materials. Because of the many variables which affect diffusion characteristics, the values in this table indicate order of magnitude only. The listed temperatures are based on diffusion characteristics and are the maximum interface temperatures between the fuel material and cladding. It should be noted that some of the listed temperatures are much higher than the material could withstand because of other limitations, such as a maximum core temperature; therefore this tabulation can be taken as an indication of the safety factor involved in the use of a particular combination.

The maximum coolant temperatures for the various cladding materials are listed in Table III. Values from this table should be compared to the maximum fuel element core temperature since, in many designs, it may be the limiting factor.

These data lead to the conclusion that only a minor technological incentive exists for the use of any fuel cladding in a high temperature gas cooled reactor. Indeed, if one selects either helium or any of the other inert gases or carbon monoxide then most of the ceramic fuel materials are compatible. The possible difficulty to be anticipated in such a fuel system is derived from the attrition of the fuel material and the release of fission products from the unclad fuel element. This will necessitate the design of an off-gas system which will separate the fission products and possibly the fuel material which is carried in the hot gas stream.

Present fabrication experience with high temperature fuel elements is limited primarily to uranium dioxide clad in stainless steel or zirconium. Conventional methods of sintering, roll cladding and swaging

have been used in the fabrication of these elements. Uranium carbide, one of the promising ceramic fuels under development could be fabricated by impregnating a graphite mix with uranium oxide, forming to the desired shape and graphitization. The need of cladding an element of this type would depend primarily on its ability to withstand thermal fracture.

This concludes the initial phase of our study and indicates the parameters which must be considered in establishing fuel element operational limits. With this data and specific reactor operating requirements, detailed fuel elements can be developed.

TABLE I

GAS COOLANT AND BARE FUEL ELEMENT COMPATIBILITY
MAXIMUM SURFACE TEMPERATURES, ^{o} C

	U	U_{alloy}	UO_2	UC	UN
CO_2	400	-	500	?	?
N_2	450	-	?	1100	700+
CO	400	-	700+	700+	700+
H	250	-	700	700	?
He, Ne, A	Limited by melting temperature of core material.				
Melting Temp.	1100	1100	2000-2500	2000-2500	2000-2500
Heat Transfer-KΔT					
Cal./Cm. Sec	30.3	-	16.8	80	?
Δ T	400	-	1300	1300	-
Uranium Concentration G/cc-Theoretical	19.0	-	9.7	13	13.6
Neutron Capture Cross Section for Combining element, Barns	None	-	0.0002	0.0032	1.9

TABLE II

FUEL ELEMENT CORE AND JACKET COMBINATIONS
MAXIMUM ALLOWABLE INTERFACE TEMPERATURES WITH NO DIFFUSION BARRIER-°C

Core Material	Maximum Core Temp.	Al	Be	Mg	Zr	SS	Ti	Fe	C	Mo	Nb
U	620	200	600	600	600	700	500	600	1100	600	600
U_{alloy}	1100	-	-	-	-	-	-	-	1100	-	-
UO_2	2000	500	500	450	600	950	700 +	950	2000	-	-
UC	2000	600	700 +	650	700 +	700 +	700 +	500	2000	-	-
UN	2000	600	700 +	650	700 +	700 +	<700	500	2000	-	-

TABLE III

GAS COOLANT AND FUEL ELEMENT JACKET COMPATIBILITY
ALLOWABLE OPERATING TEMPERATURES, °C

	Cross Section Barns	Al	Be	Mg	Zr	SS	Ti	Fe	C	Mo	Nb
CO_2	.003	600	500	450	700	950	-	500	500	-	-
N	1.9	600	500	400	700	700	400	450	2000	-	300
He	.007	600	1200	600	1400	1350	1650	1450	3000	2500	2000
CO	.002	600	-	500	700	950	-	500	3000	-	-
H	.33	400	700	-	300	800	120	-	-	2500	250
Cross Section		.23	.01	.063	.18	3.0	6.0	2.5	.0032	2.5	1

REACTOR PHYSICS STUDY

The physics calculations for the Gas Cooled Reactor concept were broken down into individual groups of equations. Each group (see Figure 1) is interdependent upon the results of every other group. Many of the individual calculations are quite lengthy and have been programmed for solution by the IBM-702 high speed computing machine. The individual components will be described in detail and referred to by the number appearing in the upper righthand corner of each box. The general results of the study appear as Figures 10 through 99.

1 Input Data

The majority of the thermal microscopic cross sections used as input data to the entire program were taken directly out of BNL-325. Values of the cross sections (absorption and fission) were tabulated at energy intervals of 0.01 ev from 0.001 to 2.5 ev for the elements, U-235, U-238, Pu-239, Pu-240, Pu-241, Xenon 135, Samarium 149, Carbon (normalized to 3.9×10^{-3} barns for 1.6 g/cc graphite at 0.025 ev) and a composite curve for stainless steel. These cross sections were then blackness weighted (β weighted) to properly account for the mutual and self-shielding of the various isotopes. A brief description of the method follows:

Blackness Weighting (β weighted) Cross Sections

Diffusion theory, which is the easiest and by far the fastest method of calculating the various physics data, suffers from its inability to accurately calculate the so-called fuel rod disadvantage factor F. This factor being the ratio of the flux at the surface of the rod to the volume average flux in the fuel. G. W. Stuart[1] has developed a powerful but easily calculable method for F based upon his "Successive Generations" approach:

Briefly, the method consists of the following. Define,

$$(1) \quad F = \frac{\phi|_R}{\langle\phi\rangle}$$

Conservation of neutrons in the rod is expressed by,

$$(2) \quad 2\pi RD \left.\frac{\partial \phi}{\partial r}\right|_R = \pi R^2 \sigma_a \langle\phi\rangle$$

While the rod blackness is defined by,

$$(3) \quad \beta = \frac{J^{in} - J^{out}}{J^{in}} = \frac{D \left.\frac{\partial\phi}{\partial r}\right|_R}{\frac{\phi}{4} + \frac{D}{2}\left.\frac{\partial\phi}{\partial r}\right|_R}$$

(1) "Method of Successive Generations", G. W. Stuart and R. W. Woodruff, unpublished paper written in 1956 for Hanford Laboratories Operation.

Combining Equations (1), (2), and (3) yields,

$$(4)\quad F = \frac{\Sigma_a R(2-\beta)}{\beta}$$

This expression is not exact within the framework of the "Successive Generations" approach as it requires that the rod exit neutron distributions have the functional form of the diffusion theory. However, Stuart has compared the simple form (4) with his exact expression for ϕ,

$$(5)\quad \phi = \frac{J_1^{in}}{1 + \frac{\beta}{2-\beta}} \sum_{m=1,2}^{\infty} \sum_{n=0}^{\infty} \left(\sigma_s R\right)^n \delta_m \pi_{n,m}(x,T),$$

and has shown that the agreement between Equation (4) and (5) is within 2 percent for fuel rods of less than two inches in diameter. Thus, a useful relation between neutron current entering an absorbing rod and the Maxwellian flux at the fuel rod surface is,

$$(6)\quad J^{in} = \frac{\phi|_R}{2(2-\beta)}$$

Where ϕ_R is the Marxwellian flux at the surface of the rod.

The use of this relation instead of the straight diffusion theory expression of $J^{in} = \frac{\phi|_R}{4}$ will enable us to account for the hardening of the spectrum when calculating average cross sections. Rather than use the well known but inaccurate "f" factor, the cross sections were averaged over energy by β weighting by means of the following formulae:

$$(7)\quad \langle \sigma^i \rangle_{kT} = \frac{2}{R} \int_0^{\infty} J^{in}(E,kT) \frac{\beta(E)}{\Sigma_a(E)} \sigma^i(E)\, dE,$$

where the current is expressed by (6). Notice that average cross sections now vary with rod size, initial composition and exposure. The average values at energy kT as calculated by means of Equation (7) are significantly different than the usual "f" factor average values.

In the limit of a thin foil,

$$J^{in} \longrightarrow \frac{\phi(E,kT)}{4}$$

$$\beta \longrightarrow 2\Sigma_a R$$

Substituting these into Equation (7), it becomes,

$$(8)\quad \langle \sigma^i \rangle_{kT} = \int_0^{\infty} \phi(E,kT)\, \sigma^i(E)\, dE = \frac{\sqrt{\pi}}{2} f_i(kT)\, \sigma_i(kT)$$

or the usual "f" factor formulation.

This method, a transport theoretic technique has the advantage of accounting for the neutron behavior within a rod.

2 Calculation of Resonance Escape Probability

An eight region modified one-group diffusion equation[2] is used for this calculation. In order to solve these equations, it is necessary to have some kind of symmetry. For rod cluster geometries, it has been shown experimentally by R. Nilson[3] that one may convert this geometry into an equivalent internally-externally cooled slug if one divides the void volume in the cluster geometry such that two-thirds of the void volume is on the outside of the slug and one-third on the inside. This geometric change must be accompanied by a method which properly accounts for the increase in the effective resonance integral due to the increased surface to mass ratio of the fuel.

A method[4] consistent with the above procedure describes the effective inner surface area as just the total surface of all the rods minus the surface enclosed by a rubber band stretched around the outside of the cluster. This method combined with the new data for UO_2 resonance integrals[5],

$$RI = 4.15 + 26.6 \left(\frac{S}{M}\right)^{\frac{1}{2}} \qquad 0.08 \leq \frac{S}{M} \leq 0.7$$

(where the 1/v absorptions have been subtracted out), gives one values for the resonance escape probability which are in good agreement with experimentally determined values using the Physical Constants Test Reactor.

3 Neutron Temperature, Exposure and Geometric Buckling

It has been assumed that the neutron temperature is determined by the flux square weighted graphite temperature and that for all reactor cases studied, the average operating graphite temperatures are limited to the range of 600-700°C. The effect of neutron temperature is extremely important in determining the amount of plutonium present in the highly exposed fuel element (~10,000 MWD/T) due to the prominent resonances at low neutron temperatures in the plutonium isotopes. The experimental data available on the effective resonance integral of Pu-240 is insufficient to allow proper self-shielding allowances in long exposure studies. However, an error of 50 percent in the plutonium yield of a reactor using the private financing scheme would amount to an error of only 0.5 mils/kw-hr in the net power costs.

(2) HW-42580, Diffusion Equation Solution of an Eight Region Lattice, E. R. Astley, May 3, 1956.

(3) Private communication from R. Nilson, HLO.

(4) Report AEFI-58-1, Carlvick and B. Pershagen, A. B. Atomenergi, Sweden, 1957.

(5) Measurements of the Effective Resonance Integral in Uranium Metal and Oxide in Different Geometries, Eric Hellestrand, Journal of Applied Physics, Vol.28, No. 12, December 1957.

The calculation of exposure dependent characteristics are facilitated if one chooses the throughput exposure and then makes certain assumptions as regards charge-discharge procedures. Box No. 6 calculated the exposure variation of k_{eff} as a function of generalized parameters such as neutron leakage, resonance escape probability, fast fission effect as well as the isotopic composition of the fuel. Assuming a continuous tube by tube discharge such that there is a uniform distribution of exposures throughout the reactor, then the pile average reactivity may be expressed by,

$$\int_0^{E_p} (Z - \overline{Z})\, dE = 0$$

where E_p = fuel discharge exposure

E = exposure

Z = pile reactivity at any exposure E

$\overline{Z}$ = average pile reactivity during operation while discharging fuel of exposure E_p

The solution of the above integral equation is most easily handled by graphical integration since the Z function is not an explicit function of exposure. Graphical plots of Z versus exposure for various resonance escape probabilities and operating enrichments were prepared for all the cases studied; for example, see Figure 3. At 5000 MWD/T, the total variation between cases for $\overline{Z}$ was about 2 percent.

The total neutron leakage was calculated by means of the multiplier,

$$\text{Non-leakage multiplier} = \frac{e^{-\tau B_g^2}}{1 + L^2 B_g^2}$$

where τ = volume weighted age of the lattice

L^2 = volume-flux-weighted lattice diffusion length

B_g^2 = geometric buckling including a constant 40 cms reflector savings

A typical non-leakage multiplier is plotted in Figure 2 as a function of the front face dimension where the length is always $\sqrt{2}$ times the height. Although the leakage varies with initial enrichment through its effect on the thermal diffusion length, the variation was not considered large enough to justify plotting every case individually. Figure 2 represents a composite average of all the cases considered.

5 & 6 Reactivity Changes and Isotope Yields at High Exposures

The basic problem here was to determine the changes in composition of the fuel resulting from the three processes of neutron capture, fission and radioactive decay. When the changes are sufficiently small (low exposure), the mathematical description can be treated with sufficient accuracy as linear perturbations of the initial system. The formulation chosen[6] incorporates non-linear as well as feed back effects. The form of the equations and of the feed back and non-linear terms depends upon the choice of the independent variable. If time is chosen as the independent variable, some specification of the neutron flux is required. If the flux is held constant with respect to time, it is found that the fission rate will vary. If the reactor power is held constant, the flux becomes a function of the concentrations of the fissionable isotopes introducing both non-linearity and feedback. If one neglects all radioactive decay terms, the flux can be factored out and incorporated in the independent variable which then becomes a thermal exposure parameter such as nvt. The method of Triplett[6] uses $T = \sigma_{25} \int \phi \, dt$ as the dimensionless independent variable. He points out that since he represented the epithermal cross sections by effective resonance integrals, one should include concentrations dependent self-shielding factors and interactions between overlapping resonance levels such as Pu-239 and U-235 at 0.3 ev. These effects are most predominate at high fuel exposures (10,000 MWD/T). These effects were not included in this study.

The equations assume a simplified model of resonance absorption in which a neutron slows down first through a region in which U-238 resonances predominate, then through a region in which U-235 resonances predominate, then through a narrow region in which the 1 ev resonance of Pu-240 predominates, and finally through a region in which the 0.3 ev resonance of Pu-239 predominates. The resonance capture in each energy region was then assumed to take place only in the isotope predominant in that region, with a probability proportional to the concentration of the isotope.

The following equations were then set up and solved by the standard Runge-Kutta method:

$$\dot{N}_{28} = -N_{28} \frac{\sigma_{28}}{\sigma_{25}} - HG\varepsilon(1 - P_{28}) - HG \frac{\varepsilon - 1}{\nu_{28} - 1}$$

$$\dot{N}_{25} = -N_{25} - HG\varepsilon P_{28} (1 - P_{25})$$

$$\dot{N}_{26} = N_{25} \frac{\alpha_{25}}{1 + \alpha_{25}} + HG\varepsilon P_{28} (1 - P_{25C}) - N_{26} \frac{\sigma_{26}}{\sigma_{25}}$$

$$\dot{N}_{49} = N_{28} \frac{\sigma_{28}}{\sigma_{25}} - N_{49} \frac{\sigma_{49}}{\sigma_{25}} + HG\varepsilon(1 - P_{28}) - HG\varepsilon P_{28} P_{25} P_{410} (1 - P_{49})$$

(6) HW-33912, Reactivity Changes and Isotope Yields, High Exposures, J. R. Triplett,

$$\dot{N}_{410} = N_{49} \frac{\alpha_{49}}{1+\alpha_{49}} \frac{\sigma_{49}}{\sigma_{25}} - N_{410} \frac{\sigma_{410}}{\sigma_{25}} + HG\varepsilon P_{28} P_{25}$$

$$\left[P_{410}(1 - P_{49C}) - (1 - P_{410})\right]$$

$$\dot{N}_{411} = N_{410} \frac{\sigma_{410}}{\sigma_{25}} - N_{411} \frac{\sigma_{411}}{\sigma_{25}} + HG\varepsilon P_{28} P_{25} (1 - P_{410})$$

$$\dot{N}_F = N_{25} \frac{1}{1+\alpha_{25}} + N_{49} \frac{\sigma_{49}}{\sigma_{25}} \frac{1}{1+\alpha_{49}} + N_{411} \frac{\sigma_{411}}{\sigma_{25}} \frac{1}{1+\alpha_{411}}$$

$$+ HG\varepsilon P_{28}\left[1 - P_{25f} + P_{25} P_{410}\left(1 - P_{49f}\right)\right] + HG \frac{\varepsilon - 1}{\nu_{28} - 1}$$

$$H = N_{25} \eta_{25} + N_{49} \frac{\sigma_{49}}{\sigma_{25}} \eta_{49} + N_{411} \frac{\sigma_{411}}{\sigma_{25}} \eta_{411}$$

$$G = e^{-B^2\tau}\left[1 - \varepsilon P_{28} P_{25} P_{410} (1 - P_{49f}) \nu_{49} - \varepsilon P_{28} (1 - P_{25f}) \nu_{25}\right]^{-1}$$

$$P_i = 1 - \left[1 - P_{28}(o)\right] \frac{\tau_i}{N_{28}(o)} N_i$$

$$G = \left[1 - \varepsilon P_{28} (1 - P_{25f}) \nu_{25}\right]^{-1} e^{-\tau B^2}$$

The regeneration factor, Z, which is a function of exposure is calculated by means of the formula,

$$Z = G P \eta \varepsilon$$

where P is the net resonance escape probability of the fuel accounting for all resonance structure. Z does not contain the change in thermal utilization or leakage as a function of exposure. These two variations are small in comparison to changes in η alone. As an example only, Z is plotted as

a function of exposure and U-235 concentration for a fuel having a net resonance escape probability of 0.82 (see Figure 3). The variation in this parameter with enrichment is most severe in the ranges of natural urnaium but is just a minor variation at enrichments of 1-2 w/o. However, the adjustment was made for each case studied.

8 Graphite Temperature Coefficient

The calculation of this parameter is considerably less complicated in the absence of water in a cell, due to the ability to specify the effective neutron temperature as equal to the flux-square weighted average graphite temperature.

The method used reduced to the calculation of,

$$\left.\frac{\Delta k_{eff}}{k_{eff}}\right|_{kT} = \frac{\Delta f}{f} + \frac{\Delta \eta}{\eta} - \frac{B^2 M^2_{KT}\left(\frac{\Delta M^2}{M^2}\right)}{1 + M^2 B^2}$$

where

$$\frac{\Delta f}{f} = \frac{\langle f\rangle_{KT} - \langle f\rangle_{.025}}{\langle f\rangle_{.025}}$$

$$\frac{\Delta \eta}{} = \frac{\langle \eta\rangle_{KT} - \langle \eta\rangle_{.025}}{\langle \eta\rangle_{.025}}$$

$$\frac{\Delta M^2}{M^2} = \frac{\langle M^2\rangle_{KT} - \langle M^2\rangle_{.025}}{\langle M^2\rangle_{.025}}$$

Thus, we have only to specify how to calculate these average ($\langle\ \rangle$) parameters. Following the method outlined by G. W. Stuart[1], we spectrally average the thermal utilization or,

$$\langle f\rangle_{kT} = \int_0^\infty f(E)\ \phi\ (E,kT)\ dE$$

where f is expressed by a diffusion expression derived by D. D. Lanning[7] from small source theory in which the fuel rod properties are accounted for by fuel rod blackness or,

$$f(E) = \frac{1}{k^2(E)A(E) + 1}$$

(1) op. cit., Method of Successive Generations

(7) HW-30508, "Quarterly Report - Physics Unit", January 1954, D. D. Lanning

where

$$A(E) = \frac{2D\,b^2}{\pi R \beta} + \frac{b^2}{2\pi} K_o(kR) - \frac{Dk}{\pi} b^2 K_1(kR) - \frac{1}{k^2}\left[1 - \frac{bk}{\sqrt{\pi}} K_1\left(k \frac{b}{\sqrt{\pi}}\right)\right]$$

The average value of η is calculated by β-weighting,

$$\langle \eta \rangle_{kT} = \frac{\int_o^\infty \eta(E)\beta(E)\phi(E,kT)\,dE}{\int_o^\infty \beta(E)\phi(E,kT)\,dE}$$

This equation as pointed out earlier now incorporates the so-called hardening effect of the neutron spectrum within the fuel rod. $\langle \eta \rangle$ is now a function of fuel rod radius which is a result of allowing for self-shielding within the rod.

The third expression in $\frac{\Delta k_{eff}}{k_{eff}}$ is the term accounting for the variation of leakage of neutrons from the finite reactor. This is a significant term for any but extremely large reactors. In order to reduce this part to a calculable form, it was assumed that,

$$\langle M^2 \rangle = \langle L^2 \rangle + \tau(kT)$$

where the neutron age is specified according to Fermi age treatment.[8]

$$\tau_{(kT)} = \tau_{.025} - \left(\frac{1}{3\xi\Sigma_s\Sigma_t}\right) \ln \frac{kT}{.025}$$

The larger variation in M^2 is due to the changes in L^2 where L^2 is determined by,

$$L^2(E) = \frac{1 - f(E)}{k^2(E)}$$

(8) Glasstone and Edlund, Elements of Nuclear Reactor Theory.

Then the average value of the lattice diffusion length squared is,

$$\langle L^2 \rangle_{kT} = \int_0^\infty L^2 (E)\, \phi (E,kT)\, dE$$

The over-all temperature coefficient was investigated over the entire range of cases and three widely different cases are plotted for comparison as Figures 4, 5, and 6.

9 Steady State Xenon Poisoning

Xenon poisoning in a reactor is a function of the reactor power level, flattening ratio, fuel enrichment and other poisons in the lattice. An expression derived by P. F. Gast[9] for the xenon poisoning in a heterogeneous lattice is,

$$X = \frac{1679 f \eta \varepsilon - 682.7 f \eta}{1 + \dfrac{3.568 \times 10^{-25} R^2 N_{25}}{P} \dfrac{\Sigma F_i^2}{\Sigma F_i^3}}$$

where f = lattice thermal utilization

$\eta = \nu \dfrac{\Sigma_f}{\Sigma_a}$

ε = fast fission effect

R = radius of fuel in cms.

N_{25} = number of atoms of U-235 per cc.

P = total pile power in MW divided by the product of the number of tubes in the pile times the length of the charge in centimeters

$$\frac{\Sigma F_i^2}{\Sigma F_i^3} = \frac{\phi^3}{\phi^2} \frac{\int_0^{R'} \phi^2\, dV}{\int_0^{R'} \phi^3\, dV}$$

where R' = bare pile radius plus extrapolation distance

(9) HW-23721, "Review of Xenon Problems", P. F. Gast, March 12, 1952.

This last ratio corrects the steady state xenon poisoning for the effect of the eight inch lattice for helium and nitrogen. Figures 7 and 8 demonstrate the variation in xenon poisoning with reactor power level, outlet temperature and reactor Δt.

10 Steady State Samarium Poisoning

The steady state value of the samarium 149 poisoning is independent of the flux in the reactor so that there is no need to average it over the reactor. The steady state samarium has been shown[10] to be equal to,

$$\frac{\Delta k}{k} = -\frac{0.014}{1+\alpha}\,\frac{1}{1+\frac{\Sigma_{28}}{\Sigma_{25}}}$$

11 Cold Clean Effective Pile Reactivity

The only part of the four part factor formula yet unexplained is the description of the thermal utilization calculation. It has been shown experimentally by several authors[11,12,13] that the standard definition of the thermal utilization (where the average fluxes in the various regions are calculated by the one-group diffusion theory) may be used to accurately predict the thermal utilization of a heterogeneous cell. With this verification, an eight region one-group diffusion theory[2] in cylindrical coordinates was programmed for solution by the IBM-702. The boundary conditions imposed on the equations were:

1. Continuity of flux and neutron current at the interfaces of the regions.

2. Flux at the center of the region must remain finite and non-negative.

3. Slope of the flux at the outside boundary of the cell must be zero at equilibrium.

4. The flux in every region must obey the equation,

$$\phi = AI_o(kr) + bK_o(kr) + \frac{q}{\Sigma_a}$$

Unfortunately at the present time, the entire program as described by Figure 1 is not one-integrated program on the IBM-702 due to the machines limited capacity. The separate boxes must be run independently one at

(10) HW-17171, P. F. Gast, March 9, 1950.
(11) HW-38738, W. E. Niemuth, June, 1955.
(12) HW-46117, R. Nilson, February, 1957.
(13) HW-54516, R. E. Smith, February, 1958.
(2) op. cit., Page 3.

a time, the feedback being accomplished by the physicist adjusting the input data at each step.

After one has interated the over-all program such that equilibrium is obtained for each case, the final results are read from the program of Box 5. The results for the Gas Cooled Reactor Study for all the cases studied are listed as Figures 10 through 99.

COMPLETE CLOSED LOOP REACTOR PHYSICS CALCULATIONS

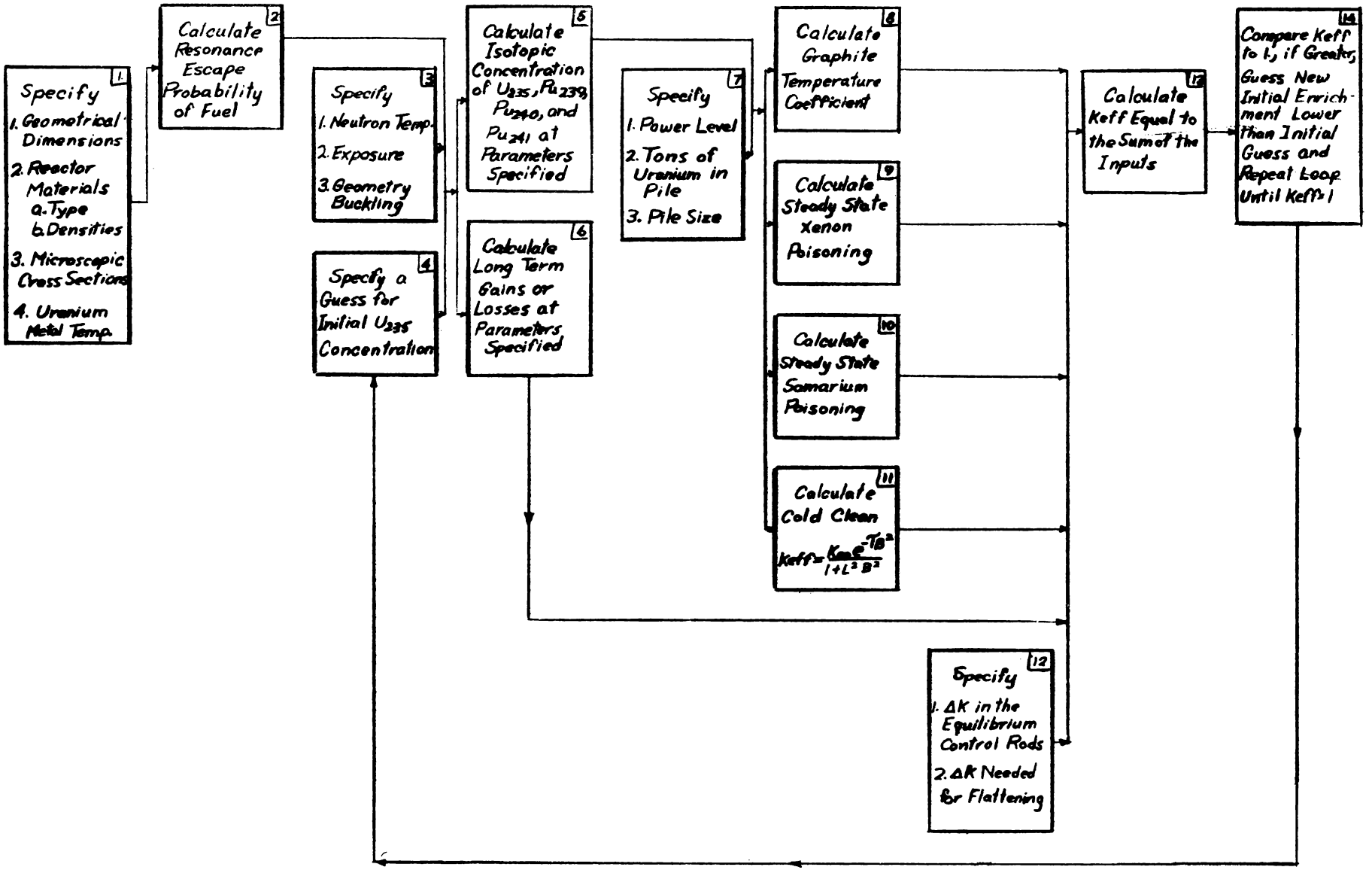

UNCLASSIFIED

UNCLASSIFIED

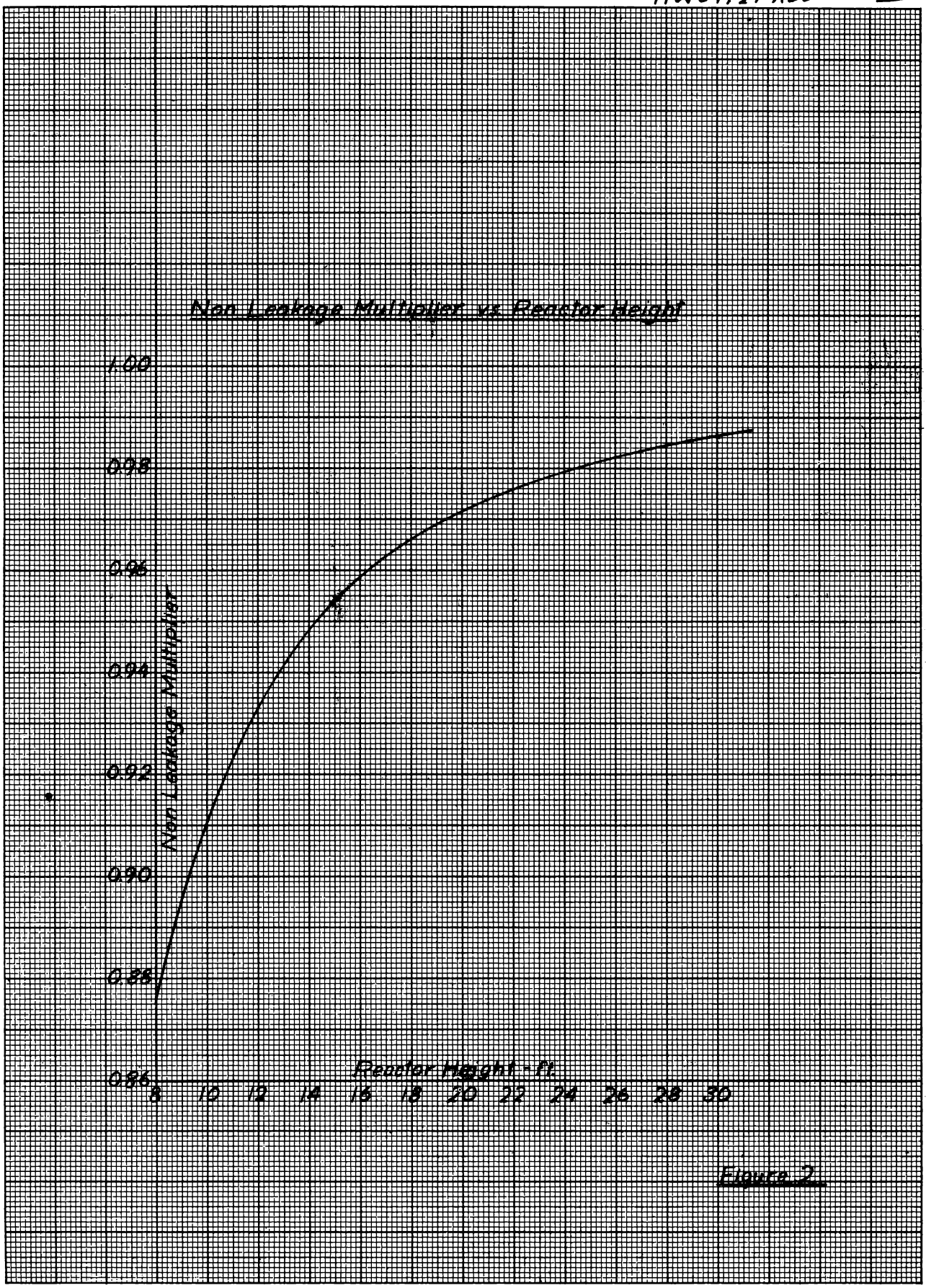
Non Leakage Multiplier vs Reactor Height
1.00
0.98
0.96
0.94
0.92
0.90
0.88
0.86
Non Leakage Multiplier
8
10
12
14
16
18
20
22
24
26
28
30
Reactor Height - ft

Figure 2.

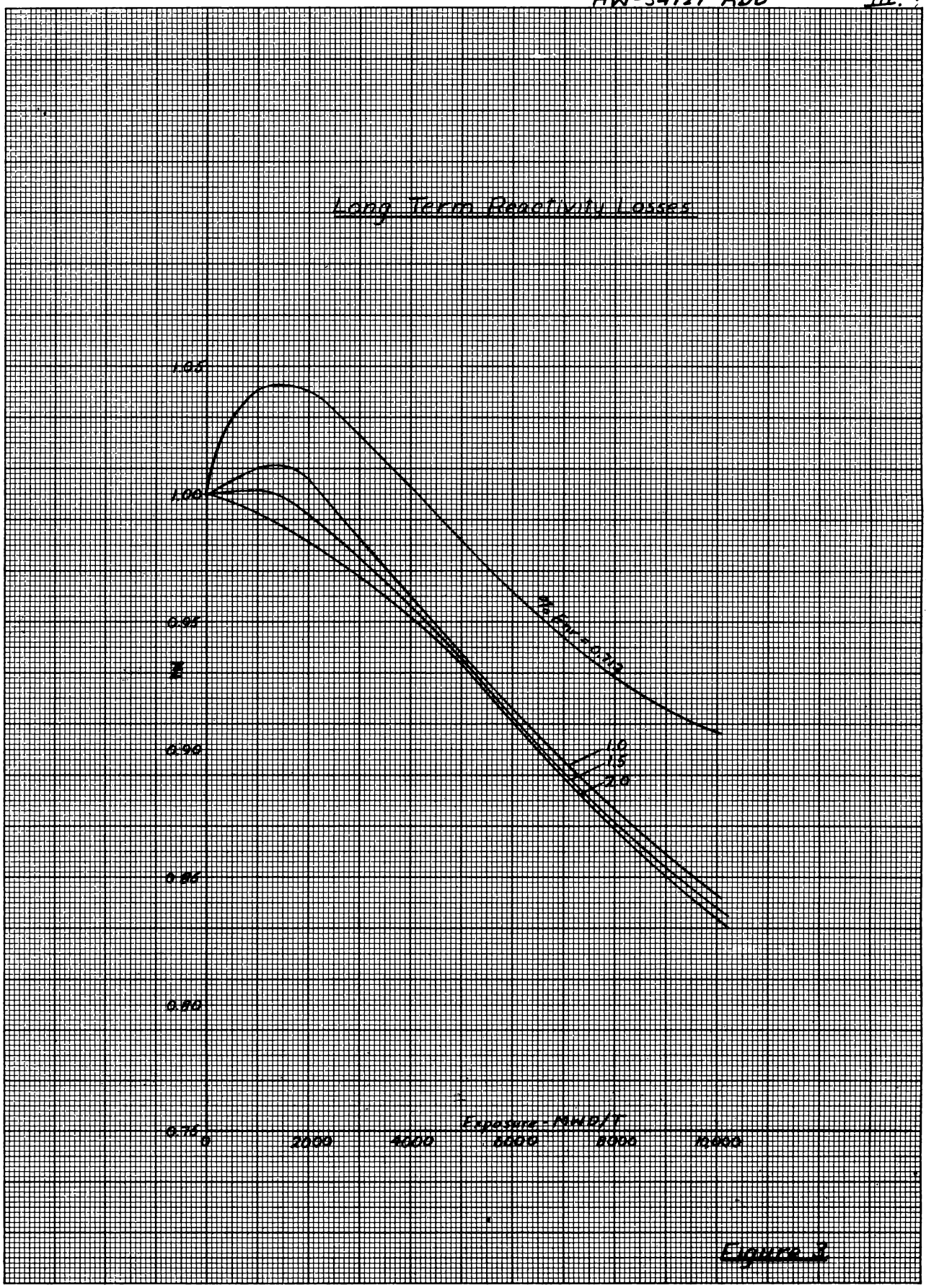
Long Term Reactivity Losses
1.05
1.00
0.95
0.90
0.85
0.80
0.75
0
2000
4000
6000
8000
10,000
Exposure - MWD/T
% Enr = 0.712
1.0
1.5
2.0

Figure 3

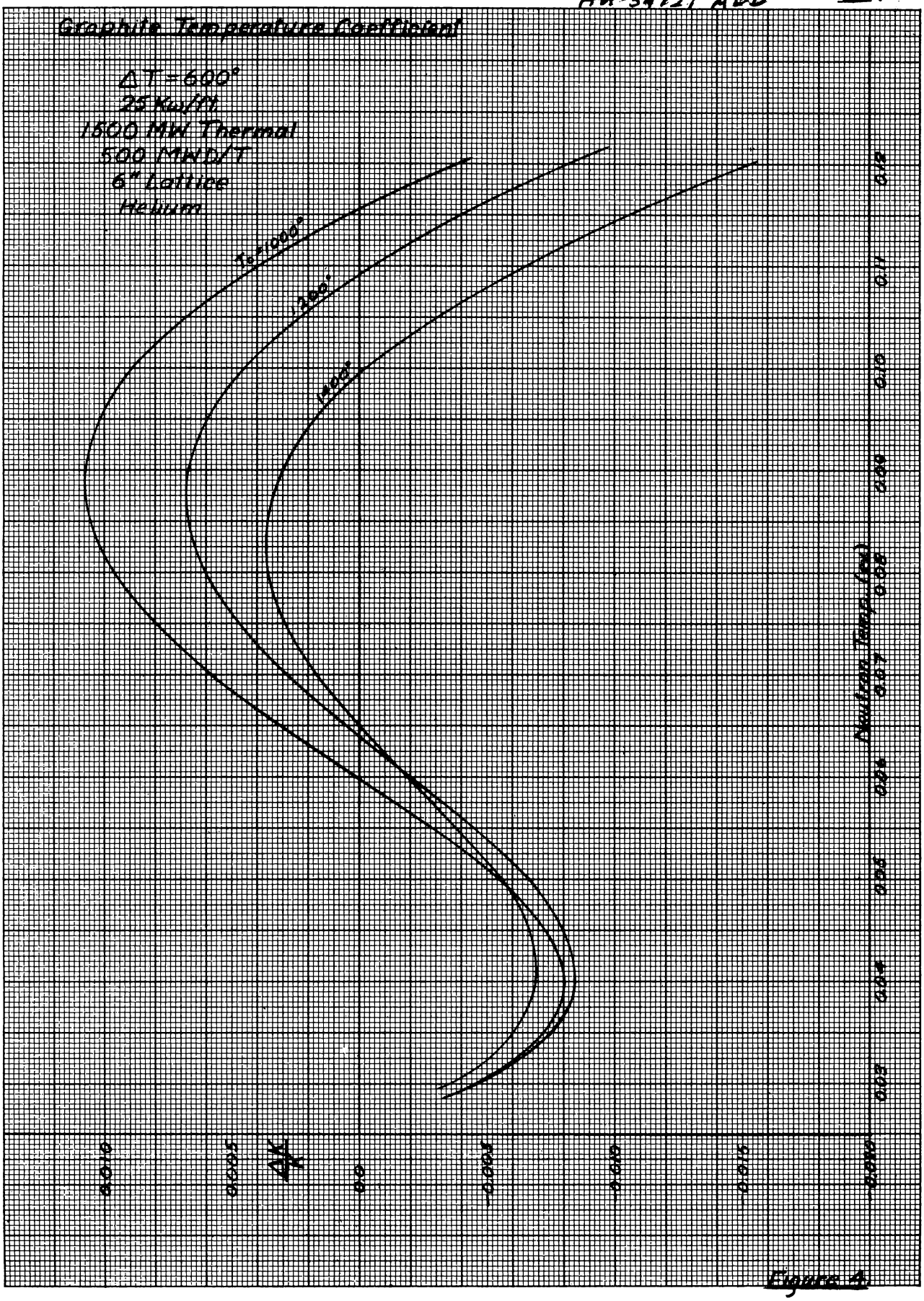
Graphite Temperature Coefficient
ΔT = 600°
25 Kw/ft.
1500 MW Thermal
500 MWD/T
6" Lattice
Helium
T₀ = 1000°
1200°
1400°
Neutron Temp. (°C)
0.03
0.04
0.05
0.06
0.07
0.08
0.09
0.10
0.11
0.12
ΔK/K
0.010
0.005
0.0
-0.005
-0.010
-0.015
-0.020

Figure 4.

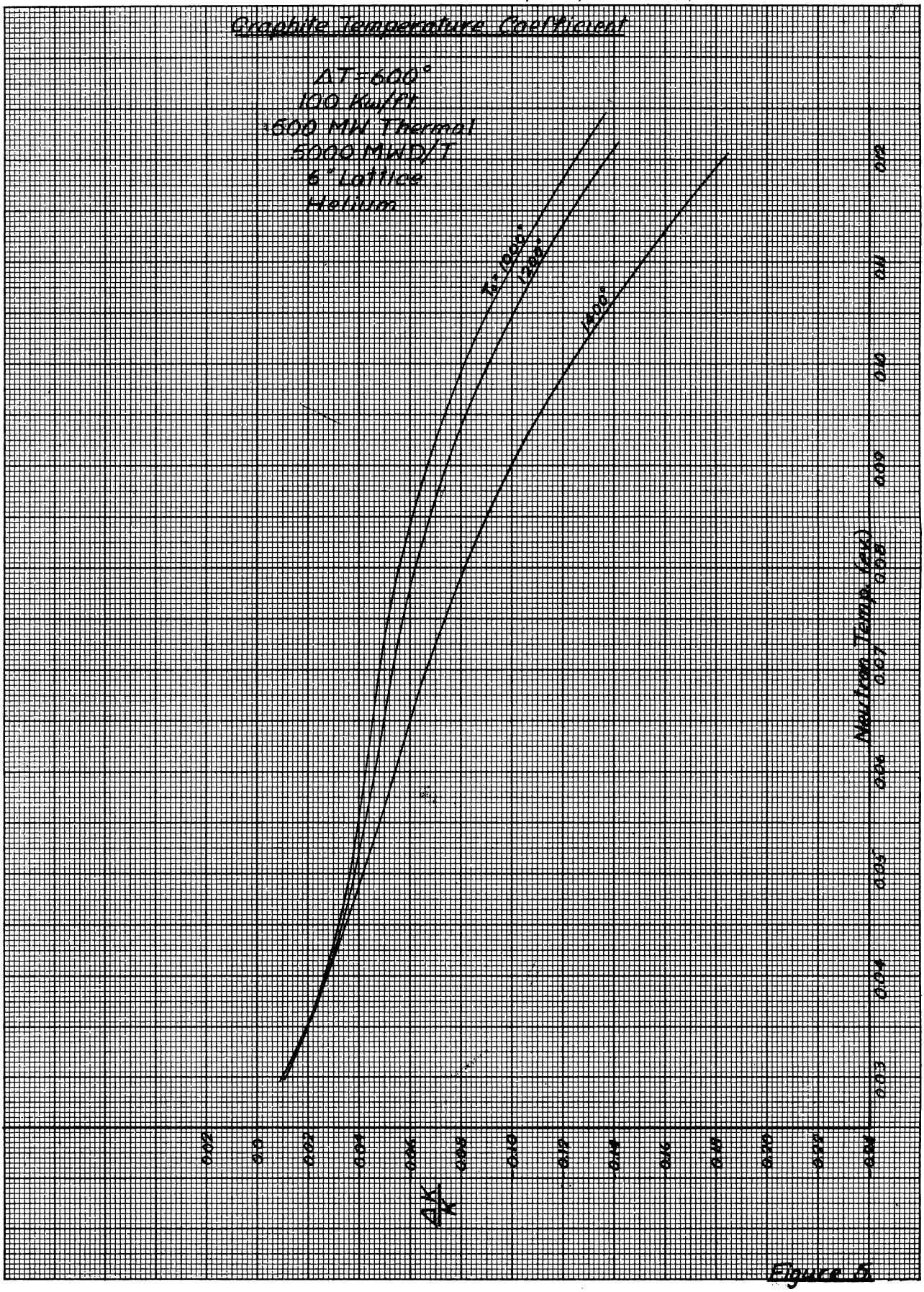
Graphite Temperature Coefficient
ΔT=600°
100 Kw/Ft
600 MW Thermal
5000 MWD/T
6" Lattice
Helium
Neutron Temp. (eV)

Figure 6

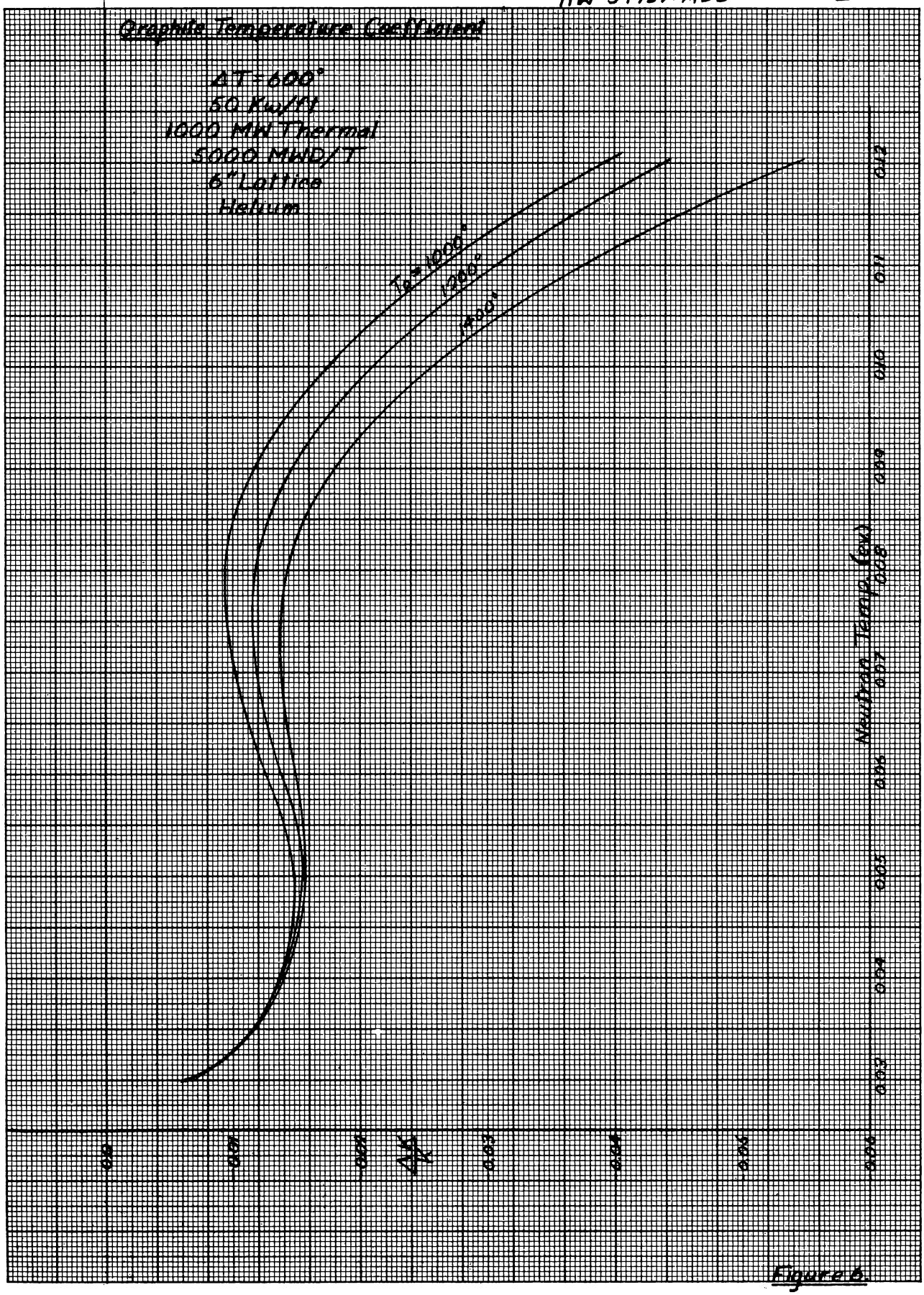
Graphite Temperature Coefficient
ΔT = 600°
50 Kw/ft
1000 MW Thermal
5000 MWD/T
6" Lattice
Helium
T_0 = 1000°
1200°
1400°
Neutron Temp. (ev)
0.03
0.04
0.05
0.06
0.07
0.08
0.09
0.10
0.11
0.12
ΔK/K
-0.00
-0.01
-0.02
-0.03
-0.04
-0.05
-0.06

Figure 6.

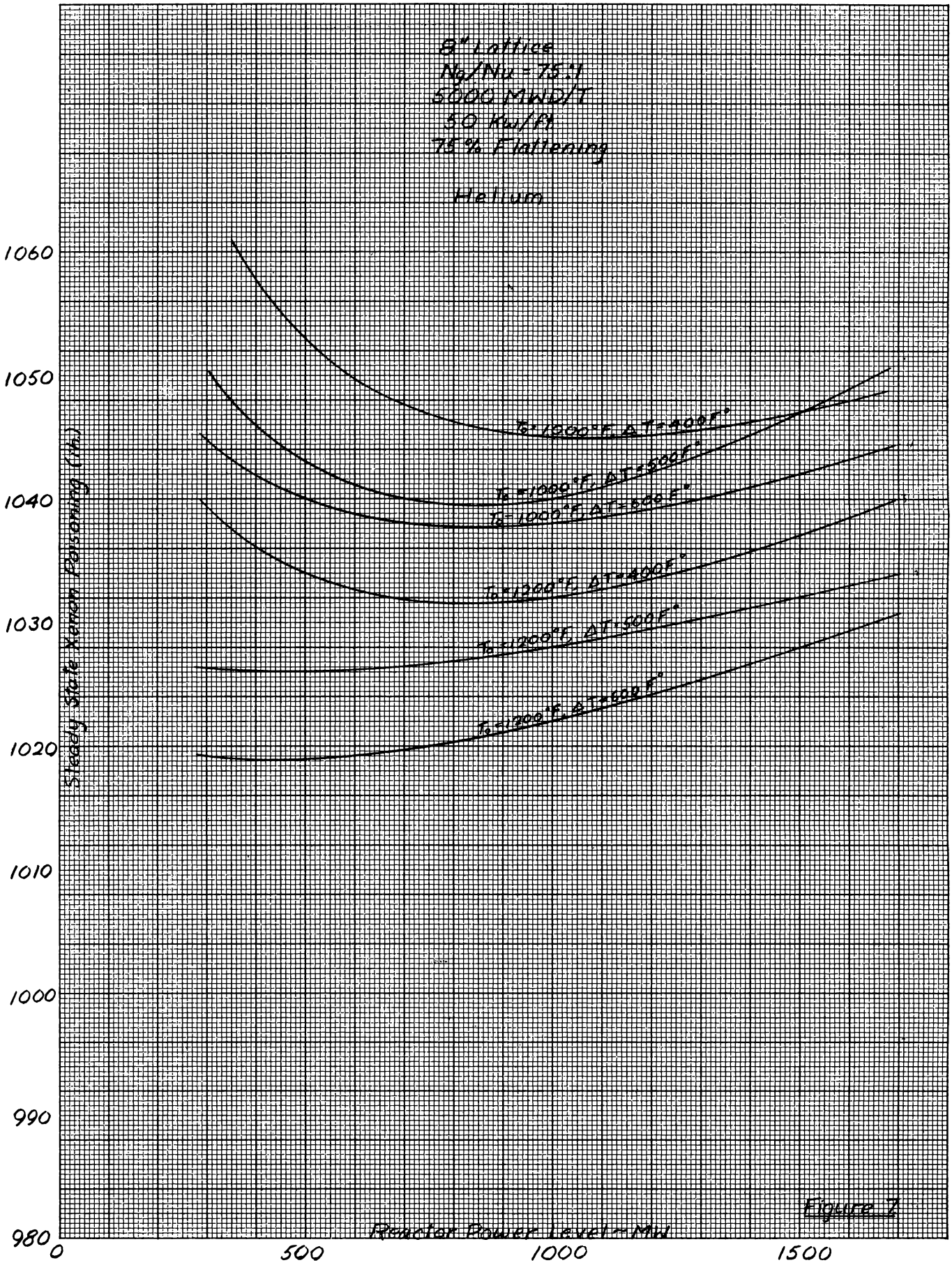
8" Lattice
Ng/Nu = 75:1
5000 MWD/T
50 Kw/ft
75% Flattening
Helium
T_0=1000°F, ΔT=400F°
T_0=1000°F, ΔT=500F°
T_0=1000°F, ΔT=600F°
T_0=1200°F, ΔT=400F°
T_0=1200°F, ΔT=500F°
T_0=1200°F, ΔT=600F°
Steady State Xenon Poisoning (in.)
1060
1050
1040
1030
1020
1010
1000
990
980
0
500
1000
1500
Reactor Power Level ~ MW

Figure 7

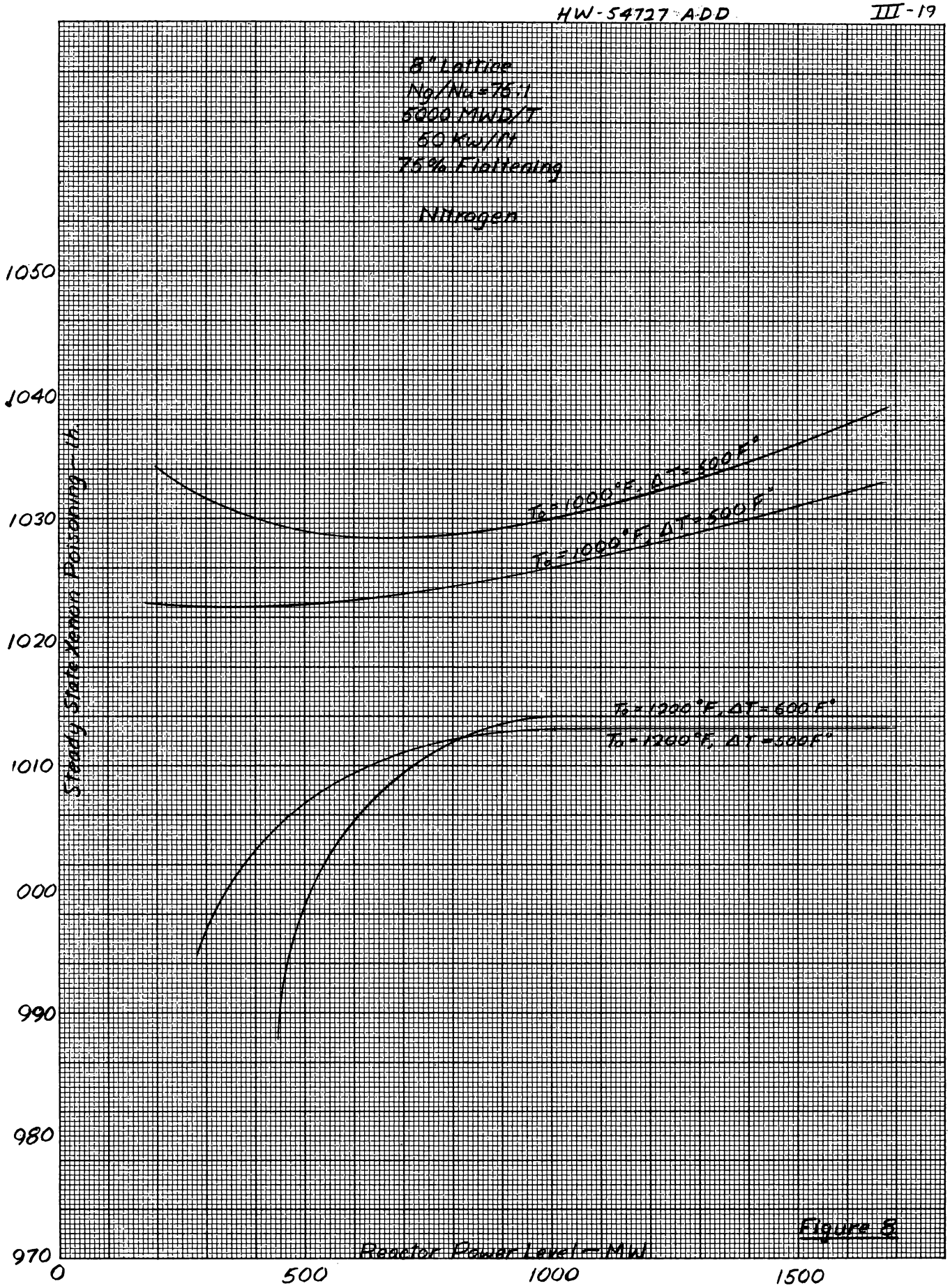
8" Lattice
No/Nu=75:1
6000 MWD/T
50 Kw/ft
75% Flattening
Nitrogen
Tc=1000°F, ΔT=500 F°
Tc=1000°F, ΔT=500 F°
Tc=1200°F, ΔT=600 F°
Tc=1200°F, ΔT=500 F°
Steady State Xenon Poisoning — Lb.
1050
1040
1030
1020
1010
000
990
980
970
0
500
1000
1500
Reactor Power Level — Mwt

Figure 8

Figure 9 has been deleted

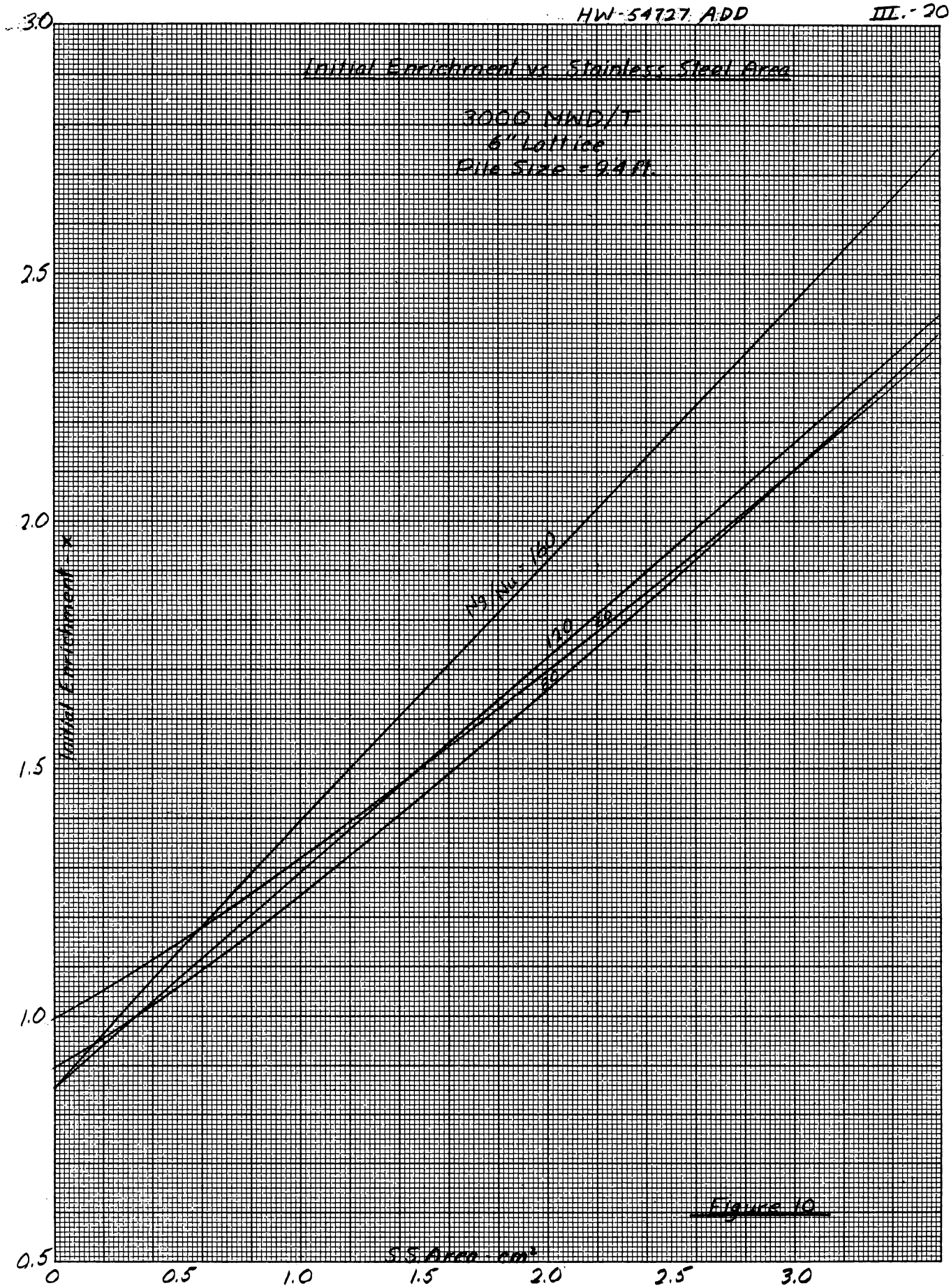
Initial Enrichment vs Stainless Steel Area
3000 MWD/T
6" Lattice
Pile Size = 9.4 ft.
Initial Enrichment - x
S.S. Area - cm²
Ng/Nu = 160
120
80
60
3.0
2.5
2.0
1.5
1.0
0.5
0
0.5
1.0
1.5
2.0
2.5
3.0

Figure 10

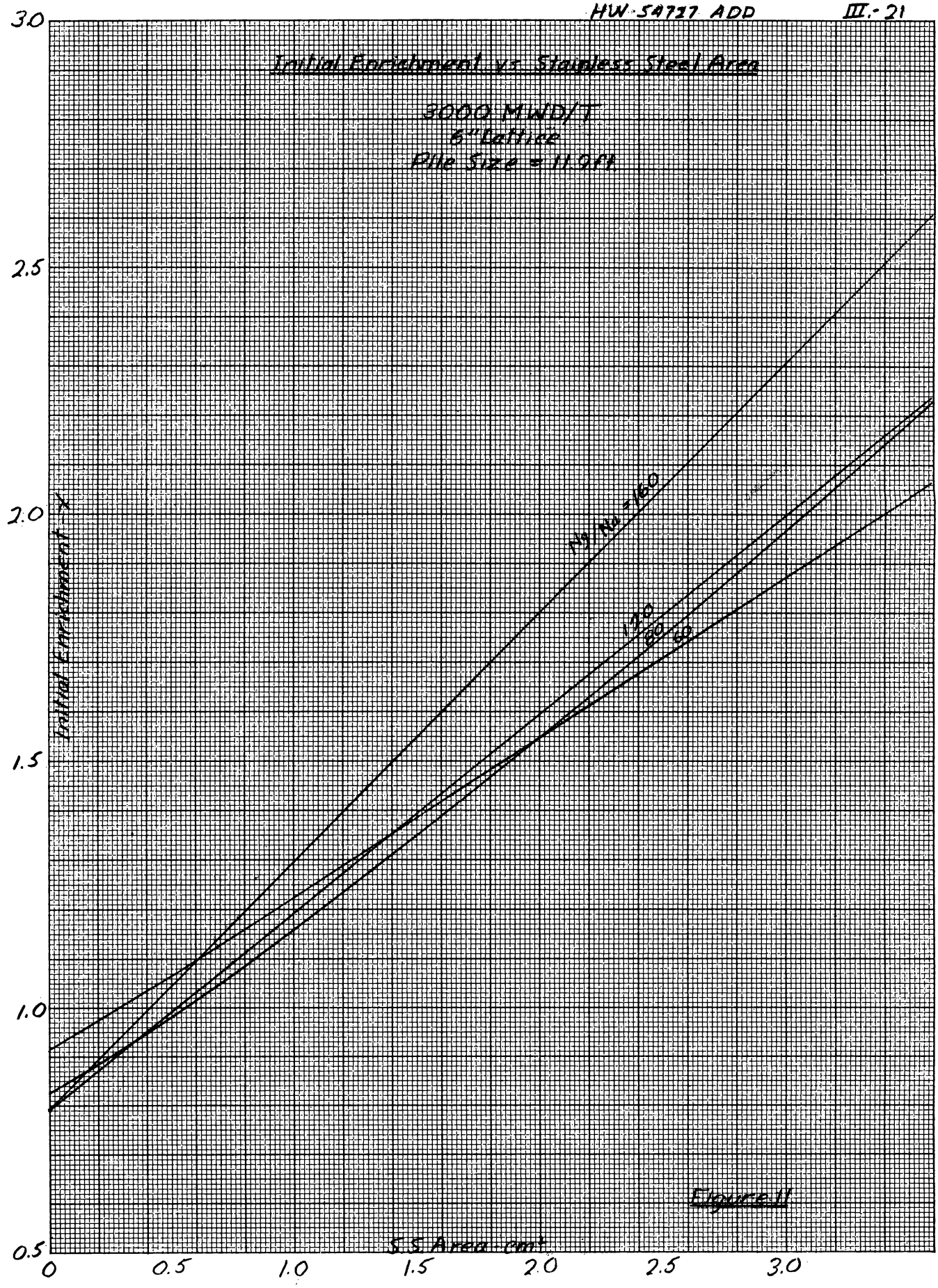
Initial Enrichment vs Stainless Steel Area
3000 MWD/T
6" Lattice
Pile Size = 11.9 ft
Ng/Na = 160
120
80
60
Initial Enrichment - X
S.S. Area - cm²
3.0
2.5
2.0
1.5
1.0
0.5
0
0.5
1.0
1.5
2.0
2.5
3.0

Figure 11

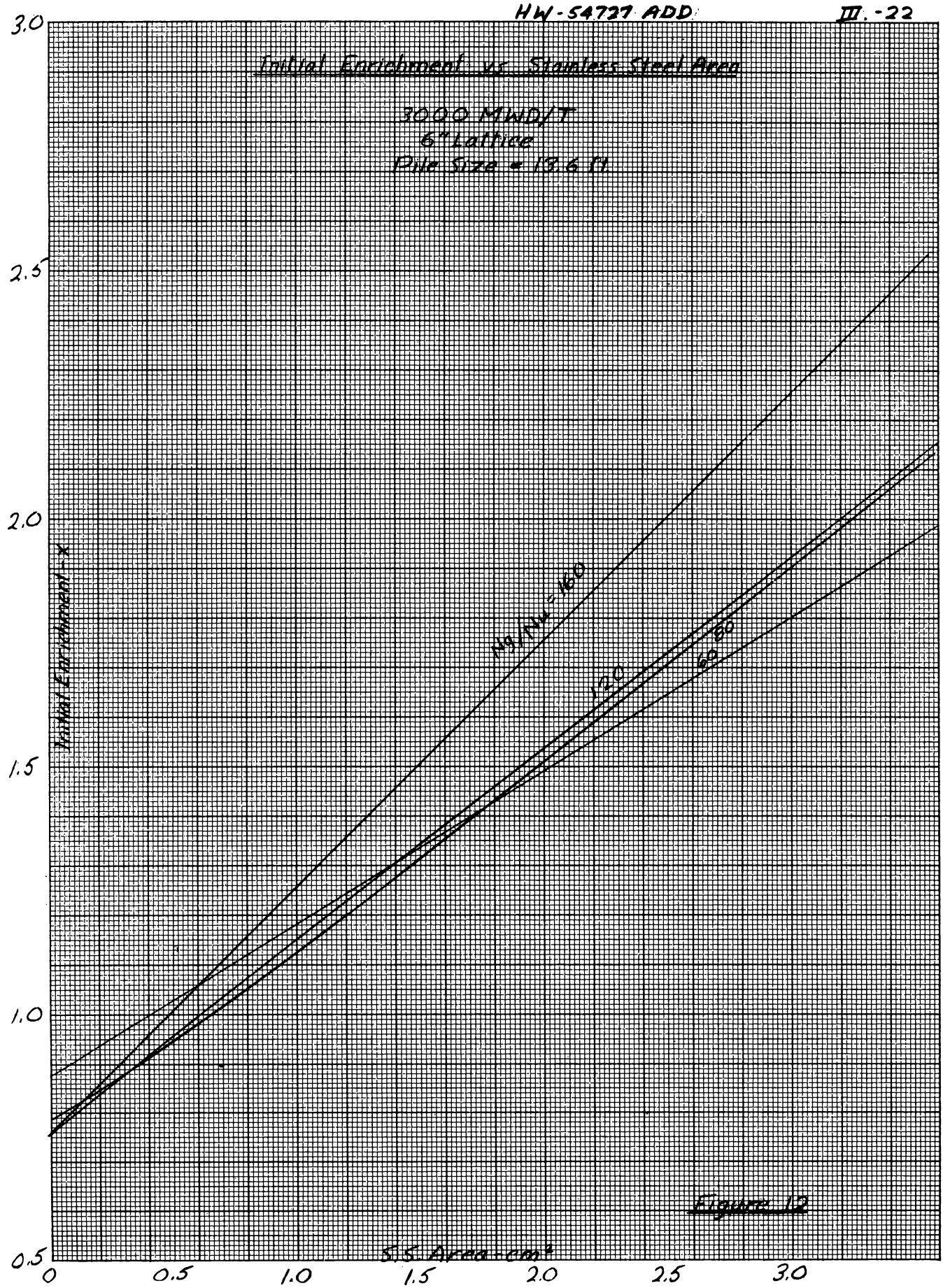
Initial Enrichment vs Stainless Steel Area
3000 MWD/T
6" Lattice
Pile Size = 13.6 ft
Initial Enrichment - X
S.S. Area - cm²
Ng/Nu = 160
120
80
60
3.0
2.5
2.0
1.5
1.0
0.5
0
0.5
1.0
1.5
2.0
2.5
3.0

Figure 12

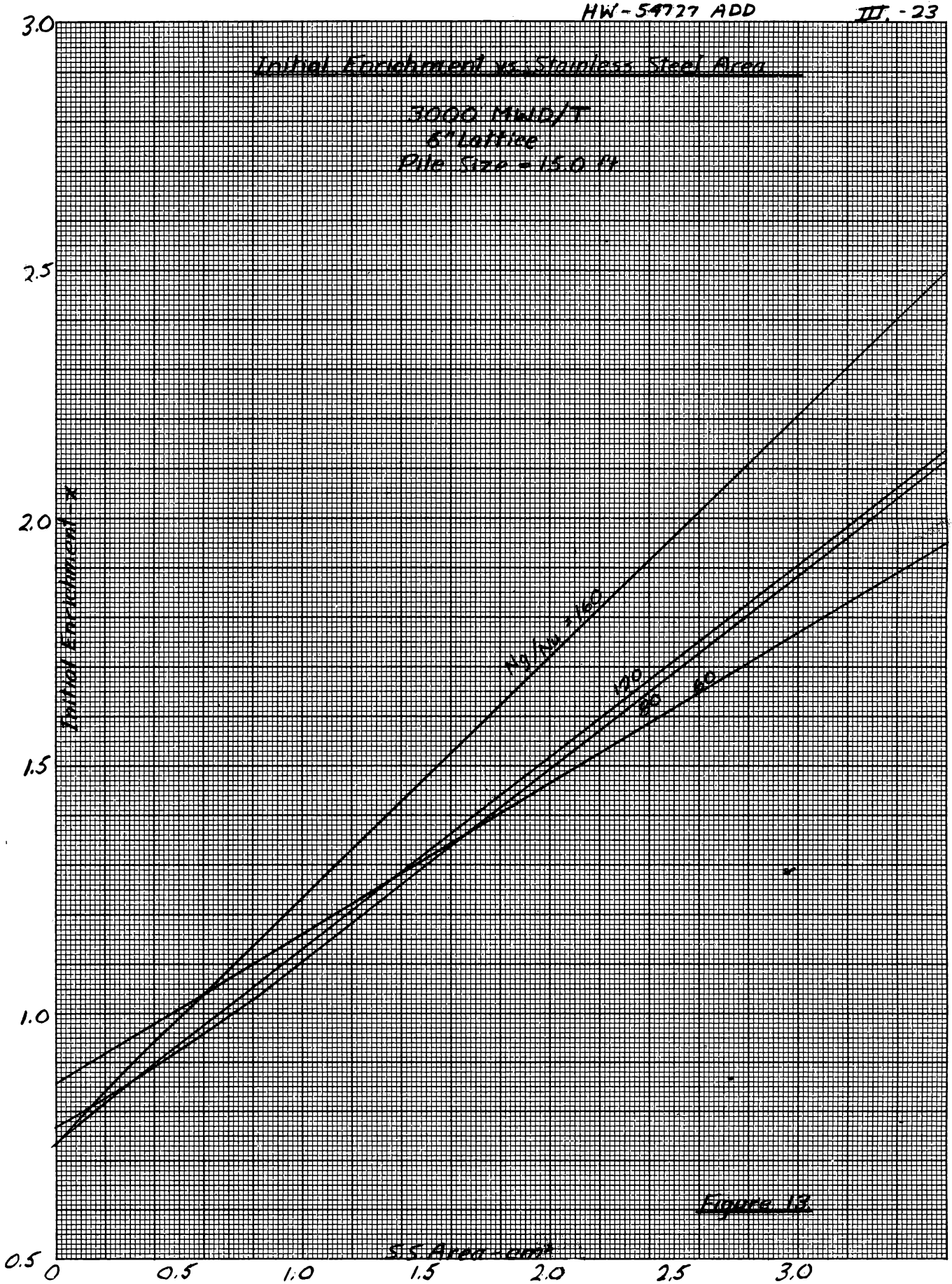
Initial Enrichment vs. Stainless Steel Area
3000 MwD/T
6" Lattice
Pile Size = 15.0 ft
Initial Enrichment, w/o
SS Area - cm²
160
140
120
100
80
60
3.0
2.5
2.0
1.5
1.0
0.5
0
0.5
1.0
1.5
2.0
2.5
3.0

Figure 13

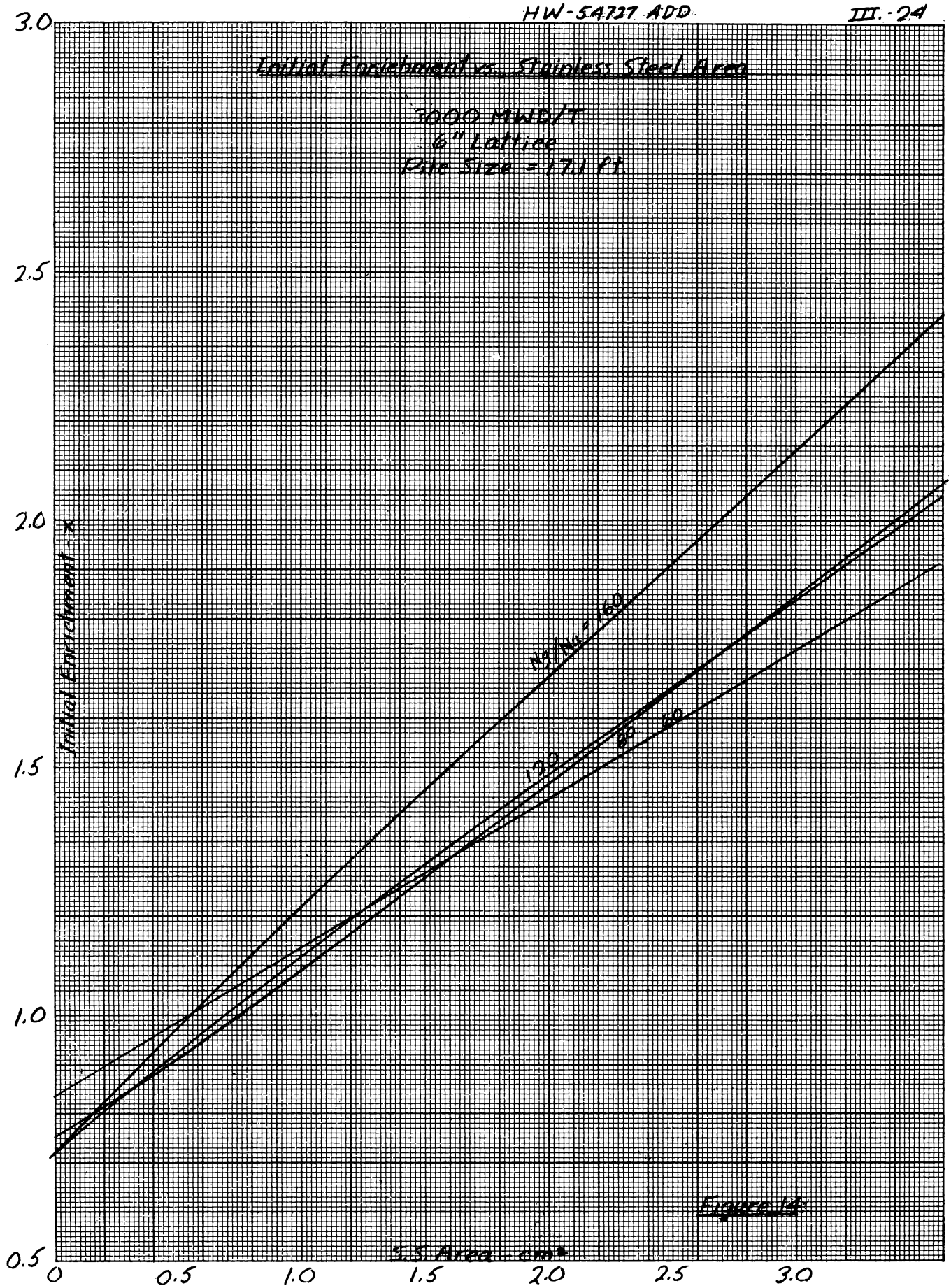
Initial Enrichment vs. Stainless Steel Area
3000 MWD/T
6" Lattice
Pin Size = 1.71 Pt.
Initial Enrichment - %
S.S. Area - cm²
160
120
80
60
3.0
2.5
2.0
1.5
1.0
0.5
0
0.5
1.0
1.5
2.0
2.5
3.0

Figure 14

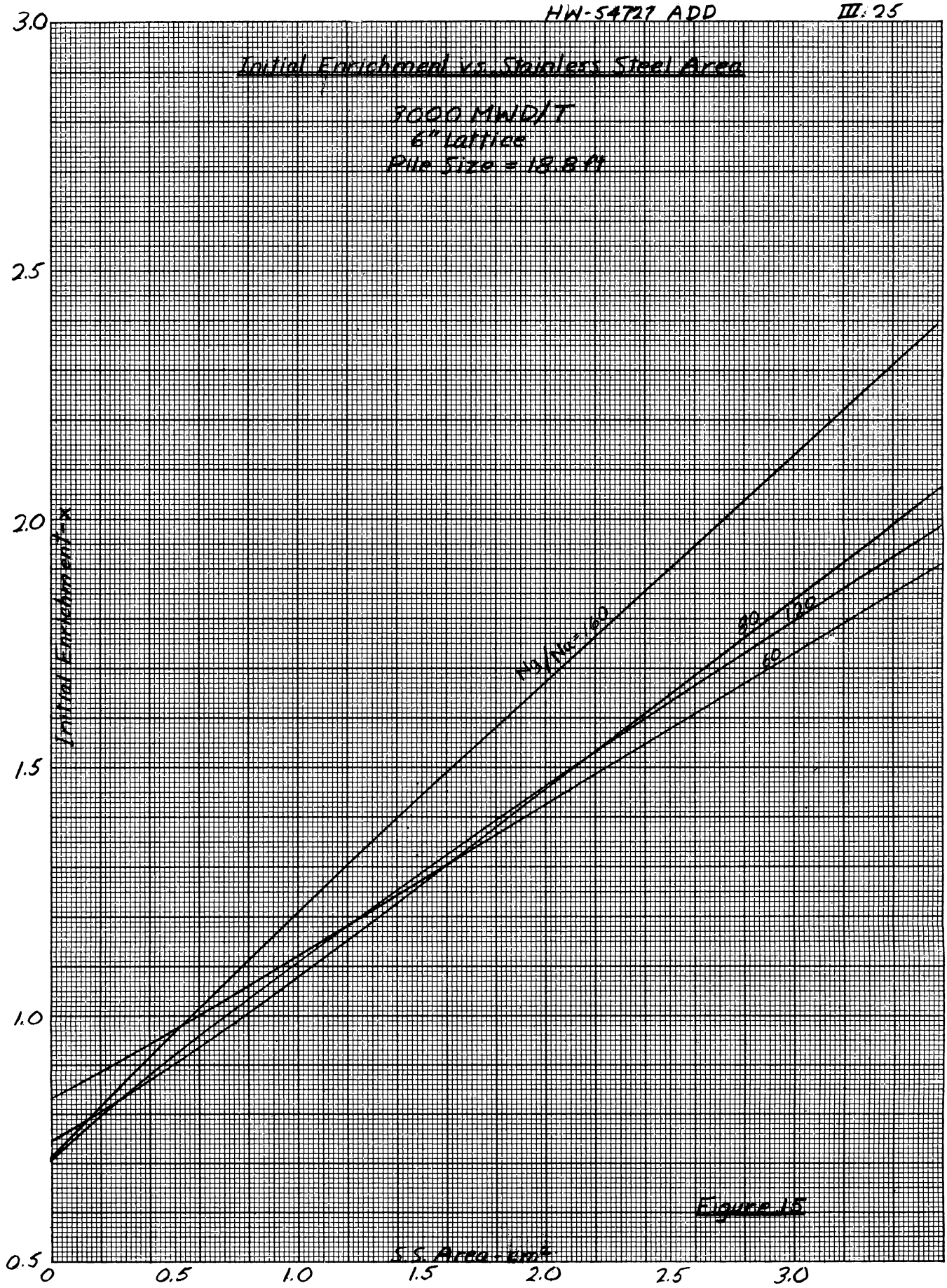
Initial Enrichment vs. Stainless Steel Area
3000 MWD/T
6" Lattice
Pile Size = 18.8 ft
Initial Enrichment - x
S.S. Area - cm²
Ng/Na = 160
80
120
60
3.0
2.5
2.0
1.5
1.0
0.5
0
0.5
1.0
1.5
2.0
2.5
3.0

Figure 15

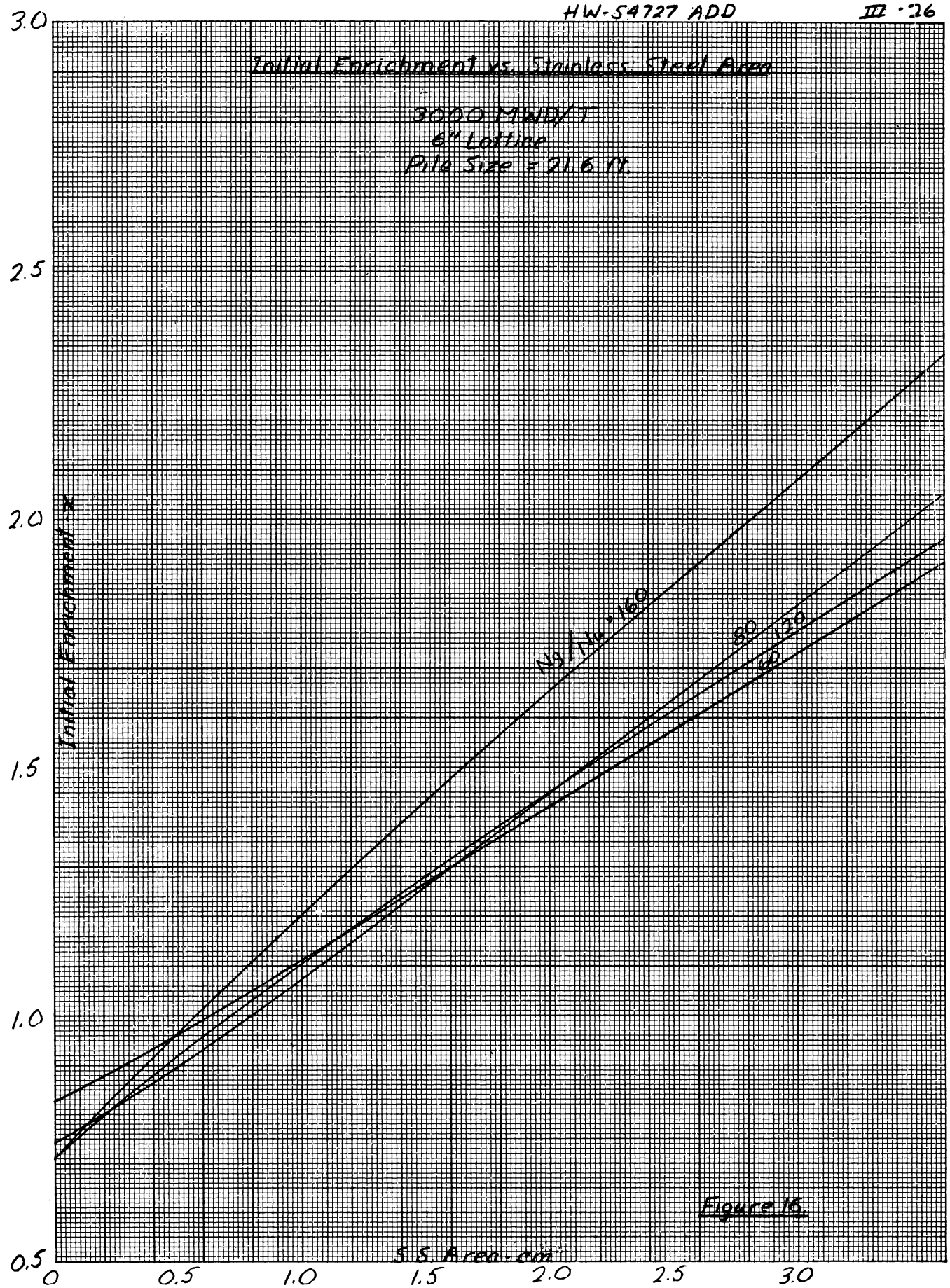
Initial Enrichment vs. Stainless Steel Area
3000 MWD/T
6" Lattice
Pile Size = 21.6 ft.
Initial Enrichment - x
S.S. Area - cm
Ng/Nu = 160
80
120
60
3.0
2.5
2.0
1.5
1.0
0.5
0
0.5
1.0
1.5
2.0
2.5
3.0

Figure 16

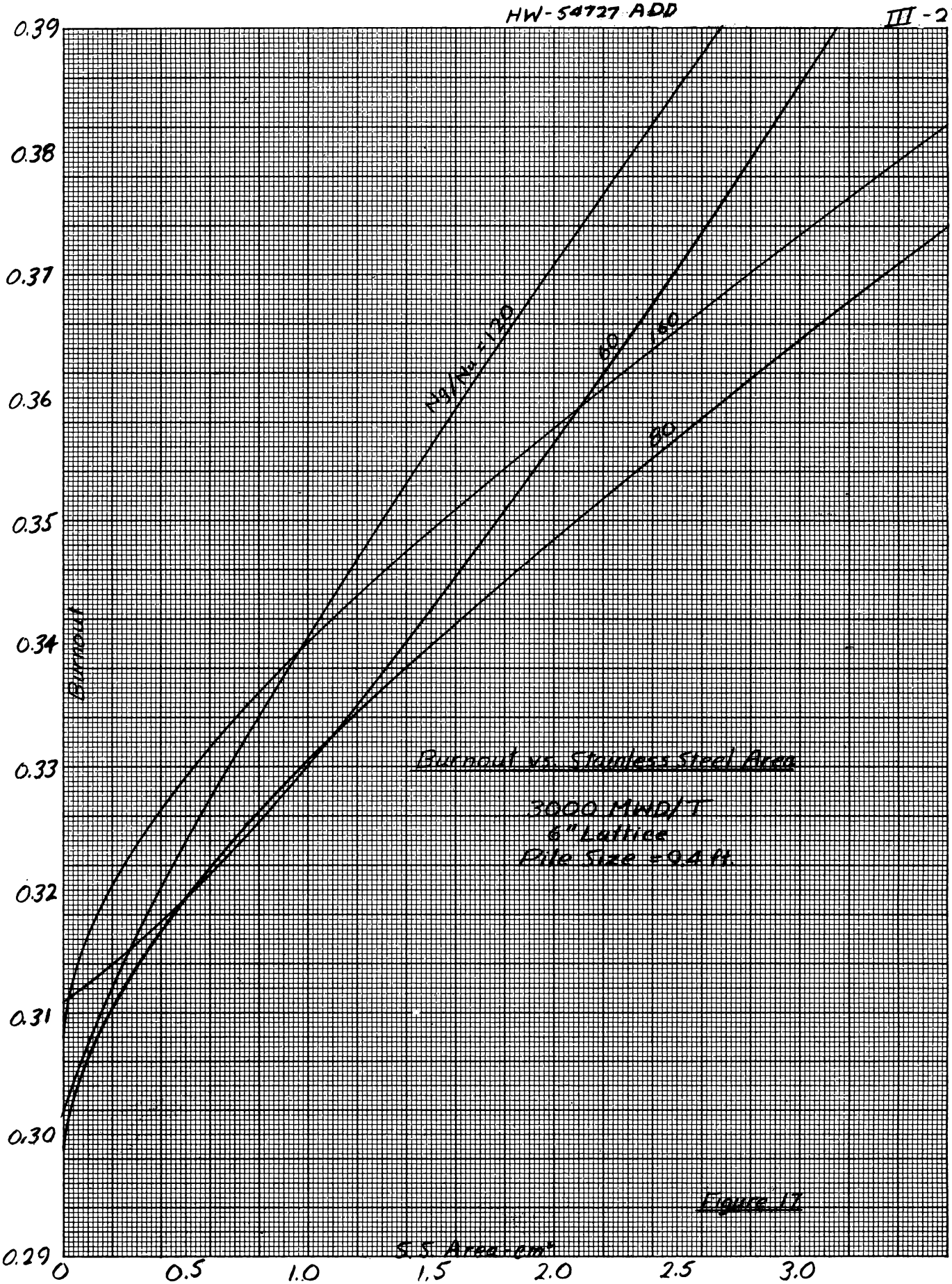
0.39
0.38
0.37
0.36
0.35
0.34
0.33
0.32
0.31
0.30
0.29
BURNOUT
0
0.5
1.0
1.5
2.0
2.5
3.0
S.S. Area - cm²
60
60
60
Burnout vs. Stainless Steel Area
3000 MWD/T
6" Lattice
Pile Size = 0.4 ft.

Figure 12

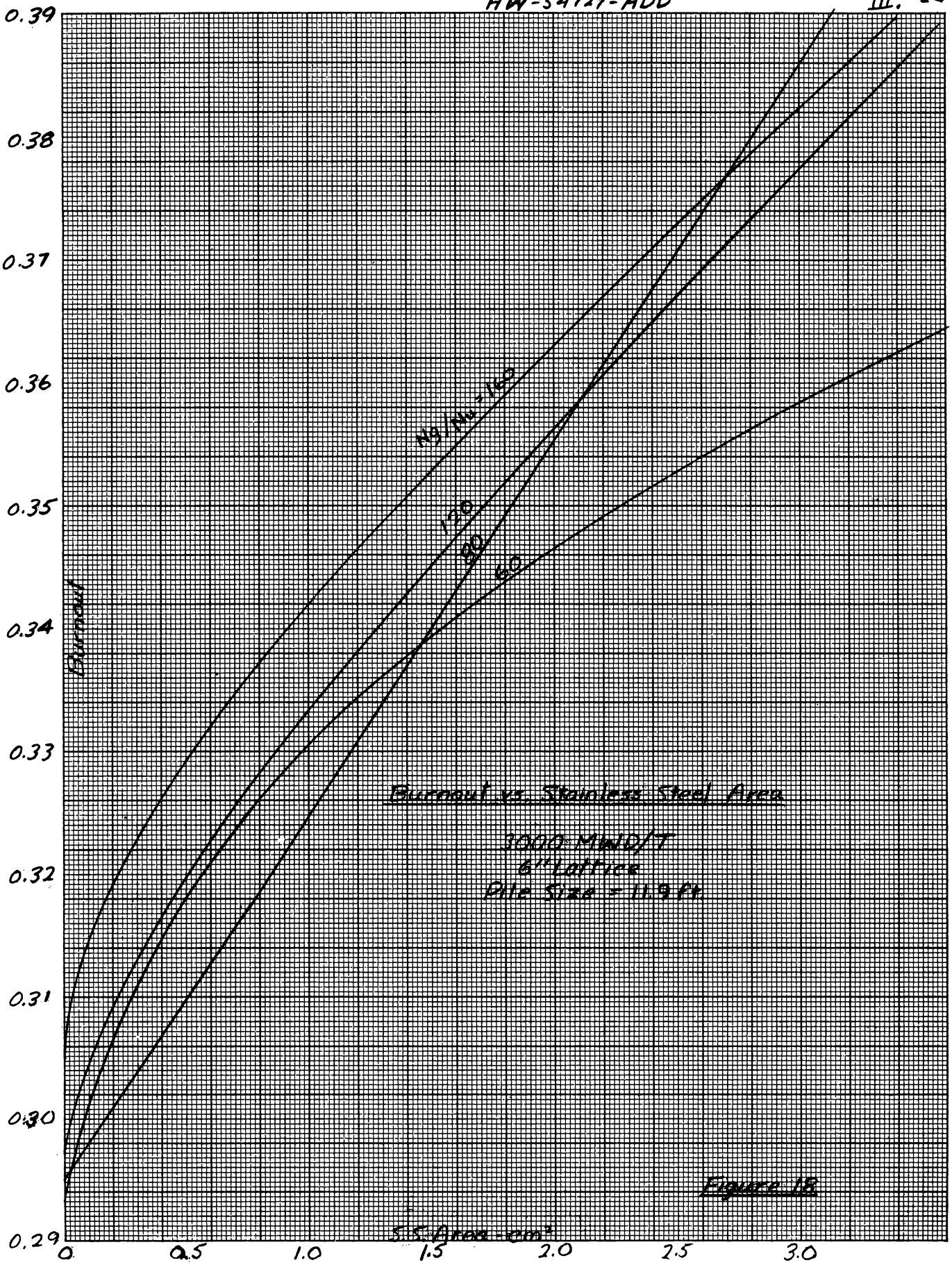
0.39
0.38
0.37
0.36
0.35
0.34
0.33
0.32
0.31
0.30
0.29
Burnout
Ng/Nu = 160
120
80
60
Burnout vs. Stainless Steel Area
3000 MWD/T
6" Lattice
Pile Size = 11.9 ft.
S.S. Area - cm²
0
0.5
1.0
1.5
2.0
2.5
3.0

Figure 18

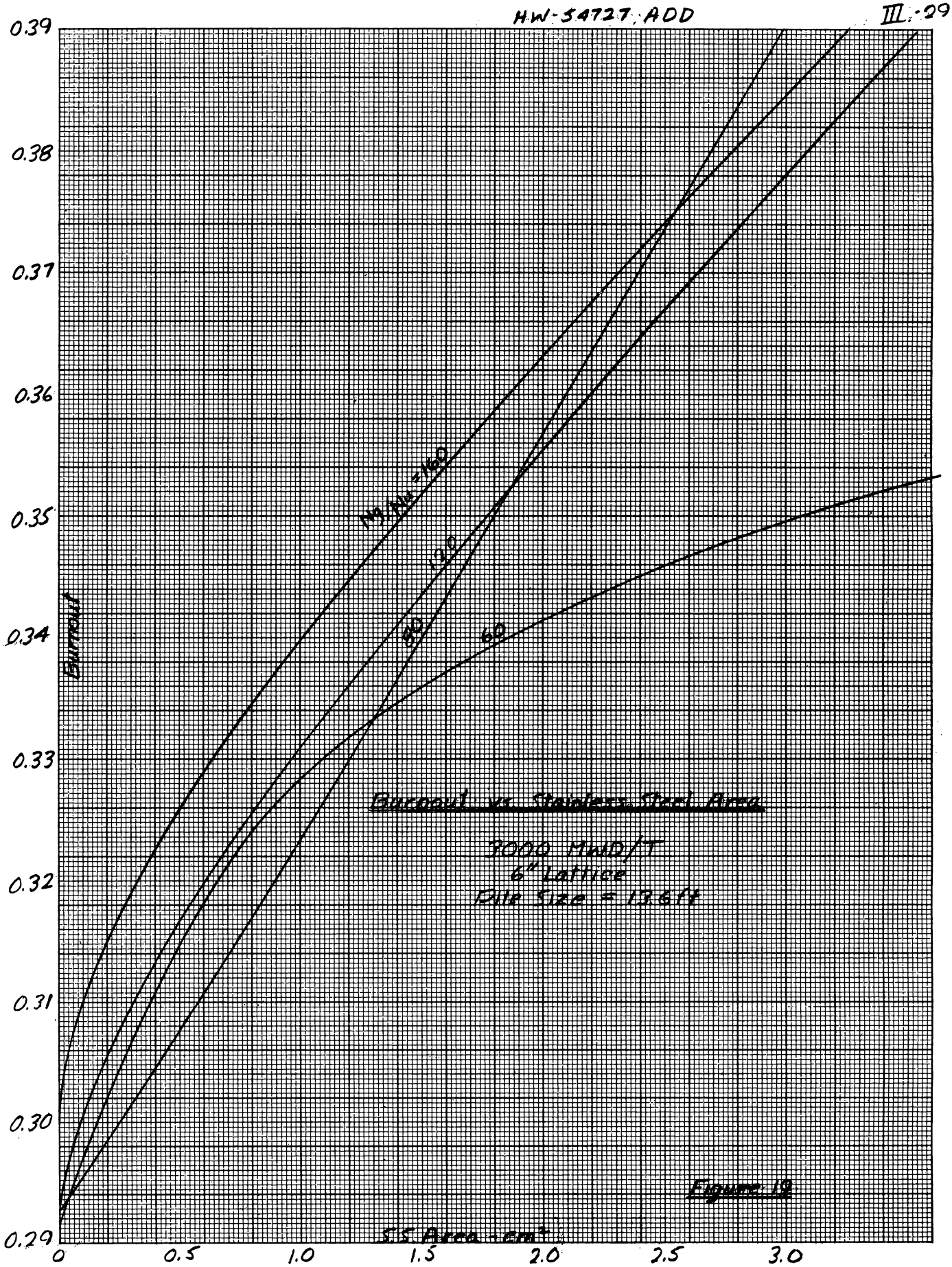
0.39
0.38
0.37
0.36
0.35
0.34
0.33
0.32
0.31
0.30
0.29
Bucsq
0
0.5
1.0
1.5
2.0
2.5
3.0
SS Area - cm²
160
120
80
60
Bucsq vs Stainless Steel Area
3000 MWD/T
6" Lattice
Pin Size = 13.6 ft

Figure 18

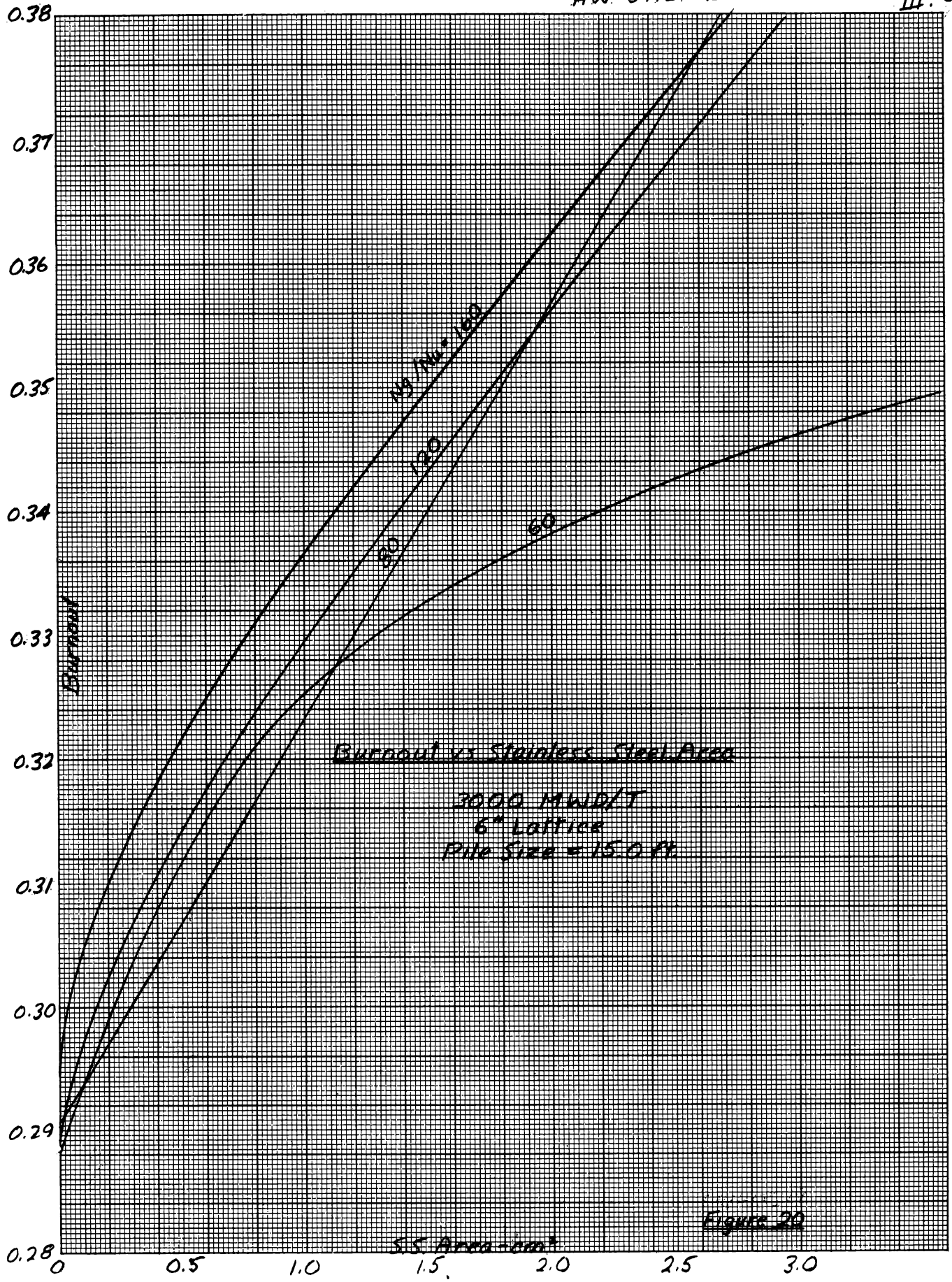
0.38
0.37
0.36
0.35
0.34
0.33
0.32
0.31
0.30
0.29
0.28
Burnout
0
0.5
1.0
1.5
2.0
2.5
3.0
5.5 Area-cm²
60
60
60
Burnout vs Stainless Steel Area
30000 MWD/T
6" Lattice
Pile Size = 15.0 Ft.

Figure 20

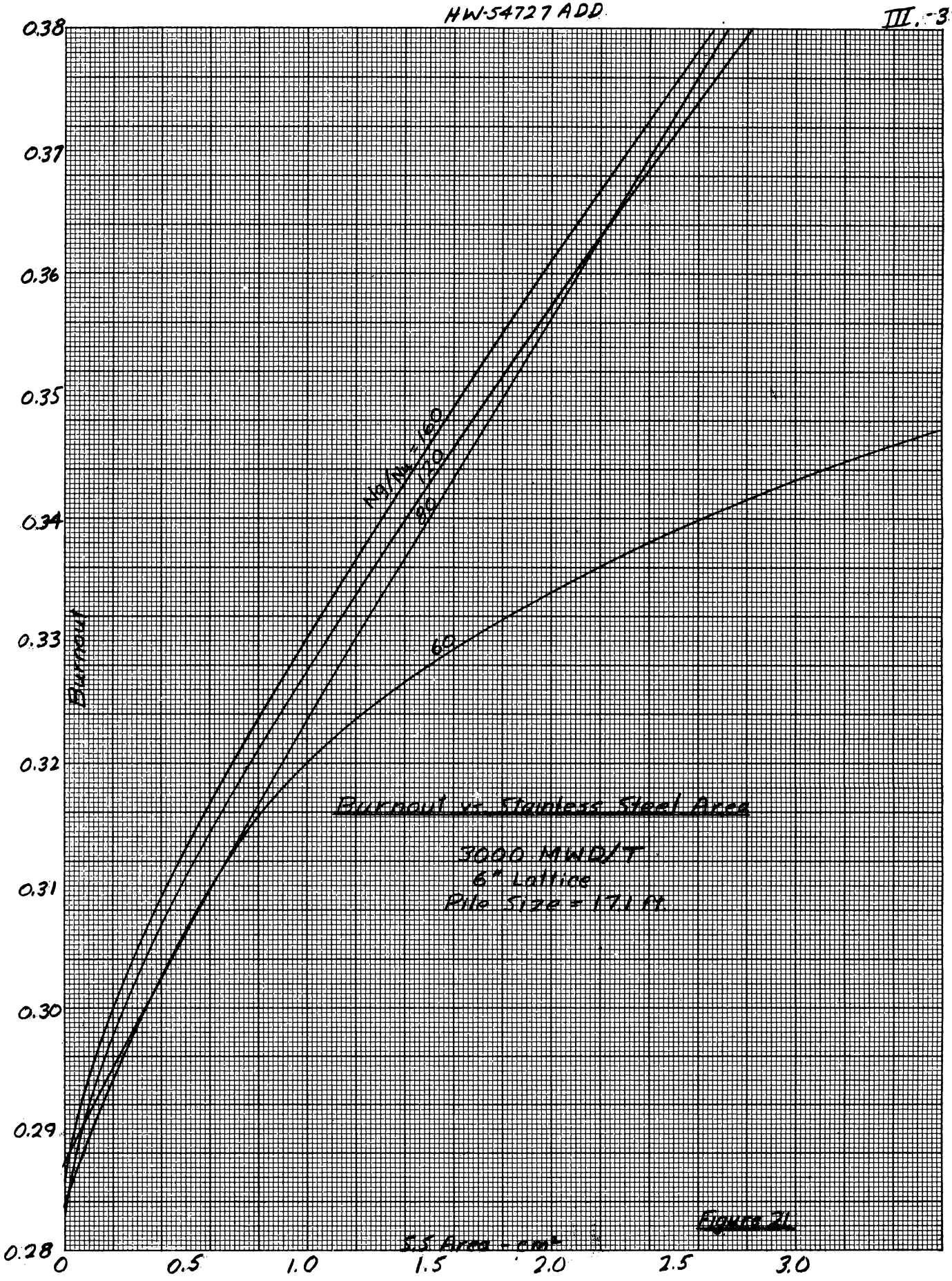
0.38
0.37
0.36
0.35
0.34
0.33
0.32
0.31
0.30
0.29
0.28
Burnout
0
0.5
1.0
1.5
2.0
2.5
3.0
S.S Area - cm²
60
60
60
60
Burnout vs. Stainless Steel Area
3000 MWD/T
6" Lattice
Pile Size = 17.1 ft.

Figure 2L

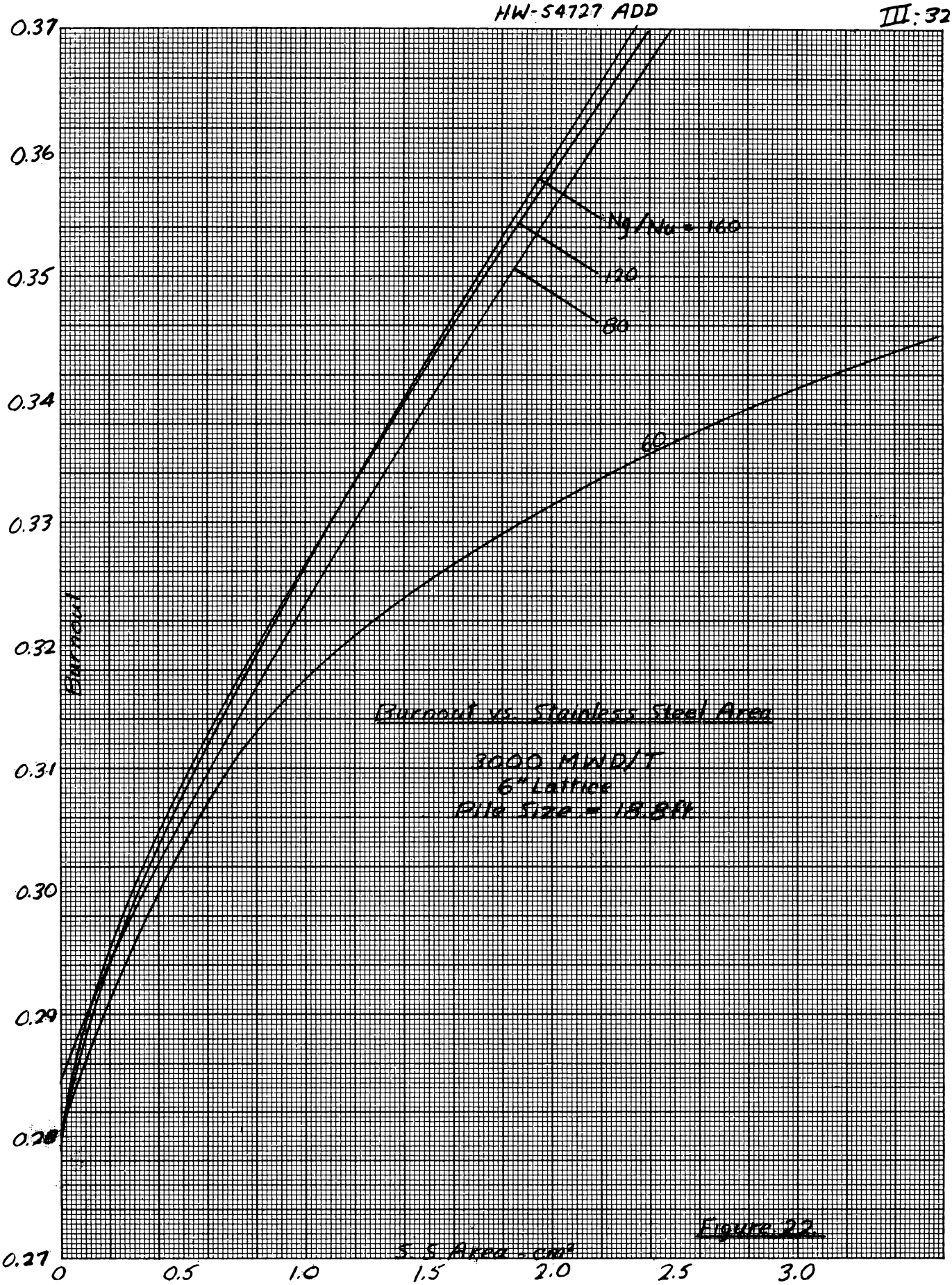
0.37
0.36
0.35
0.34
0.33
0.32
0.31
0.30
0.29
0.28
0.27
Burnout
0
0.5
1.0
1.5
2.0
2.5
3.0
S.S Area - cm²
Ng/Nu = 160
120
80
60
Burnout vs. Stainless Steel Area
30000 MWD/T
6" Lattice
Pile Size = 18.8 ft

Figure 22.

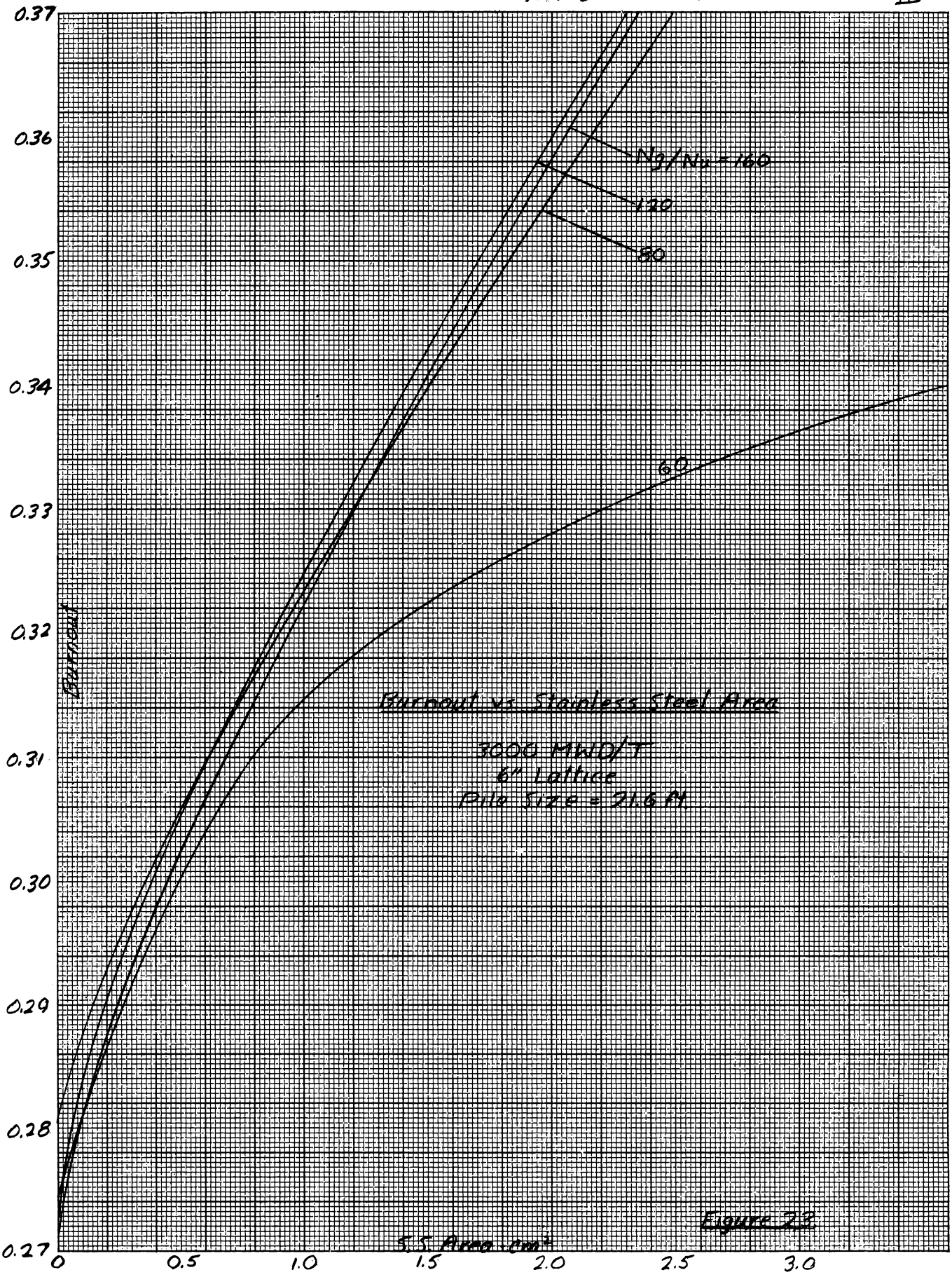
0.37
0.36
0.35
0.34
0.33
0.32
0.31
0.30
0.29
0.28
0.27
Burnout
0
0.5
1.0
1.5
2.0
2.5
3.0
S.S. Area, cm²
N_g/N_u = 160
120
80
60
Burnout vs. Stainless Steel Area
3000 MWD/T
6" Lattice
Pile Size e = 21.6 ft

Figure 2.2

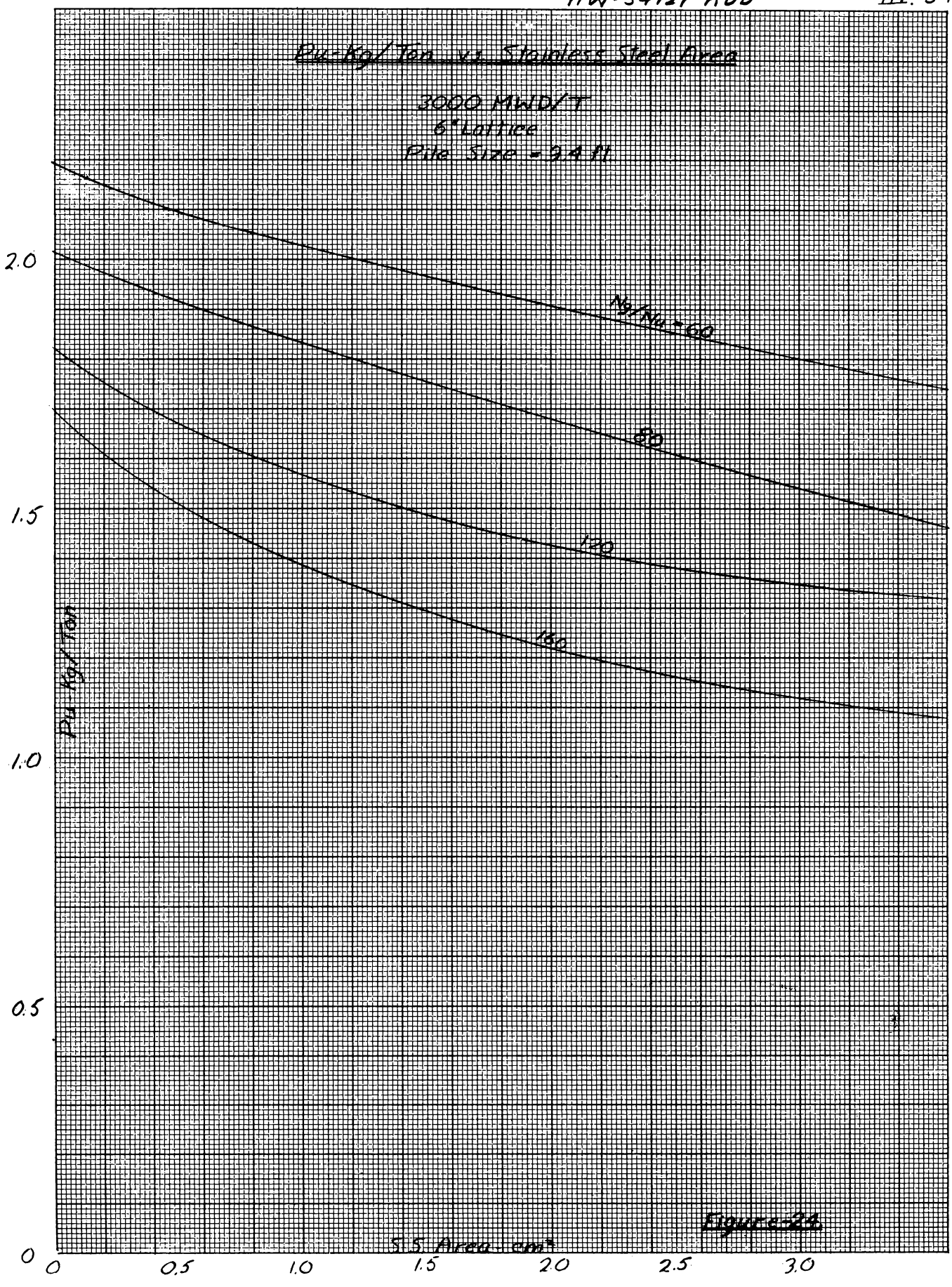
Pu-Kg/Ton vs Stainless Steel Area
3000 MWD/T
6" Lattice
Pile Size = 9.4 ft
Ng/Nu = 60
80
120
160
Pu Kg/Ton
2.0
1.5
1.0
0.5
0
0
0.5
1.0
1.5
2.0
2.5
3.0
S.S. Area - cm²

Figure-24

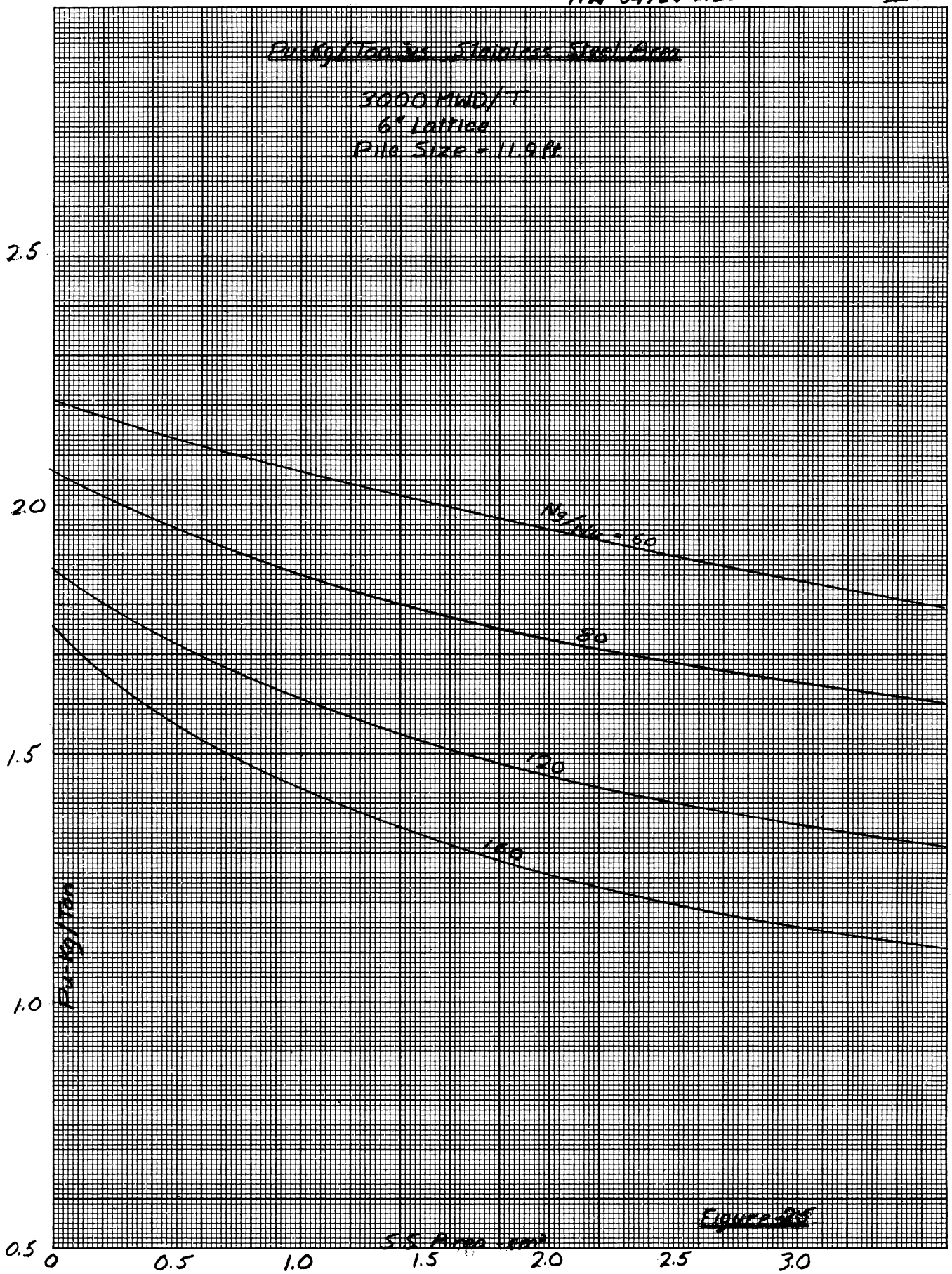
Pu-Kg/Ton vs. Stainless Steel Area
3000 MWD/T
6" Lattice
Pile Size = 11.9 ft
Ns/Nu = 60
80
120
160
Pu-Kg/Ton
S.S. Area - cm²
2.5
2.0
1.5
1.0
0.5
0
0.5
1.0
1.5
2.0
2.5
3.0

Figure 25

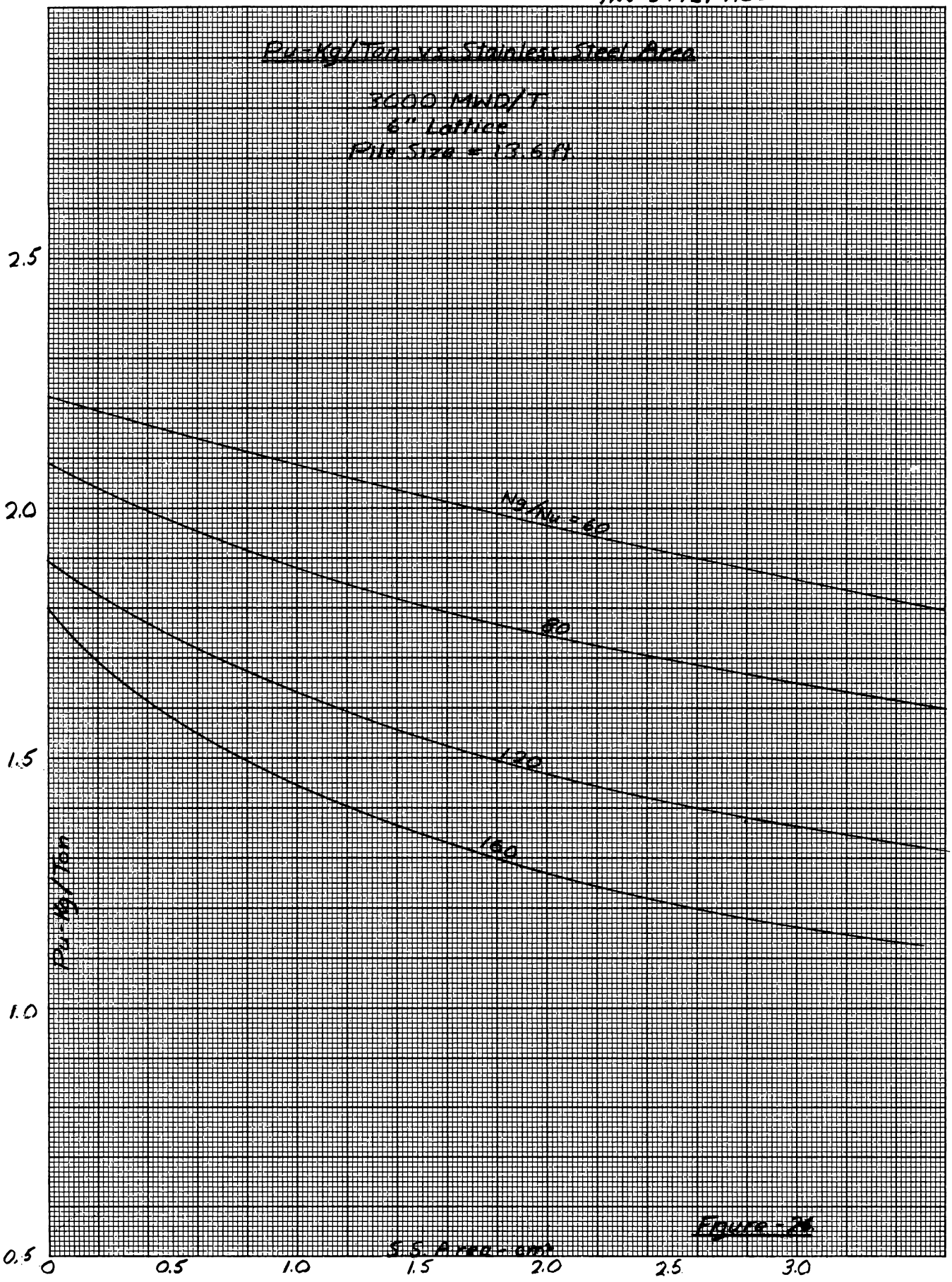
Pu-Kg/Ton vs Stainless Steel Area
3000 MWD/T
6" Lattice
Pile Size = 13.6 ft
Ng/Nu = 60
80
120
160
Pu-Kg/Ton
S.S. Area - cm²
2.5
2.0
1.5
1.0
0.5
0
0.5
1.0
1.5
2.0
2.5
3.0

Figure - 26

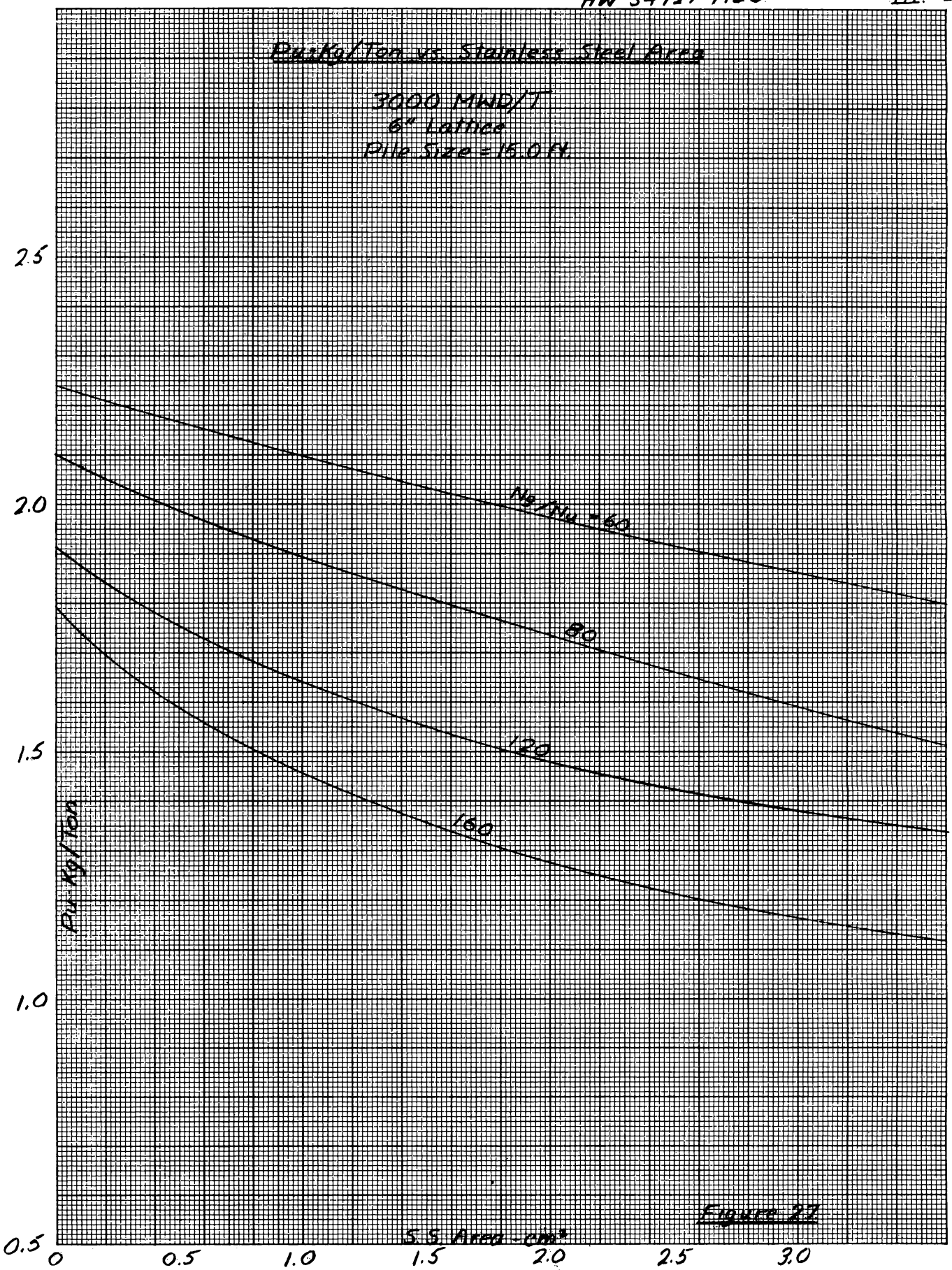
Pu:Kg/Ton vs. Stainless Steel Area
3000 MWD/T
6" Lattice
Pile Size = 15.0 ft.
Ng/Nu = 60
80
120
160
Pu Kg/Ton
S.S. Area - cm²
2.5
2.0
1.5
1.0
0.5
0
0.5
1.0
1.5
2.0
2.5
3.0

Figure 27

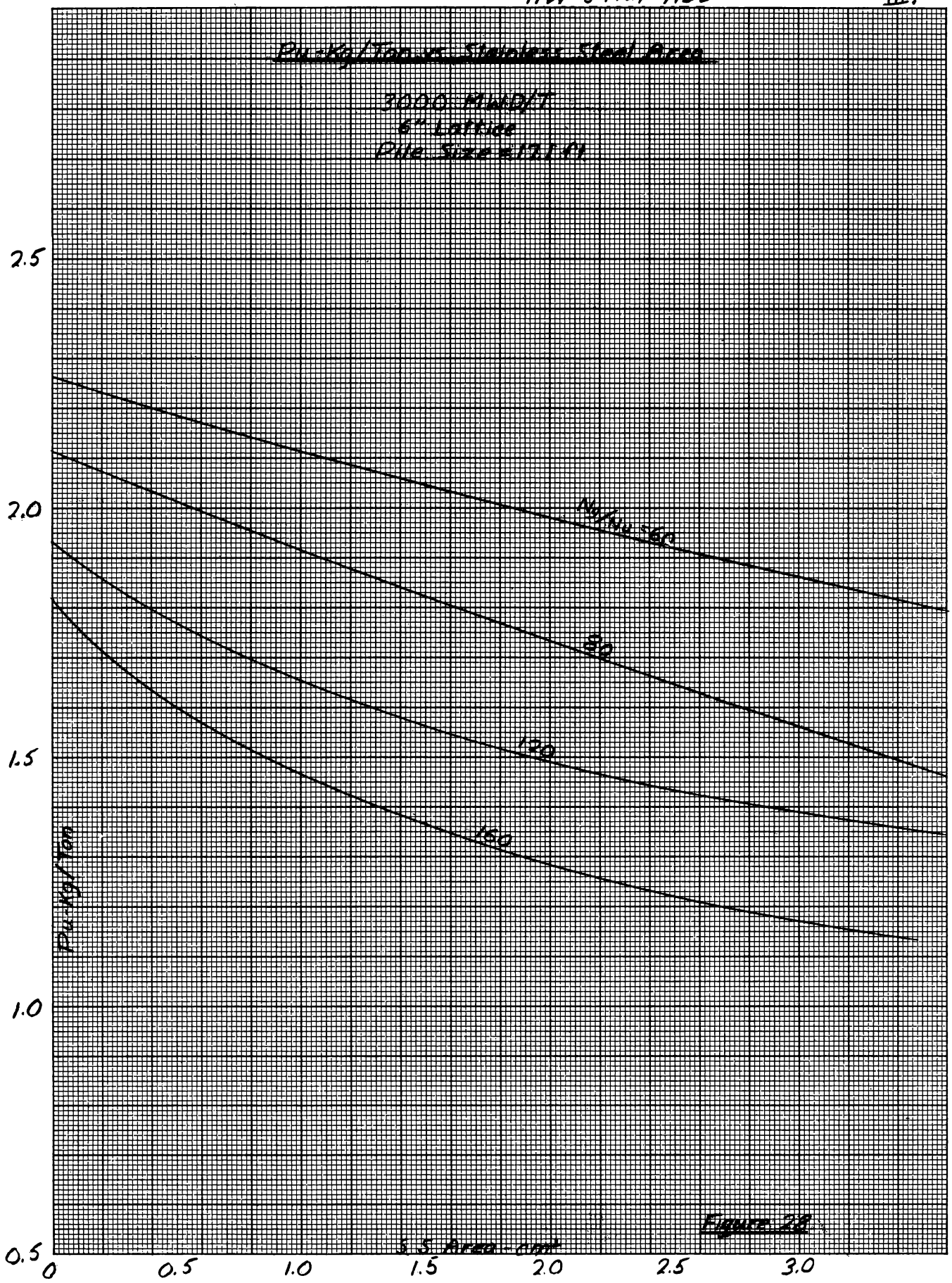
Pu-Kg/Ton vs Stainless Steel Area
3000 MWD/T
6" Lattice
Pile Size = 12.1 ft
Ng/Nu = 60
80
120
160
Pu-Kg/Ton
S.S. Area - cm²
2.5
2.0
1.5
1.0
0.5
0
0.5
1.0
1.5
2.0
2.5
3.0

Figure 28

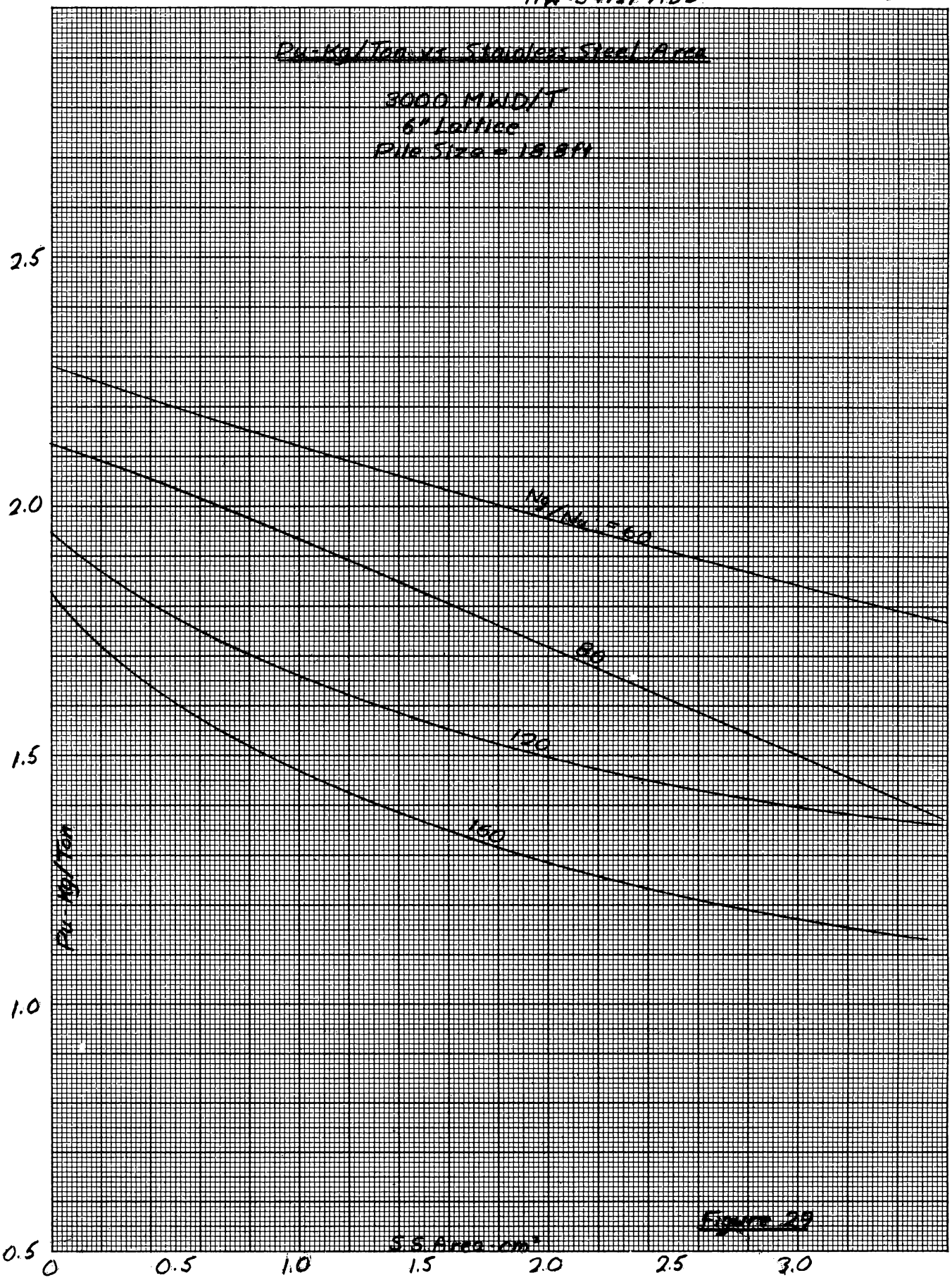
Pu-Kg/Ton-xt. Stainless Steel Area
3000 MWD/T
6" Lattice
Pile Size = 18.8 ft
Pu Kg/Ton
2.5
2.0
1.5
1.0
0.5
0
0.5
1.0
1.5
2.0
2.5
3.0
S.S. Area - cm²
Na/Na = 60
60
120
180

Figure 29

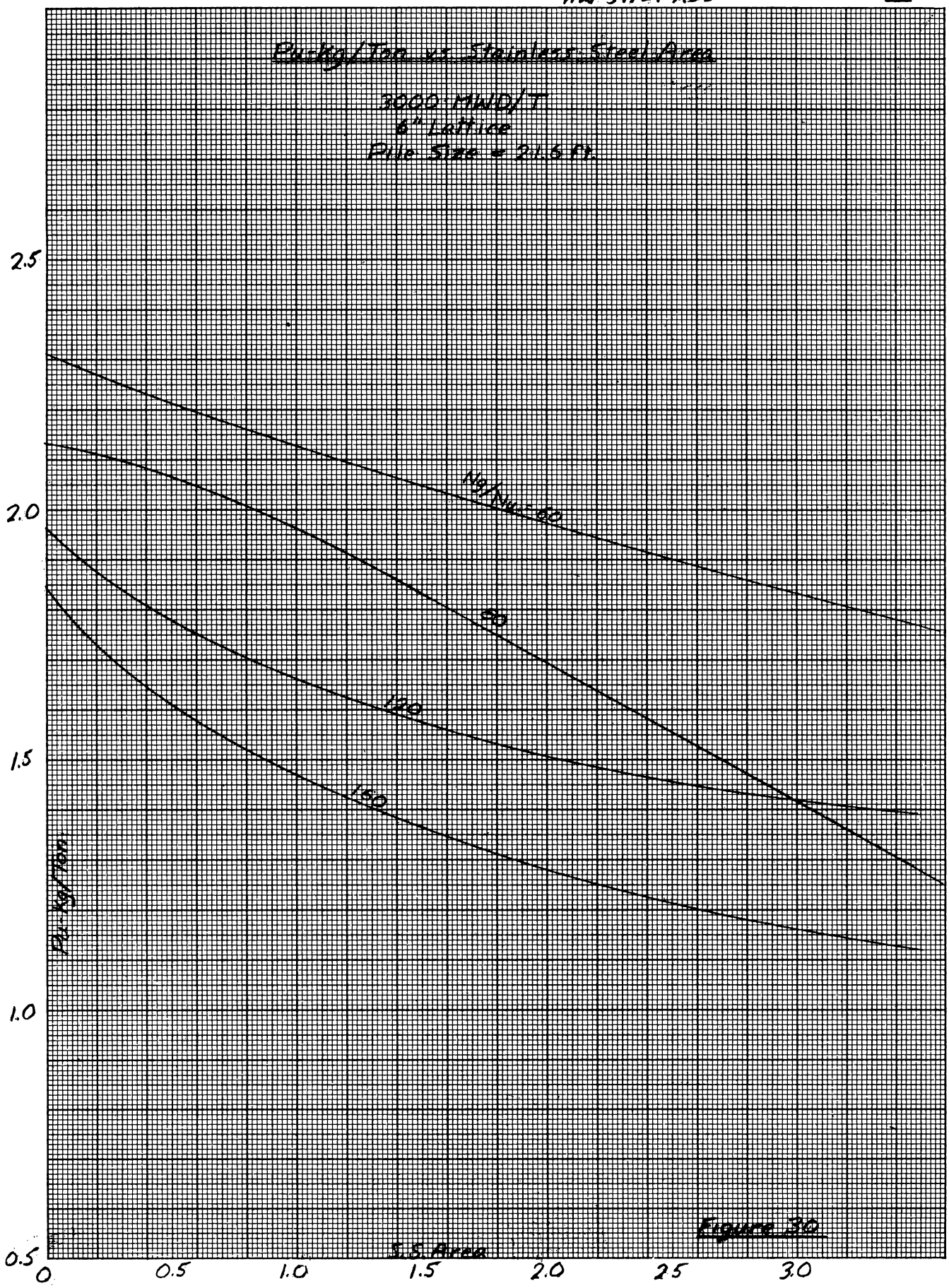

Pu-240 Ton vs. Stainless Steel Area

3000 MWD/T
6" Lattice
Pile Size = 21.6 ft.

Figure 30

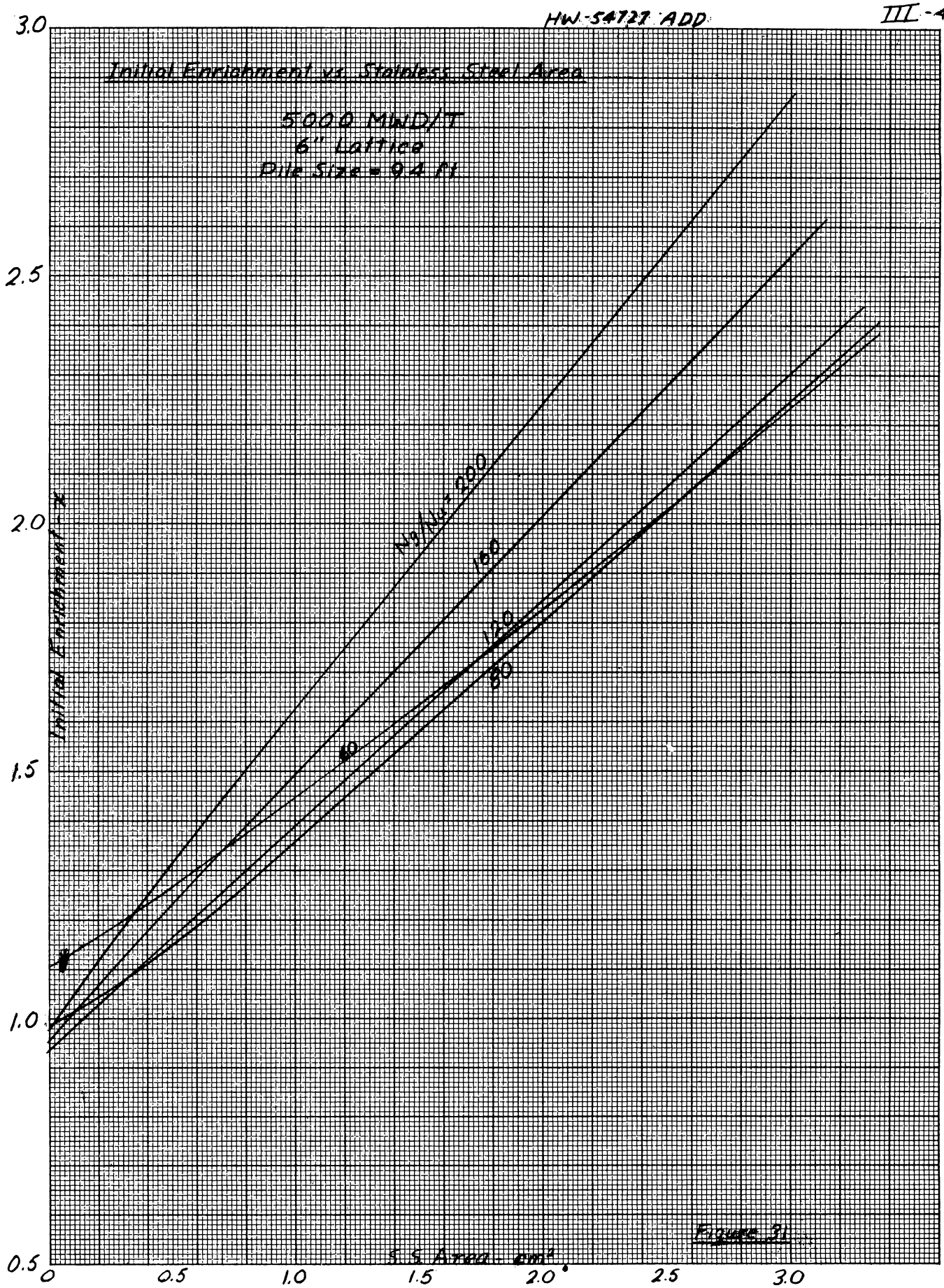
Initial Enrichment vs. Stainless Steel Area
5000 MWD/T
6" Lattice
Pile Size = 9.4 ft
Ng/Nu = 200
160
120
80
60
Initial Enrichment - x
S.S. Area - cm²
3.0
2.5
2.0
1.5
1.0
0.5
0
0.5
1.0
1.5
2.0
2.5
3.0

Figure 31

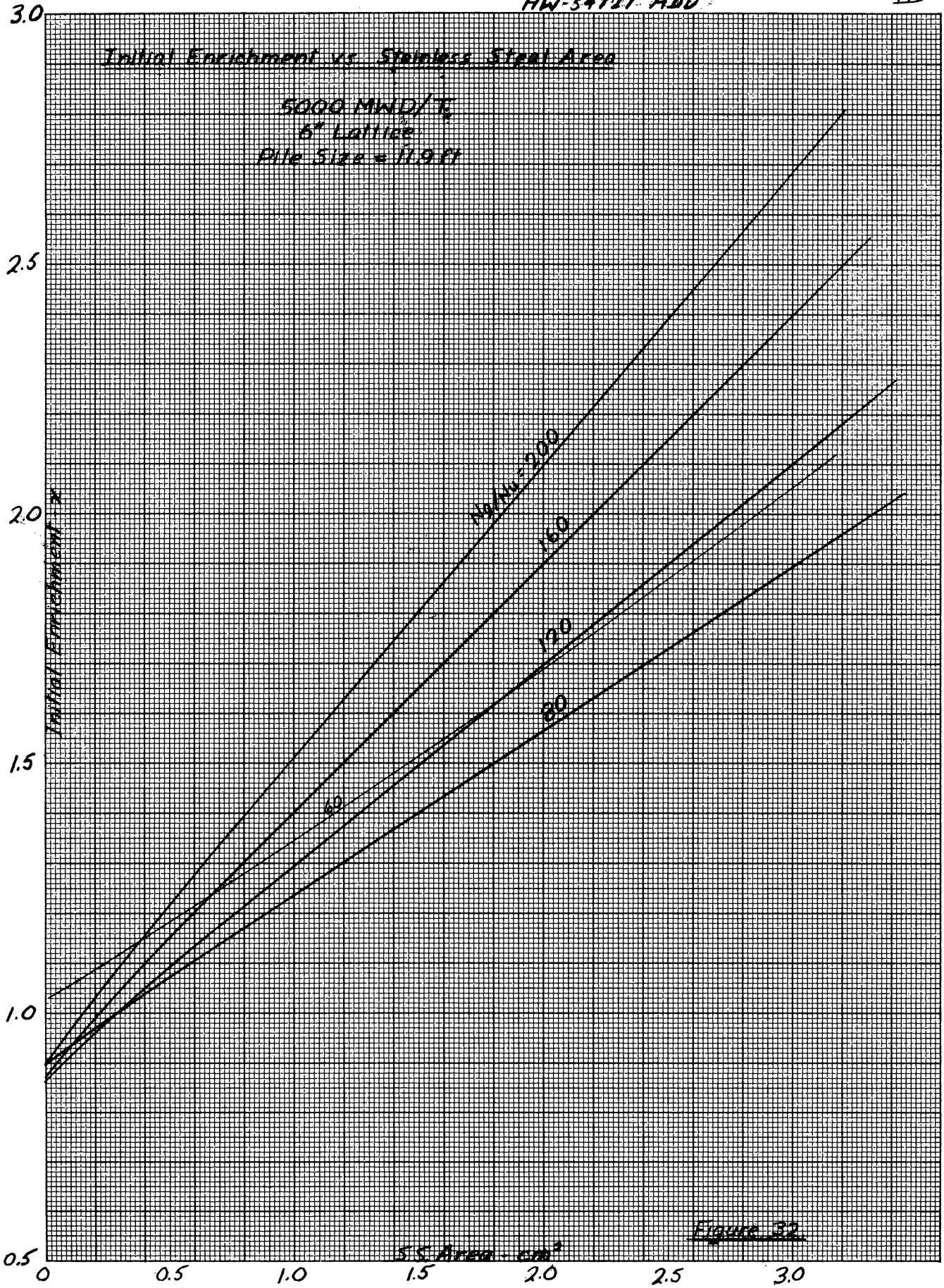
Initial Enrichment vs. Stainless Steel Area
5000 MWD/T
6" Lattice
Pile Size = 11.9 ft
Ng/Nu = 200
160
120
80
60
Initial Enrichment x
S.S. Area - cm²
3.0
2.5
2.0
1.5
1.0
0.5
0
0.5
1.0
1.5
2.0
2.5
3.0

Figure 32

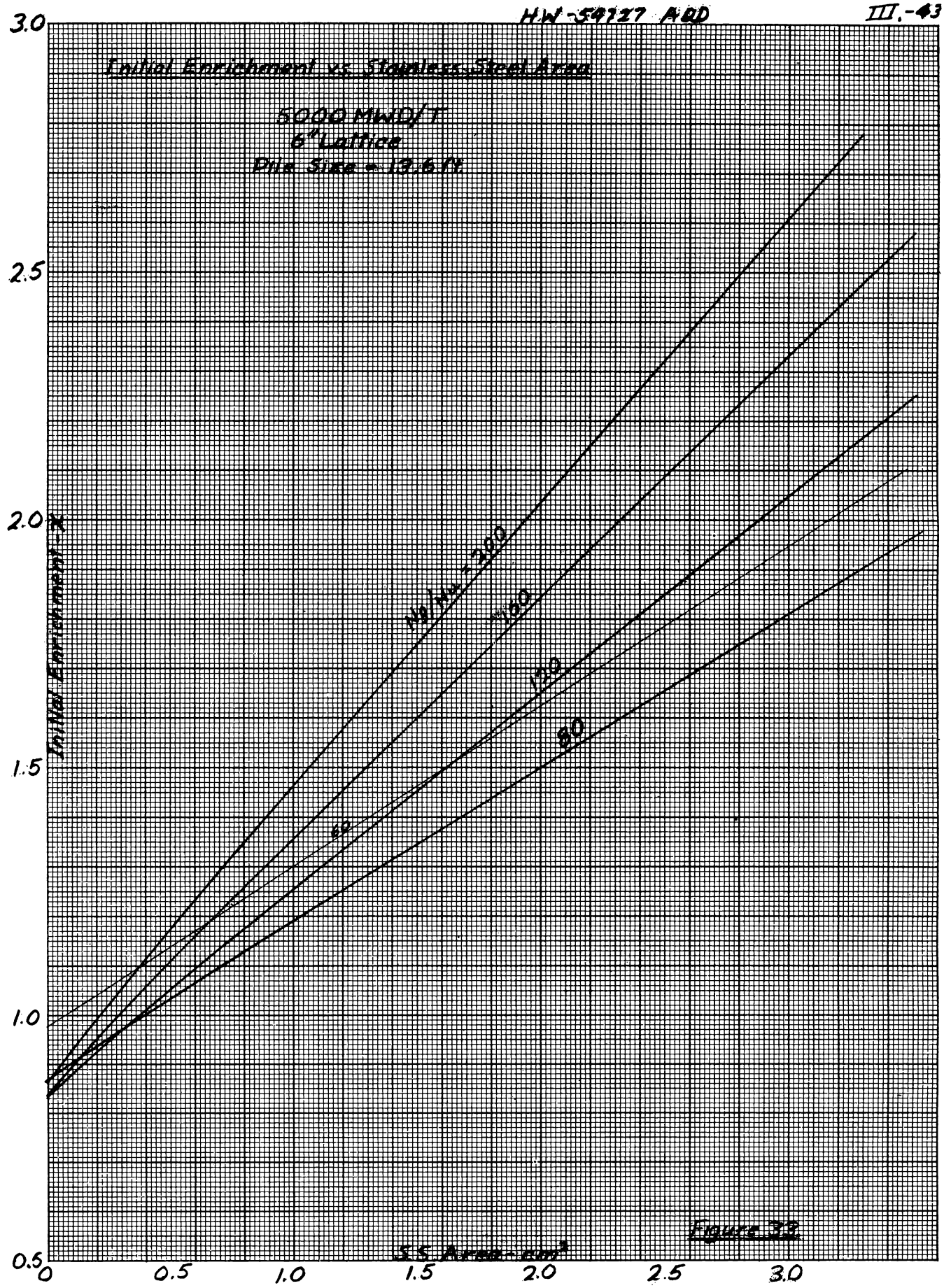
Initial Enrichment vs. Stainless Steel Area
5000 MWD/T
6" Lattice
Pile Size = 12.6 ft.
Initial Enrichment - %
SS Area - cm²
3.0
2.5
2.0
1.5
1.0
0.5
0
0.5
1.0
1.5
2.0
2.5
3.0
200
150
120
90
60

Figure 32

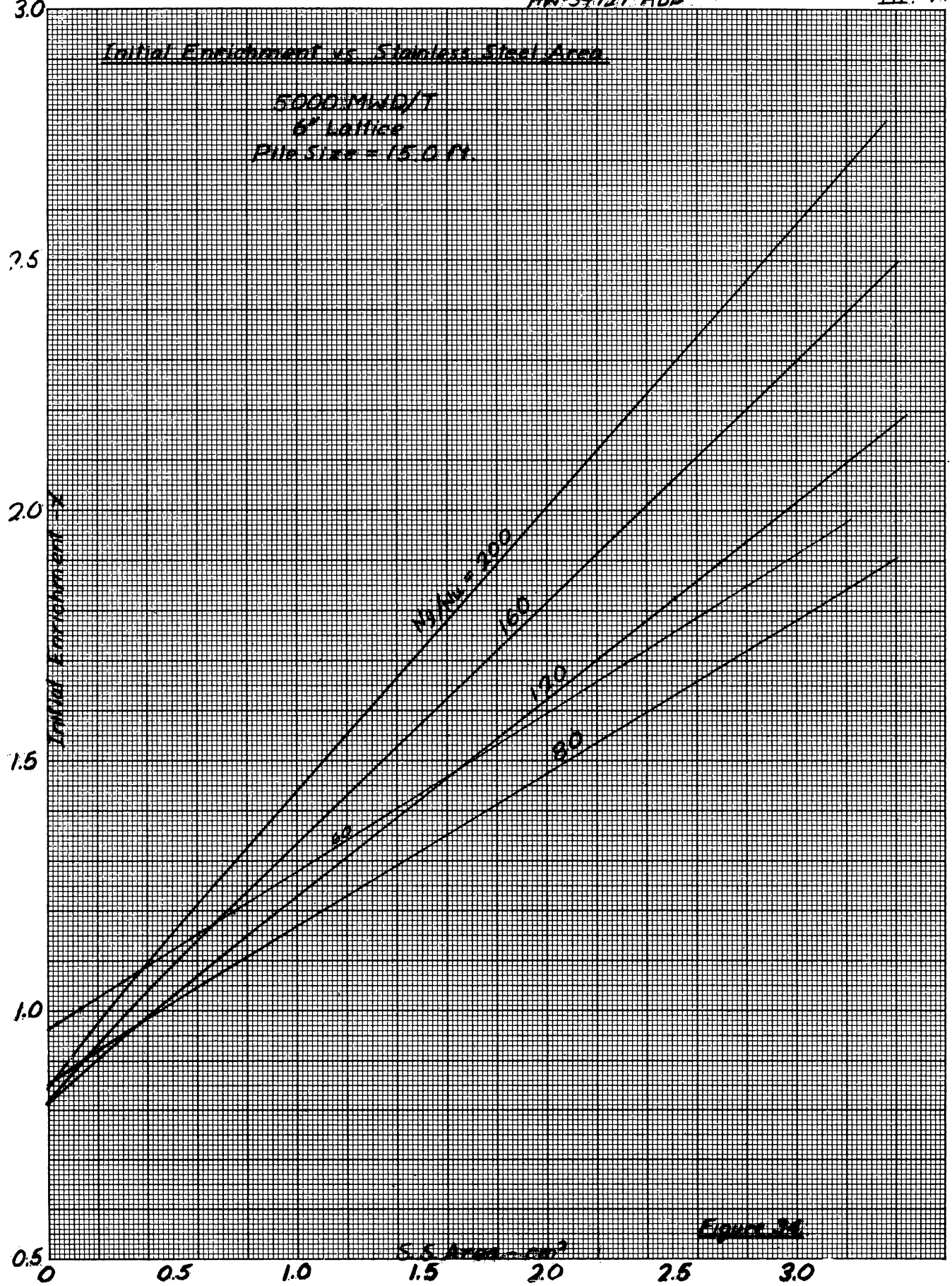
Initial Enrichment vs. Stainless Steel Area
5000 MWD/T
6" Lattice
Pile Size = 15.0 ft.
MWD/T = 200
160
120
80
40
Initial Enrichment, w/o
S.S. Area - cm²
3.0
2.5
2.0
1.5
1.0
0.5
0
0.5
1.0
1.5
2.0
2.5
3.0

Figure 24

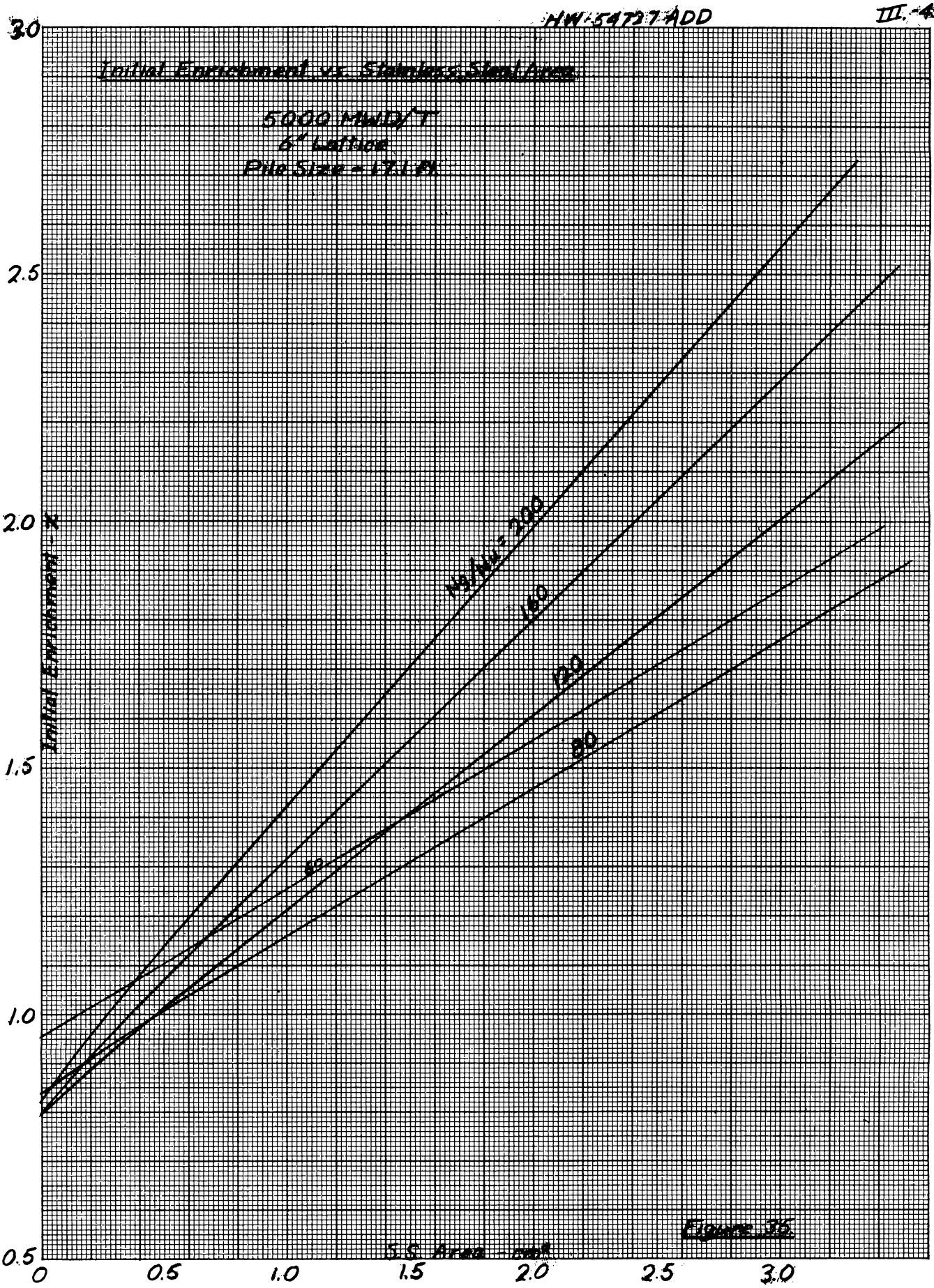
Initial Enrichment vs. Stainless Steel Area
5000 MWD/T
6" Lattice
Pile Size = 17.1 ft
Initial Enrichment - w/o
S.S. Area - cm²
0
0.5
1.0
1.5
2.0
2.5
3.0
0.5
1.0
1.5
2.0
2.5
3.0
200
150
100
80
60

Figure 36

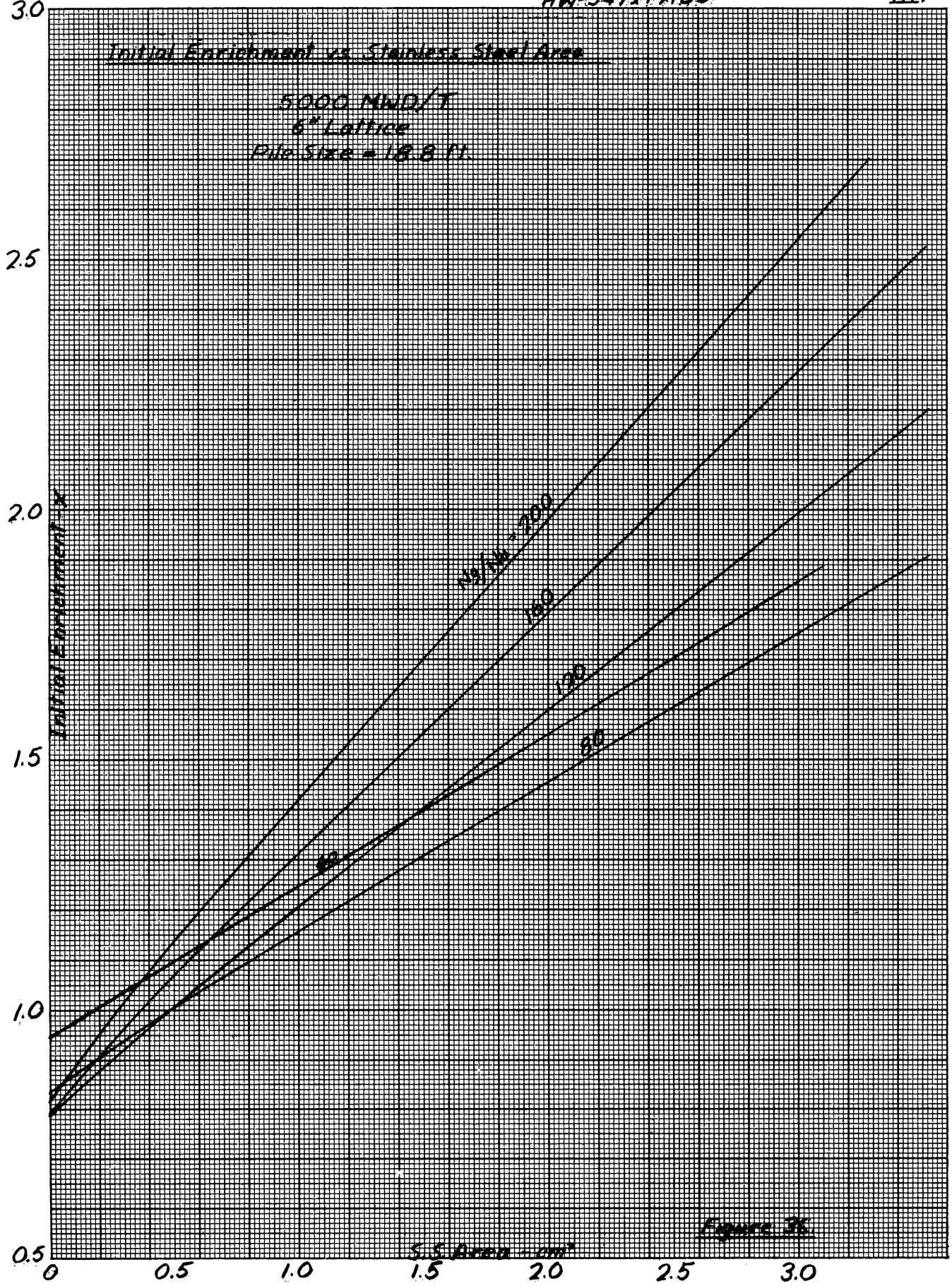
Initial Enrichment vs Stainless Steel Area
5000 MWD/T
6" Lattice
Pile Size = 18.8 ft.
Initial Enrichment - x
S.S. Area - cm²
3.0
2.5
2.0
1.5
1.0
0.5
0
0.5
1.0
1.5
2.0
2.5
3.0
400
300
200
100
60

Figure 36.

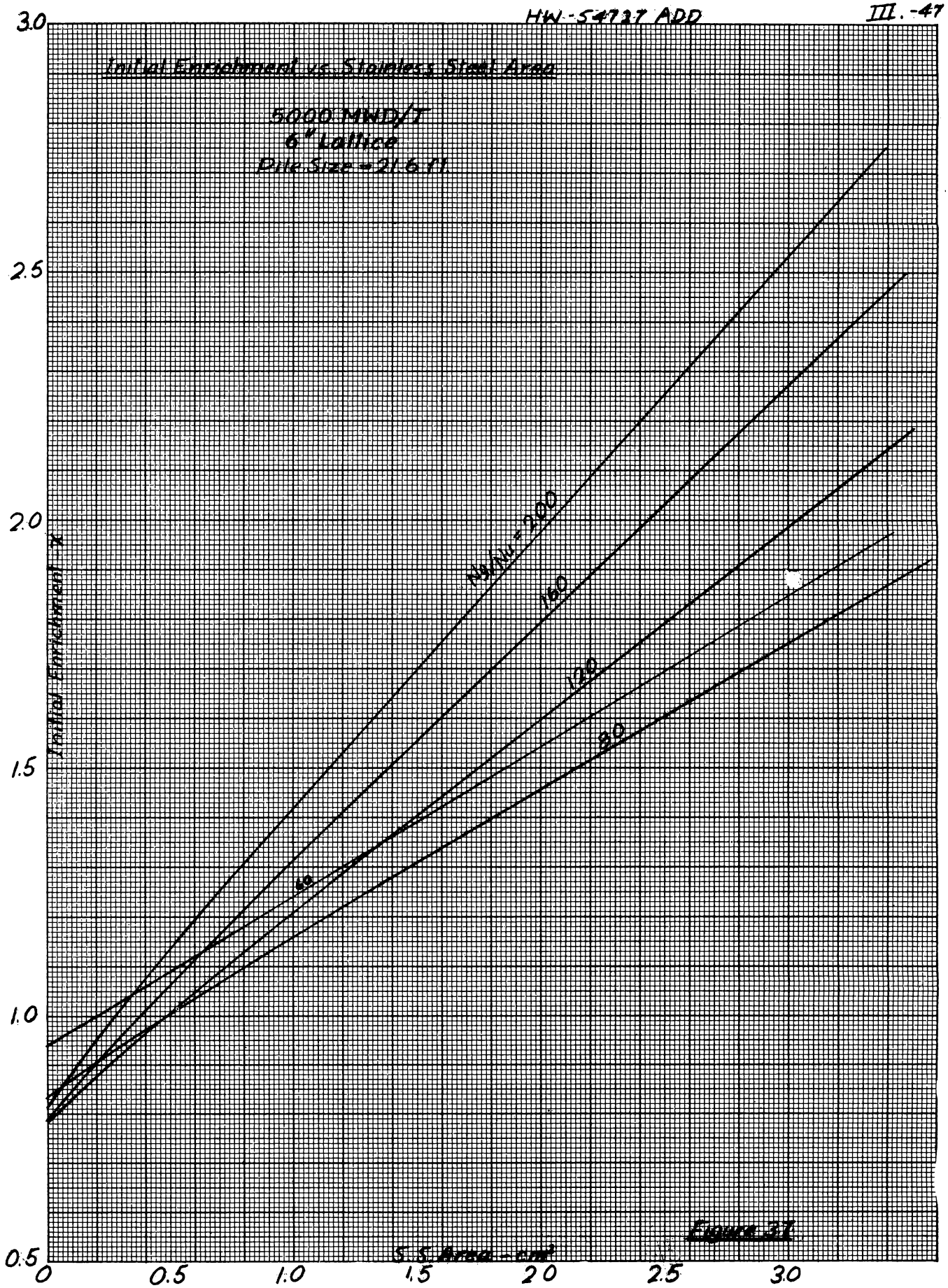
Initial Enrichment vs. Stainless Steel Area
5000 MWD/T
6" Lattice
Pile Size = 21.6 ft.
Ng/Nu = 200
160
120
80
60
Initial Enrichment - x
S.S. Area - cm²
3.0
2.5
2.0
1.5
1.0
0.5
0
0.5
1.0
1.5
2.0
2.5
3.0

Figure 37

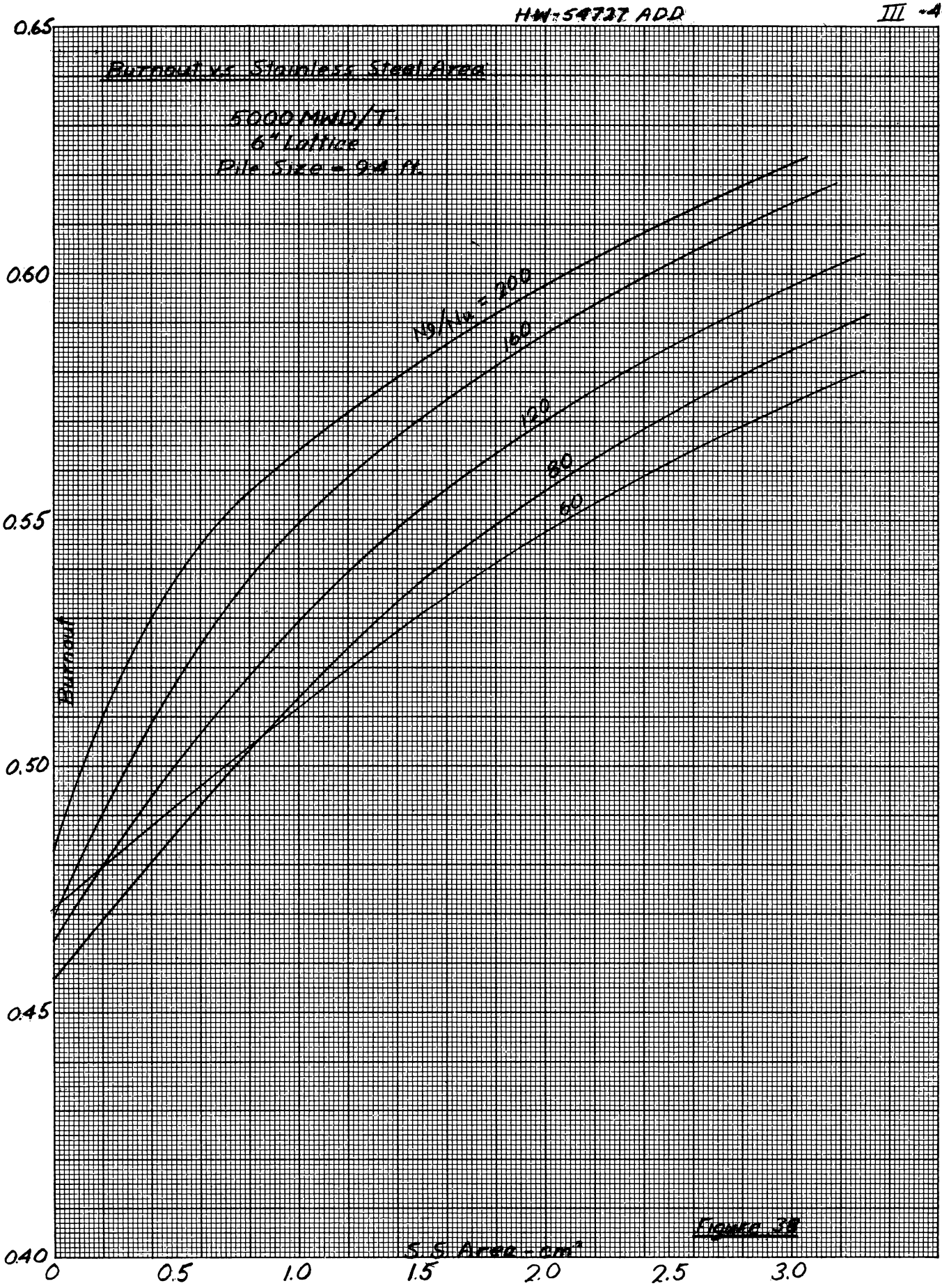
Burnout vs. Stainless Steel Area
5000 MWD/T
6" Lattice
Pile Size = 9.4 ft.
kw/ft = 200
180
120
80
60
Burnout
0.65
0.60
0.55
0.50
0.45
0.40
0
0.5
1.0
1.5
2.0
2.5
3.0
S.S. Area - cm²

Figure 38

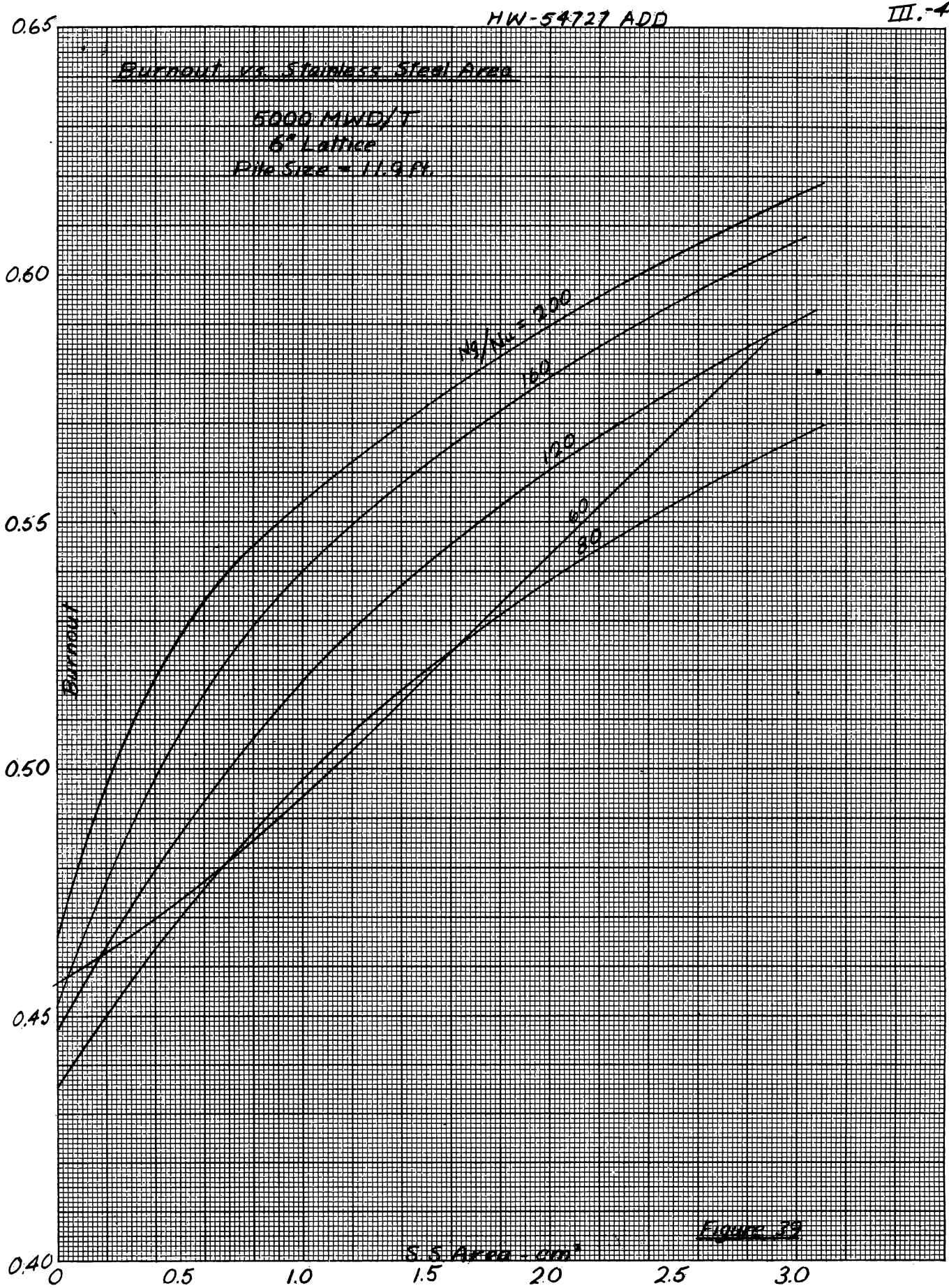
Burnout vs. Stainless Steel Area
5000 MWD/T
6" Lattice
Pile Size = 11.9 ft.
Ng/Nu = 200
160
120
60
80
Burnout
S.S. Area - cm²
0.65
0.60
0.55
0.50
0.45
0.40
0
0.5
1.0
1.5
2.0
2.5
3.0

Figure 39

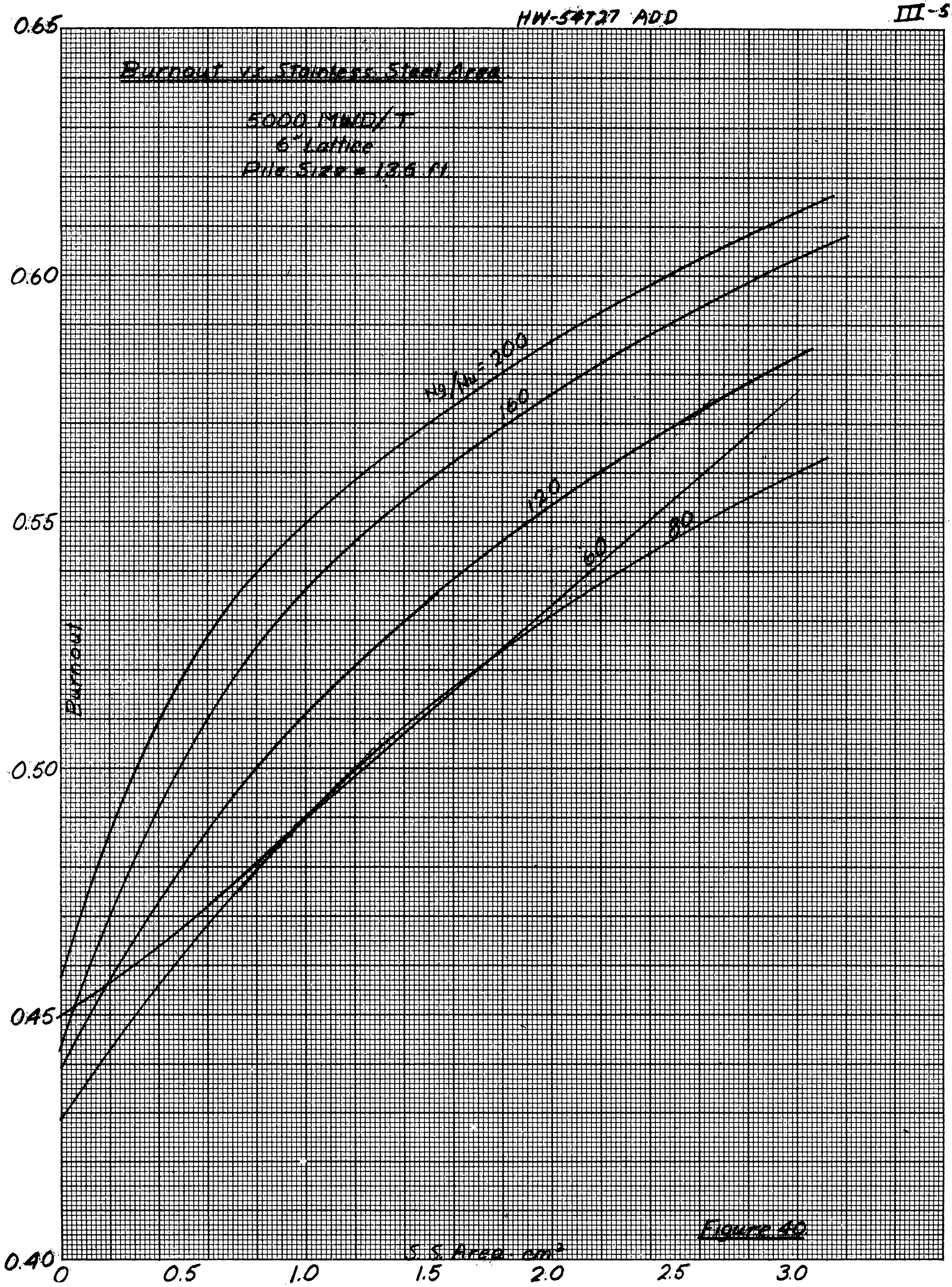
Burnout vs. Stainless Steel Area
5000 MWD/T
6" Lattice
Pile Size = 13.6 ft
kg/hr-ft² 300
200
100
80
60
Burnout
0.65
0.60
0.55
0.50
0.45
0.40
0
0.5
1.0
1.5
2.0
2.5
3.0
S.S. Area cm²

Figure 60

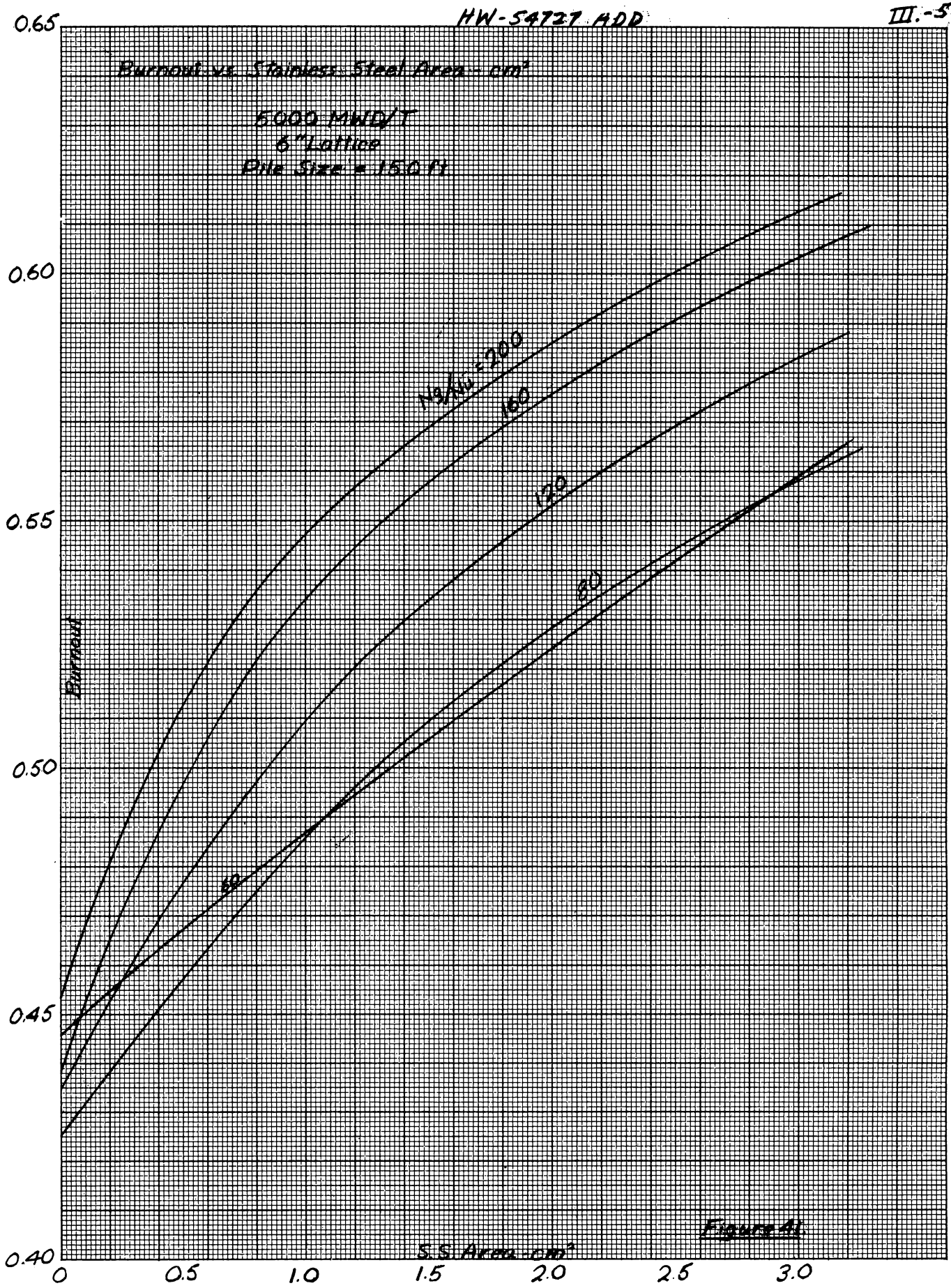
Burnout vs. Stainless Steel Area - cm²
5000 MWD/T
6" Lattice
Pile Size = 15.0 ft
MW/Ft = 200
160
120
80
60
Burnout
0.65
0.60
0.55
0.50
0.45
0.40
0
0.5
1.0
1.5
2.0
2.5
3.0
S.S. Area - cm²

Figure 41

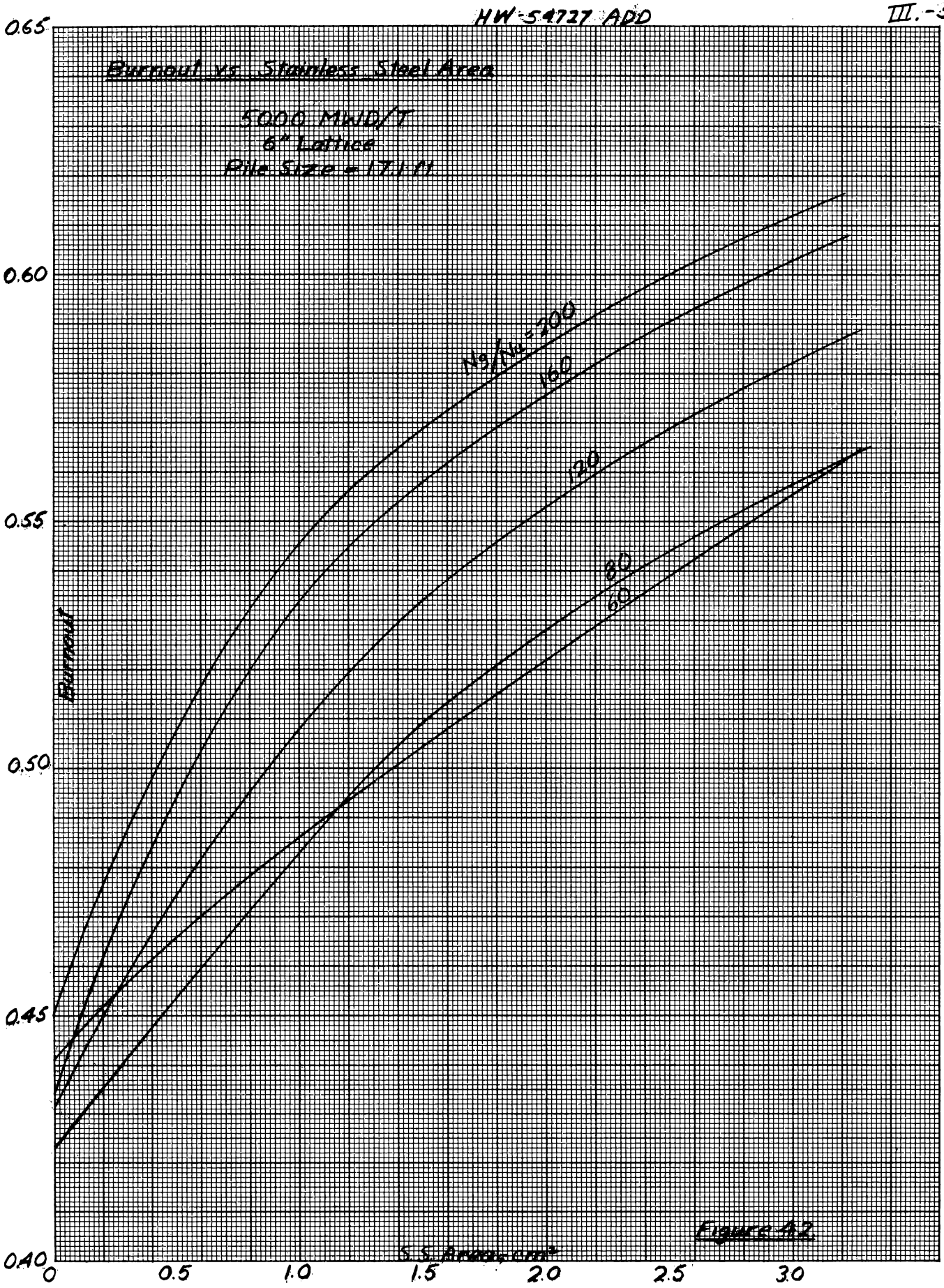
Burnout vs Stainless Steel Area
5000 MWD/T
6" Lattice
Pile Size = 17.1 ft
Ng/Nu = 200
160
120
80
60
Burnout
0.65
0.60
0.55
0.50
0.45
0.40
0
0.5
1.0
1.5
2.0
2.5
3.0
S.S. Area, cm²

Figure 4.2

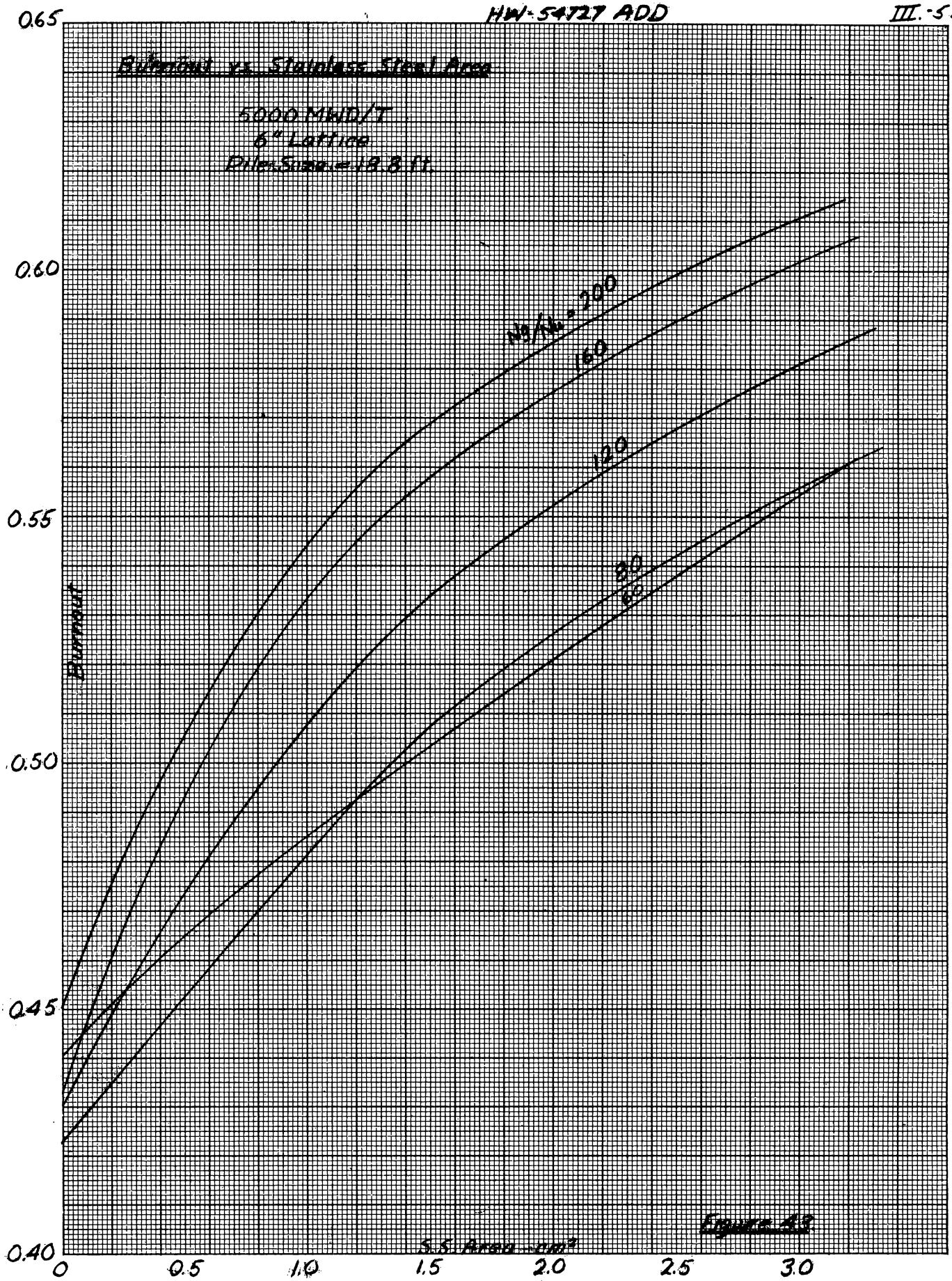
Burnout vs. Stainless Steel Area
5000 MWD/T
6" Lattice
Pile Size = 18.8 ft.
Ng/Nu = 200
160
120
80
60
Burnout
0.65
0.60
0.55
0.50
0.45
0.40
0
0.5
1.0
1.5
2.0
2.5
3.0
S.S. Area - cm²

Figure 43

Burnout vs. Stainless Steel Area

5000 MWD/T
8" Lattice
Pile Size = 216 ft.

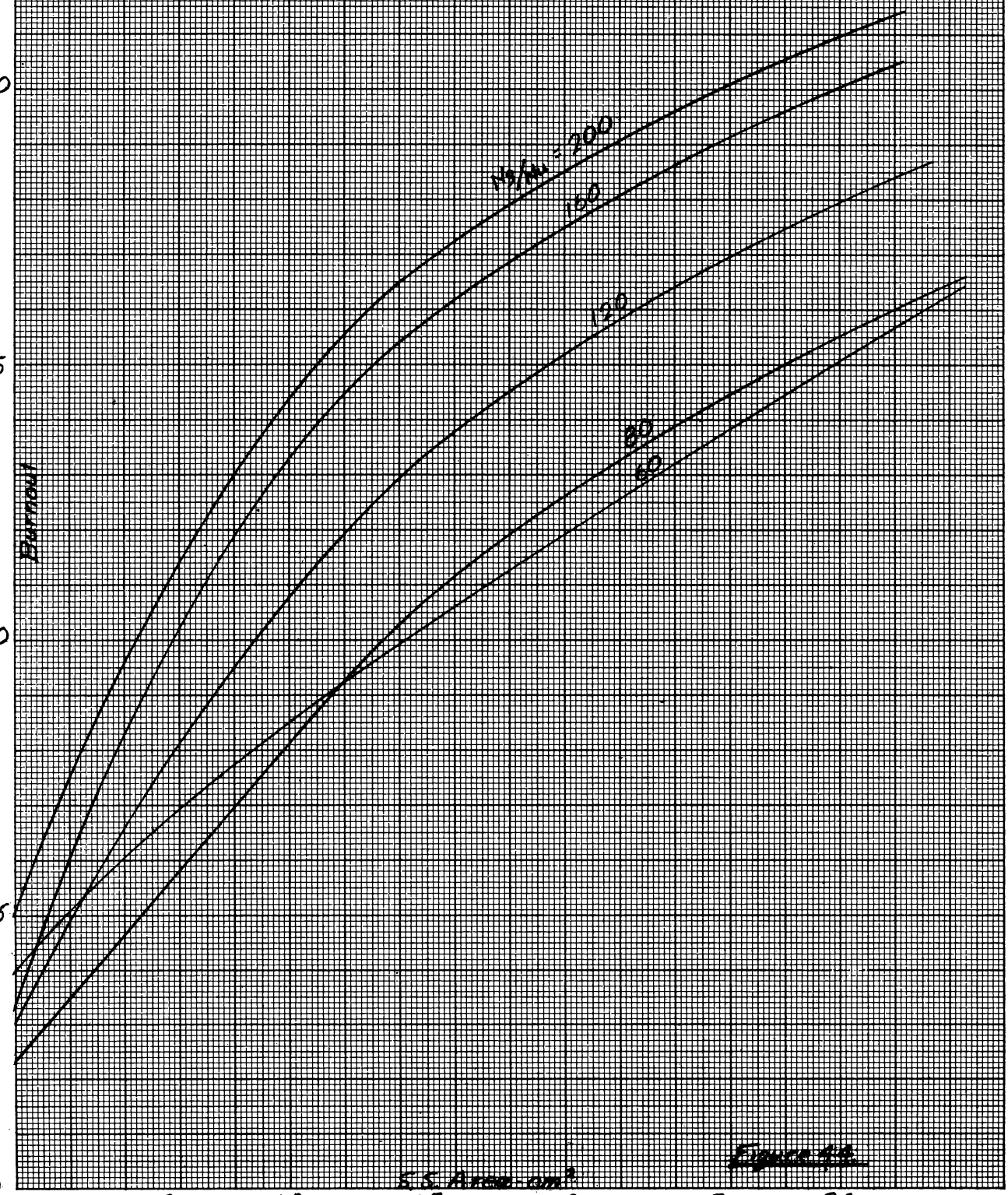

Figure 4.8

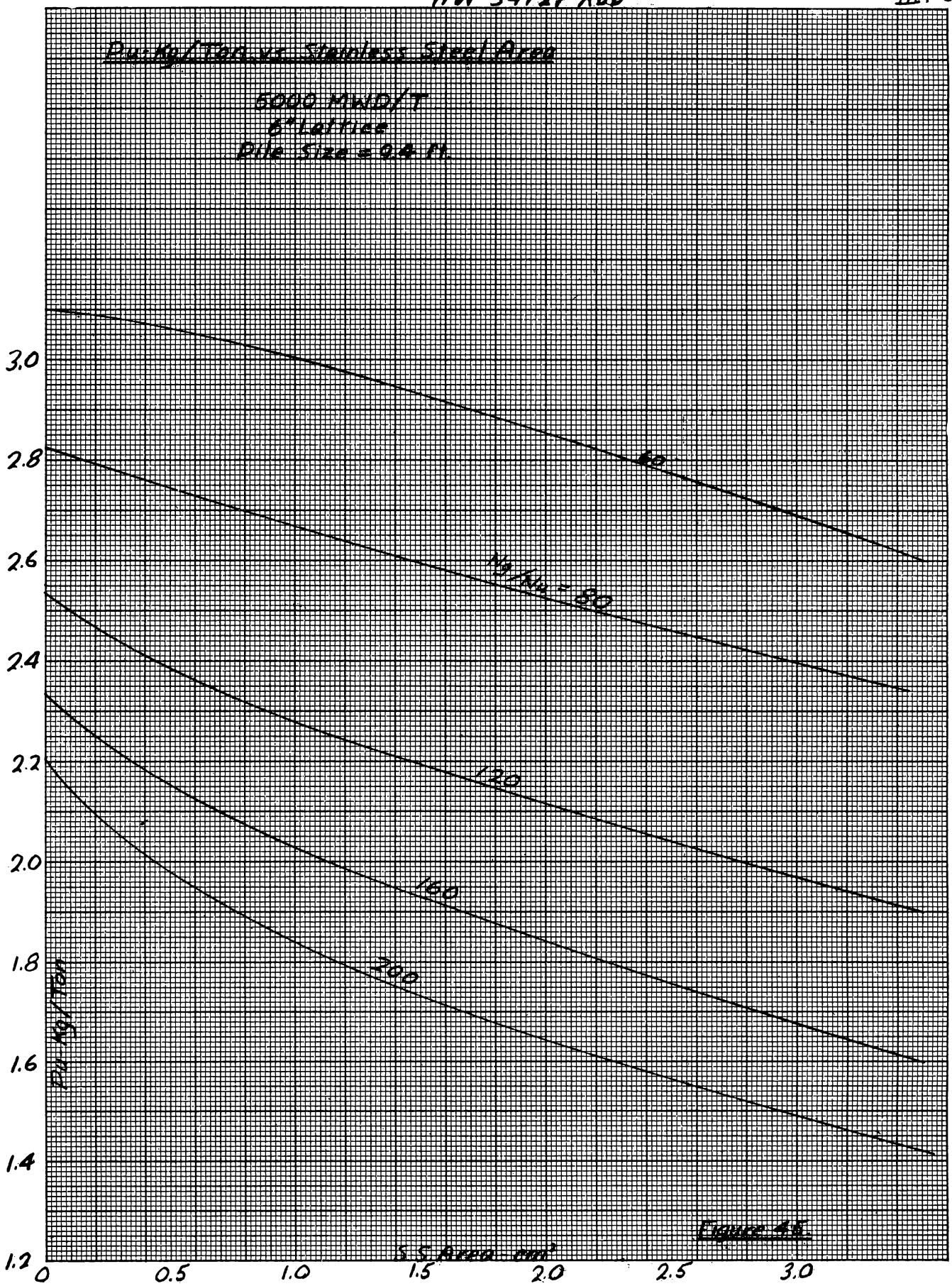
Pu-Kg/Ton vs. Stainless Steel Area
6000 MWD/T
6" Lattice
Pile Size = 0.4 Ft.
3.0
2.8
2.6
2.4
2.2
2.0
1.8
1.6
1.4
1.2
Pu-Kg/Ton
40
80
120
160
200
0
0.5
1.0
1.5
2.0
2.5
3.0
S.S. Area cm²

Figure 4.5

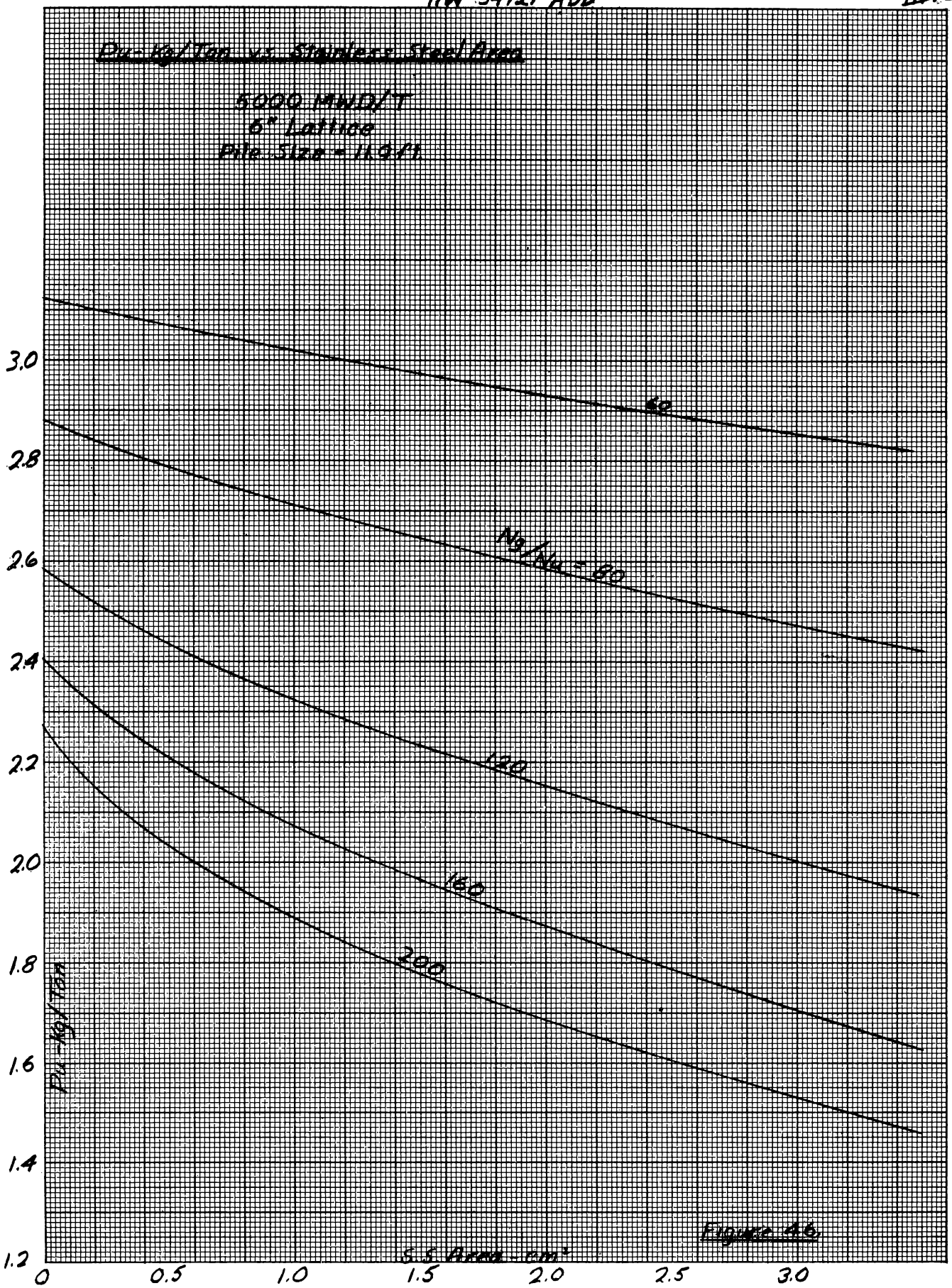
Pu-Kg/Ton vs. Stainless Steel Area
5000 MWD/T
6" Lattice
Pile Size = 11.9 ft.
60
Ng/Nu = 80
120
160
200
Pu-Kg/Ton
S.S. Area - cm²
3.0
2.8
2.6
2.4
2.2
2.0
1.8
1.6
1.4
1.2
0
0.5
1.0
1.5
2.0
2.5
3.0

Figure 46

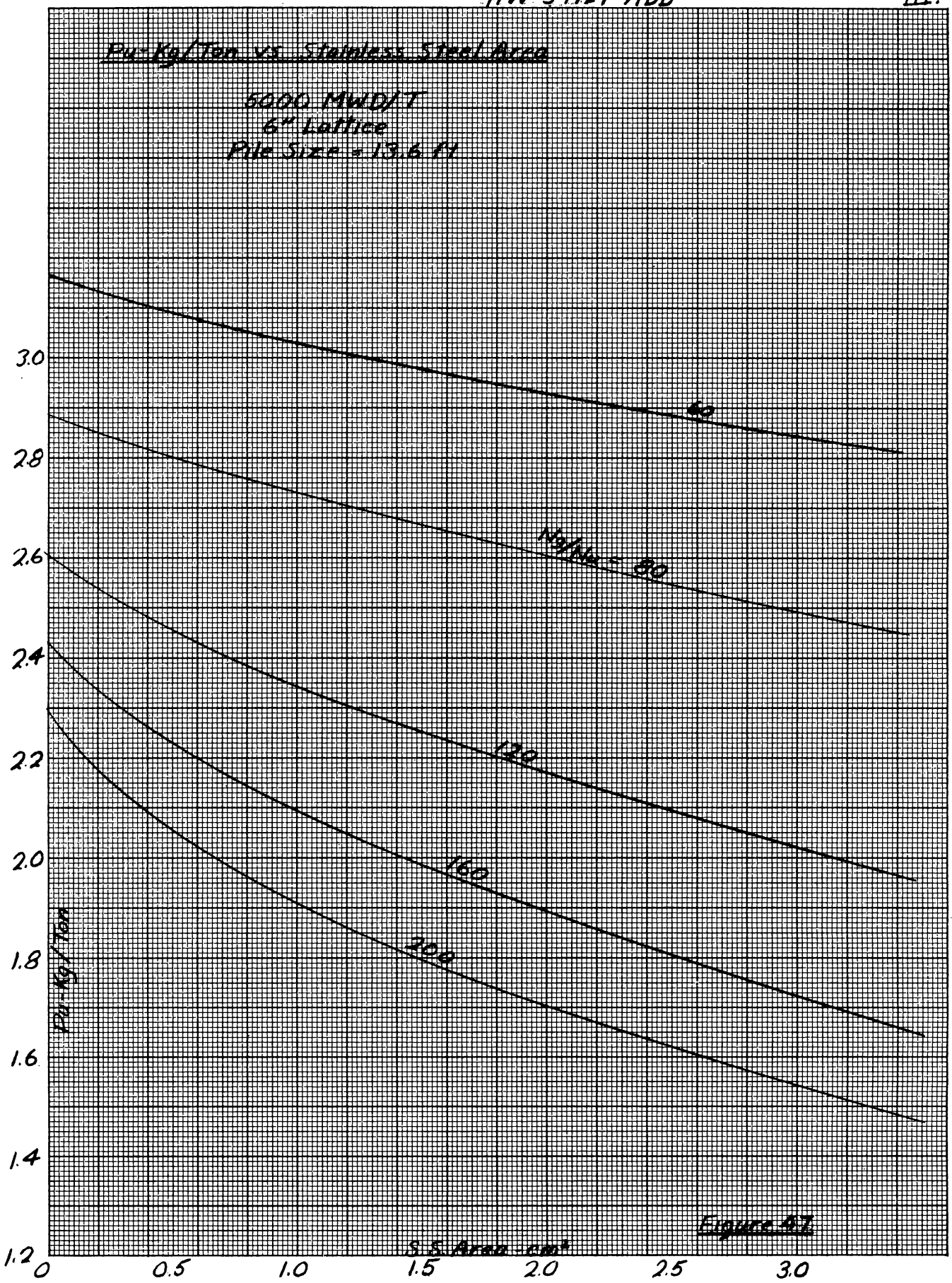
Pu-Kg/Ton vs. Stainless Steel Area
6000 MWD/T
6" Lattice
Pile Size = 13.6 ft
Pu-Kg/Ton
3.0
2.8
2.6
2.4
2.2
2.0
1.8
1.6
1.4
1.2
40
80
120
160
200
0
0.5
1.0
1.5
2.0
2.5
3.0
S.S. Area cm²

Figure A7

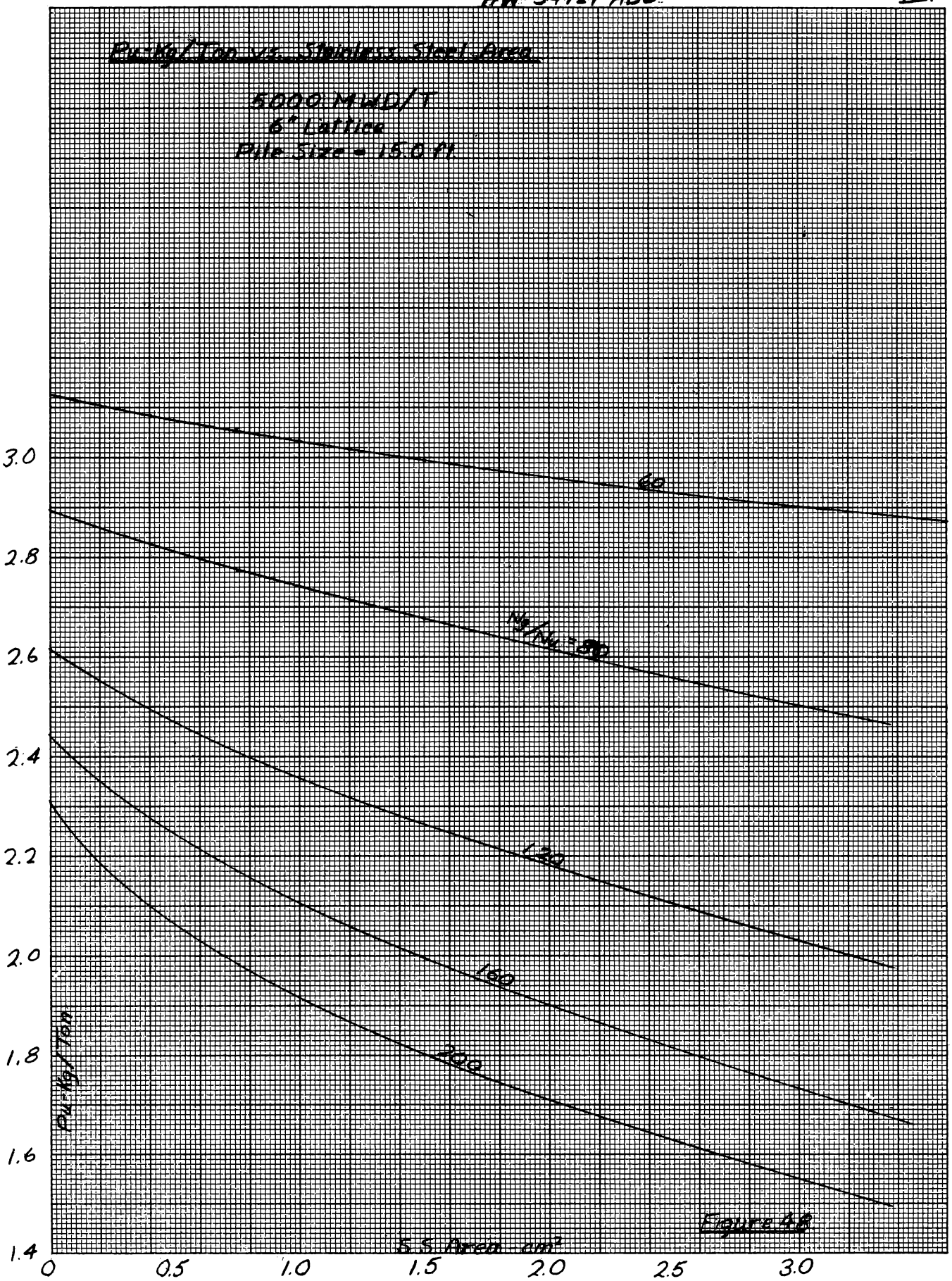
Pu-Kg/Ton vs. Stainless Steel Area
5000 MWD/T
6" Lattice
Pile Size = 15.0 ft
60
Ng/Nu = 80
120
160
200
Pu-Kg/Ton
S.S. Area - cm²
3.0
2.8
2.6
2.4
2.2
2.0
1.8
1.6
1.4
0
0.5
1.0
1.5
2.0
2.5
3.0

Figure 48

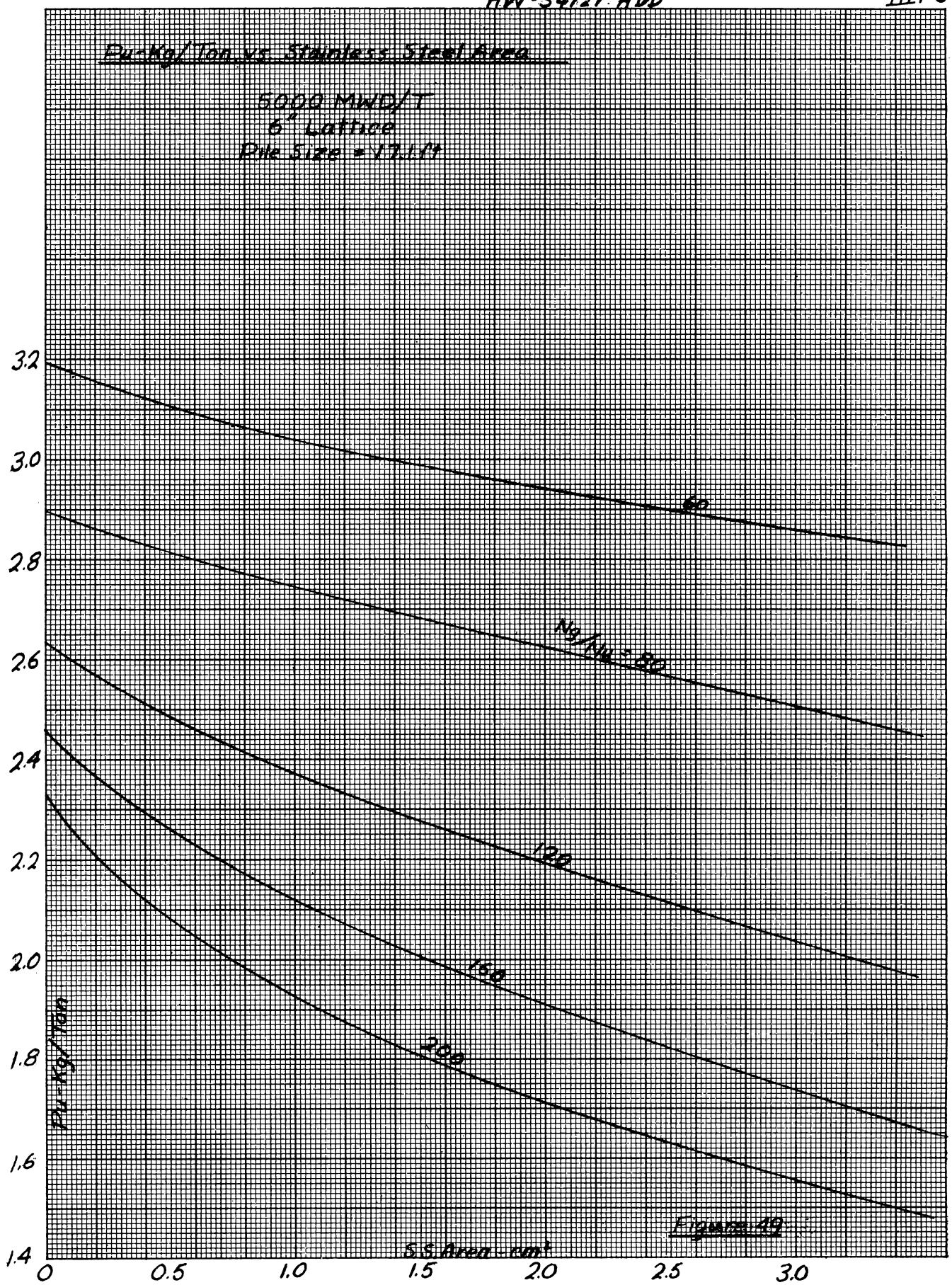
Pu-Kg/Ton vs Stainless Steel Area
5000 MWD/T
6" Lattice
Pile Size = 17.1 ft
60
Ng/Nu = 80
120
160
200
Pu-Kg/Ton
S.S. Area - cm²
3.2
3.0
2.8
2.6
2.4
2.2
2.0
1.8
1.6
1.4
0
0.5
1.0
1.5
2.0
2.5
3.0

Figure 49

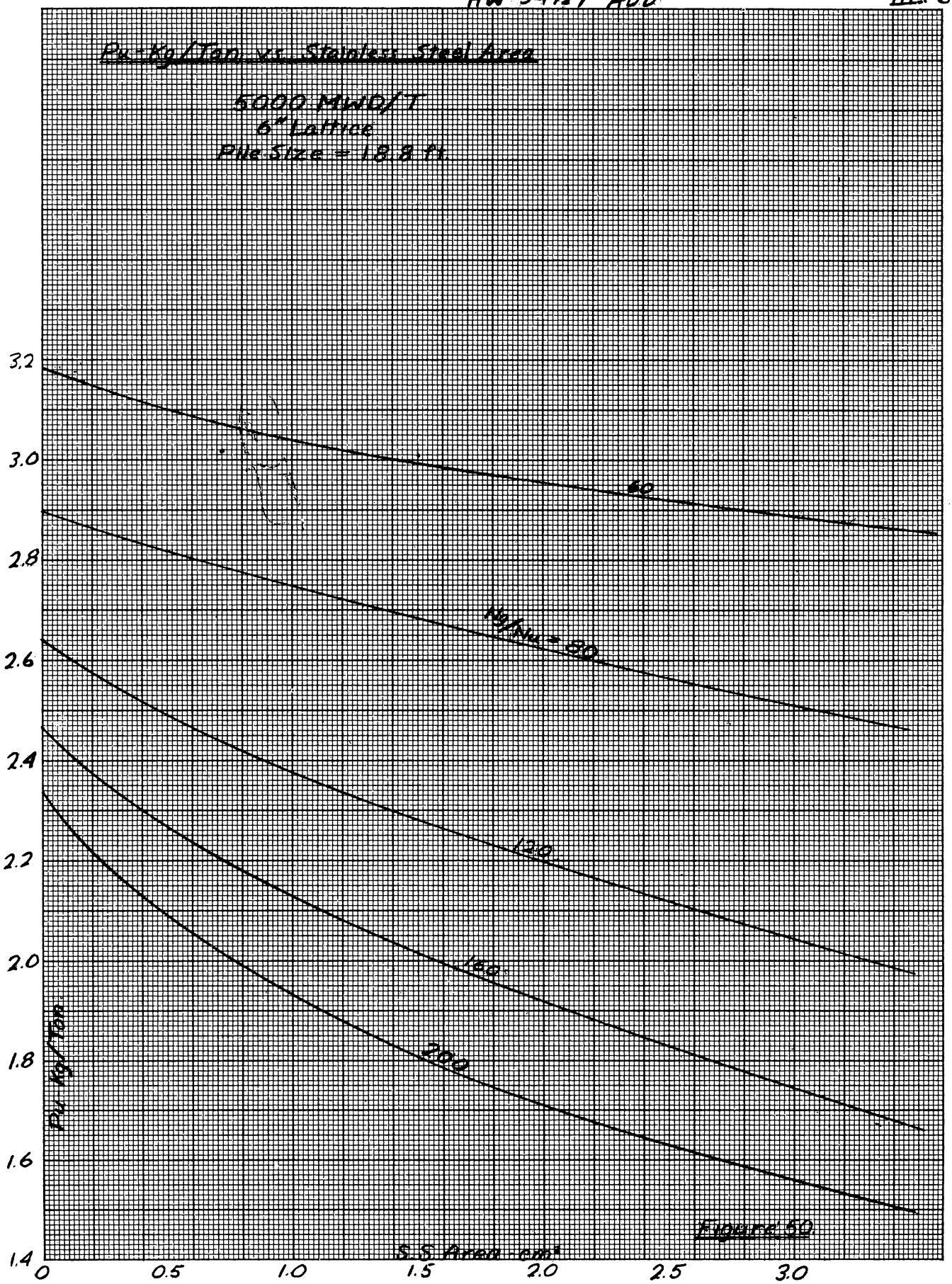
Pu-Kg/Ton vs. Stainless Steel Area
5000 MWD/T
6" Lattice
Pile Size = 18.8 ft.
3.2
3.0
2.8
2.6
2.4
2.2
2.0
1.8
1.6
1.4
Pu Kg/Ton
0
0.5
1.0
1.5
2.0
2.5
3.0
S.S. Area - cm²
40
Mg/Nu = 80
120
160
200

Figure 50

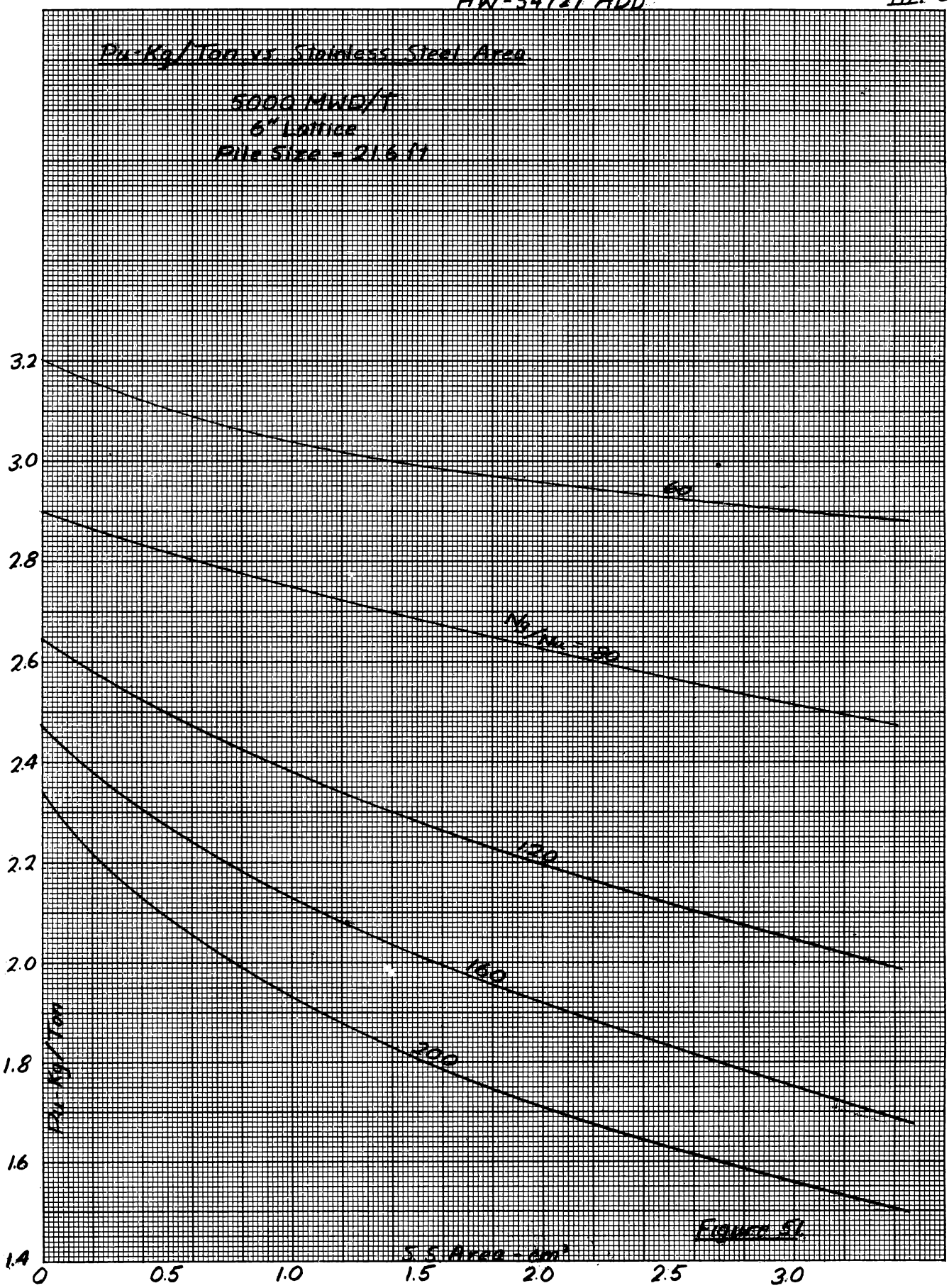
Pu-Kg/Ton vs. Stainless Steel Area
5000 MWD/T
6" Lattice
Pile Size = 21.6 ft
3.2
3.0
2.8
2.6
2.4
2.2
2.0
1.8
1.6
1.4
Pu-Kg/Ton
0
0.5
1.0
1.5
2.0
2.5
3.0
S.S. Area - cm²
60
N6/N4 = 80
120
160
200

Figure 51

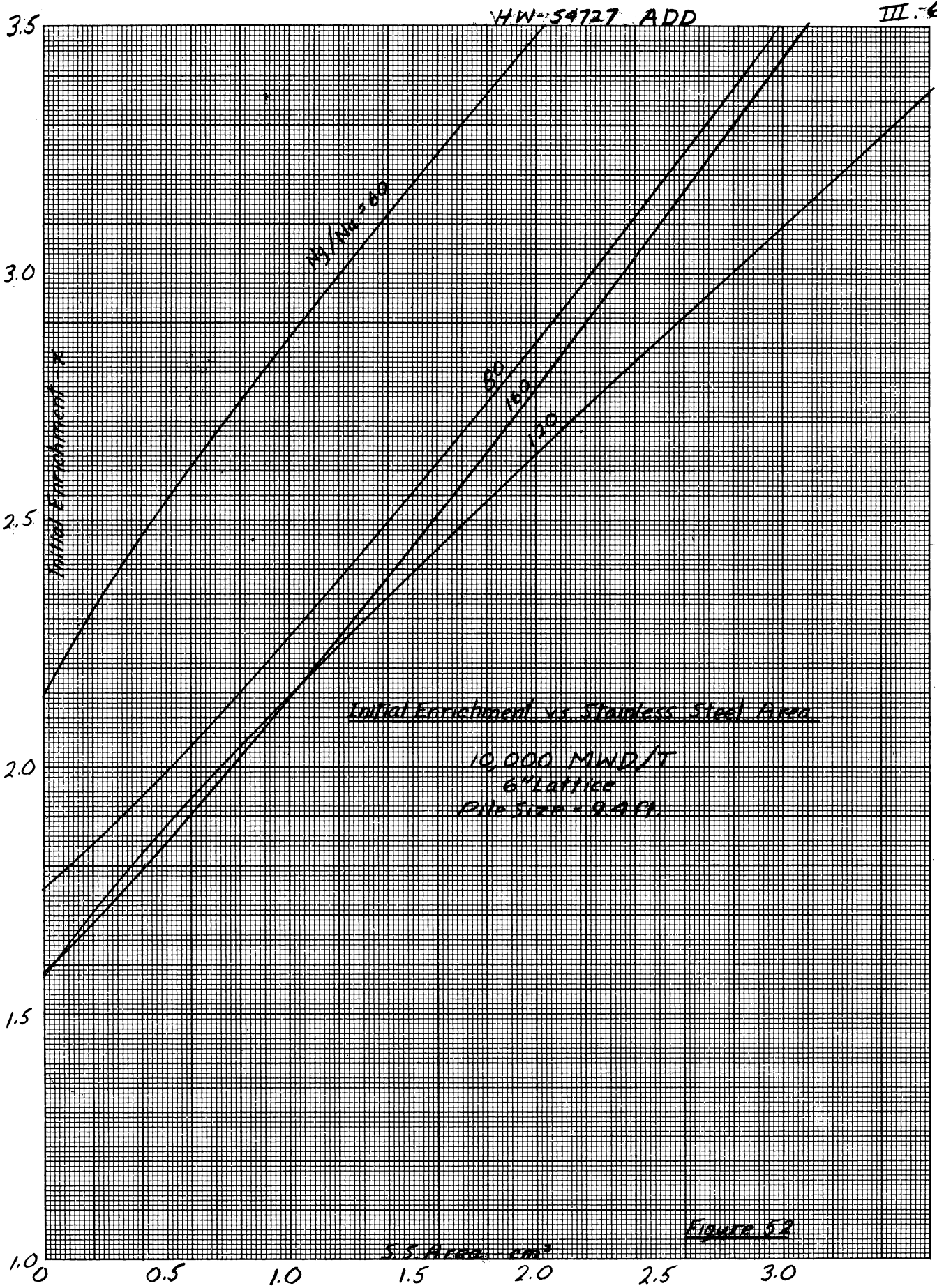
3.5
3.0
2.5
2.0
1.5
1.0
0
0.5
1.0
1.5
2.0
2.5
3.0
Initial Enrichment - %
S.S. Area - cm²
M/Mw = 6.0
6.0
6.0
6.0
Initial Enrichment vs. Stainless Steel Area
10,000 MWD/T
6" Lattice
Pin Size = 0.44"

Figure 5.2

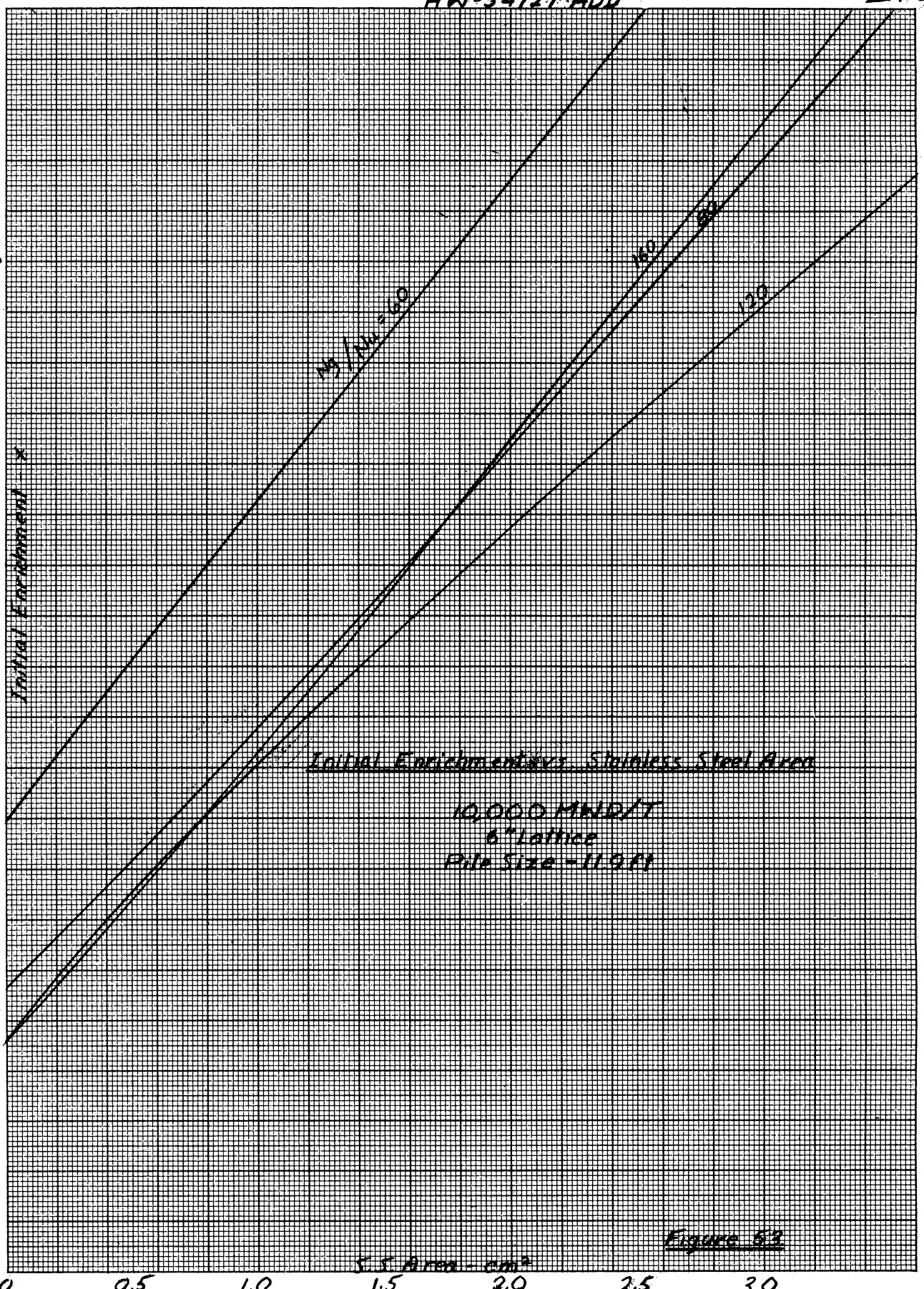
3.5
3.0
2.5
2.0
1.5
1.0
0
0.5
1.0
1.5
2.0
2.5
3.0
Initial Enrichment, w/o
S.S. Area - cm²
Initial Enrichment vs. Stainless Steel Area
10,000 MWD/T
6" Lattice
Pile Size - 11.9 ft
160
120

Figure 53

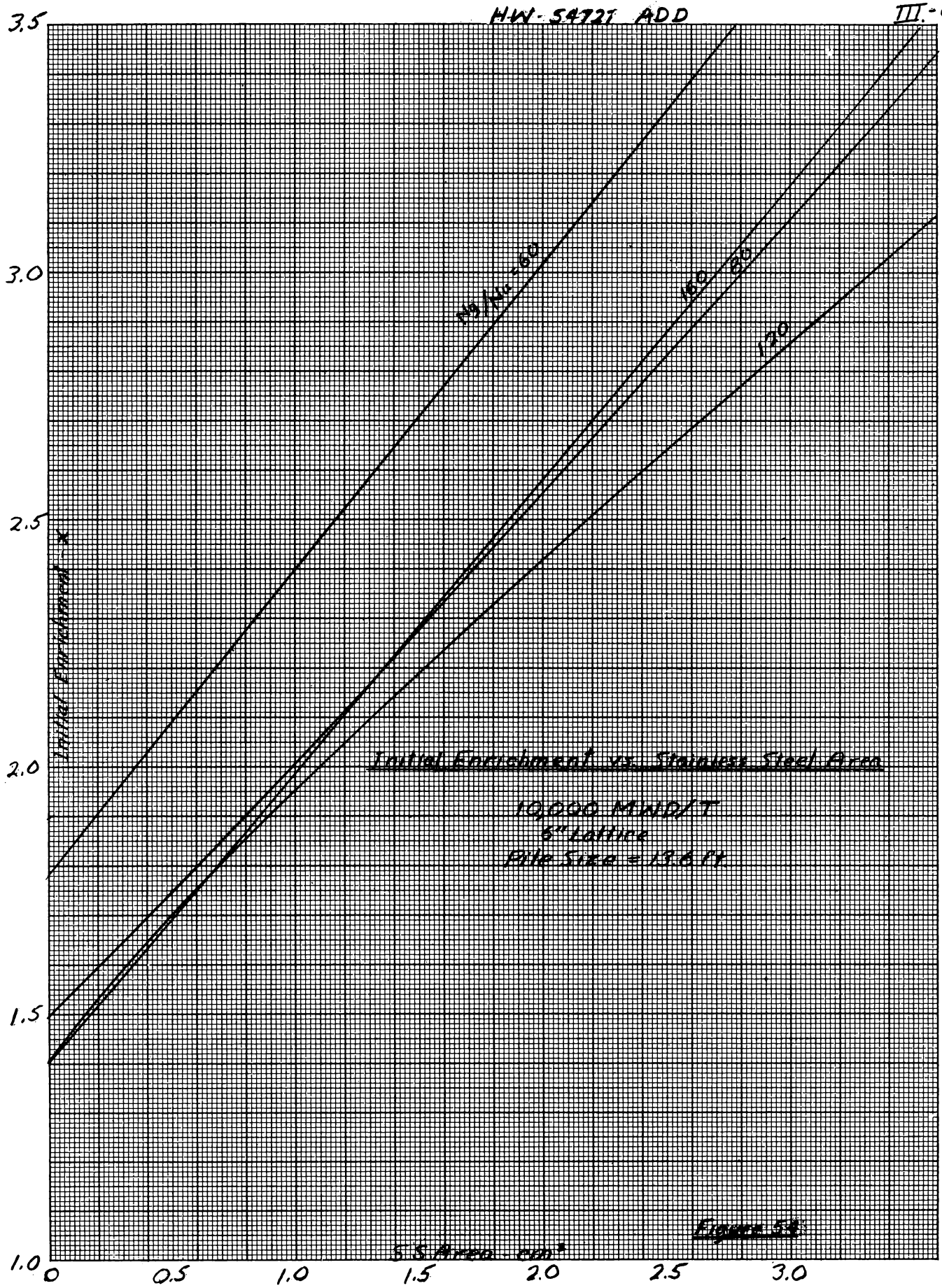
3.5
3.0
2.5
2.0
1.5
1.0
Initial Enrichment - x
0
0.5
1.0
1.5
2.0
2.5
3.0
S.S. Area - cm²
Ng/Nu = 60
160
80
120
Initial Enrichment vs. Stainless Steel Area
10,000 MWD/T
6" Lattice
Pile Size = 13.6 ft.

Figure 54

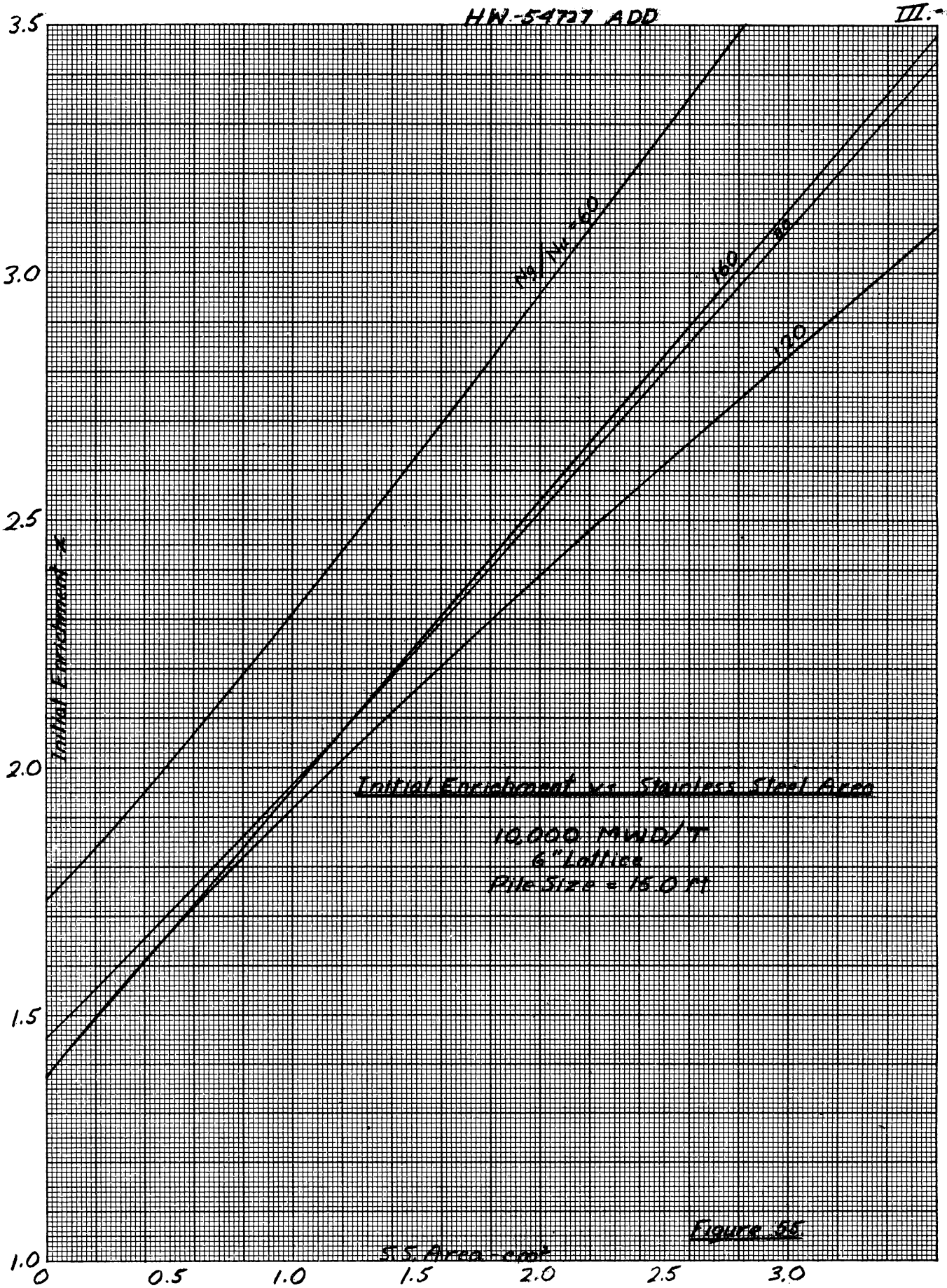
Initial Enrichment %
3.5
3.0
2.5
2.0
1.5
1.0
0
0.5
1.0
1.5
2.0
2.5
3.0
S.S. Area - cm²
Psi W
0
60
80
120
Initial Enrichment vs. Stainless Steel Area
10,000 MWD/T
6" Lattice
Pile Size = 16.0 ft

Figure 38

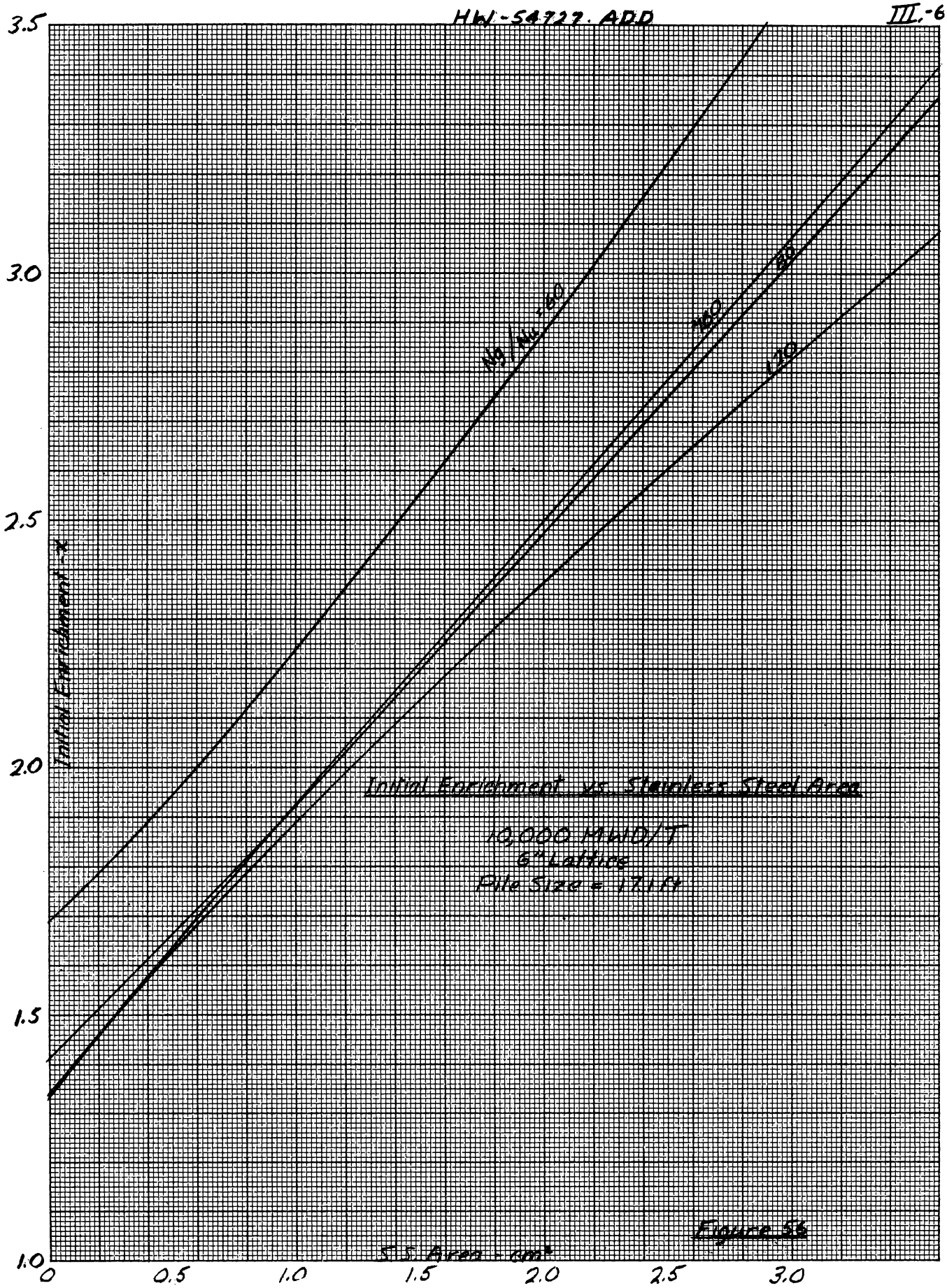
3.5
3.0
2.5
2.0
1.5
1.0
Initial Enrichment - X
0
0.5
1.0
1.5
2.0
2.5
3.0
S.S. Area - cm²
Ng/Nu = 60
80
100
120
Initial Enrichment vs. Stainless Steel Area
10,000 MWD/T
6" Lattice
Pile Size = 17.1 ft

Figure 56

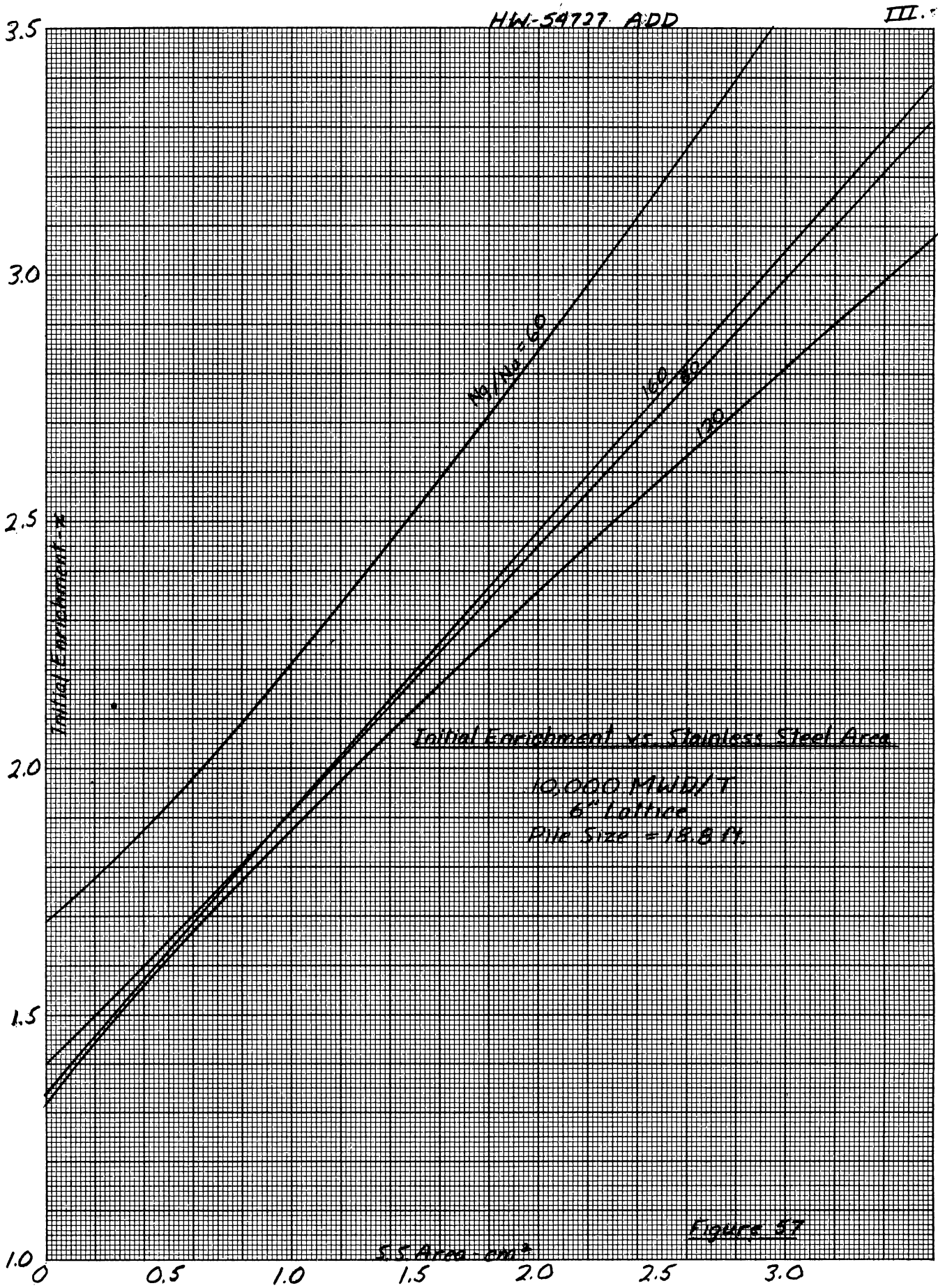
Initial Enrichment - w/o
3.5
3.0
2.5
2.0
1.5
1.0
0
0.5
1.0
1.5
2.0
2.5
3.0
S.S Area - cm²
Initial Enrichment vs. Stainless Steel Area
10,000 Mwd/T
6" Lattice
Pin Size = 18.8 ft.

Figure 37

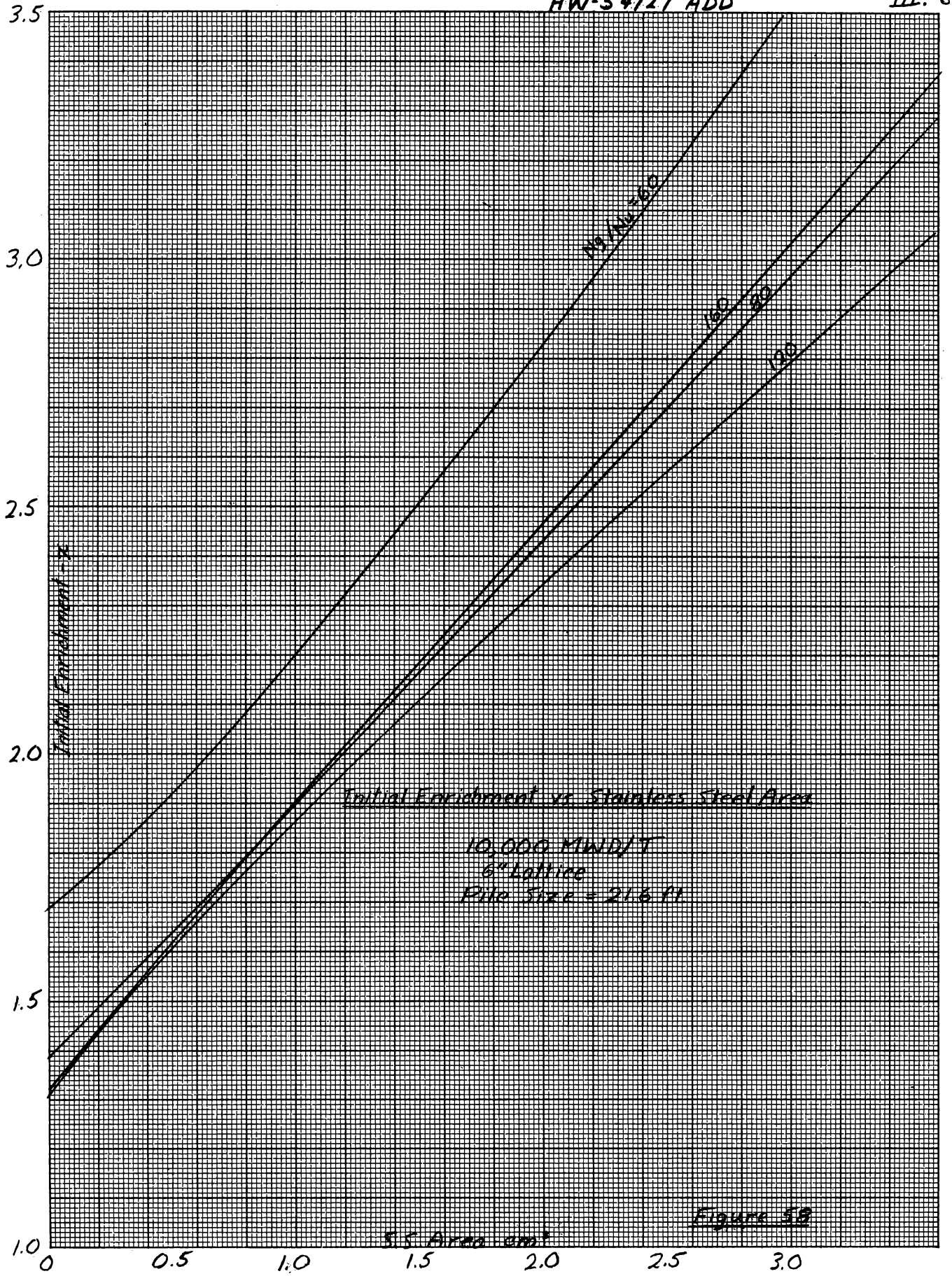
3.5
3.0
2.5
2.0
1.5
1.0
0
0.5
1.0
1.5
2.0
2.5
3.0
Initial Enrichment - %
S.S. Area cm²
Initial Enrichment vs Stainless Steel Area
10,000 MWD/T
6" Lattice
Pile Size = 21.6 ft
Figure 58

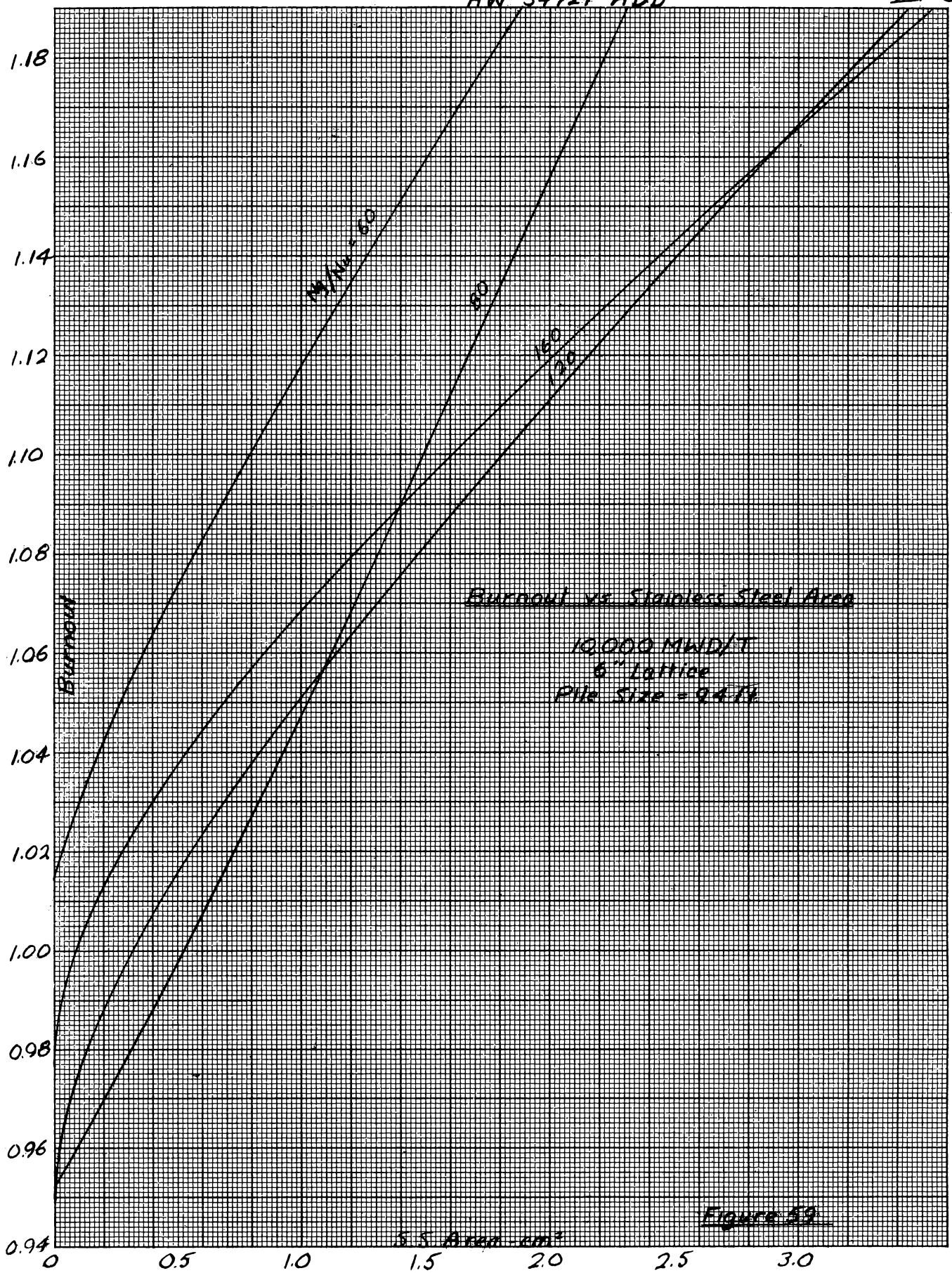
1.18
1.16
1.14
1.12
1.10
1.08
1.06
1.04
1.02
1.00
0.98
0.96
0.94
Burnout
0
0.5
1.0
1.5
2.0
2.5
3.0
S.S. Area - cm²
Burnout vs. Stainless Steel Area
10,000 MWD/T
6" Lattice
Pile Size = 9.4 ft
0°
8°
16°

Figure 59

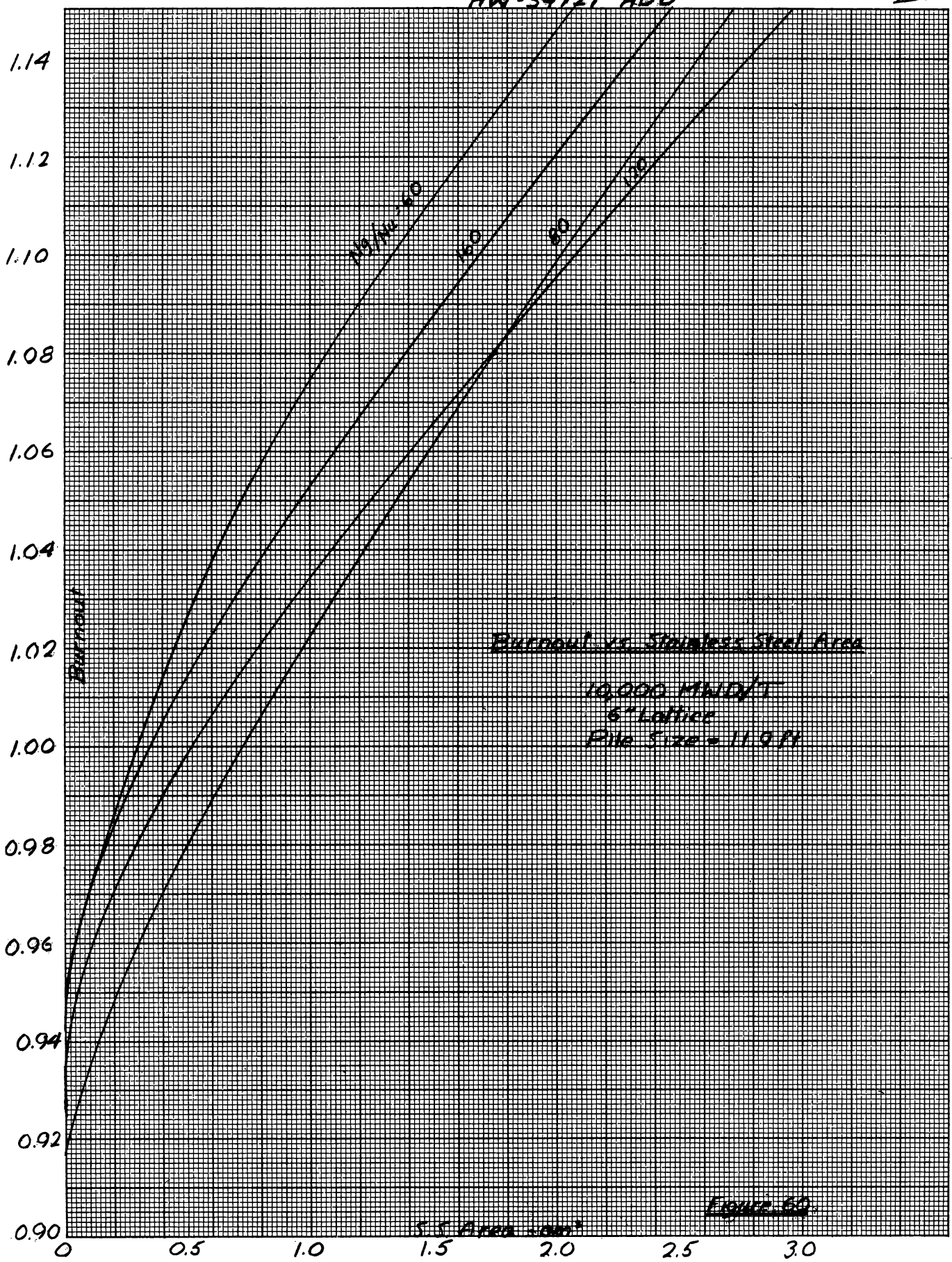
Burnout vs. Stainless Steel Area
10,000 MWD/T
6" Lattice
Pile Size = 11.9 ft
Ng/Nu = 60
160
80
120
Burnout
S.S. Area - cm²
1.14
1.12
1.10
1.08
1.06
1.04
1.02
1.00
0.98
0.96
0.94
0.92
0.90
0
0.5
1.0
1.5
2.0
2.5
3.0

Figure 60

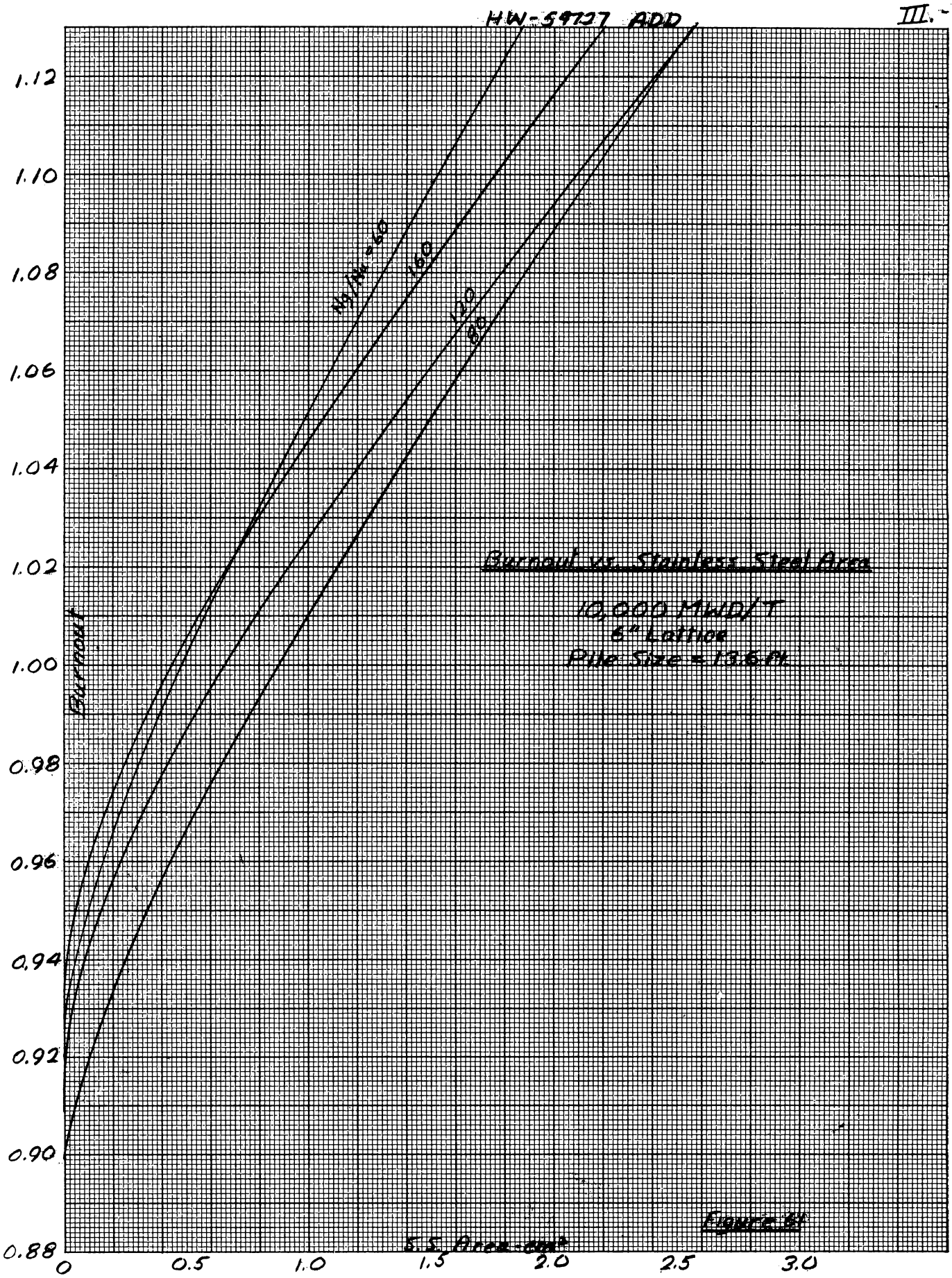
HW-59737 ADD
Burnout
1.12
1.10
1.08
1.06
1.04
1.02
1.00
0.98
0.96
0.94
0.92
0.90
0.88
0
0.5
1.0
1.5
2.0
2.5
3.0
S.S. Area-ft²
Burnout vs. Stainless Steel Area
10,000 MWD/T
6" Lattice
Pile Size = 13.6 ft.
Figure 61

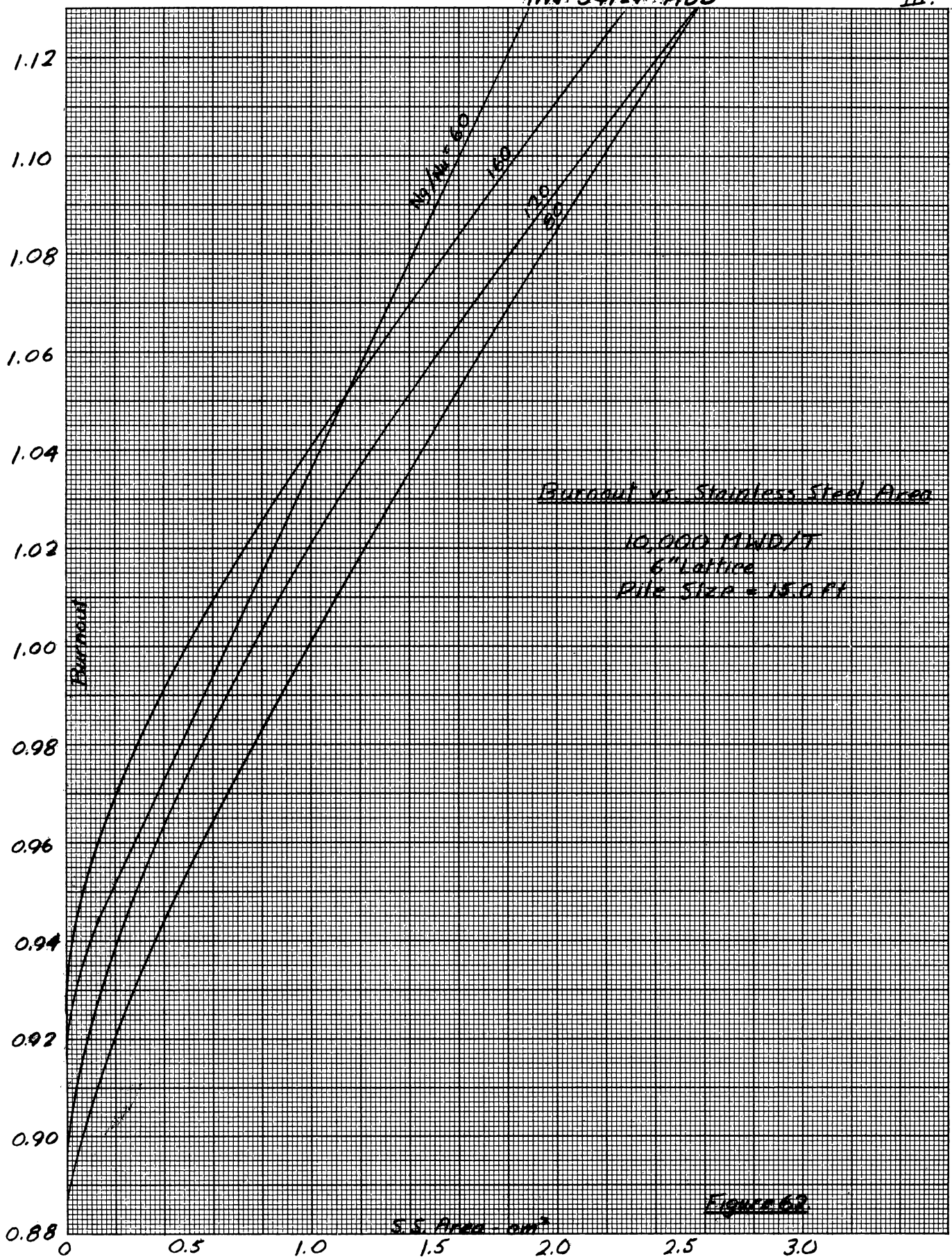
1.12
1.10
1.08
1.06
1.04
1.02
1.00
0.98
0.96
0.94
0.92
0.90
0.88
Burnout
0
0.5
1.0
1.5
2.0
2.5
3.0
S.S. Area - cm²
Burnout vs. Stainless Steel Area
10,000 MWD/T
6" Lattice
Pile Size = 15.0 Ft

Figure 62

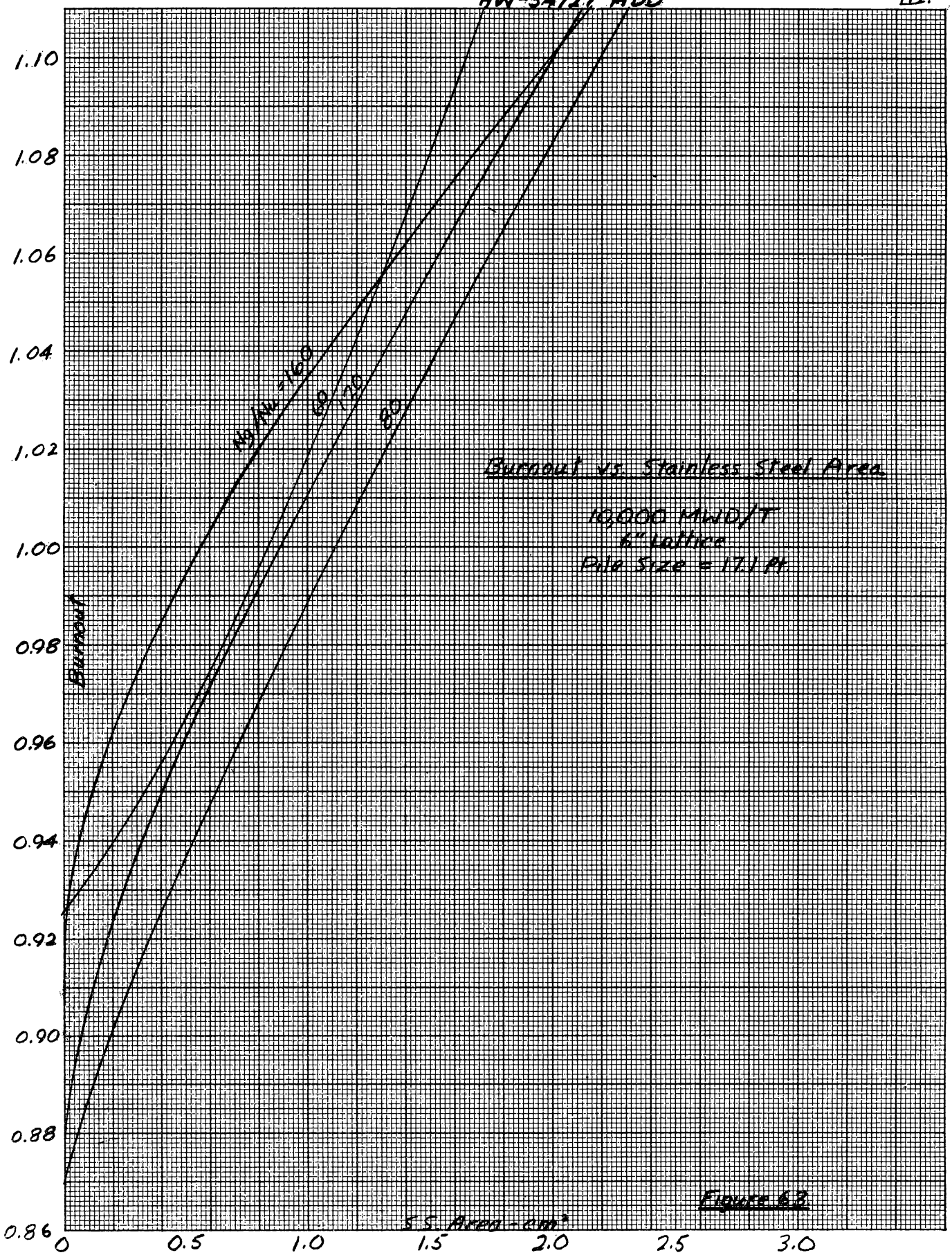
Burnout vs. Stainless Steel Area
10,000 MWD/T
6" Lattice
Pile Size = 17.1 ft.
Ng/Nu = 160
60
120
80
Burnout
S.S. Area - cm²
1.10
1.08
1.06
1.04
1.02
1.00
0.98
0.96
0.94
0.92
0.90
0.88
0.86
0
0.5
1.0
1.5
2.0
2.5
3.0

Figure 6.3

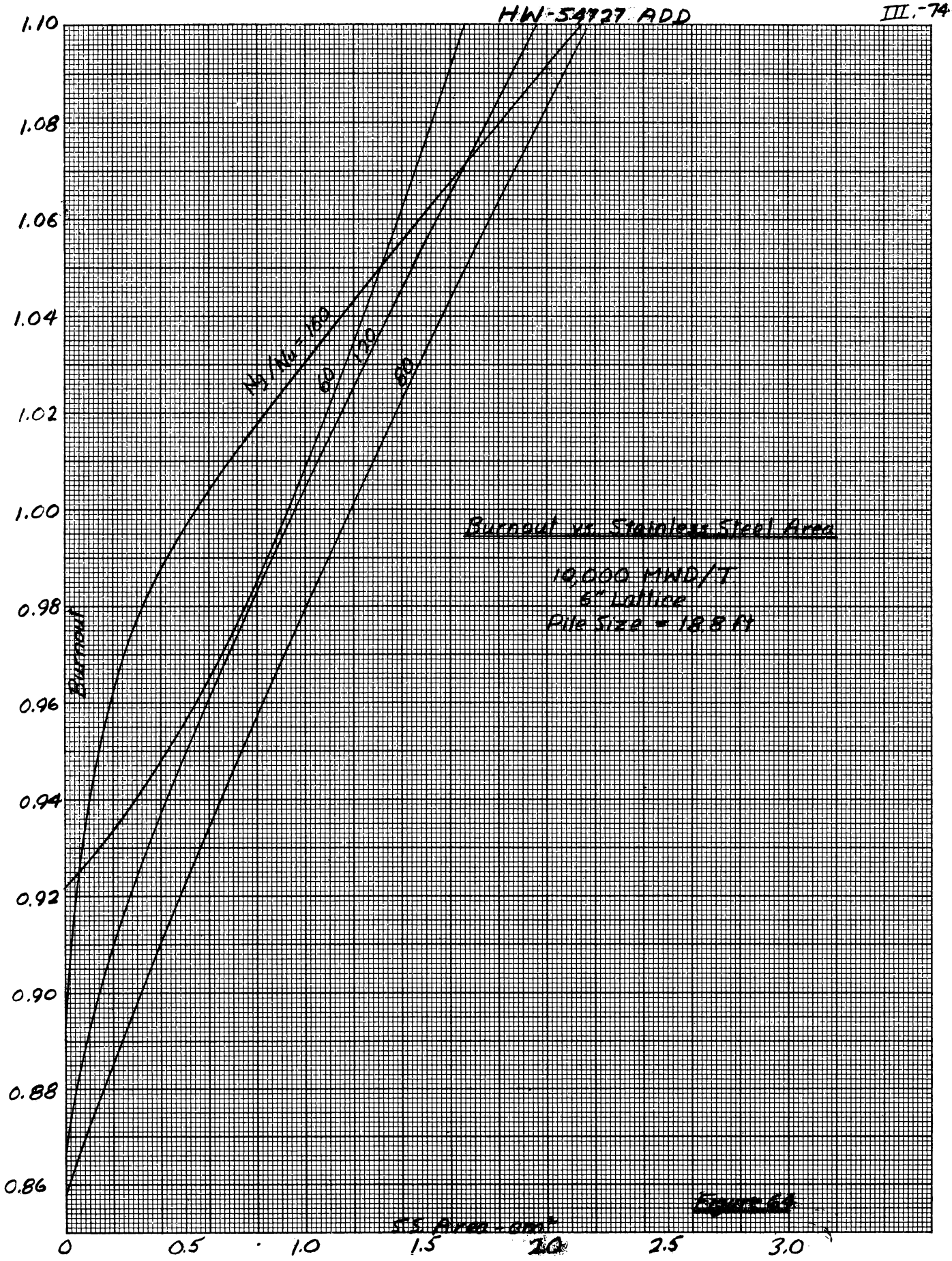
Burnout
1.10
1.08
1.06
1.04
1.02
1.00
0.98
0.96
0.94
0.92
0.90
0.88
0.86
0
0.5
1.0
1.5
2.0
2.5
3.0
S.S. Area - cm²
Burnout vs. Stainless Steel Area
10,000 MWD/T
6" Lattice
Pile Size = 18.8 ft
Figure 64

HW-54727 ADD

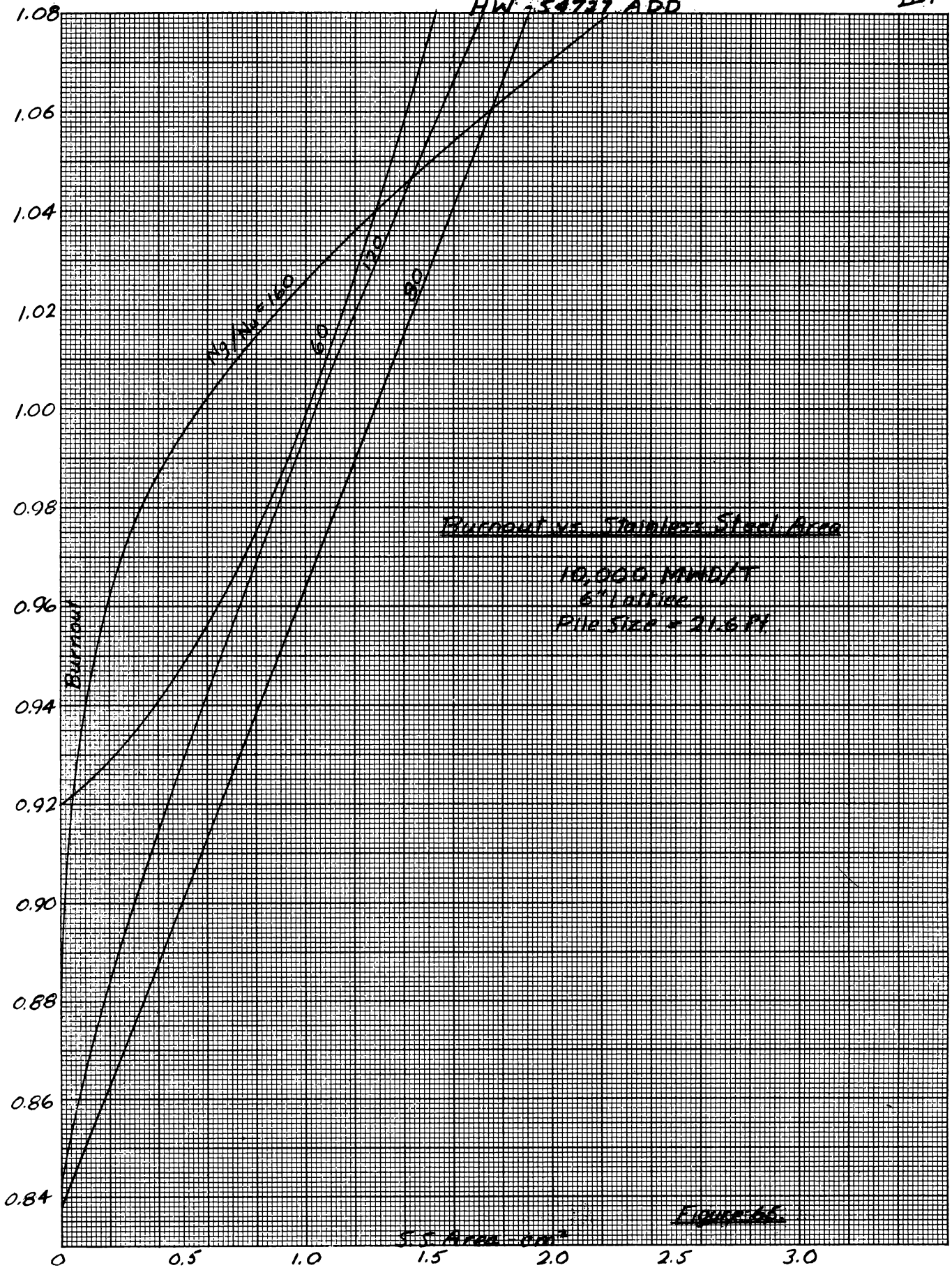
1.08
1.06
1.04
1.02
1.00
0.98
0.96
0.94
0.92
0.90
0.88
0.86
0.84
Burnout
0
0.5
1.0
1.5
2.0
2.5
3.0
S.S. Area cm²
Burnout vs. Stainless Steel Area
10,000 MWD/T
6" Lattice
Pile Size = 21.6 Ft
Equivalent

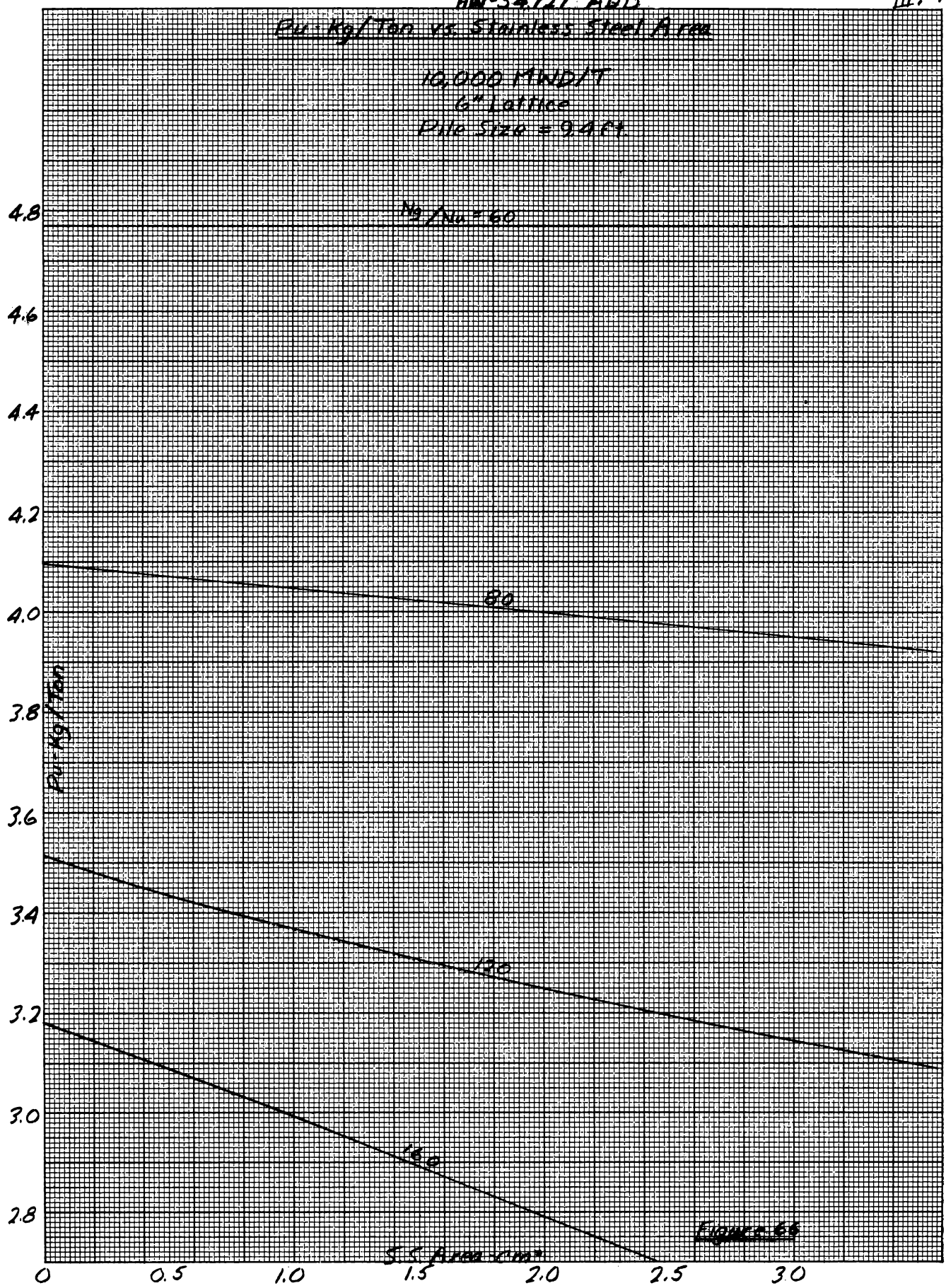
Pu-Kg/Ton vs. Stainless Steel Area
10,000 MWD/T
6" Lattice
Pile Size = 9.4 ft.
Ng/Nu = 60
80
120
160
Pu-Kg/Ton
4.8
4.6
4.4
4.2
4.0
3.8
3.6
3.4
3.2
3.0
2.8
S.S. Area-cm²
0
0.5
1.0
1.5
2.0
2.5
3.0

Figure 66

HW-54727 ADD

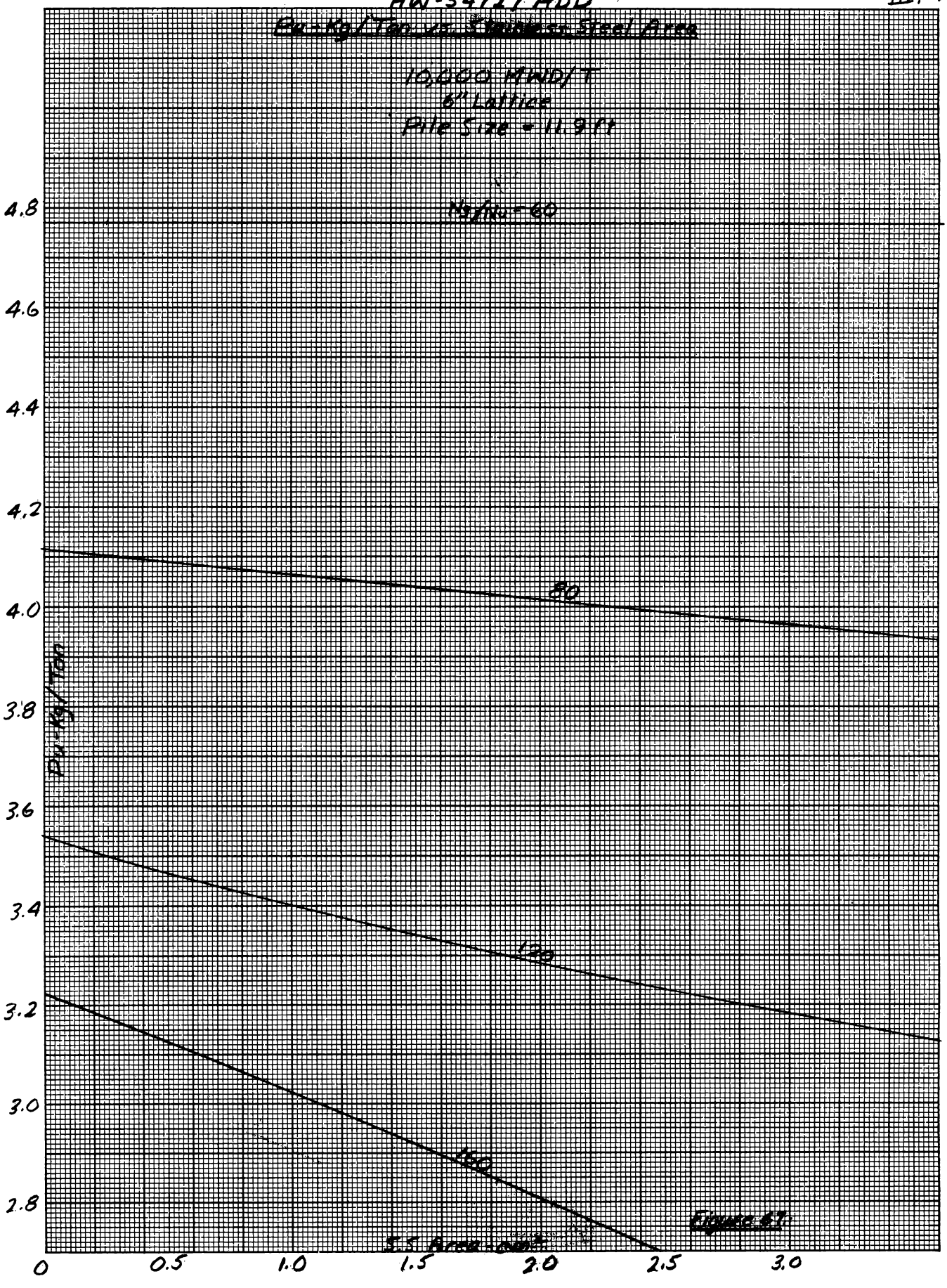

Figure 67

HW-54727 ADD

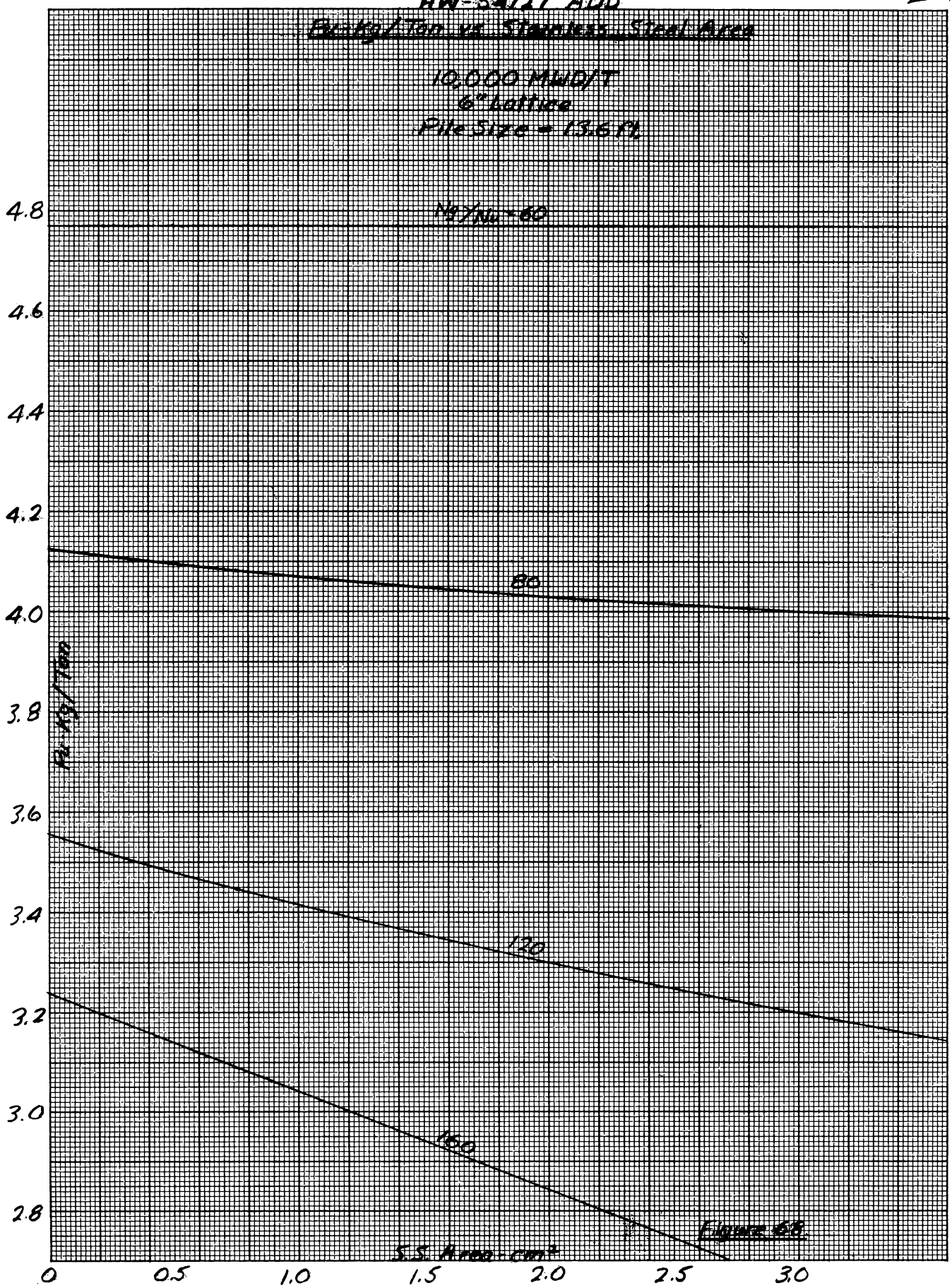

Figure 68.

HW-54727 ADD

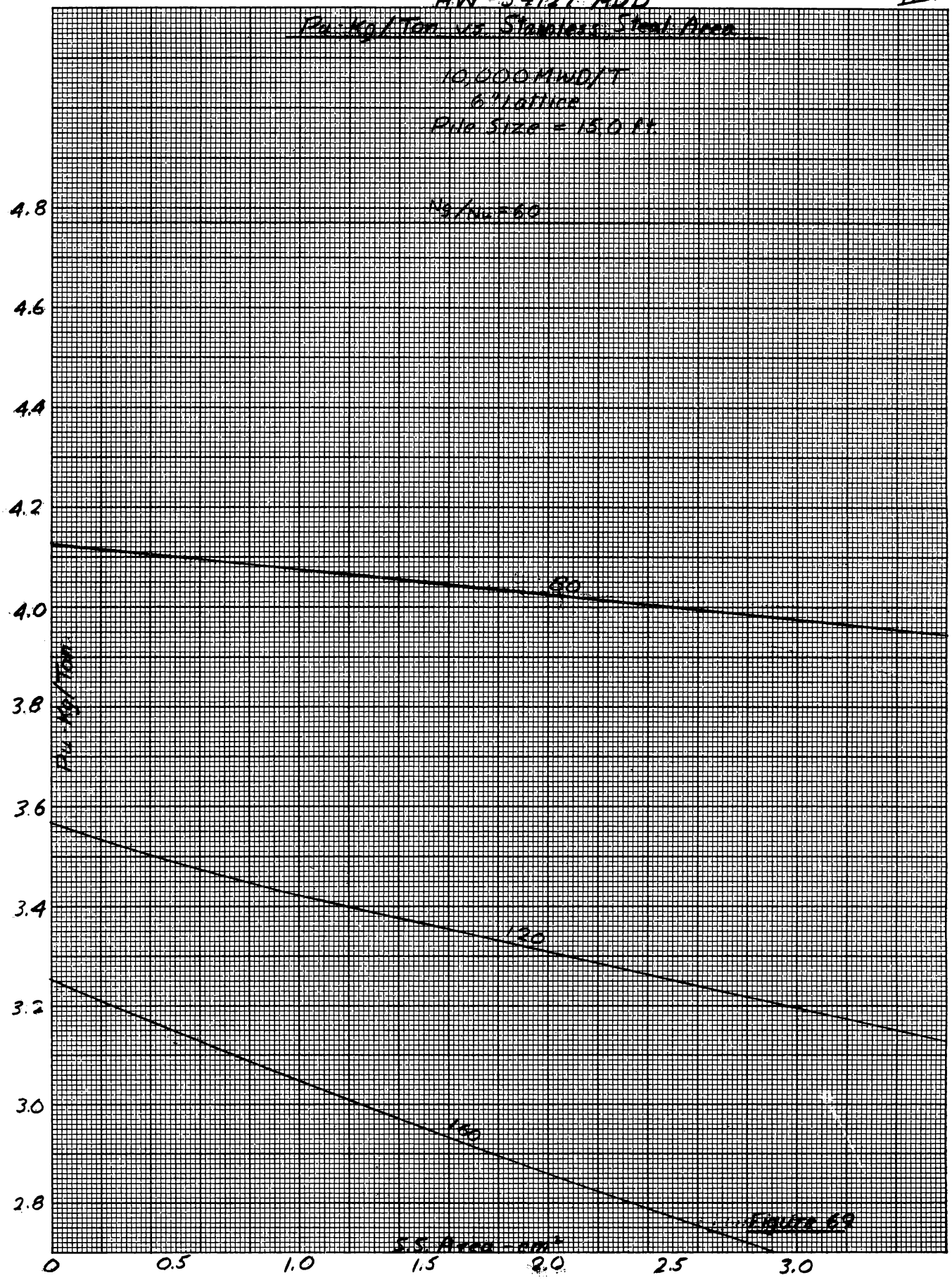

Figure 69

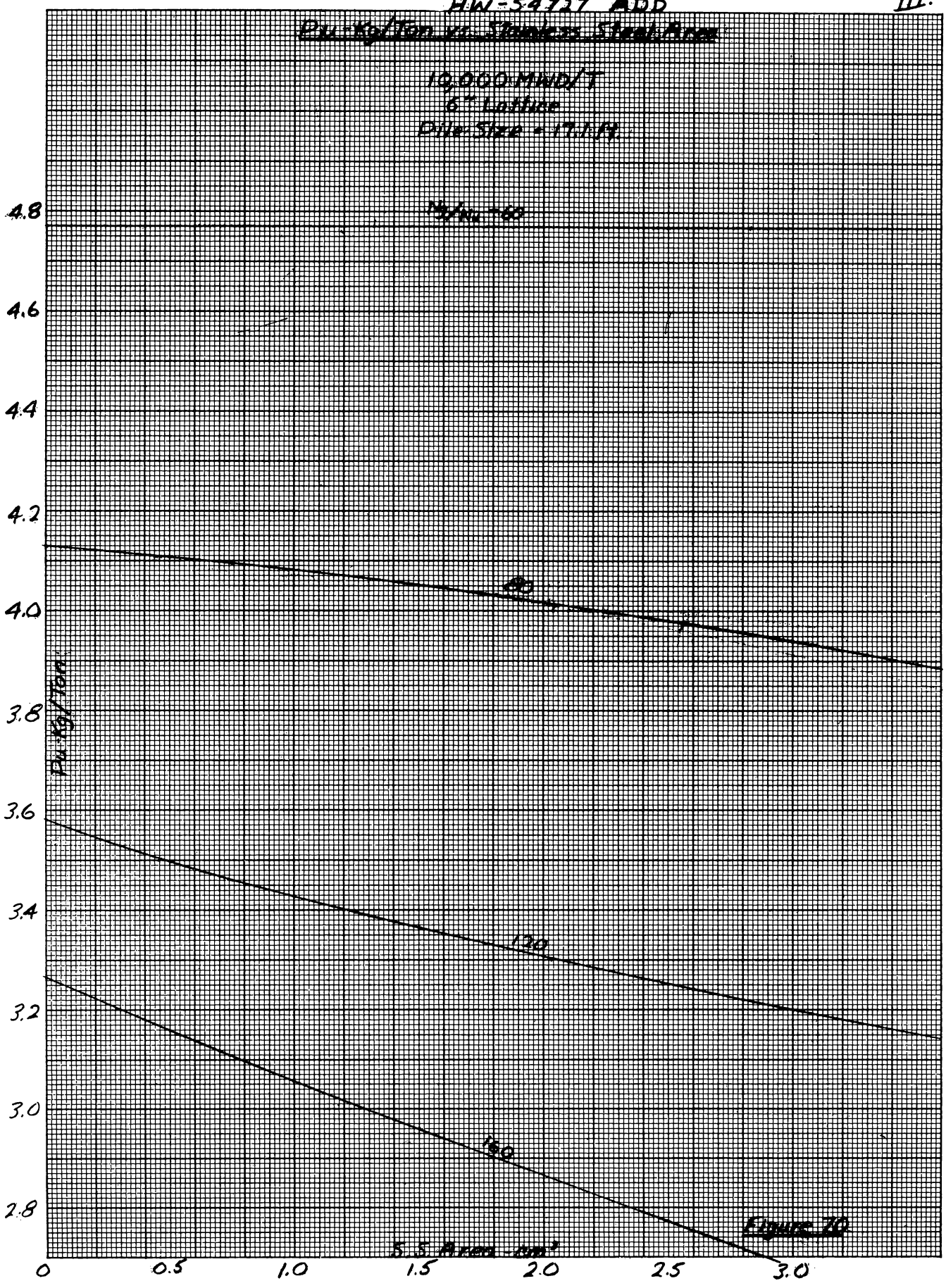
Pu-Kg/Ton vs. Stainless Steel Area
10,000 MWD/T
6" Lattice
Pile Size = 17.1 ft.
Ng/Nu = 60
80
120
160
Pu-Kg/Ton
4.8
4.6
4.4
4.2
4.0
3.8
3.6
3.4
3.2
3.0
2.8
S.S. Area - cm²
0
0.5
1.0
1.5
2.0
2.5
3.0

Figure 70

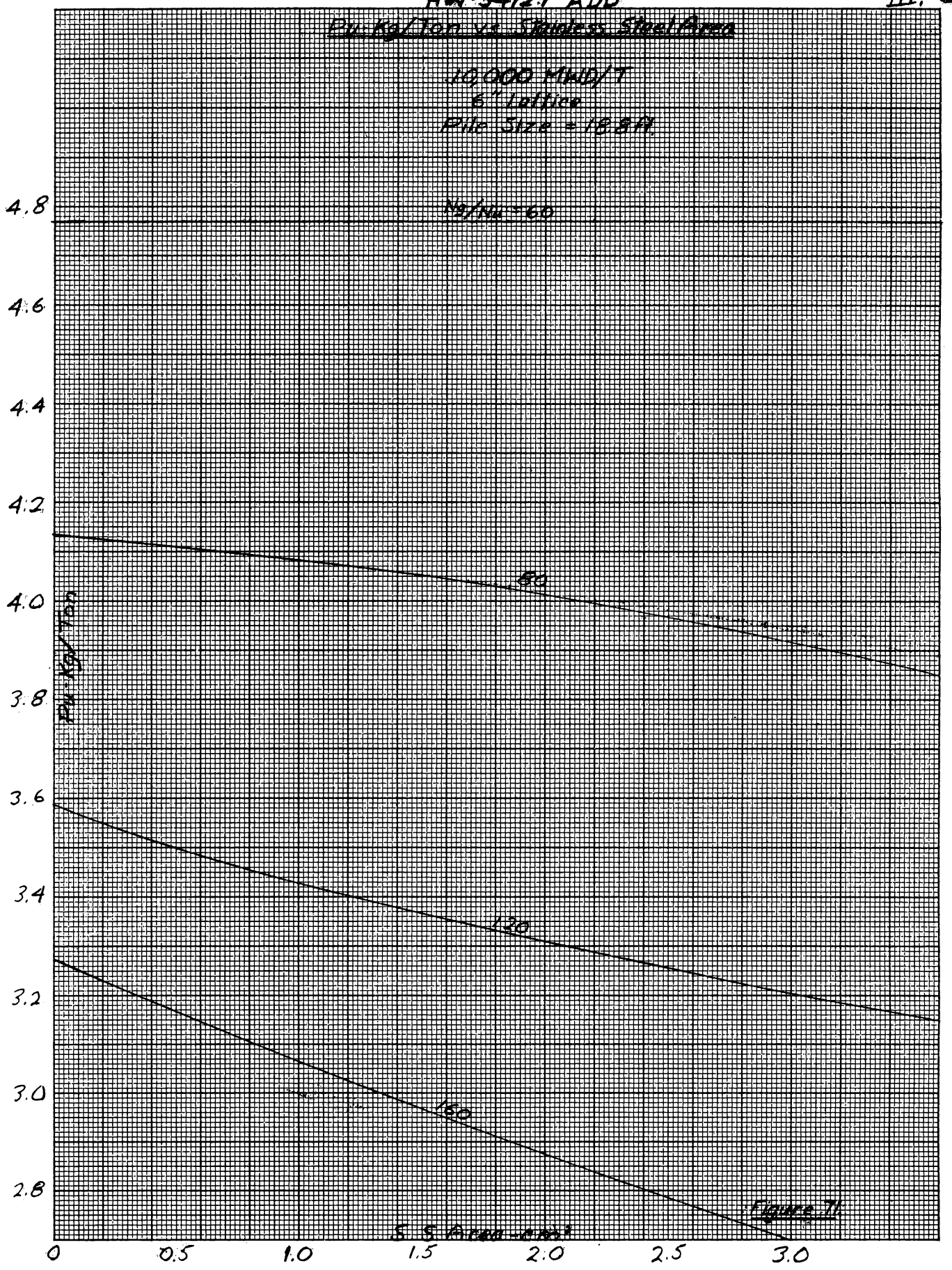
Pu-Kg/Ton vs Stainless Steel Area
10,000 MWD/T
6" lattice
Pile Size = 18.8 ft.
Ng/Nu = 60
80
120
160
Pu-Kg/Ton
4.8
4.6
4.4
4.2
4.0
3.8
3.6
3.4
3.2
3.0
2.8
S.S. Area-cm²
0
0.5
1.0
1.5
2.0
2.5
3.0

Figure 71

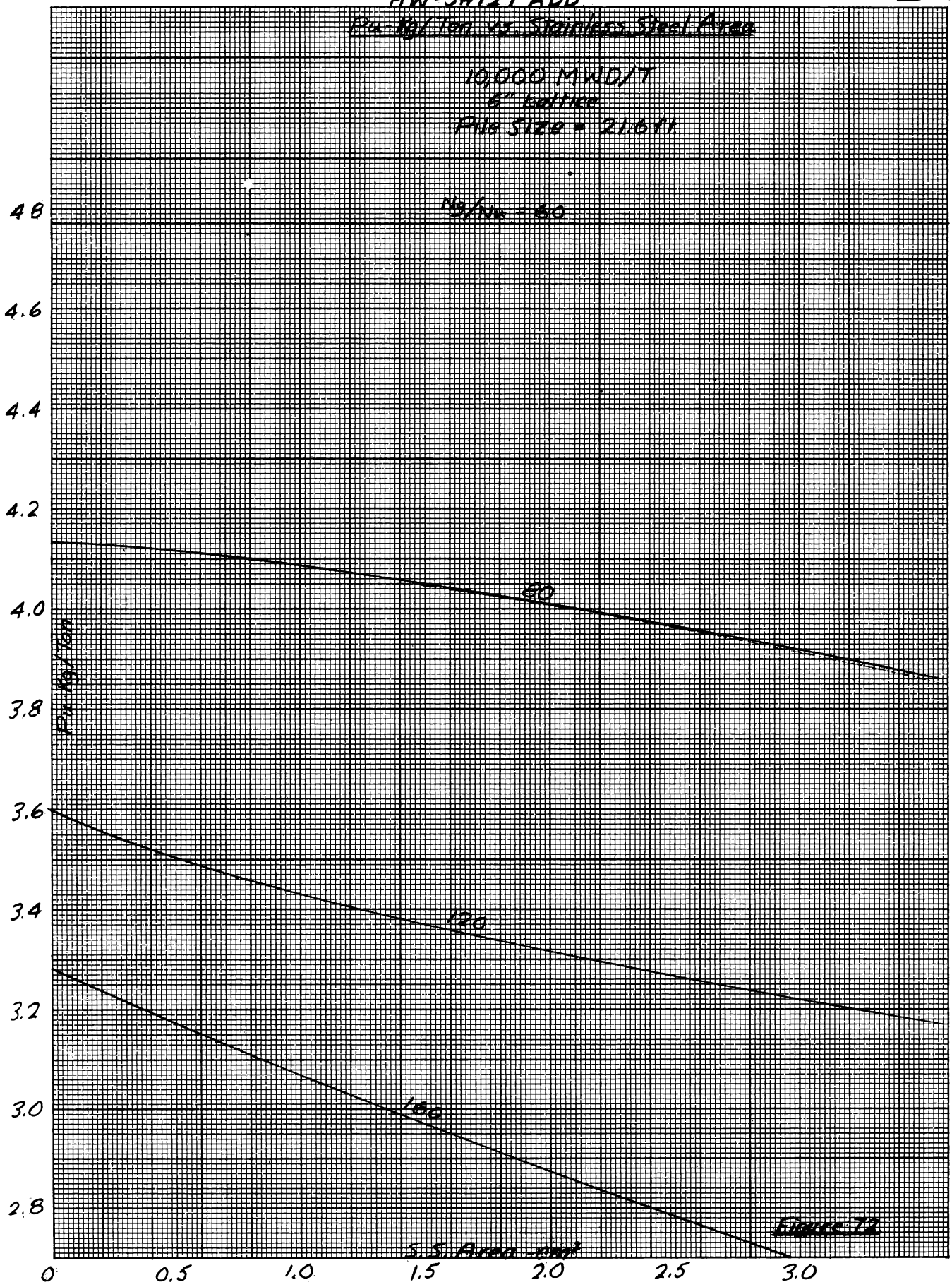
Pu-239/Ton vs. Stainless Steel Area
10,000 MWD/T
6" Lattice
Pile Size = 21.6 ft
Ns/Nu = 60
4.8
4.6
4.4
4.2
4.0
3.8
3.6
3.4
3.2
3.0
2.8
Pu-239 Kg/Ton
60
120
160
0
0.5
1.0
1.5
2.0
2.5
3.0
S.S. Area - cm²

Figure 72

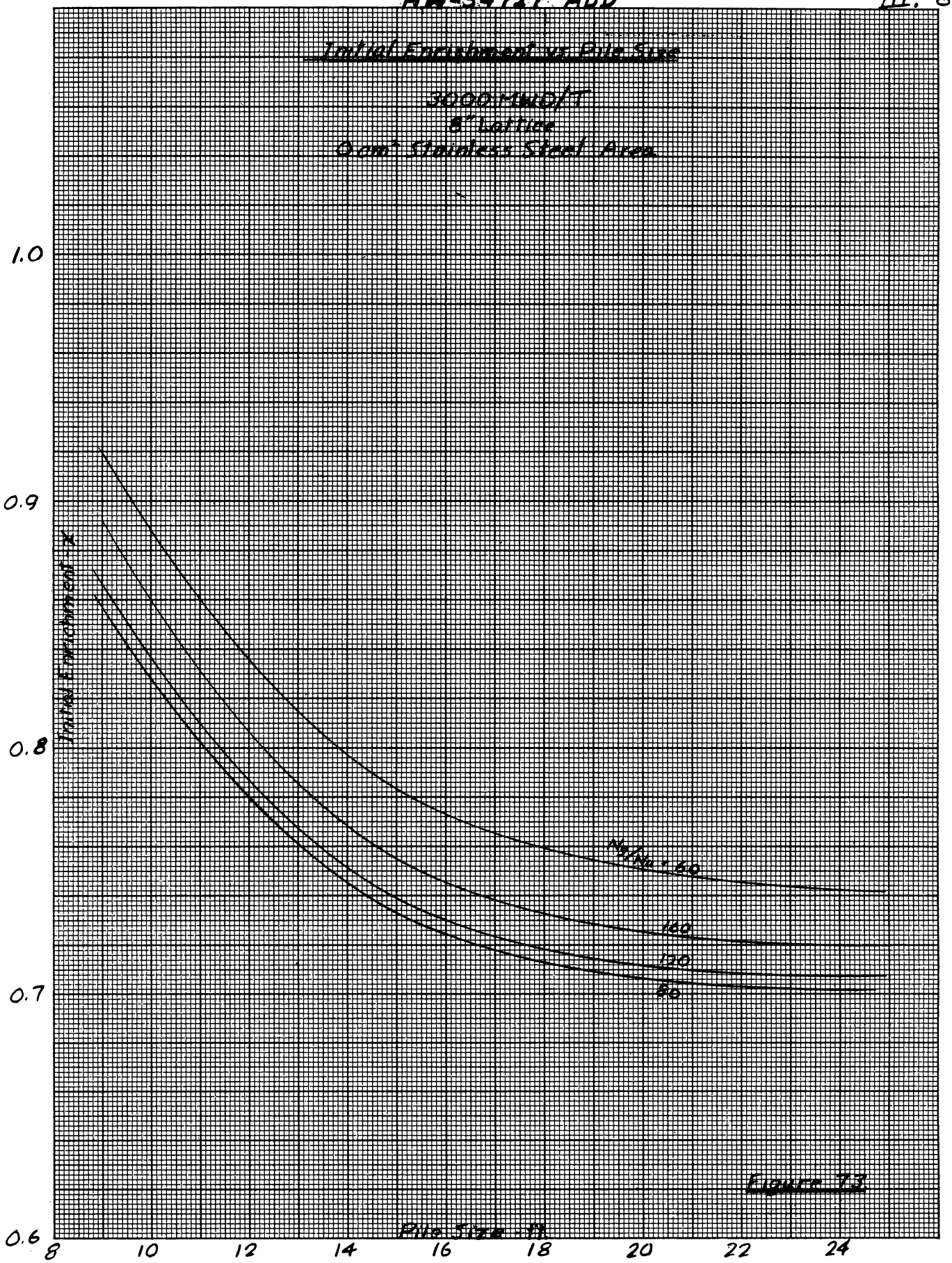
Initial Enrichment vs. Pile Size
3000 MWD/T
8" Lattice
0 cm² Stainless Steel Area
Initial Enrichment - x
1.0
0.9
0.8
0.7
0.6
Ng/Nu = 60
160
120
80
Pile Size - ft
8
10
12
14
16
18
20
22
24

Figure 73

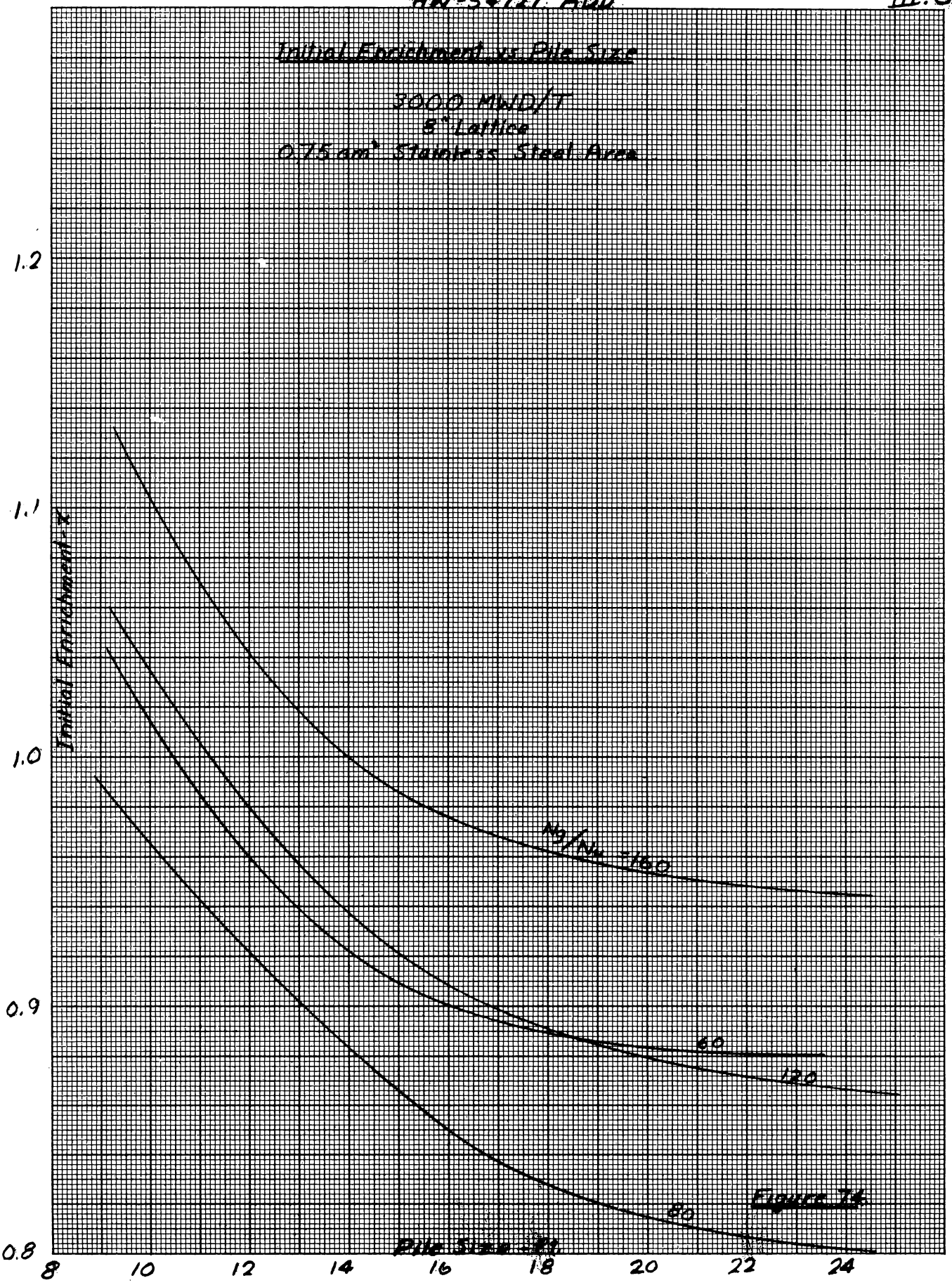
Initial Enrichment vs Pile Size
3000 MWD/T
8" Lattice
0.75 cm² Stainless Steel Area
Initial Enrichment - %
1.2
1.1
1.0
0.9
0.8
8
10
12
14
16
18
20
22
24
Pile Size - In.
N9/N5 = 160
60
120
80

FIGURE 74

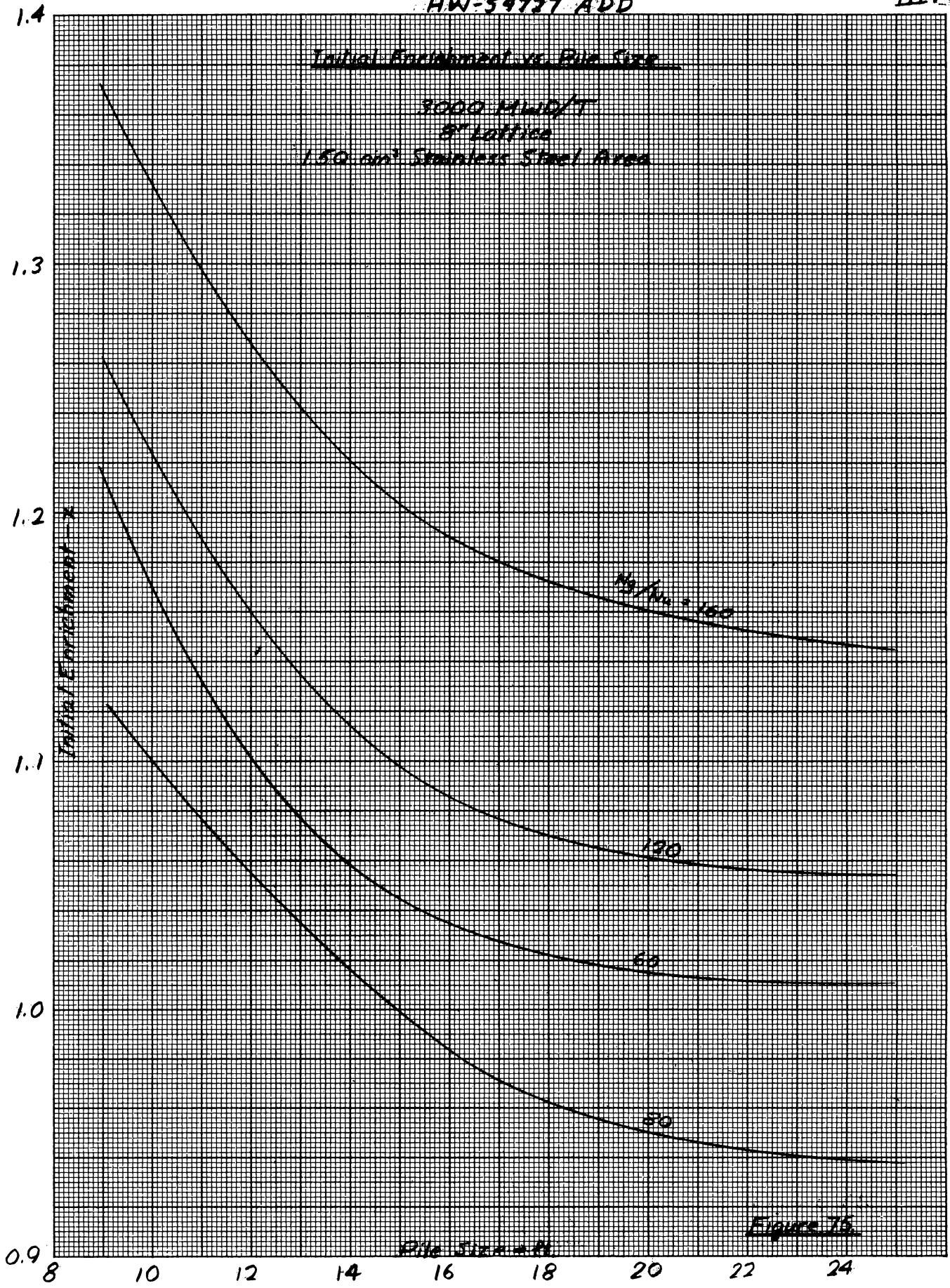
Initial Enrichment vs. Pile Size
3000 MWD/T
8" Lattice
150 cm² Stainless Steel Area
Initial Enrichment - %
1.4
1.3
1.2
1.1
1.0
0.9
8
10
12
14
16
18
20
22
24
Pile Size - Ft.
N_g/N_u = 160
120
60
30

Figure 16.

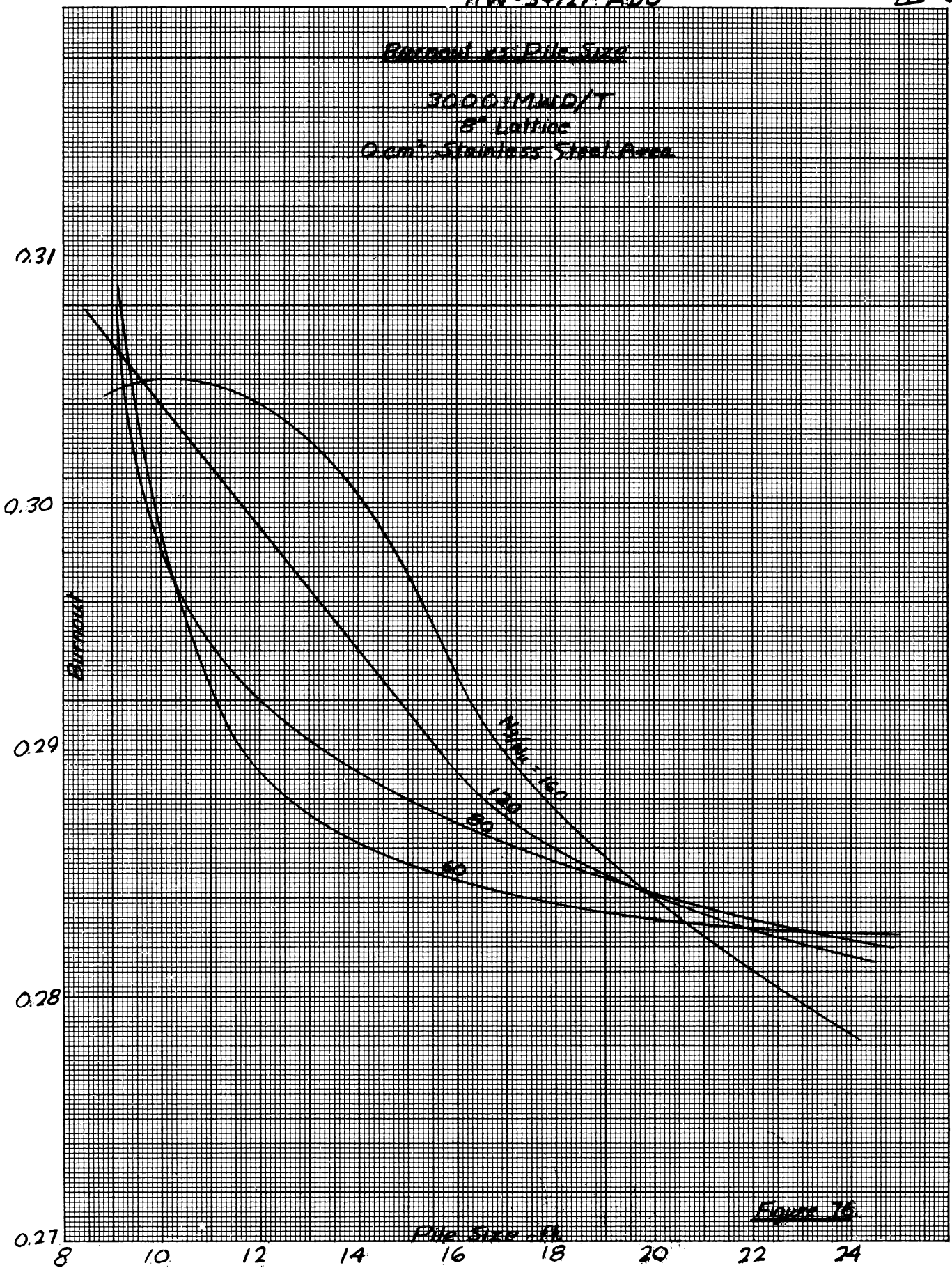
Burnout vs. Pile Size
3000 MWD/T
8" Lattice
0 cm² Stainless Steel Area
0.31
0.30
0.29
0.28
0.27
Burnout
Ng/Nu = 160
120
80
60
Pile Size - ft
8
10
12
14
16
18
20
22
24

Figure 76

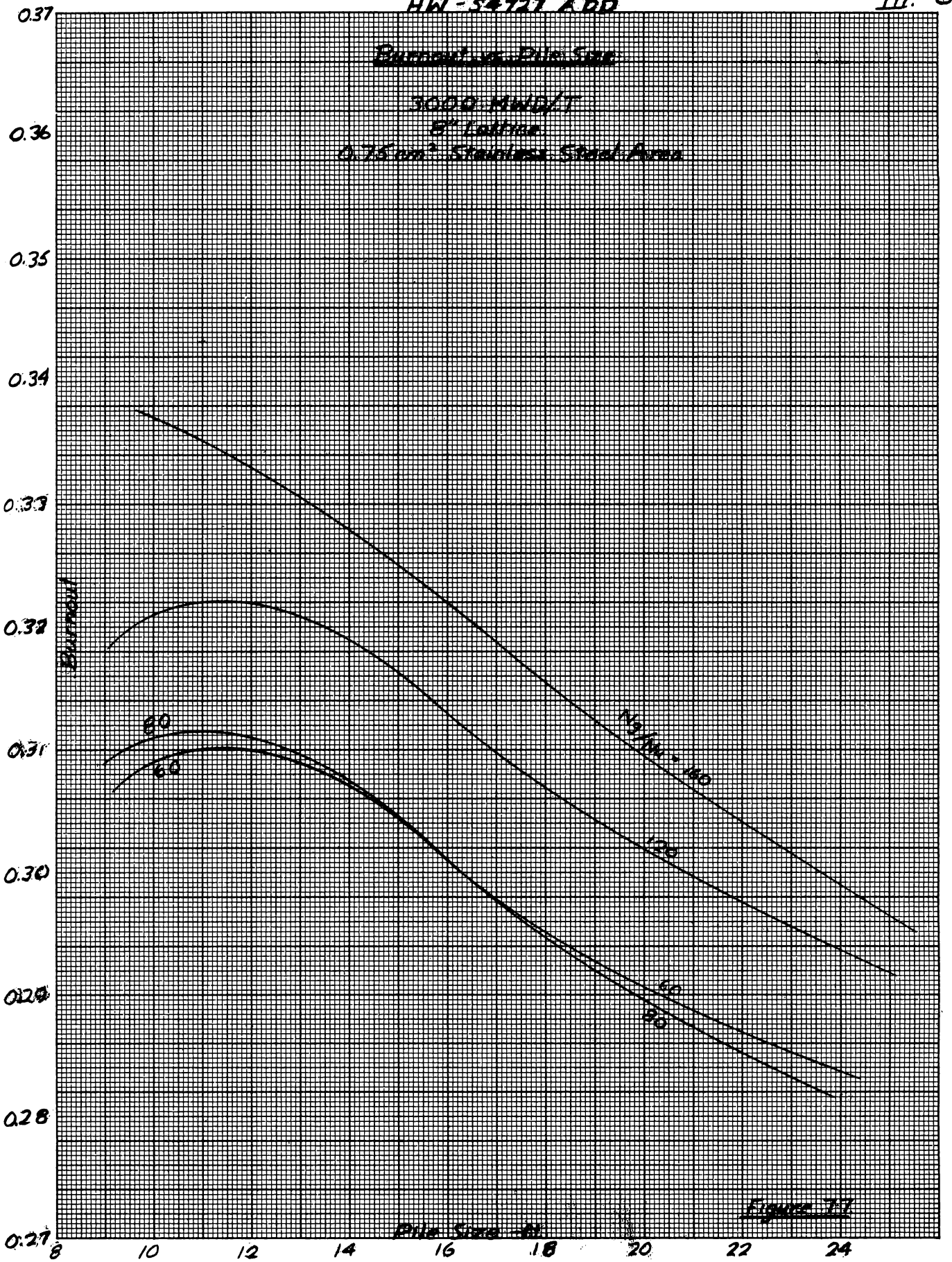
Burnout vs. Pile Size
3000 MWD/T
8" Lattice
0.75 cm² Stainless Steel Area
Burnout
Pile Size - ft
0.37
0.36
0.35
0.34
0.33
0.32
0.31
0.30
0.29
0.28
0.27
8
10
12
14
16
18
20
22
24
80
60
Ng/Nu = 160
120
60
80

Figure 77

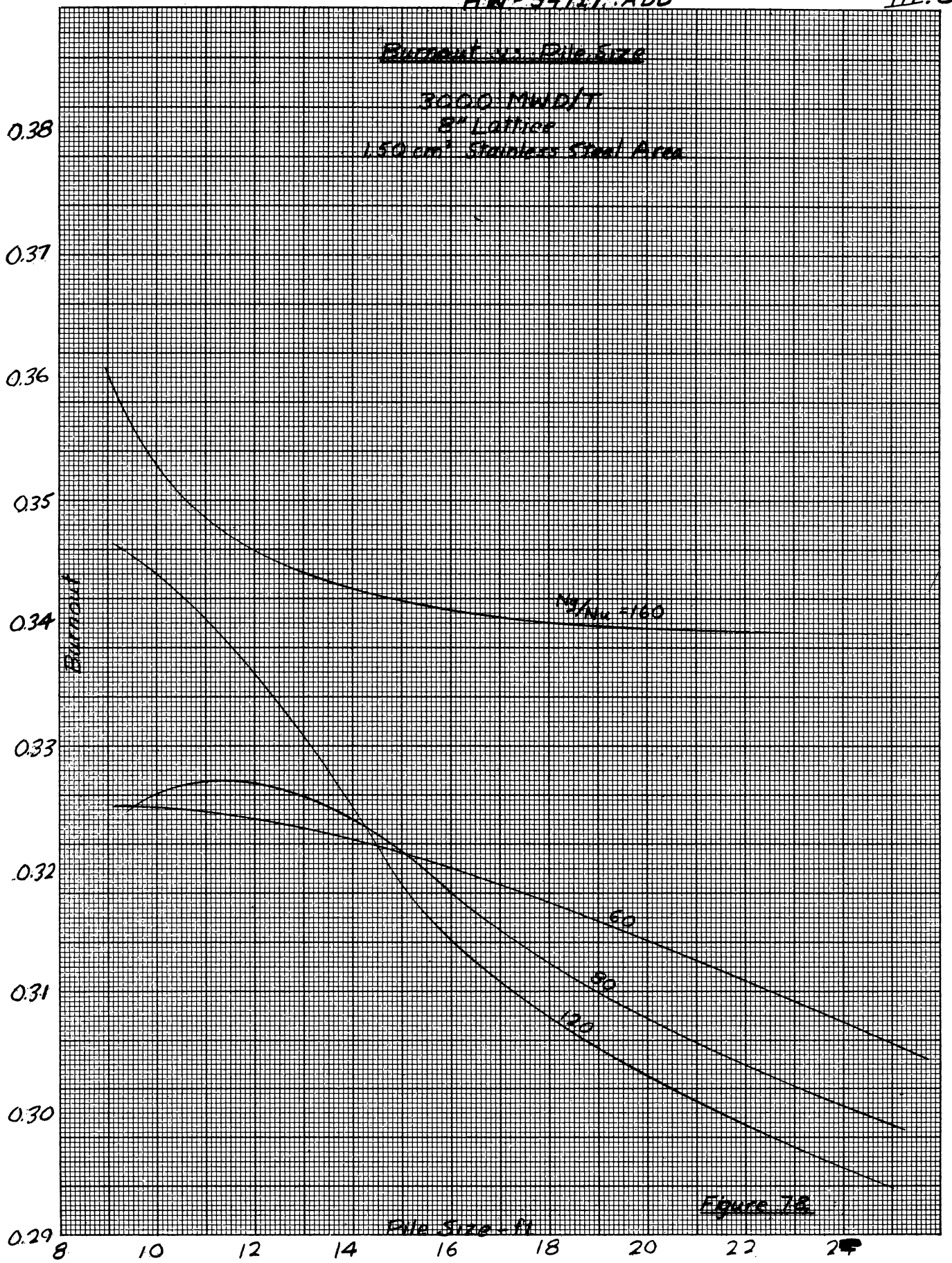
Burnout vs. Pile Size
3000 Mwd/T
8" Lattice
150 cm² Stainless Steel Area
Burnout
0.38
0.37
0.36
0.35
0.34
0.33
0.32
0.31
0.30
0.29
8
10
12
14
16
18
20
22
24
Pile Size - ft
Mg/Mu = 160
60
80
120

Figure 18.

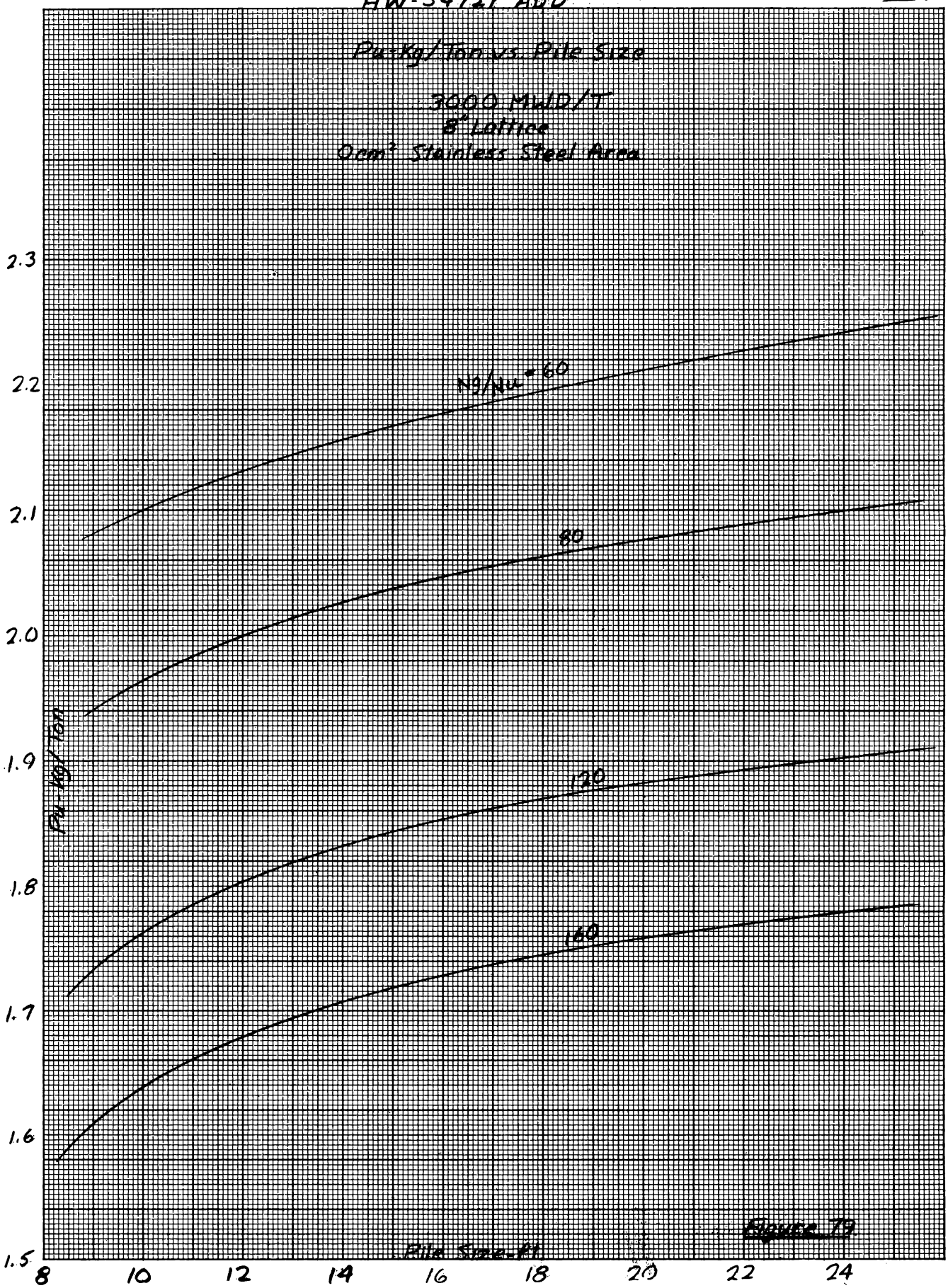
Pu-Kg/Ton vs. Pile Size
3000 MWD/T
8" Lattice
0cm² Stainless Steel Area
N9/Nu = 60
80
120
160
Pu-kg/Ton
Pile Size-ft
2.3
2.2
2.1
2.0
1.9
1.8
1.7
1.6
1.5
8
10
12
14
16
18
20
22
24

Figure 79

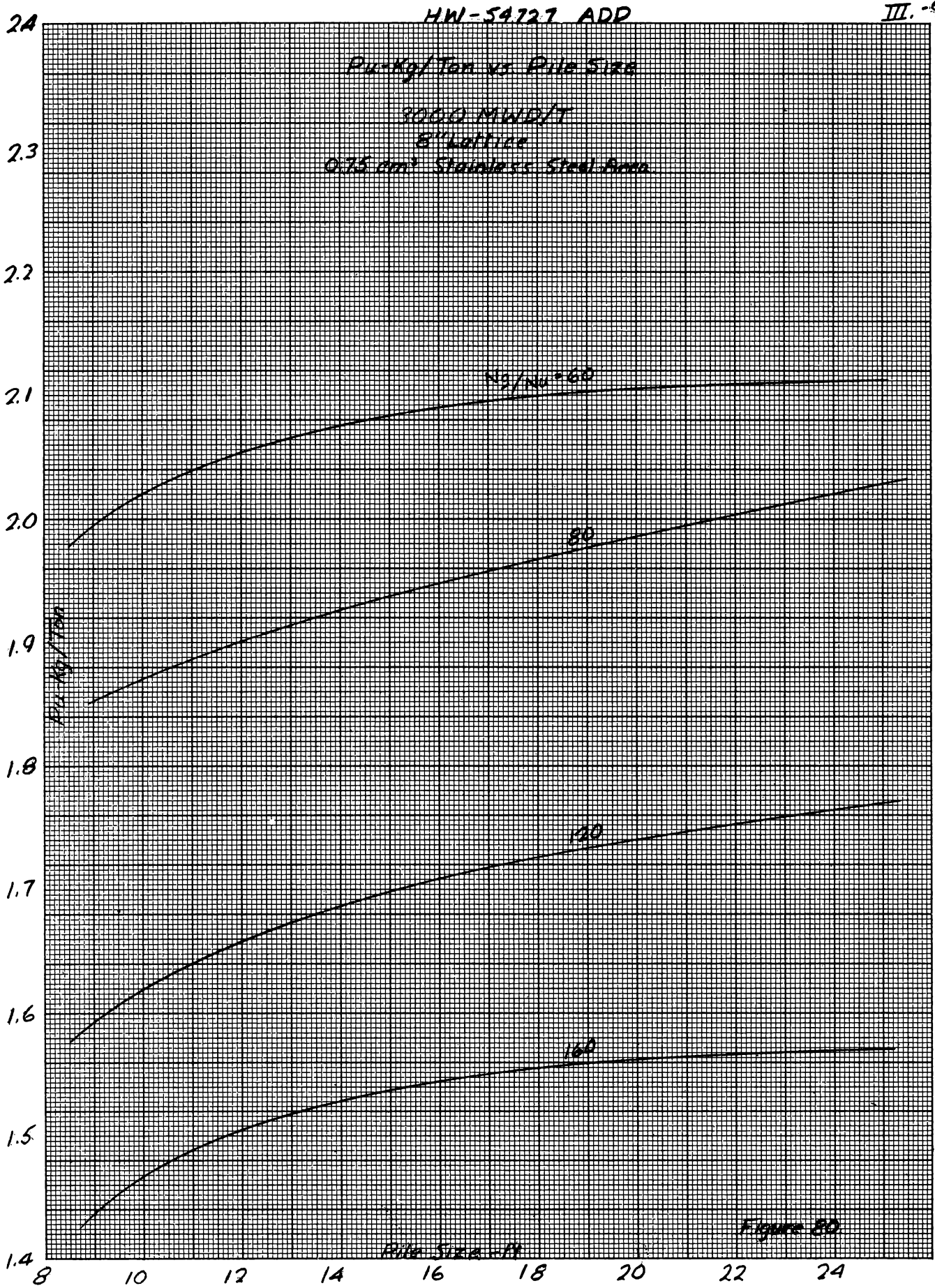
Pu-Kg/Ton vs. Pile Size
3000 MWD/T
8" Lattice
0.75 cm³ Stainless Steel Area
Ng/Nu = 60
80
120
160
Pu-Kg/Ton
Pile Size - ft
2.4
2.3
2.2
2.1
2.0
1.9
1.8
1.7
1.6
1.5
1.4
8
10
12
14
16
18
20
22
24

Figure 80

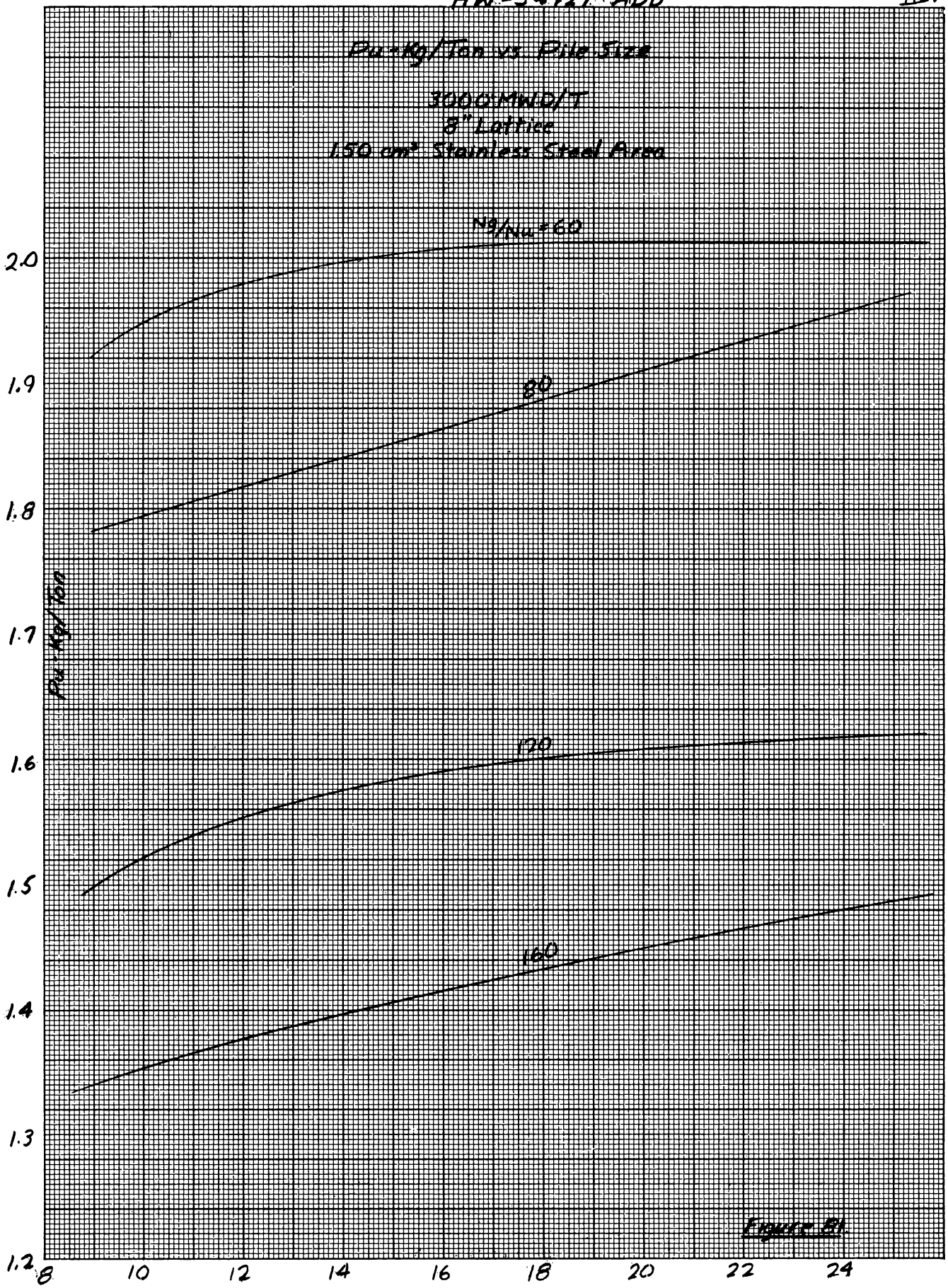
Pu-Kg/Ton vs Pile Size
3000 MWD/T
8" Lattice
150 cm² Stainless Steel Area
Ng/Nu = 60
80
120
160
Pu-Kg/Ton
2.0
1.9
1.8
1.7
1.6
1.5
1.4
1.3
1.2
8
10
12
14
16
18
20
22
24

Figure 81.

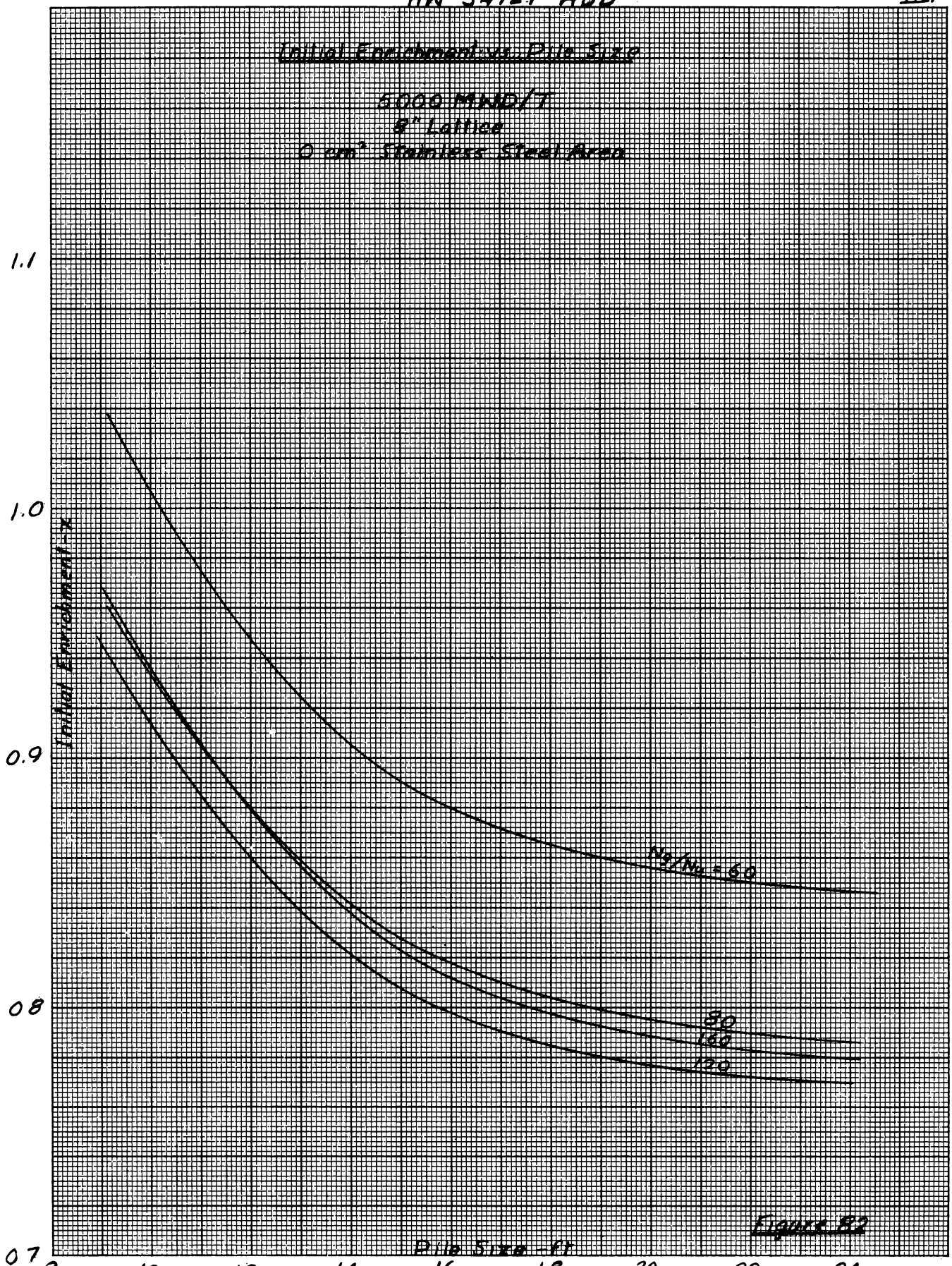
Initial Enrichment vs. Pile Size
5000 MWD/T
8" Lattice
0 cm² Stainless Steel Area
Initial Enrichment - %
1.1
1.0
0.9
0.8
0.7
8
10
12
14
16
18
20
22
24
Pile Size - ft
Na/Nu = 60
80
100
120

Figure 82

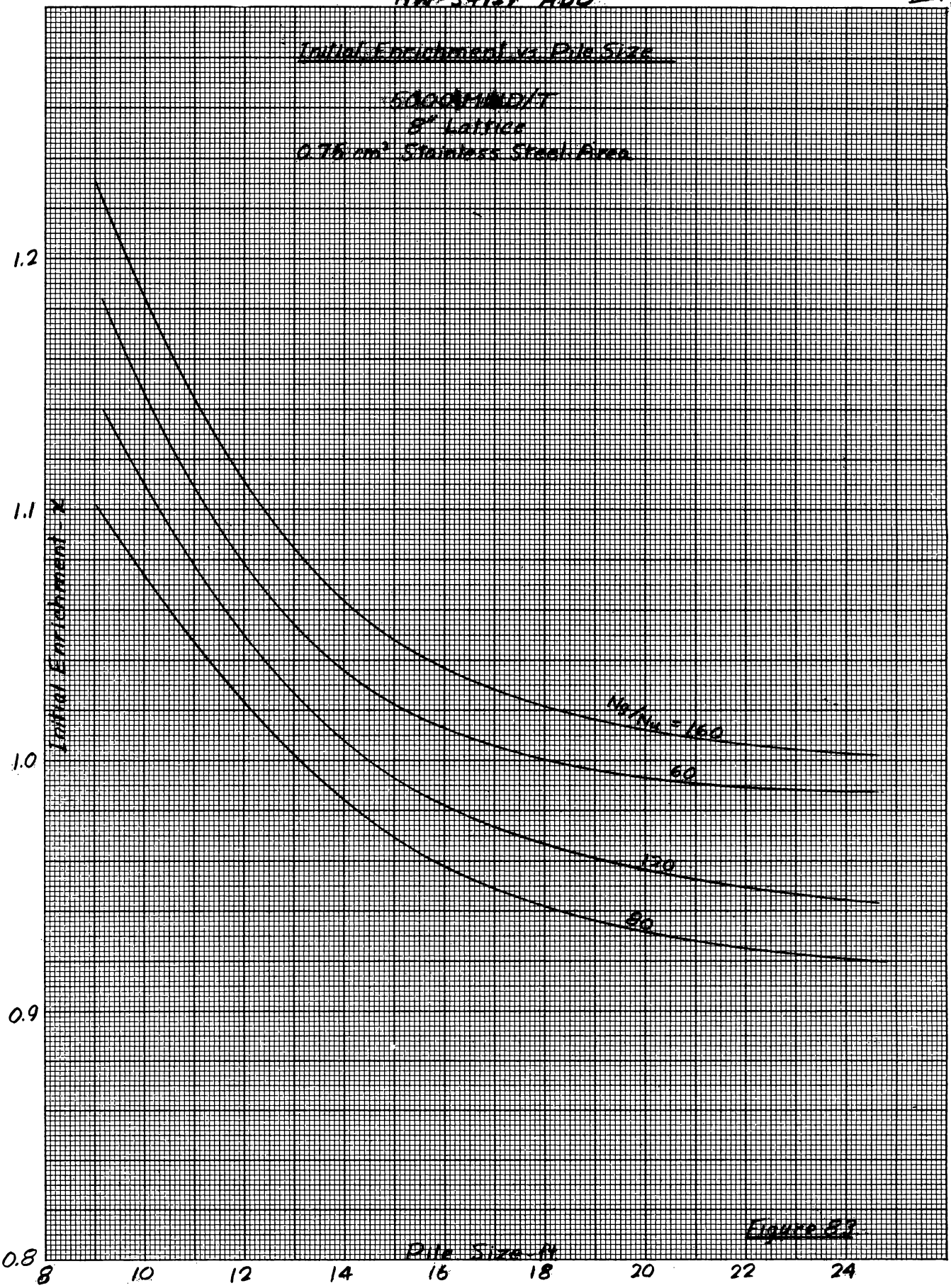
Initial Enrichment vs. Pile Size
5000 MWD/T
8" Lattice
0.75 cm² Stainless Steel Area
1.2
1.1
1.0
0.9
0.8
Initial Enrichment
N_8/N_H = 160
60
120
80
8
10
12
14
16
18
20
22
24
Pile Size - N

Figure 83

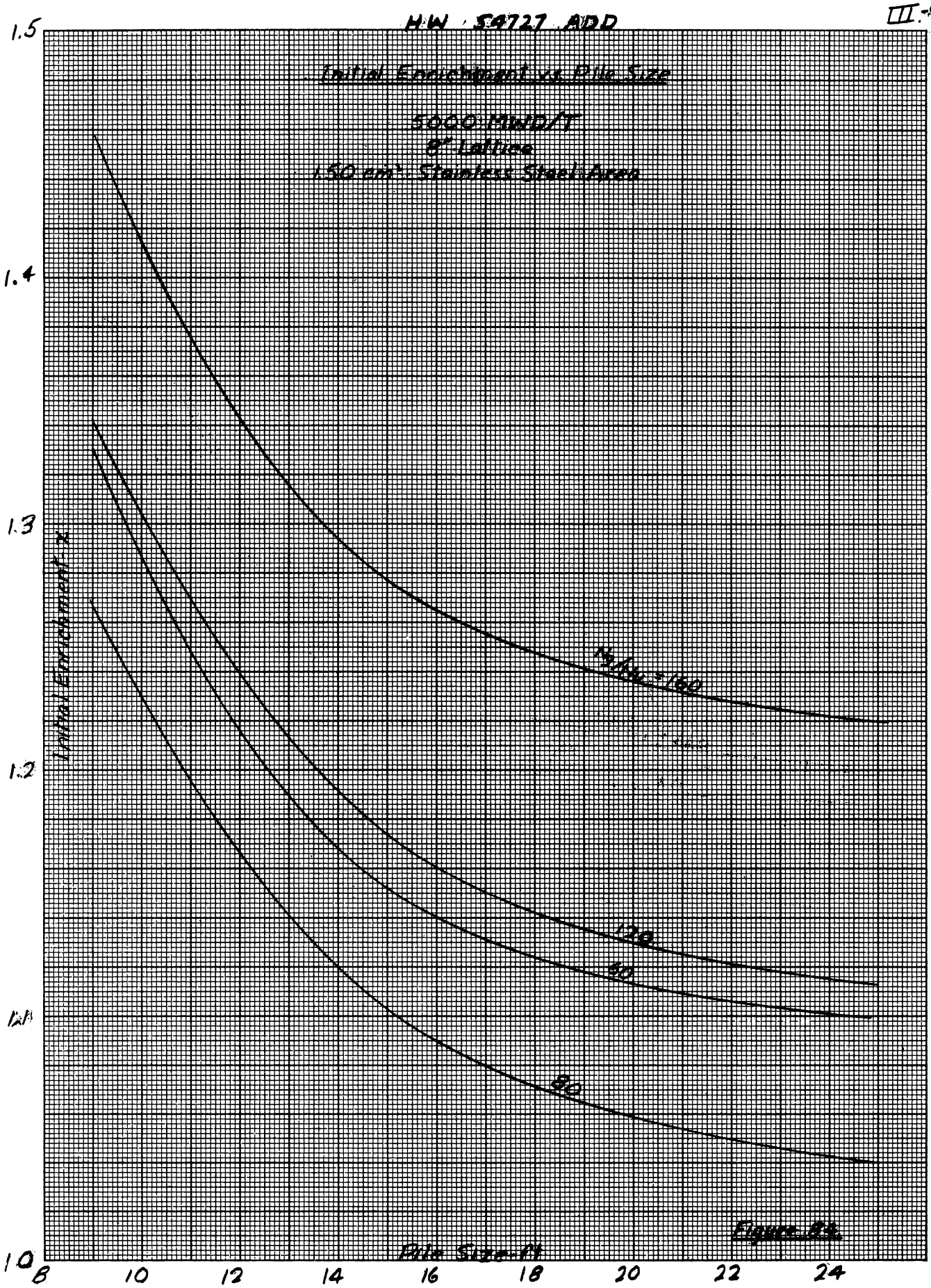
Initial Enrichment vs Pile Size
5000 MWD/T
8" Lattice
150 cm² Stainless Steel Area
Initial Enrichment, w/o
1.5
1.4
1.3
1.2
1.1
1.0
8
10
12
14
16
18
20
22
24
Pile Size-ft
160
120
80
40

Figure 8.4

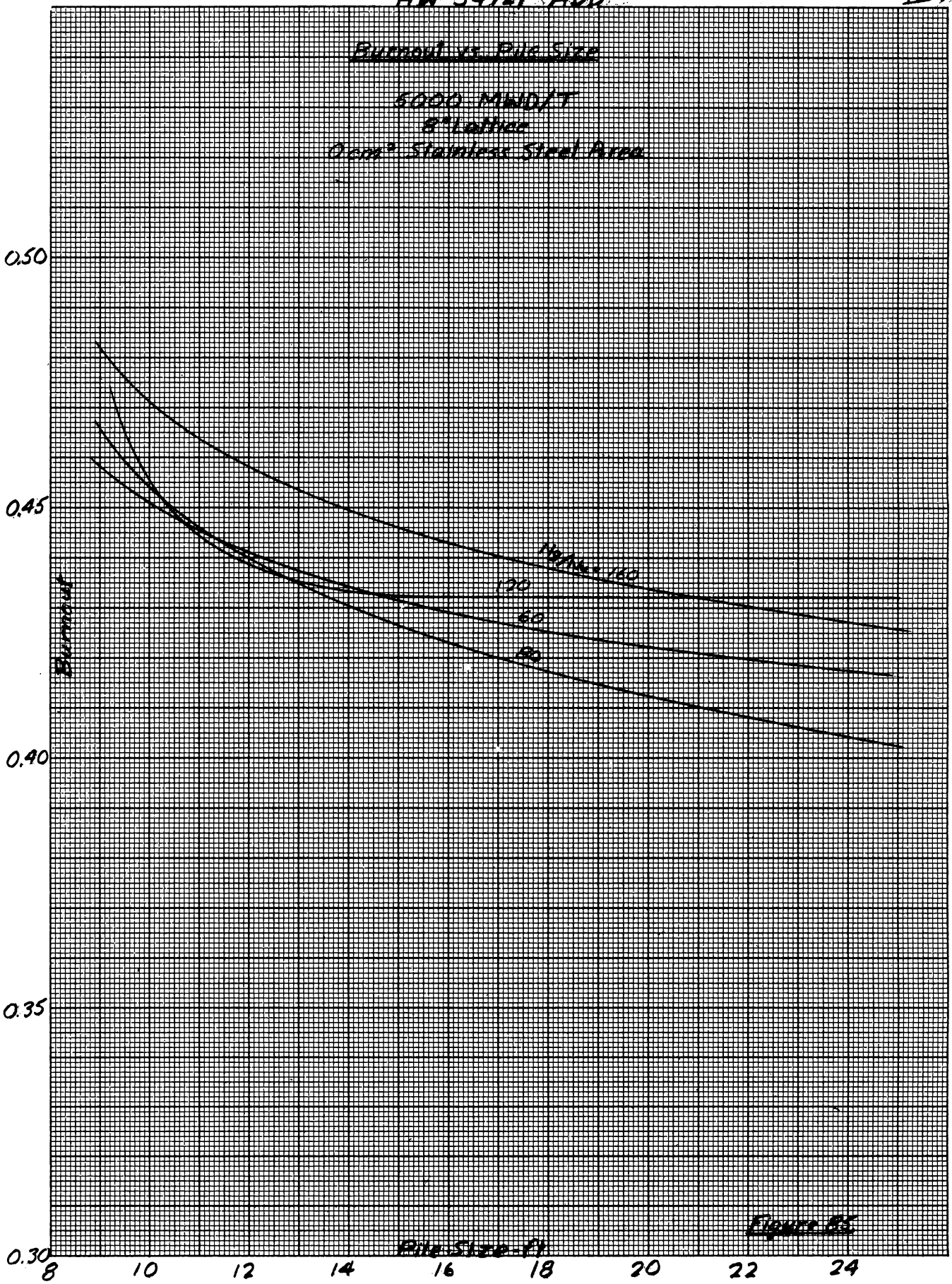
Burnout vs. Pile Size
5000 MWD/T
8" Lattice
0 cm² Stainless Steel Area
Burnout
0.50
0.45
0.40
0.35
0.30
Ng/Nu = 160
120
60
80
Pile Size-ft
8
10
12
14
16
18
20
22
24

Figure 85

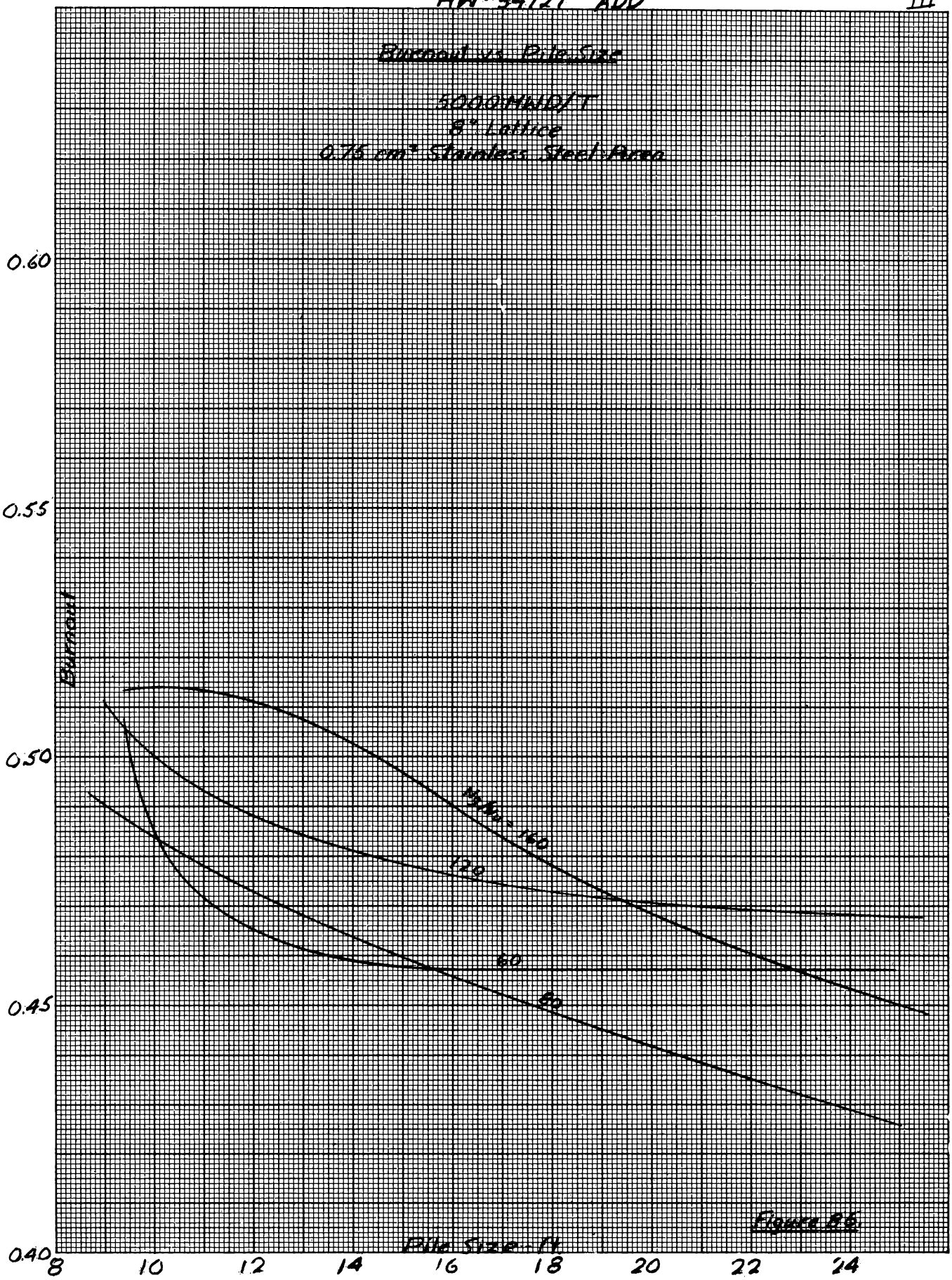
Burnout vs. Pitch Size
5000 MWD/T
8" Lattice
0.75 cm² Stainless Steel Area
0.60
0.55
0.50
0.45
0.40
Burnout
160
120
80
60
8
10
12
14
16
18
20
22
24
Pitch Size - IN

Figure 8.6

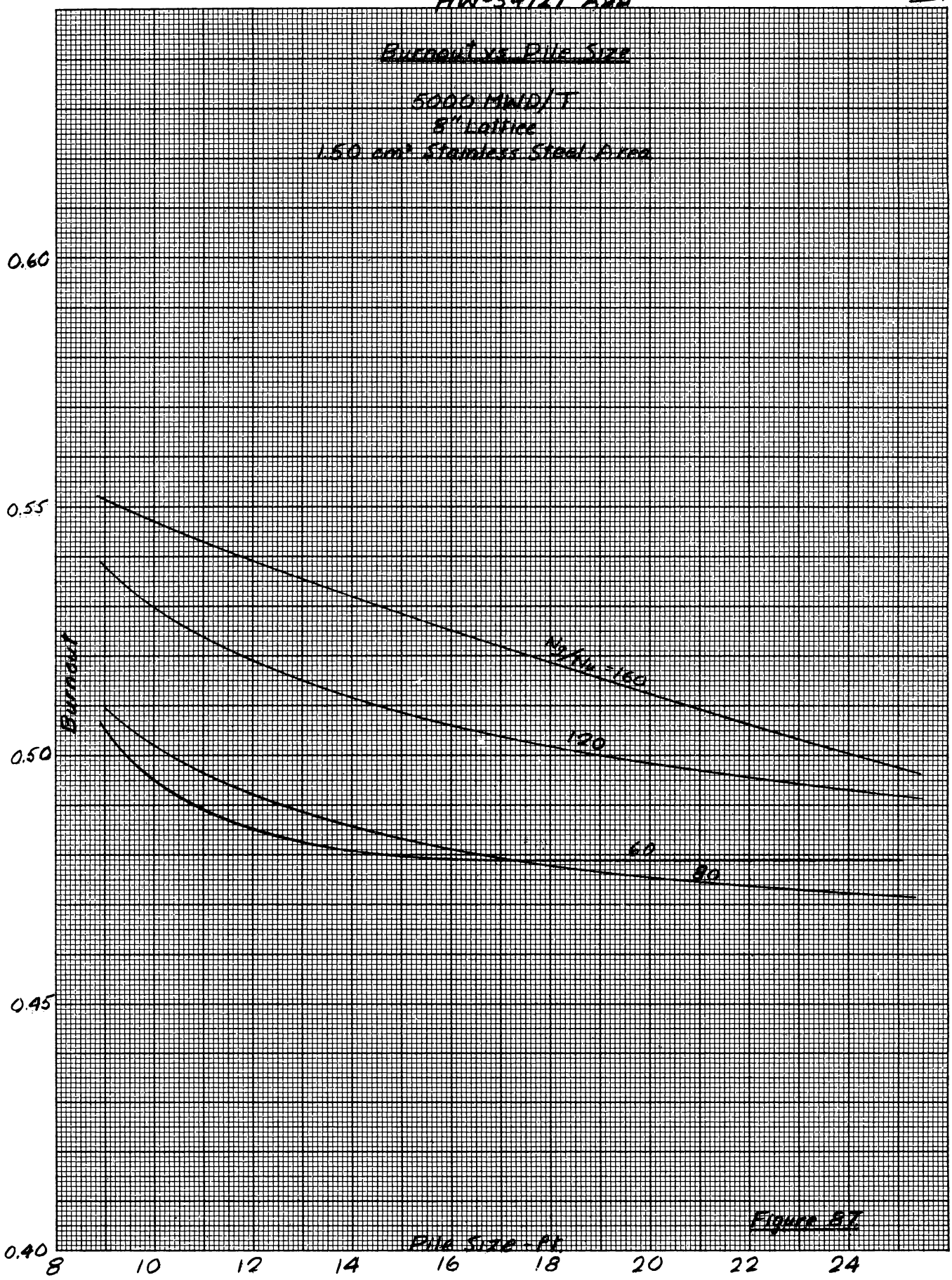
Buckling vs Pile Size
5000 MWD/T
8" Lattice
1.50 cm² Stainless Steel Area
0.60
0.55
0.50
0.45
0.40
Buckling
N_2/K_e = 160
120
60
30
8
10
12
14
16
18
20
22
24
Pile Size - Ft.

Figure 87

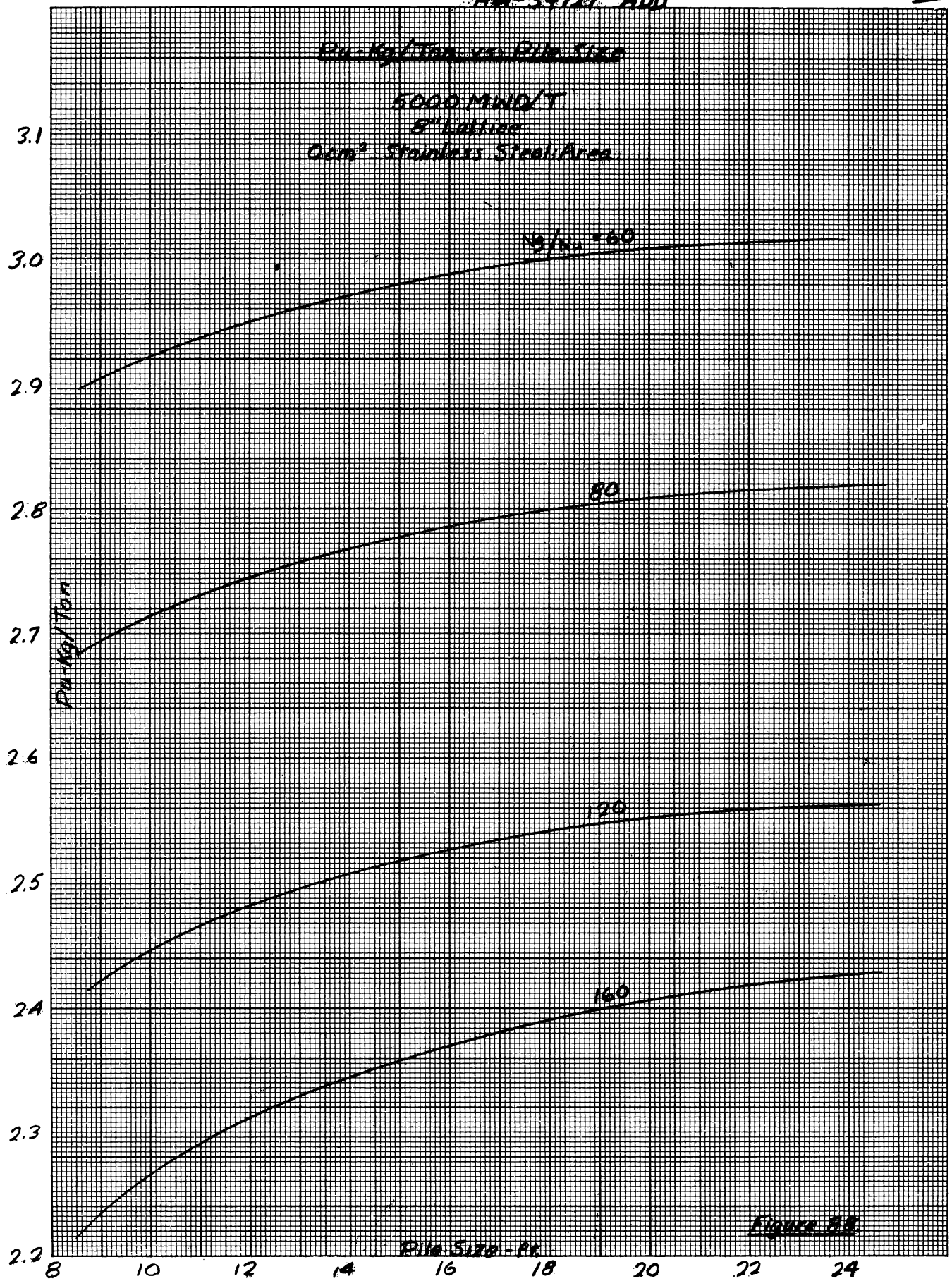
Pu-Kg/Ton vs. Pile Size
5000 MWD/T
8" Lattice
0 cm² Stainless Steel Area
Ng/Nu = 60
80
120
160
Pu-Kg/Ton
3.1
3.0
2.9
2.8
2.7
2.6
2.5
2.4
2.3
2.2
Pile Size - ft.
8
10
12
14
16
18
20
22
24

Figure 88.

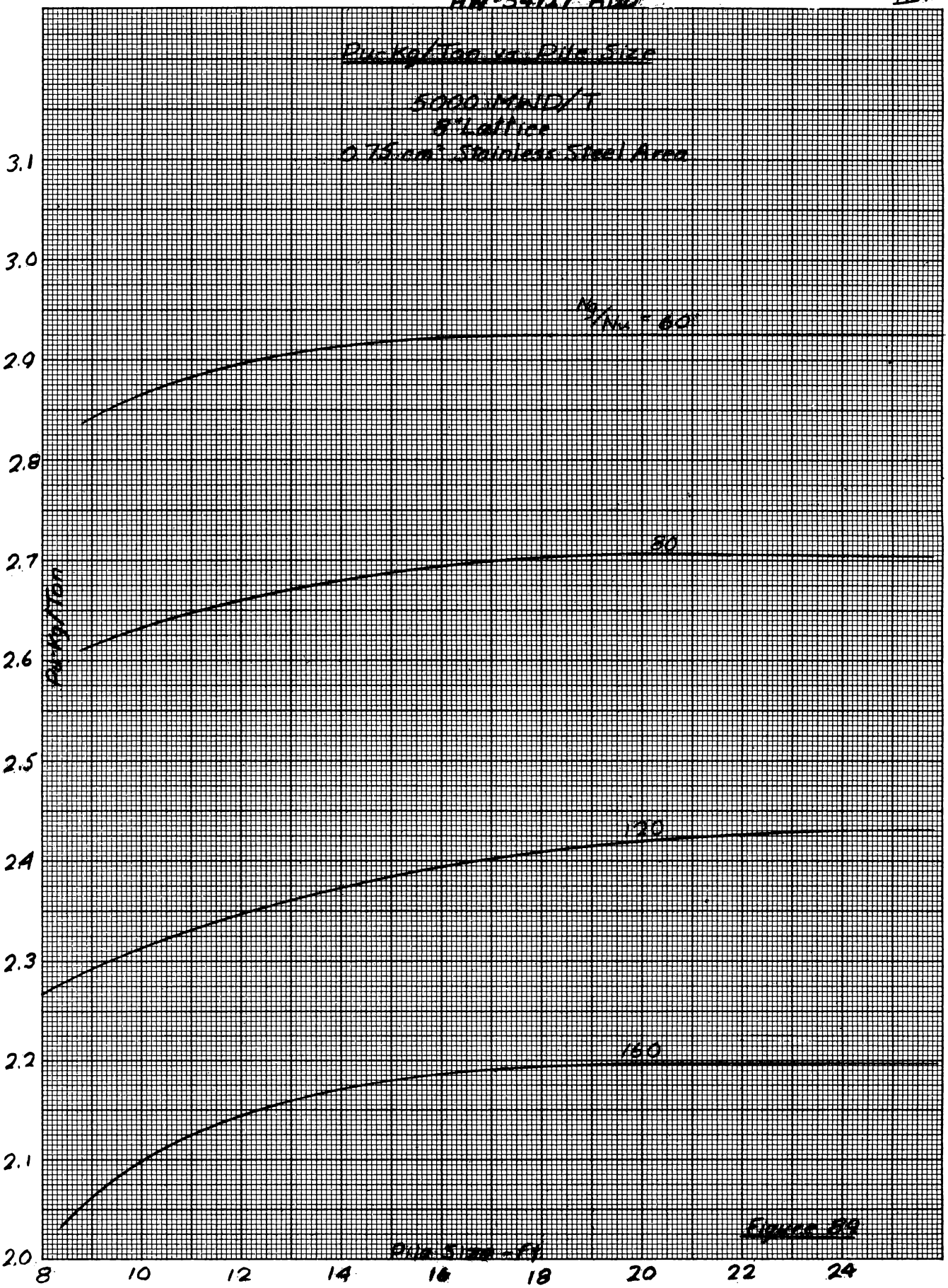
Pu-Kg/Ton vs. Pile Size
50000 MWD/T
8" Lattice
0.75 cm² Stainless Steel Area
N_2/N_{H_2} = 60
80
120
160
Pu-Kg/Ton
3.1
3.0
2.9
2.8
2.7
2.6
2.5
2.4
2.3
2.2
2.1
2.0
8
10
12
14
16
18
20
22
24
Pile Size - Ft

Figure 59

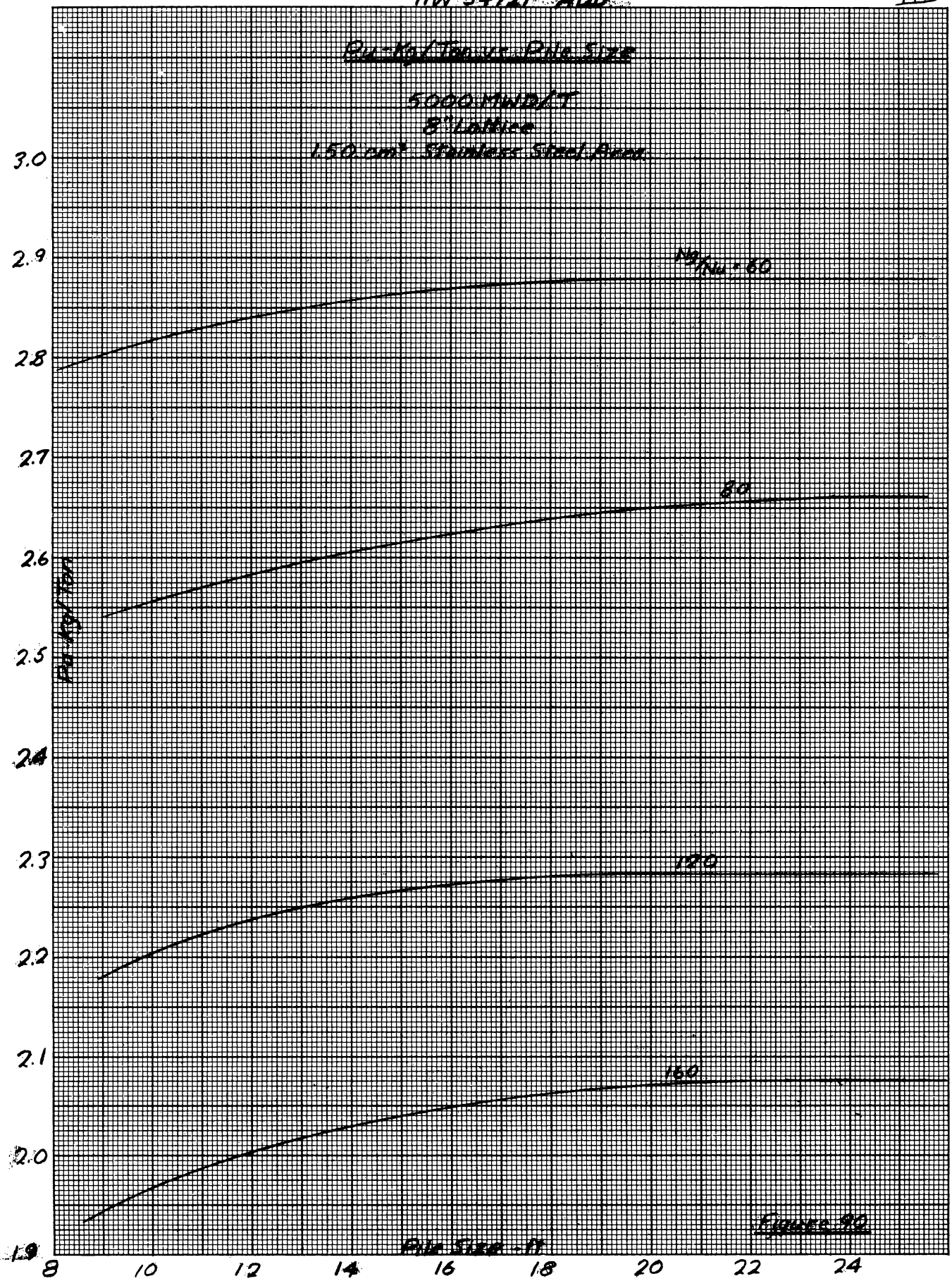
Pu-Kg/Ton vs Pile Size
5000 MWD/T
8" Lattice
1.50 cm² Stainless Steel Area
Ng/Nu = 60
80
120
160
Pu-Kg/Ton
3.0
2.9
2.8
2.7
2.6
2.5
2.4
2.3
2.2
2.1
2.0
1.9
Pile Size - ft
8
10
12
14
16
18
20
22
24

Figure 90

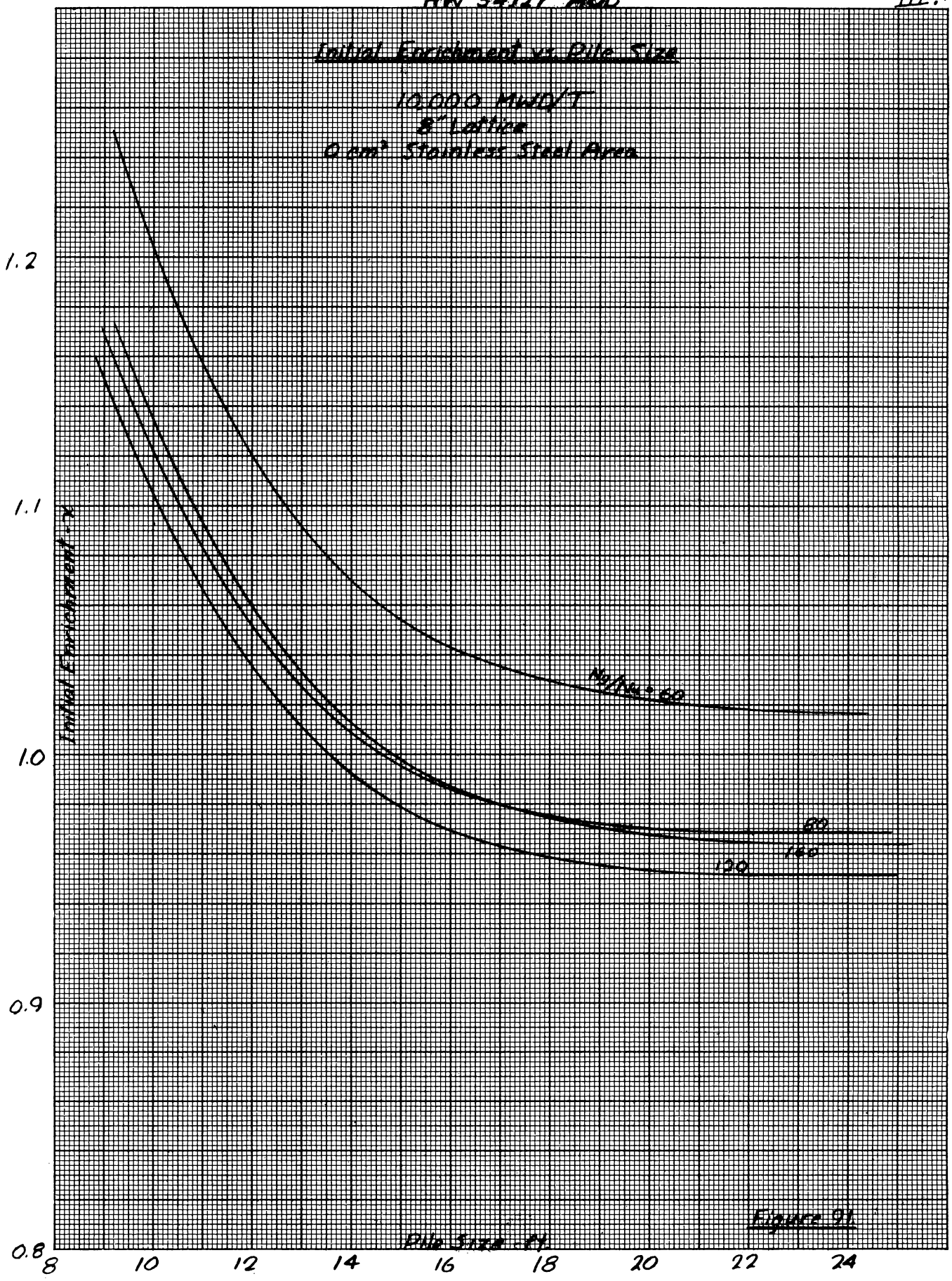
Initial Enrichment vs. Pile Size
10,000 MWD/T
8" Lattice
0 cm² Stainless Steel Area
Initial Enrichment - X
1.2
1.1
1.0
0.9
0.8
Pile Size - ft.
8
10
12
14
16
18
20
22
24
Ng/Nu = 60
80
140
120

Figure 91

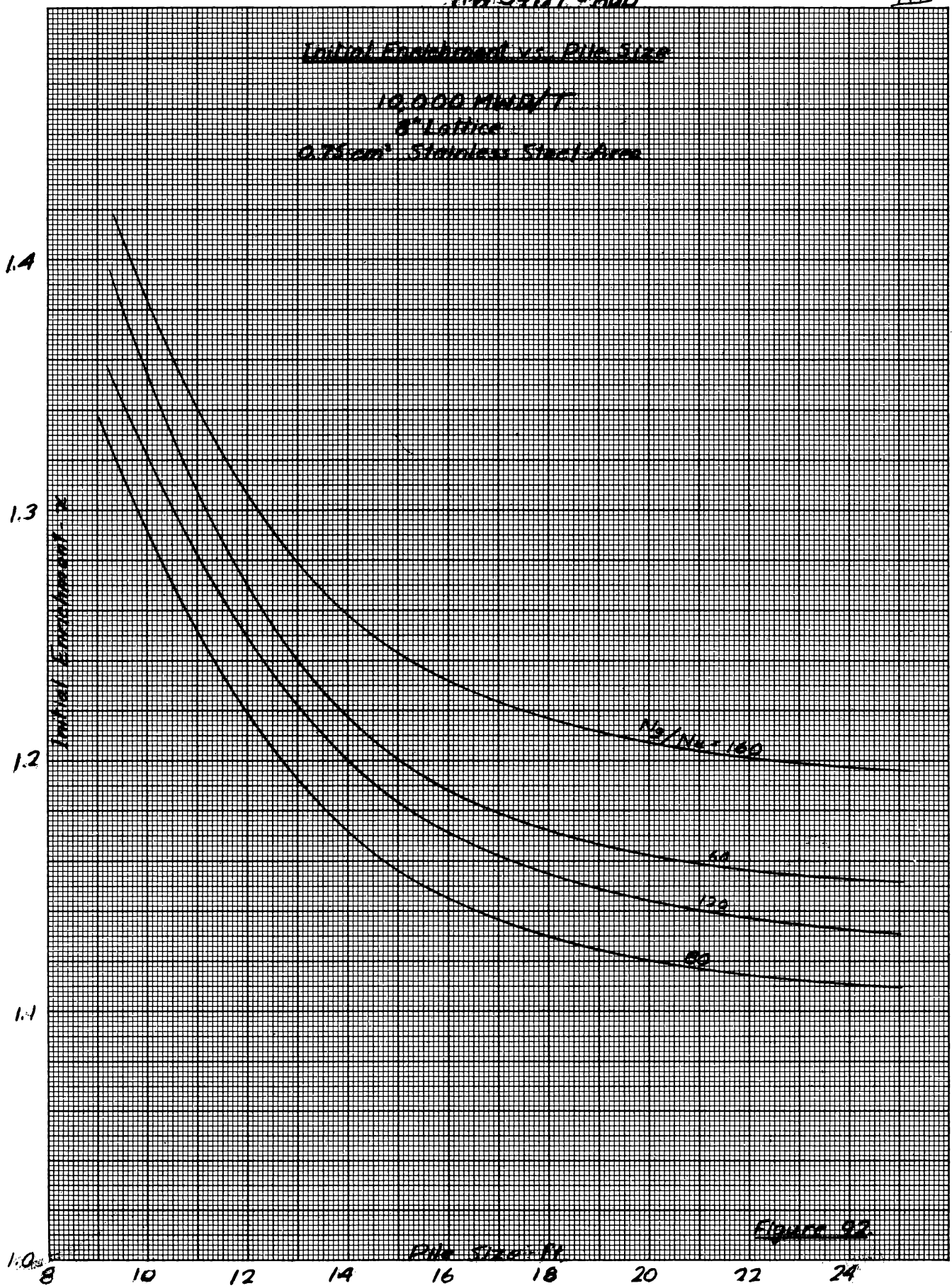
Initial Enrichment vs. Pile Size
10,000 MWD/T
8" Lattice
0.75 cm² Stainless Steel Area
Initial Enrichment - x
1.4
1.3
1.2
1.1
1.0
Ng/Nu = 160
60
120
80
Pile Size - ft
8
10
12
14
16
18
20
22
24

Figure 92

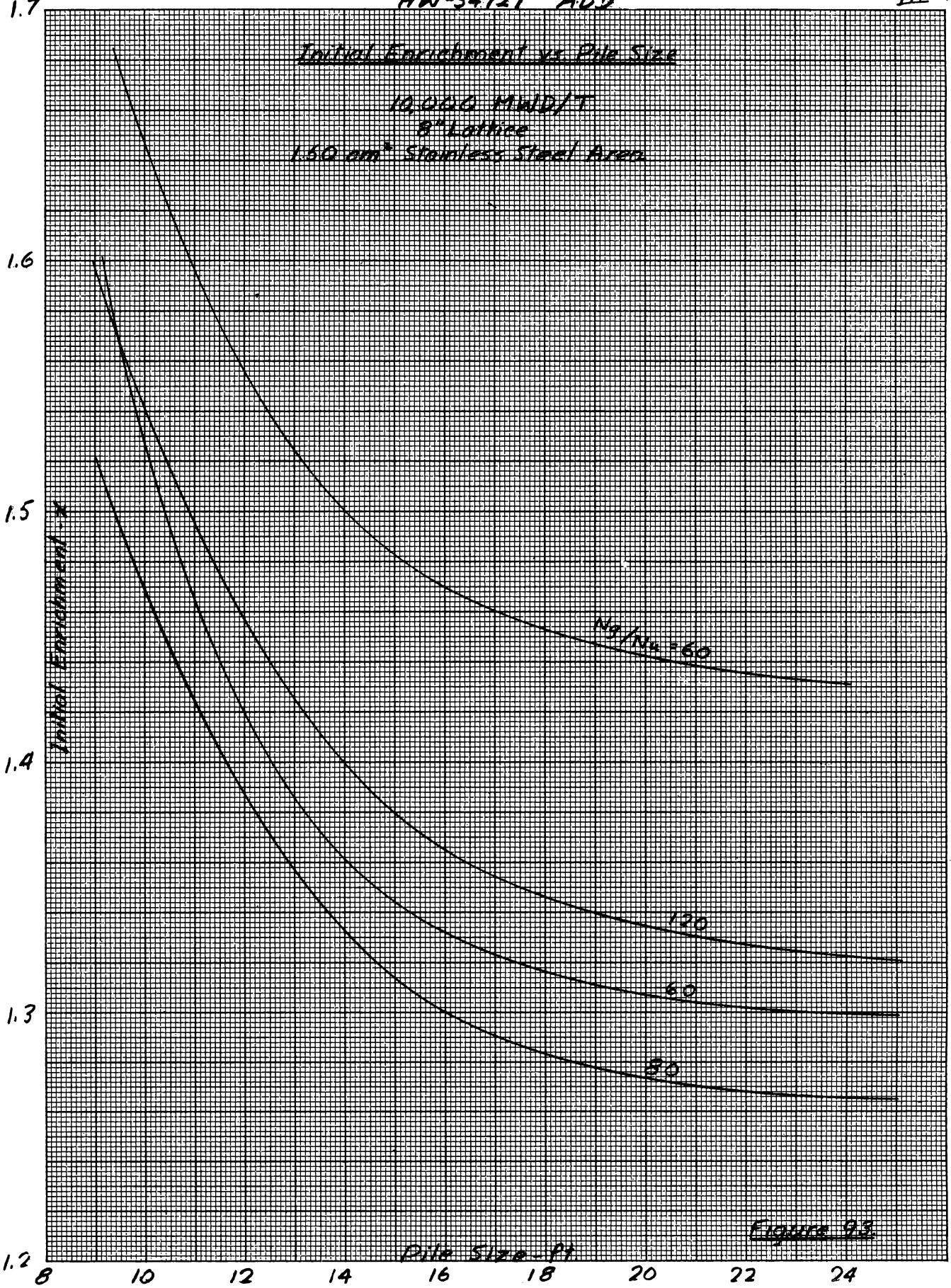
Initial Enrichment vs Pile Size
10,000 MWD/T
8" Lattice
1.60 cm² Stainless Steel Area
Initial Enrichment - w/o
1.7
1.6
1.5
1.4
1.3
1.2
8
10
12
14
16
18
20
22
24
Pile Size - ft
$N_8/N_5 = 60$
120
60
80

Figure 23

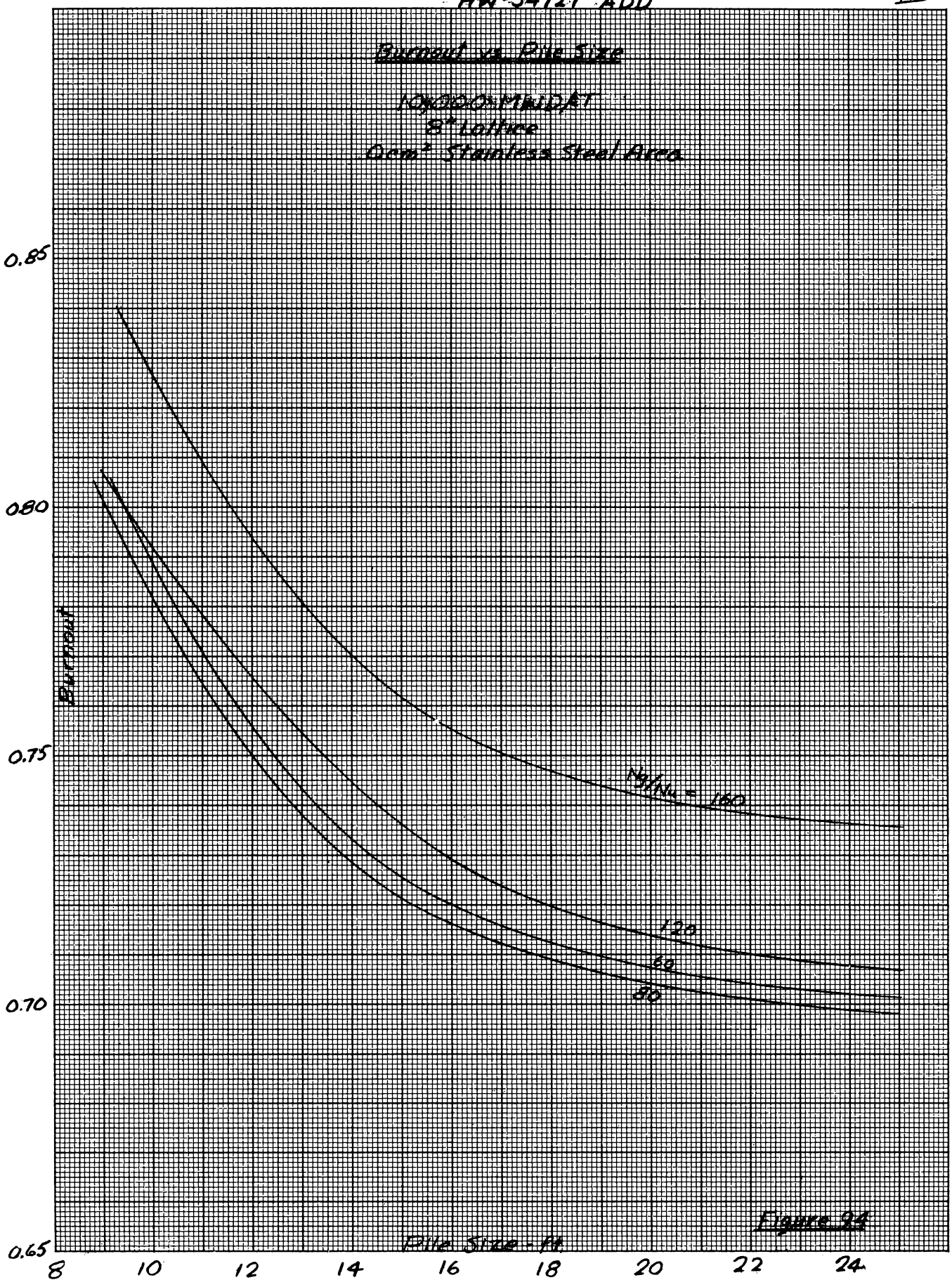
Burnout vs. Pile Size
10,000 MWD/AT
8" Lattice
0cm² Stainless Steel Area
0.85
0.80
0.75
0.70
0.65
Burnout
Ng/Nu = 160
120
60
80
Pile Size - ft
8
10
12
14
16
18
20
22
24

Figure 94

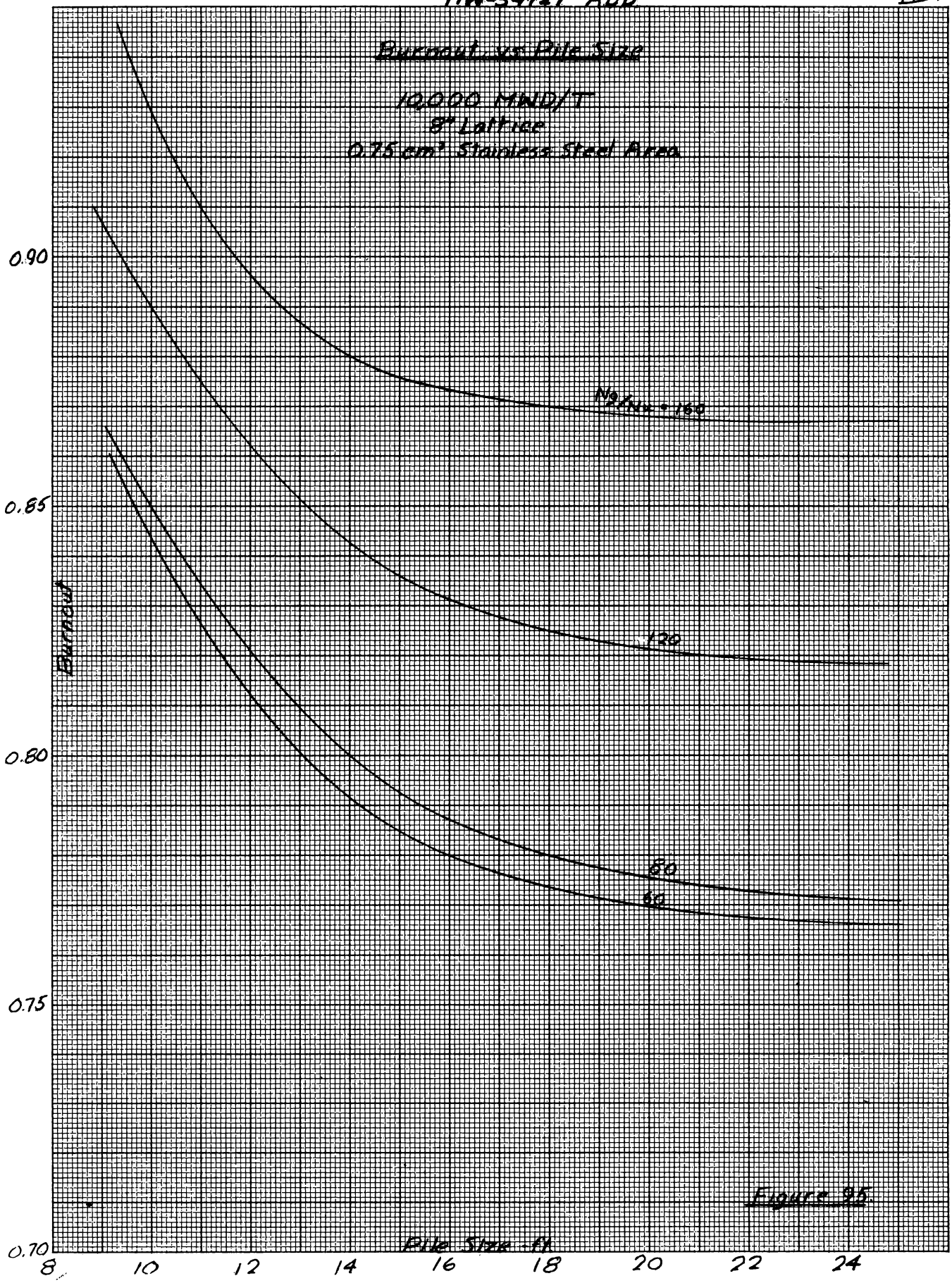
Burnout vs Pile Size
10,000 MWD/T
8" Lattice
0.75 cm² Stainless Steel Area
Ng/Nx = 160
120
80
60
Burnout
0.90
0.85
0.80
0.75
0.70
Pile Size - ft
8
10
12
14
16
18
20
22
24

Figure 95.

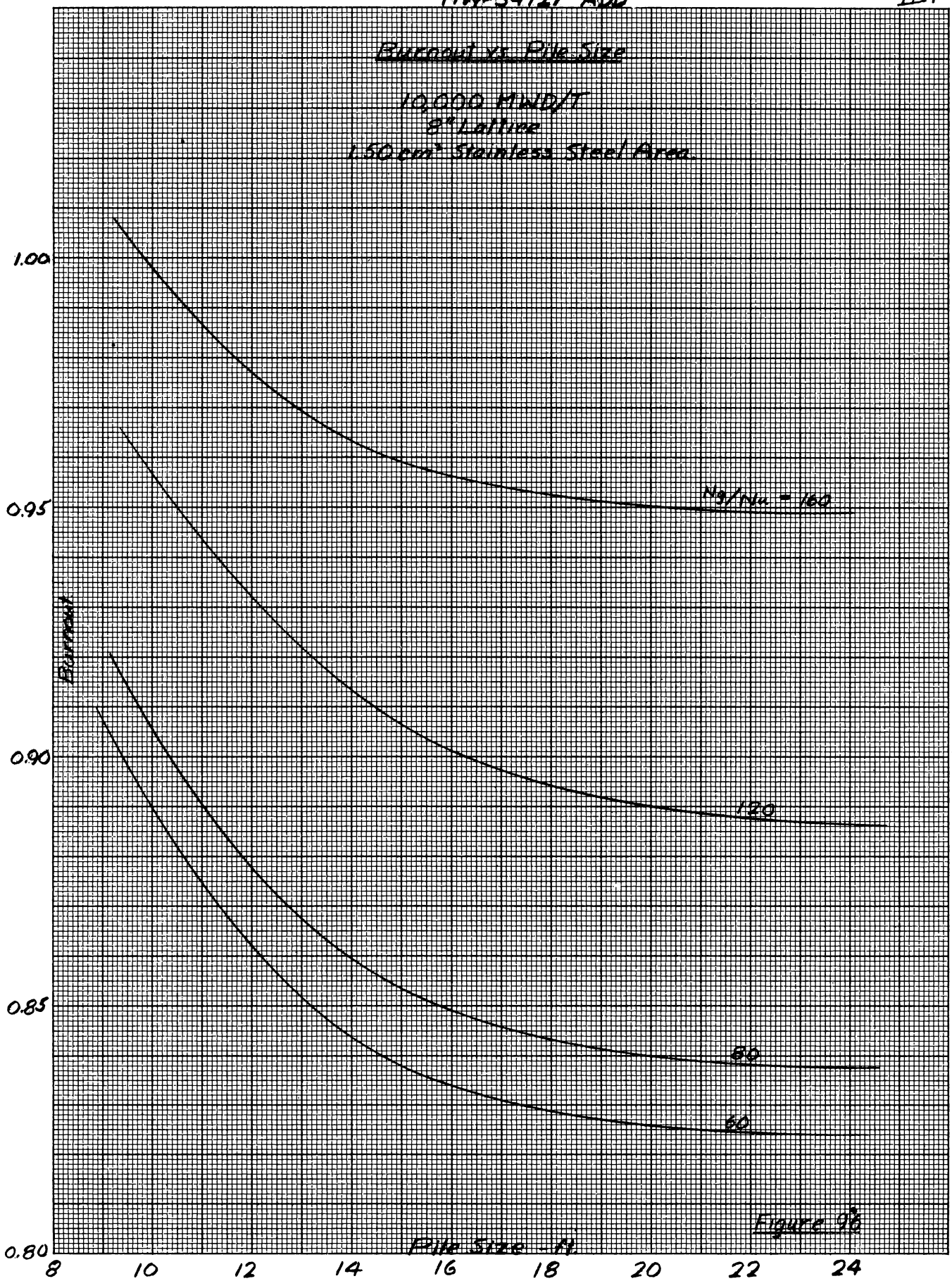
Burnout vs. Pile Size
10,000 MWD/T
8" Lattice
1.50 cm² Stainless Steel/Area
1.00
0.95
0.90
0.85
0.80
Burnout
N9/Nu = 160
120
80
60
8
10
12
14
16
18
20
22
24
Pile Size - ft

Figure 96

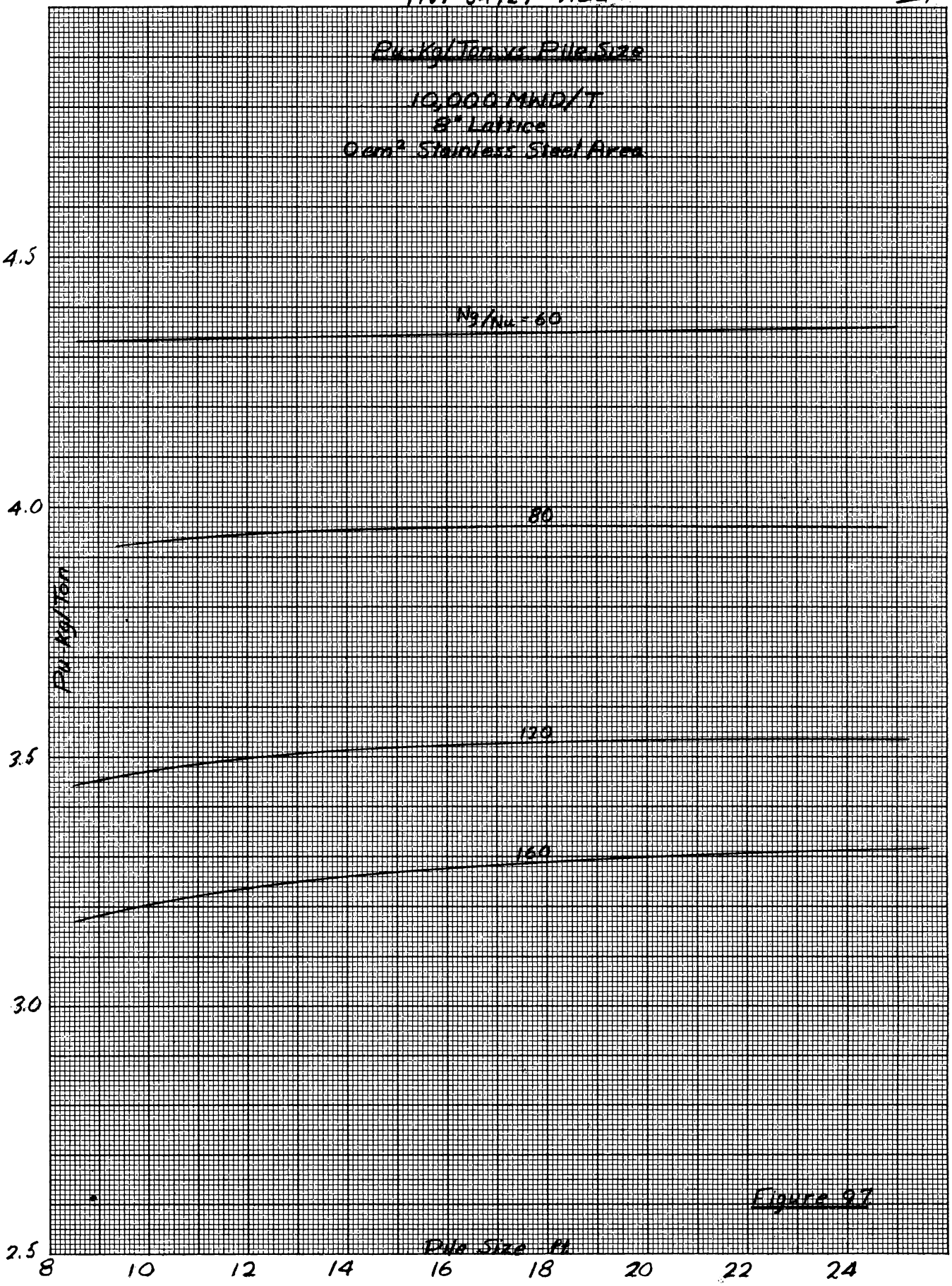
Pu-Kgl Ton vs Pile Size
10,000 MWD/T
8" Lattice
0 cm² Stainless Steel Area
Pu-Kgl/Ton
4.5
4.0
3.5
3.0
2.5
N3/Nu = 60
80
120
160
8
10
12
14
16
18
20
22
24
Pile Size ft

Figure 97

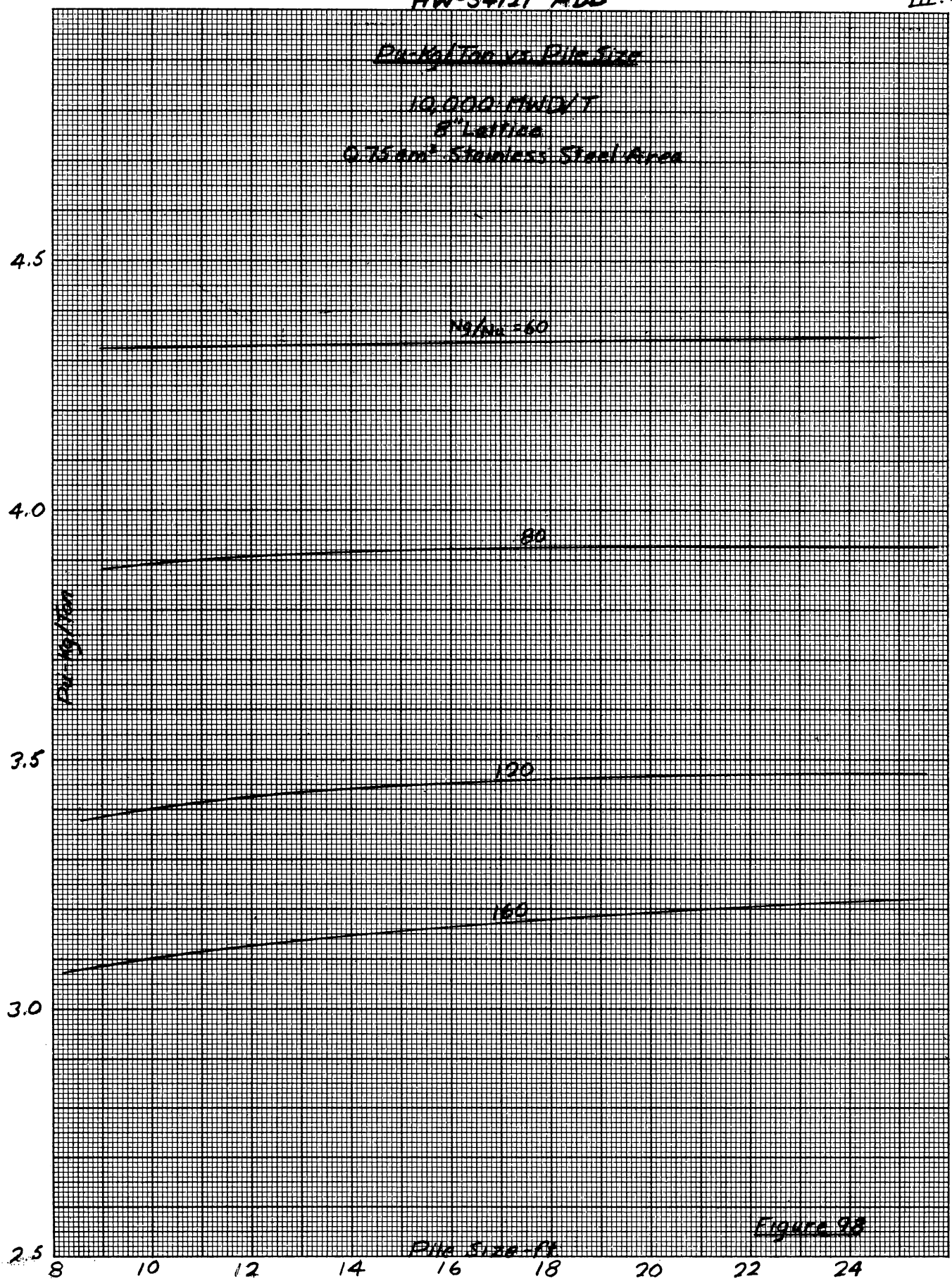
Pu-Kg/Ton vs. Pile Size
10,000 MWD/T
8" Lattice
0.75 cm² Stainless Steel Area
NP/Na = 60
80
100
160
Pu-kg/Ton
4.5
4.0
3.5
3.0
2.5
8
10
12
14
16
18
20
22
24
Pile Size - ft

Figure 98

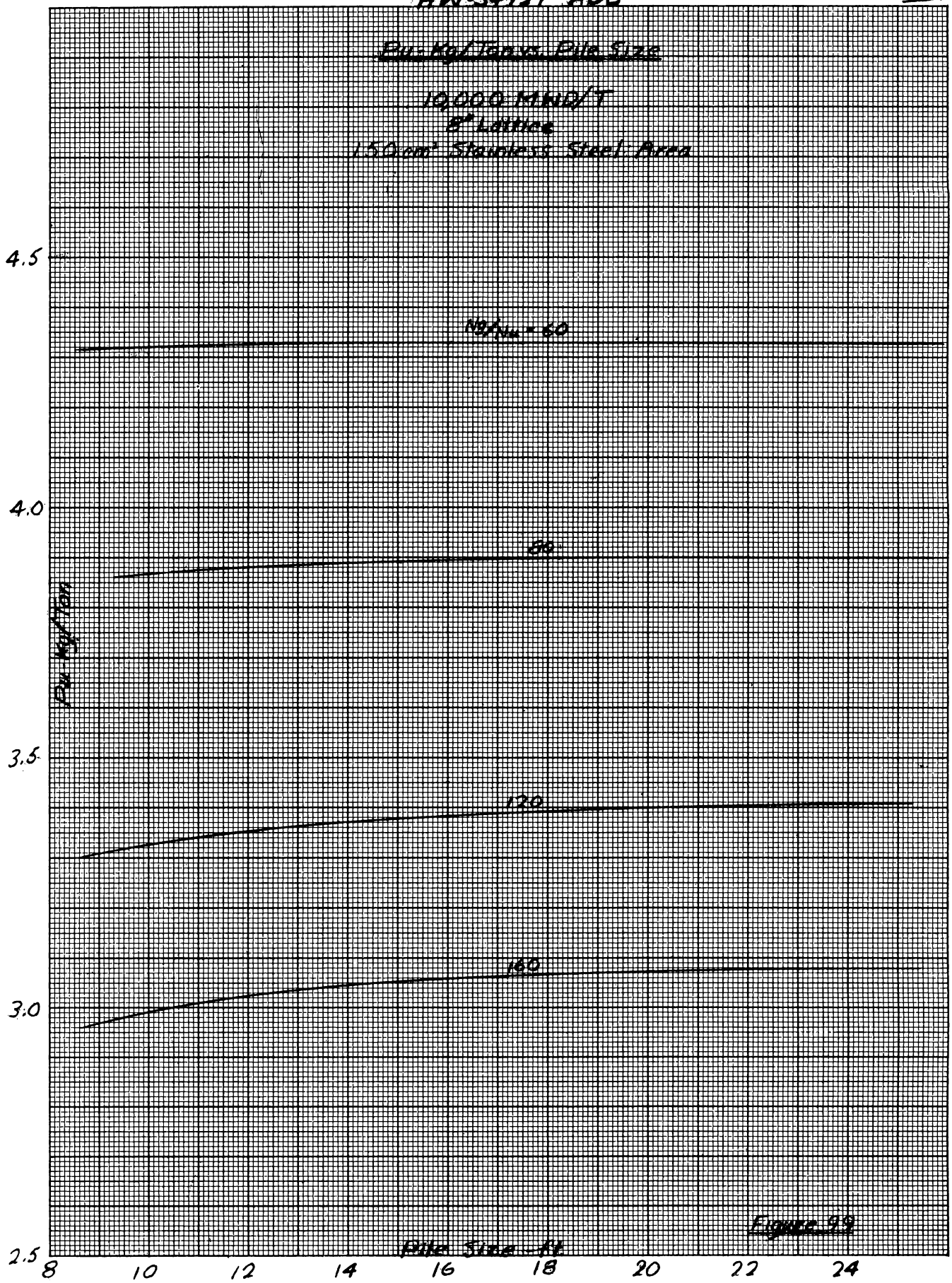
Pu-Kg/Ton vs. Pile Size
10,000 MWD/T
8" Lattice
150 cm² Stainless Steel Area
Ng/Nu = 60
80
120
160
Pu-Kg/Ton
4.5
4.0
3.5
3.0
2.5
Pile Size - ft
8
10
12
14
16
18
20
22
24

Figure 99

SECTION IV

REACTOR HEAT TRANSFER AND FLUID FLOW

by

W. A. Massena
Reactor Design Analysis Operation
Process Design Operation
IRRADIATION PROCESSING DEPARTMENT

REACTOR HEAT TRANSFER AND FLUID FLOW

INTRODUCTION

The purpose of this report is to present the methods and assumptions used to determine the reactor core configuration, fuel element configuration and reactor flow characteristics for each case considered in the preliminary study. It was decided that the cases to be examined would be characterized by the following variables: Reactor power level, coolant bulk ΔT, coolant bulk outlet temperature, specific tube power, lattice spacing and coolant gas. Any combination of these variables fixes the reactor core and fuel element configurations and also the gas flow requirements.

SUMMARY

The active zone length, core diameter and number of fuel-bearing tubes was determined for each case. This information has not been plotted. The number and size of fuel rods in the cluster was calculated for each case. Figures 1 and 2 show the number of rods needed in all the 1000 megawatt and 1500 megawatt cases considered. Reactor flows and pressure drops were computed for each case considered in the study. Pressure drops have been plotted in Figure 3 for the 1000 megawatt, 8-inch lattice cases.

GENERAL REACTOR CHARACTERISTICS

A. Core Geometry

The reactor under consideration is a graphite moderated, pressure vessel type with a cylindrical core. It utilizes a square lattice and square fuel element channels with straight-through cooling. The ratio of core length to core diameter is $\sqrt{\pi}$:1 or approximately 1.77:1.

B. Fuel Element Geometry

The fuel element consists of a cluster of stainless steel clad, massive UO_2 fueled cylinders equally spaced within the flow channel. The UO_2 is clad by swaging the jacket onto it. The number of rods in the cluster is determined by the heat transfer requirements within the channel.

REACTOR CORE CONFIGURATION

For each case of reactor power level, coolant bulk ΔT, reactor bulk outlet temperature, specific tube power and lattice spacing, it is possible to determine the number of fuel-bearing channels and the reactor core diameter and active zone length. The following analyses demonstrate how this was done. Note: The nomenclature is listed on Page 11. Important equations are underlined.

A. Number of Flow Channels Required

It is defined that

(1) $P.L. \times 10^3 = N_T L Q_A$

Also that

(2) $\eta_F = \frac{L\, Q'_A}{L\, Q'_{MA}}$

(3) $\therefore N_T = \frac{P.L. \times 10^3}{\eta_F\, L\, Q'_{MA}}$

For this study

(4) $L = \sqrt{\pi} D$

By definition

(5) $N_T \times \left(\frac{\ell^2}{144}\right) = \frac{\pi}{4} D^2$

Combining Equations (3), (4), and (5) yields

(6) $N_T = 400 \left(\frac{P.L.}{\ell\, Q'_{MA}}\right)^{2/3}$ (with $\eta_F = 0.75$)

B. Active Zone Length

Substituting Equation (4) into Equation (5) yields

(7) $L = \frac{\ell}{6} N_T^{1/2} = 0.167 \ell\, N_T^{1/2}$

FUEL ELEMENT CONFIGURATION

In order to evaluate fuel element fabrication costs and enrichment costs (due to the steel cladding), the size and number of fuel rods required in each case must be computed. In general, enough rods are needed to prevent the maximum allowable cladding temperature or the maximum allowable fuel temperature from being exceeded in the maximum performance tube. The following are calculations of maximum power tube parameters which are ultimately used to calculate n_r, the number of fuel rods in the cluster.

A. Maximum Power Tube Flow Rate

In order to obtain the minimum total gas flow through the reactor, all power tubes should have the same outlet temperature. Since the radial heat generation is not uniform, this requires that the power-producing tubes be orificed in each channel.

It is defined then, that

$$(8)\quad \eta \text{ or } = \frac{c_p \Delta T_{bulk}}{c_p \Delta T_{max.}}$$

Since

$$(9)\quad W c_p \Delta T_{max.} = 3413\ L\ Q'_{MA}$$

Substituting

$$(10)\quad W = \frac{\eta \text{ or } 3413\ L\ Q'_{MA}}{c_p \Delta T_{bulk}}$$

For the two gases considered, helium and nitrogen, c_p can be approximated in the temperature range of 600 - 1400° F by an equation of the form

$$(11)\quad c_p = c_1 + c_2\ T$$

To simplify computation, an average c_p is defined for each case at

$$(12)\quad T = T_i + \frac{\Delta T_{bulk}}{2}$$

---

where

$$T_i = T_o - \Delta T_{bulk}$$

B. Coolant Longitudinal Temperature Distribution

In a cylindrical reactor with reflector, the longitudinal heat generation is approximated by a chopped cosine curve. This means that

$$(13)\quad Q'_{(x)} = Q'_{max} \sin \frac{\pi (x + Z)}{L + 2Z}$$

The average heat generation Q'_{MA} is related to Q'_{Max} by

$$(14)\quad Q'_{MA} = \frac{Q'_{max}}{L} \int_{0}^{L} \sin \frac{\pi (x + Z)}{L + 2Z}\ dx$$

Integrating Equation (14) yields

$$(15)\quad Q'_{max} = \frac{\pi L Q'_{MA}}{(L + 2Z)\left[\cos\frac{\pi Z}{L + 2Z} - \cos\frac{\pi(L + Z)}{L + 2Z}\right]}$$

By performing a heat balance on the fuel element and coolant, it can be shown that

$$(16)\quad T_{(x)} - T_i = \frac{3413}{W c_p}\int_0^x Q'dx \qquad (1)$$

Substituting Equations (10), (13), and (15) into Equation (16) and integrating yields

$$(17)\quad T_{(x)} = T_i + \frac{\Delta T_{bulk}}{\eta} \text{ or } \frac{\left[\cos\frac{\pi Z}{L + 2Z} - \cos\frac{\pi(x + Z)}{L + 2Z}\right]}{\left[\cos\frac{\pi Z}{L + 2Z} - \cos\frac{\pi(L + Z)}{L + 2Z}\right]}$$

C. Fuel Cross Sectional Area

The cross sectional area A_f of UO_2 in the flow channel is determined by the moderator-to-uranium ratio Ng/Nu and the lattice spacing:

$$(18)\quad A_f = 0.75\ell^2 \frac{Nu}{Ng}\frac{\rho g}{\rho UO_2} \times \frac{\text{Mol. Wt of } UO_2}{\text{Mol. Wt of graphite}}$$

Simplifying and inserting the proper constants yields

$$(19)\quad A_f = .0368\ell^2 \qquad \frac{Ng}{Nu} = 75 \qquad \rho_g = 1.6 \qquad MW_g = 12.01$$

$$\rho_{UO_2} = 9.776 \qquad M.W._{UO_2} = 270$$

Therefore

$$(20)\quad r_i = \ell\left[\frac{.0368}{\pi n_r}\right]^{\frac{1}{2}}$$

and

$$(21)\quad r_o = r_i + 12\,d$$

D. Gas Film Coefficient

The coolant channel was chosen to have a cross sectional area equal to one-quarter of the lattice area. Using this relationship, the mass flow rate G is determined by

$$(22) \quad G = \frac{144\ W}{0.25\ell^2 - n_r \pi r_o^2}$$

Likewise

$$(23) \quad D_e = \frac{4 \times \text{Flow Area}}{\text{Wetted Perimeter}} = \frac{.0417\ (\ell^2 - 4\ n_r \pi r_o^2)}{\ell + n_r \pi r_o}$$

The gas film coefficient h is calculated from a modified form of the Dittus-Boelter equation which utilizes the fact that the Prandtl numbers of the gases under consideration (helium and nitrogen) are close to 0.7.

$$(24) \quad h = \frac{.027\ c_p\ G^{0.8}\ \mu^{0.2}}{D_e^{0.2}} \qquad (2)$$

The viscosity of both helium and nitrogen can be represented with reasonable accuracy by an equation of the form

$$(25) \quad \mu = c_1 + (c_2 \times T)$$

in the temperature range of this study.

E. Fuel Element Requirements

Two fuel element temperature limits are specified; the maximum allowable cladding temperature T_j and the maximum fuel central temperature T_c. The first limit becomes operative at higher values of heat flux. The primary heat transfer requirement is that there be sufficient fuel element surface area to prevent either the cladding temperature limit or the fuel rod central temperature limit from being exceeded.

Assuming uniform heat generation Q' in the fuel, the ΔT from the fuel rod axis to the coolant is given by

$$(26) \quad \Delta T = \left[\frac{1}{4\pi k_f} + \frac{12}{2\pi r_i h_i} + \frac{1}{2\pi k_j} \ln \frac{r_o}{r_i} + \frac{12}{2\pi r_o h} \right] \frac{3210\ Q'_{(x)}}{n_r}$$

If the fuel rod is central temperature limited,

$$(27)\quad n_r = \left[\frac{1}{4\pi k_f} + \frac{12}{2\pi r_i h_i} + \frac{1}{2\pi k_j} \ln \frac{r_o}{r_i} + \frac{12}{2\pi r_o h}\right] \frac{3210\, Q'_{(x)}}{T_c - T_{(x)}}$$

The ΔT from the axis of the rod to the inner surface of the jacket is

$$(28)\quad \Delta T = \left[\frac{1}{4\pi k_f} + \frac{12}{2\pi r_i h_i}\right] \frac{3210\, Q'_{(x)}}{n_r}$$

Therefore, the fuel rod will be central temperature limited only if

$$(29)\quad T_c - T_j < \left[\frac{1}{4\pi k_f} + \frac{12}{2\pi r_i h_i}\right] \frac{3210\, Q'_{(x)}}{n_r}$$

or

$$(30)\quad n_r < \left[\frac{1}{4\pi k_f} + \frac{12}{2\pi r_i h_i}\right] \frac{3210\, Q'_{(x)}}{T_c - T_j}$$

When the jacket temperature limit applies, n_r will be given

$$(31)\quad n_r = \left[\frac{1}{2\pi k_j} \ln \frac{r_o}{r_i} + \frac{12}{2\pi r_o h}\right] \frac{3210\, Q'_{(x)}}{T_j - T_x}$$

F. Longitudinal Position of Maximum Fuel Element Temperatures

In order to utilize the fuel element temperature limits, it is necessary to know the position (along the flow channel) of the maximum fuel temperatures. The position, x_{max}, of the maximum jacket temperature T_j is determined by

$$(32)\quad x_{max} = \frac{L + 2Z}{\pi} \tan^{-1} \left[\frac{-\pi W c_p \left(\frac{1}{h} + \frac{d}{k_j}\right)}{h A_h}\right] - Z \quad (3), (7)$$

The position, x'_{max}, of the maximum fuel temperature T_c is obtained from

$$(33)\quad x'_{max} = \frac{L + 2Z}{\pi} \tan^{-1} \left[\frac{-\pi W c_p \left(\frac{1}{h} + \frac{d}{h_j} + \frac{r_i}{2k_f}\right)}{h A_h}\right] - Z \quad (3), (7)$$

where

(34) $A_h = 0.167\, n_r\, \pi\, r_o\, L$

G. Method of Solution for n_r

All computations through Equation (15) are performed sequentially for any case. It is then necessary to guess an x to use in Equation (17). This x corresponds to x_{max} or x'_{max} depending on which fuel element temperature limit applies.

To use Equation (20), it is necessary to estimate n_r in order to determine r_i and r_o. G, D_e and h are calculated using this estimated r_o. Equation (30) is used to determine whether to use Equation (27) or (31) for calculating n_r. The proper equation is then solved for n_r using the estimated values of r_i and r_o. This procedure is repeated until the estimated n_r and the calculated n_r agree.

The next step is to calculate A_h and solve for x_{max} or x'_{max} whichever is applicable. If this value does not agree with the value chosen at Equation (17), a new x is chosen and the whole cycle repeated.

Because of the two trial and error solutions and the general length of the computation, the necessary equations were programmed on the IBM-650 digital computer which was able to do a case every two minutes. n_r was calculated for each of the 324 cases considered. A plot of n_r versus Q_{MA} for the 1000 megawatt and 1500 megawatt cases utilizing a 6 and 8 inch lattices is given in Figures 1 and 2. The 500 megawatt case was not plotted because fuel costs were much higher than for the other two cases.

REACTOR FLOW CHARACTERISTICS

Reactor pressure drop contributes a significant portion of the system pumping costs. The total reactor pressure drop consists of several parts; the inlet contraction loss, the drop through the active zone and reflectors and the outlet expansion loss. The following analysis describes the computation of these values.

A. Reactor Inlet Pressure

Reactor inlet pressure is determined by using the maximum allowable pressure for the pressure vessel required in each case using a 4-1/2 inch vessel wall thickness. Seven and one-half feet are added to the core diameter to allow for the reflector, thermal shield and gas annulus, so that

(35) $R = 6\,(D + 7.5)$

The allowable inlet pressure P_o is then given by

(36) $P_o = \dfrac{62{,}000}{R + 2.64}$ (4)

B. Reactor Pressure Drop

1. Active zone- ΔP across the active zone is given by

$$\Delta P = G^2 \frac{(v_L - v_o)}{g} + \frac{fL}{D_e} \frac{G^2 v_m}{2g} \quad (5) \quad (37)$$

where

$$v_m = \frac{v_L + v_o}{2} \quad (38)$$

as a good approximation.

2. Inlet loss- ΔP is given by

$$\Delta P = 0.5 \frac{G^2 v_o}{2g} \quad (6) \quad (39)$$

3. Outlet loss- ΔP is given by

$$\Delta P = \frac{G^2 v_L}{2g} \quad (6) \quad (40)$$

4. Reflector regions - ΔP is given by

$$\Delta P = \frac{6 f B}{l} \frac{G_2^2}{2g} (v_o + v_L)$$

or

$$\Delta P = \frac{12 f B}{l} \frac{G_2^2}{2g} v_m \quad (41)$$

where

$$G_2 = G\left(\frac{l^2 - 4 n_r \pi r_o^2}{l^2}\right)$$

Total ΔP is then

$$\Delta P = \frac{G^2}{2g} (3 v_L - 1.5 v_o + \frac{fL}{D_e} v_m) + \frac{12 f B}{l} \frac{G_2^2}{2g} v_m \quad (42)$$

Reactor pressure drops were computed for each of the cases considered. To speed up calculation, the foregoining equations were programmed on the IBM-650 digital computer. The results for the 1000 megawatt, 8-inch lattice cases are shown in Figure 3 for both helium and nitrogen coolants.

REFERENCES

(1) Glasstone, Principles of Nuclear Reactor Engineering, 1st ed., Van Nostrand Book Co., July 1955, p. 669.

(2) The Reactor Handbook, Vol. II, 1st ed. May 1955, Technical Information Service, AEC, p. 425.

(3) Glasstone, op. cit., p. 672.

(4) Section VI, Reactor Core Arrangement and Vessel Studies, E. R. Rudock,

(5) The Reactor Handbook, op. cit., p. 412.

(6) Bonilla, C. F., Nuclear Engineering, 1st ed., McGraw-Hill Book Co., 1957, p. 316.

(7) Bonilla, op. cit., p. 436.

NOMENCLATURE

P.L.	power level, megawatts
N_T	number of fuel channels
L	active zone length, feet
Q'_A	average specific tube power, KW/Ft.
Q'_{MA}	average specific tube power in maximum power tube, KW/Ft.
η_F	flattening efficiency
D	core diameter, feet
ℓ	lattice spacing, inches
η or	orificing efficiency
c_p	specific heat of coolant gas, BTU/lb-^oF
ΔT_{bulk}	bulk temperature increase across the reactor, ^oF
W	flow rate in maximum power tube, lb/hr.
T_i	bulk inlet temperature, ^oF
T_o	bulk outlet temperature, ^oF
Q'_x	specific tube power at position x in maximum power tube, KW/Ft.
Q'_{max}	maximum specific tube power in maximum power tube, KW/Ft.
x	distance along channel measured from inlet end of active zone, Ft.
Z	extrapolation distance, Ft.
$T_{(x)}$	coolant temperature at x, ^oF
n_r	number of fuel rods in bundle
r_i	inside radius of fuel rod jacket, inches
r_o	outside radius of fuel rod jacket, inches
d	jacket thickness, feet
G	max flow rate, lb/hr-ft^2

NOMENCLATURE (Cont)

μ	viscosity, lb/hr-ft.
h	gas film heat transfer coefficient, Btu/hr-ft^2-^{o}F
k	thermal conductivity, Btu/hr-ft-^{o}F
h_i	heat transfer coefficient of fuel cladding bond, Btu/hr-ft^2-^{o}F
A_h	total fuel element surface area, sq. ft.
Q	volume heat generation, Btu/ft^3-hr.
α	linear coefficient of thermal expansion, in/in-^{o}F
E	modulus of elasticity, psi
ν	Poisson's ratio
ϵ	strain, in/in.
R	radius of pressure vessel, inches
v_o	inlet specific volume, ft^3/lb.
v_L	maximum power tube outlet specific volume, ft^3/lb.
f	friction factor
B	reflector thickness, ft.
A_f	cross sectional area of fuel, inches^2
C_1, C_2	constants for establishing linear functions for temperature change of C_p and μ

Constants are:

	C_p		μ	
	C_1	C_2	C_1	C_2
He	1.248	----	0.0465	0.000044
N_2	0.242	0.0000284	0.0506	0.0000341

g	conversion constant, 4.17 x 10^8 ft lb $_{mass}$/hr^2 lb $_{force}$
G_2	mass flow rate in reflector region, lb/hr ft^2
ΔT max	maximum power tube temperature increase across reactor, ^{o}F

Subscript

f	fuel
j	jacket

Number of Rods and Diameter as a Function of Specific Power

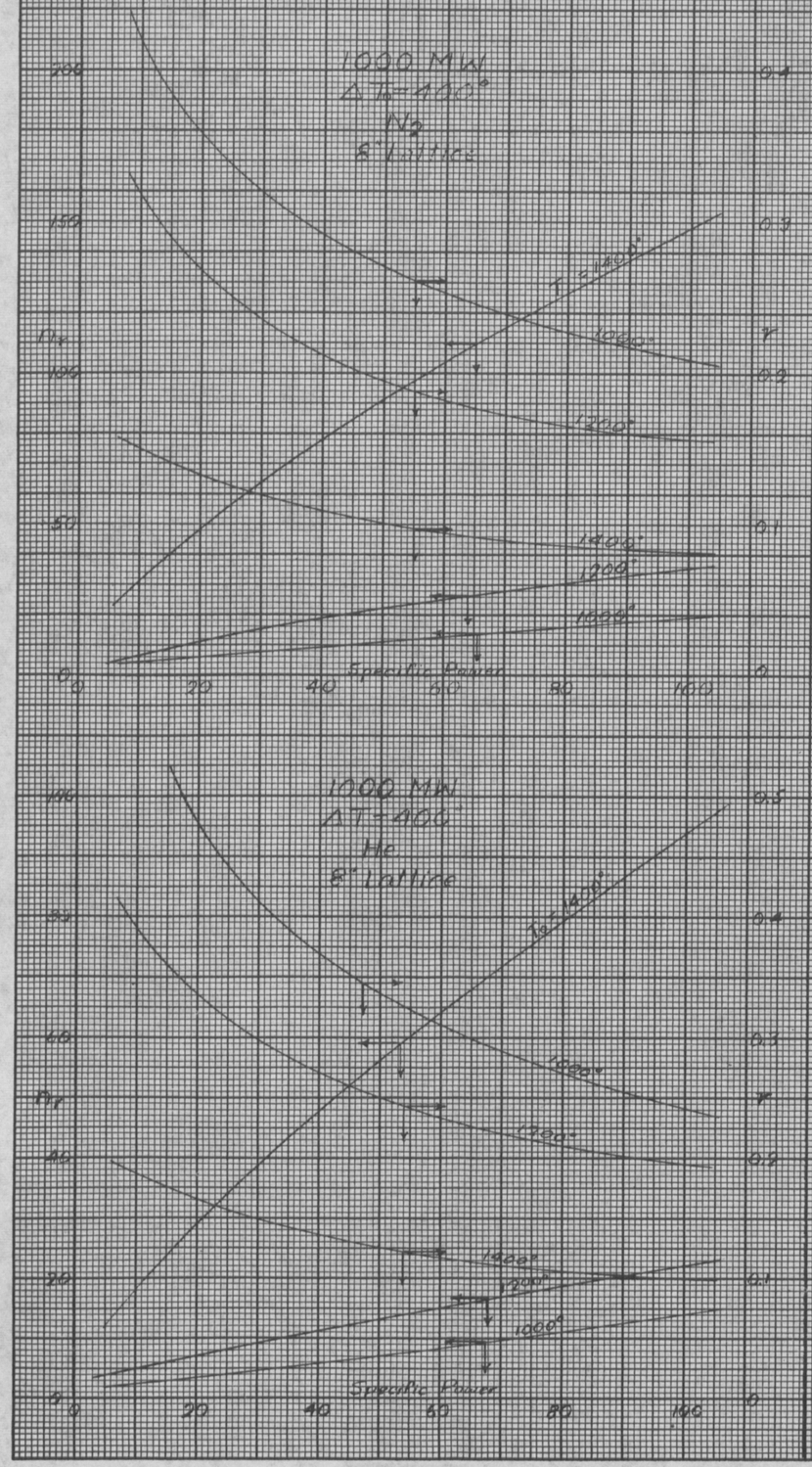

Figure 1

470381 O—58 (Face p. 138) No. 1

Number of Rods and Diameter as a Function of Specific Power

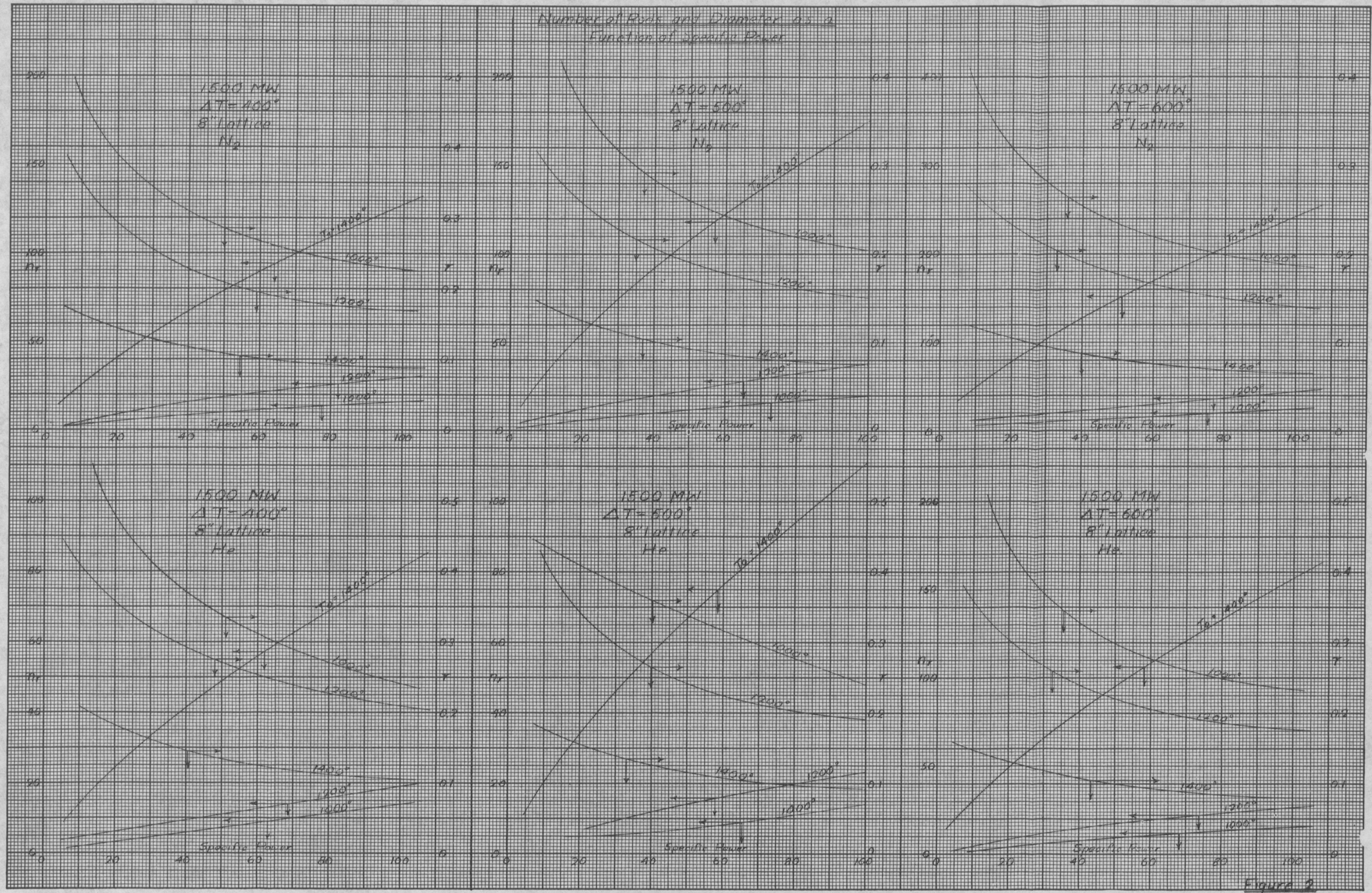

Figure 2

470381 O—58 (Face p. 138) No. 2

470381 O—58 (Face p. 138) No. 3

Reactor Pressure Drop as a Function of Specific Power

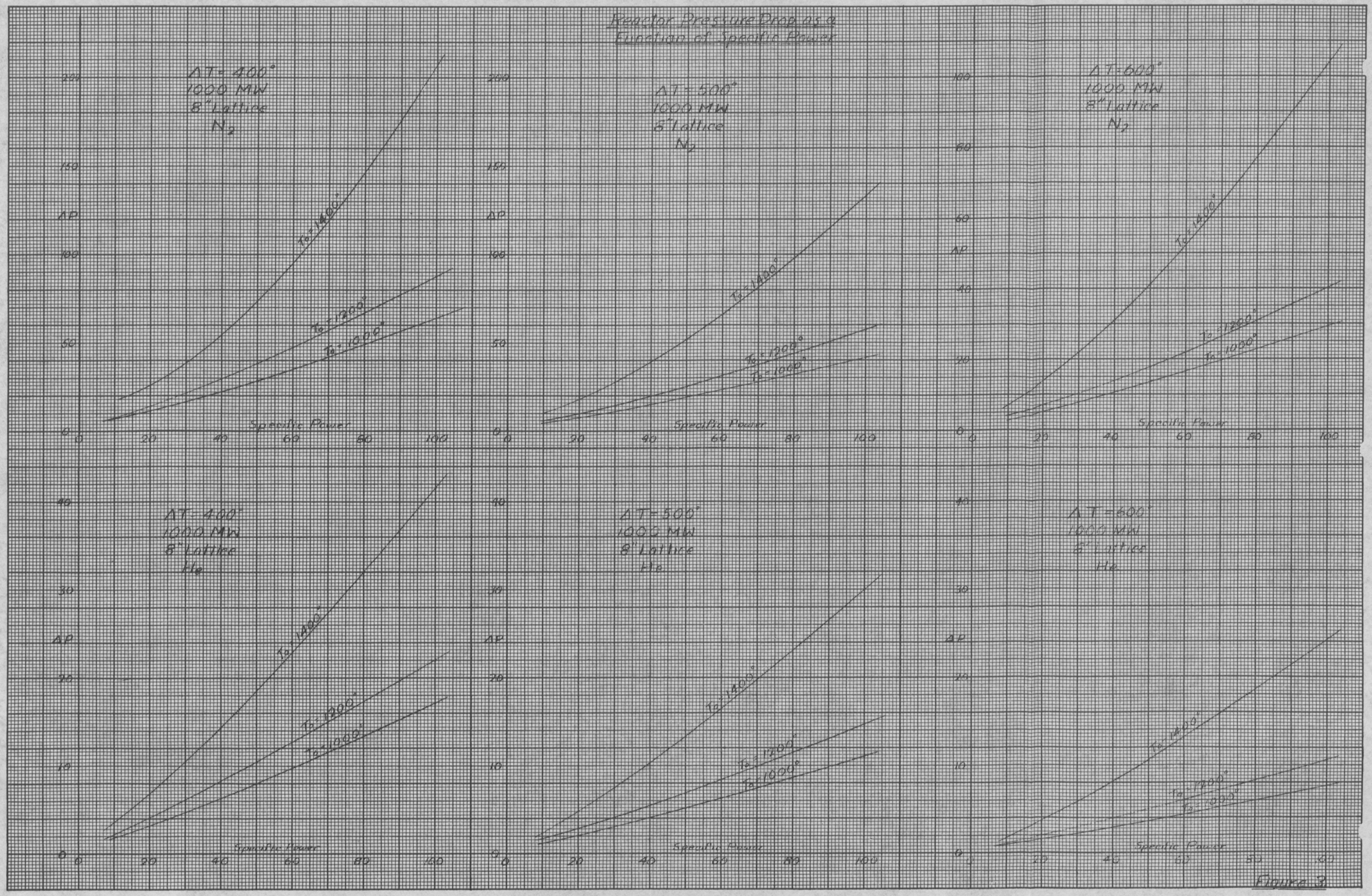

Figure 3

SECTION V

COOLANT GAS SELECTION FOR A GAS COOLED REACTOR

by

E. R. Rudock
Process Design Operation
IRRADIATION PROCESSING DEPARTMENT

COOLANT GAS SELECTION FOR A GAS COOLED REACTOR

ABSTRACT

This report has been prepared in connection with the design study for a High Temperature, Gas Cooled, Closed Loop, Direct Cycle Reactor and Power Plant now in progress at H.A.P.O. It is primarily intended to provide the background and basis for the selection of a coolant gas for the above type of power plant at reactor outlet gas temperatures between 1000° F and 1400° F. This report compares the effect of various gases on plant efficiencies, equipment and fuel elements and outlines the chemical and nuclear properties of several gases.

Comparison of several gases for the same thermodynamic and heat transfer requirements has shown that carbon dioxide will yield the highest plant efficiencies and require the lowest turbine and reactor rating for a given plant capacity. Helium will yield the next highest efficiencies. Carbon dioxide cannot be used as a coolant in the reactor type considered for this report. With the exception of the section on thermodynamics, the discussion in this report on gas coolants would also apply to a Dual Cycle Gas-Steam Reactor Power Plant.

TABLE OF CONTENTS

	Page No.
Abstract	V-1
Introduction	V-3
Conclusions	V-3
Summary	V-4
Discussion	V-6
Chemical Properties	V-6
Fuel Element Limits	V-7
Nuclear Properties	V-9
Radioactivity of Coolants	V-9
Decontamination	V-10
Thermodynamics	V-11
Heat Transfer	V-11
Equipment Size and Cost	V-12
Cost and Availability of Gases	V-13
Design and Operational Problems	V-13
Acknowledgement	V-14
References	V-15
Figures	
Figure V-1 - Schematic of Direct Cycle Gas Turbine-Reactor Plant	V-16
Figure V-2 - Plant Thermal Efficiencies versus Maximum Cycle Temperature	V-17
Figure V-3 - Pumping Power Loss per Unit of Heat Transferred Compared to Carbon Dioxide versus Reactor Outlet Temperature	V-18

SECTION V

COOLANT GAS SELECTION FOR A GAS COOLED REACTOR

INTRODUCTION

This report has been prepared in connection with a parametric study of gas cooled power reactors. The design, size and cost of equipment and the output limits of a compressor-reactor-turbine power plant are dependent upon the type of gas which is used in the cycle. The gas must possess favorable properties for the dual function of (1) a working medium in the turbine compressor cycle and (2) a heat transfer medium as the reactor coolant. The gas must also have chemical and nuclear properties which are compatible with the cycle limits and cycle equipment. A comparison of the above properties was made for helium, nitrogen, carbon monoxide, carbon dioxide and argon with the objective of determining the most desirable candidates for the application being considered.

CONCLUSIONS

Application of a number of coolant gases appears to be feasible from an engineering point of view. The largest share of net power costs is from the capital cost of the plant. Therefore, the choice of gas for a particular reactor concept must be on the basis of plant economics; considering the coolant which will result in the lowest cost power production. Since this is a general study, a precise dollar value approach to the economic selection of a coolant has not been made. However, the information developed does permit confident selection or sound arrangement of the various coolants in their order of preference with regard to the characteristics and expected efficiencies of the gas upon which plant economics are strongly dependent.

Considering all factors, helium is the preferred coolant. This gas is not perfect, it will require higher volume rates, a greater number of stages on the compressor and turbine equipment and it is more difficult to contain than the gases CO_2, N_2, CO and A, yet next to carbon dioxide, it will give the highest plant efficiency, lower pumping power losses and will require the smallest reactor rating for a given plant output.

The choice of a second most preferred gas is a little more difficult to make. Carbon monoxide is toxic and a definite personnel safety hazard. Argon is extremely poor heat transfer-wise and therefore not worthy of serious consideration. The second choice, therefore, remains between nitrogen and carbon dioxide.

Thermodynamically carbon dioxide is preferred over nitrogen and will require a smaller turbine and reactor thermal rating, but, due to the carbon dioxide-graphite reaction, the use of this gas as a graphite moderator reactor coolant would be limited to graphite temperatures below 1200° F. This limit would restrict plant output or cycle efficiencies to values that would not be acceptable for a closed direct cycle gas turbine plant. To use CO_2 at graphite temperatures above 1200° F would require a reactor design with individually pressurized

process tubes or fuel channels. The use of high temperature resistant metal materials to pressurize the fuel channel reduces neutron economy to the point where reactor enrichment costs become prohibitive.

The use of nitrogen as a coolant may require special treatment of reactor and outlet gas piping materials because of its slight nitriding effect at high temperature and possible production of active nitrogen within the reactor. Feasibility of adequate metal treatment would require more investigation; however, because of this requirement, one could expect higher material costs as compared to carbon dioxide.

Without making a rigid economic appraisal, which would require scoping the complete plant for both gases, and assuming the availability of a compatible fuel element, nitrogen must be the second choice, carbon dioxide third, carbon monoxide fourth and argon fifth.

SUMMARY

The numbers of possible gases which were considered as potential materials were reduced, as covered in the discussion, to the following: helium, carbon dioxide, carbon monoxide, nitrogen and argon. In addition to the above, hydrogen, air and neon were given preliminary consideration.

The order of preference found in comparing each of the above gases for chemical, nuclear thermodynamic and heat transfer properties and for reactor fuel element limits, availability, cost, equipment sizes, and expected degree of design and operational problems is listed in Table I.

TABLE I

ORDER OF PREFERENCE FOR
GAS COOLANTS

Chemical Properties

He, A, CO_2, N_2, CO

Nuclear Properties

Absorption

CO_2, CO, He, A, N_2

Activation

He, CO, N_2, A

Decontamination

He, A, N_2, CO, CO_2

Fuel Element Limits

He, A, CO, CO_2, N_2

Thermodynamic Properties

Cycle Efficiency

CO_2, He, CO, N_2, A

Gas Rate

He, CO, N_2, CO_2, A

Work Ratio

CO_2, CO, N_2, He, A

Heat Transfer Properties

Pumping Loss/Heat Transferred

CO_2, He, N_2, CO, A

Cost and Availability of Gas

CO_2, N_2, CO, He, A

Equipment Size

N_2, CO, CO_2, He, A

Design and Operational Problems

CO_2, N_2, CO, A, He

DISCUSSION

Chemical Properties

Undesirable chemical properties for a power plant or a reactor coolant gas are molecular unstability, corrosiveness and toxicity. A few common gases which have these properties and should not be used are listed below:

1. Disassociation: Ethane, methane, acetylene and carbon monoxide are gases which will disassociate under high temperatures or decompose under radiation. (8, 9, 10, 11)

2. Corrosiveness: Oxygen, chlorine, ammonia, hydrogen chloride, hydrogen fluoride, hydrogen sulfide, sulphur dioxide and nitric oxide gases are highly corrosive with the metallic materials that are available for use in high temperature and high pressure piping.

3. Toxicity: Of these gases only carbon monoxide has a significant toxicity. Carbon dioxide, helium, nitrogen, hydrogen, or any gas, could be considered toxic in only a very gross sense, largely through deprivation of oxygen. The tolerance limits on carbon monoxide have been well established for a number of years, and for an 8 hour/day and a lifetime basis, these have been established at 100 parts per million. In addition, automatic recording instruments are available as standard industrial equipment. In fact, such instruments have been used at Hanford for special applications. Thus we can conclude that there are no major limitations of consequence imposed by the use of carbon monoxide. Normal industrial practice would be quite adequate to prevent any significant biological hazard from the use of these materials.

4. Explosion Hazard: Hydrogen and carbon monoxide can be considered inflammable gases. The explosive limits and other pertinent parameters are listed in Table II.

TABLE II

EXPLOSIVE CHARACTERISTICS OF GASES (13)

Gas	Explosive Limits, % Lower	Upper	Autoignition Temp., °F
CO	12.5	74.2	1204
H_2	4.1	74.2	1076
CO_2, N_2,	---	---	---
He, A, Ne	None		

The problems associated with the use of corrosive, explosive or toxic gases are not insurmountable as such gases are continuously handled in the chemical processing industries. Their use, however, is because of a direct and dependent need in a process rather than from choice, and without exception, enforce an additional premium on equipment capital costs, and operating expenses.

Gases which are common, relatively available, chemically stable through the temperature range of 100° F to 2,000° F are helium, nitrogen, water, carbon dioxide, air, argon, neon and xenon. Of the above, xenon can be eliminated from the list because of its high neutron capture cross section. Air, nitrogen and water can be considered as slightly corrosive. Carbon dioxide will react with graphite at temperatures above 600° C, and since graphite will be used as a moderator for the reactors investigated in this study, the use of CO_2 will be limited to graphite temperatures below 600° C or to reactors which contain fuel elements within pressurized process tubes rather than the open graphite channel-pressure vessel type reactor. (3, 4, 14, 15)

Fuel Element Limits (13)

Perhaps the first and most important consideration is the compatibility of the coolant with the materials which can be used in fuel elements. Table III provides a summary of the maximum permissible temperature between various materials and the different coolant gases. Although there are several unknowns or uncertainties included in this data, one can conclude that:

1. For an unclad fuel element, the use of one of the inert gases - helium, neon or argon, does not limit the temperature of the core material. There is, of course, no chemical reaction.

2. Uranium metal would be unsatisfactory with any of the other non-inert coolants. Although there are no data presented for uranium alloys, it is doubtful that an alloy can be economically formulated which would be sufficiently more resistant than uranium metal to withstand the corrosive effects at temperatures high enough to permit economic power recovery.

3. Uranium dioxide offers considerable promise with nitrogen and carbon monoxide. Hydrogen is perhaps a borderline case.

4. Very little definite information is available for uranium monocarbide and uranium mononitride. However, one could feel reasonably sure of using either of these materials with carbon monoxide and nitrogen.

These considerations are limited to the reaction between the gas and the material; such factors as reaction of fuel element core and jacket are not considered. Fuel element and gas compatibility outlined in Table III assume no diffusion of the gas into the fuel.

TABLE III

GAS COOLANT AND BARE FUEL ELEMENT COMPATIBILITY
MAXIMUM SURFACE TEMPERATURES, °C

	U	U_{alloy}	UO_2	UC	UN
CO_2	400	-	500	--	--
N_2	450	-	-	1100	700 +
CO	400	-	700 +	700 +	700 +
H_2	250	-	700	700	--
He, Ne, A	Limited by melting temperature of core material.				
Melting Temp.	1100	1100	2000-2500	2000-2500	2000-2500

The use of a cladding material increases the choice of a coolant. Data are given in Table IV. Again the rare gases helium, neon, and argon present no limitations on the selection of a material for the fuel ~~element~~ jacket.

Aluminum and magnesium both have quite low melting temperatures, hence would be of little value in a high temperature gas-cooled reactor when one considers a reasonable temperature drop across the gas film in transferring heat. The only well known material compatible with carbon dioxide is stainless steel; little or no data is available on titanium, molybdenum and niobium. With nitrogen coolant, one can use graphite, the other cladding materials being of borderline or substandard compatibility. With carbon monoxide, the possibility of either stainless steel or carbon (i.e. graphite) is evident. Again, there is no data for CO_2 compatibility with beryllium, titanium, molybdenum or niobium.[2] In the use of hydrogen, one has the possibility of stainless steel, molybdenum and possibly carbon.

To summarize then, the most promising jacket materials for high temperature operation are stainless steel and graphite; stainless being compatible with helium, carbon dioxide, carbon monoxide and hydrogen, and graphite with carbon monoxide, helium, and nitrogen. The use of one of the inert gases would permit any jacketing material which is compatible with the fuel core material and had a high melting point. These in general would include beryllium, zirconium, stainless steel, titanium, iron, graphite, molybdenum, and niobium.

TABLE IV

GAS COOLANT AND FUEL ELEMENT JACKET COMPATIBILITY
MAXIMUM TEMPERATURES - °C

	Al	Be	Mg	Zr	SS	Ti	Fe	C	Mo	Nb
CO_2	600	500	450	700	950	--	500	500	--	--
N_2	600	500	400	700	700	400	450	2000	--	300
He	600	1200	600	1400	1350	1650	1450	3000	2500	2000
CO	600	--	500	700	950	--	500	3000	--	--
H_2	400	700	--	300	800	120	--	--	2500	250
Melting Temp.	660	1280	650	1680	1400	1820	1540	3500	2620	--

Nuclear Properties (1)

Total reactor fuel and enrichment requirements for a given reactor output will be influenced by the nuclear absorption cross section of the materials used in the reactor. The following table lists the gases in decreasing order of preference or neutron economy.

TABLE V

THERMAL MACROSCOPIC ABSORPTION
CROSS SECTION FOR GAS COOLANTS (standard conditions)

Gas	$cm^{-1} \times 10^{6}$
Carbon Dioxide	0.079
Carbon Monoxide	0.086
Helium	0.190
Argon	16.0
Nitrogen	102

Radioactivity of Coolants (1)

Activity in a reactor coolant is affected by the ratio of in-pile time to out-of-pile time of the coolant, the reactor power level and the concentration of enriched uranium in the reactor. The coolant will become radioactive from the reaction of neutrons with the coolant or with impurities in the coolant and by diffusion products that enter into the coolant stream. This induced radioactivity becomes a problem only insofar as the radioactive gas cannot be isolated from plant operating personnel.

Time after shutdown before entrance into or breaking open pipe and equipment for maintenance will depend on the potential hazards from long half lives of the contaminants or impurities in the gas system. For example, the energy release from disintegrating gas atoms and their respective half lives is of more significance than the actual number of decaying atoms per cc. Nitrogen-15, following a neutron, gamma reaction becomes N^{16} which decays, giving off a 6 mev gamma. During plant operation, this will impose a high radiation level around the cycle equipment, but due to its 7.35 sec. half life, entry into equipment for maintenance could begin within minutes following plant shutdown. None of the gases being considered or their impurities possess significantly long decay times except argon (A^{41}) which is about 1.8 hours.

The gas carbon dioxide and monoxide will produce the isotope of carbon-14 which has a half life of 5,600 years; however the abundance of this isotope is so insignificant that it would not constitute a serious maintenance problem except after many years of plant operation.

Decontamination (13)

Helium, argon, and neon are identical in their chemical properties. The separation of all the fission products other than the rare gases, krypton and xenon, should be relatively straightforward, although some of the separations may require further development for operation at the high temperatures of the gas cycle.

This entire field represents a considerable research and development effort in chemical separations technology. One could anticipate the easiest and least expensive separation with the use of helium, argon, or neon. The krypton and xenon could be separated from these gases if low temperature operation is permitted since fractional distillation is perhaps the most practical method of realizing this separation. Carbon dioxide and carbon monoxide may well be sufficiently inexpensive to permit their disposal after decontamination or as a part of the decontamination process. Hydrogen decontamination should be feasible though the details of the process cannot be specified at this time. Nitrogen should be fairly straightforward also.

The best which can be done with the existing data in evaluating these gases with respect to off-gas treatment is to rate them in the order of minimum difficulty.

1. Helium, neon, argon

2. Nitrogen, hydrogen

3. Carbon dioxide, carbon monoxide

Thermodynamics

In analyzing the performance of various gases in the gas turbine-compressor cycle it is necessary to take into account three factors: (1) efficiency, (2) gas rate, and (3) work ratio. Efficiency is defined as the ratio of net power output from the prime mover to the external heat supplied, the gas rate is pounds of gas pumped per hour per kilowatt output, and the work ratio represents the proportion of total installed turbine power usefully delivered to the output shaft. (5, 6, 7) The most economic or ideal system would be one that had high efficiency, low gas rate and high work ratio. A schematic of a compressor-reactor-turbine direct cycle plant is illustrated in Figure V-1. Figure V-2 graphically shows the plant thermal efficiency using helium, carbon dioxide and nitrogen gases for the same reactor output, system pressure, and equivalent plant equipment costs. The percentage η_p is the proportion of maximum system pressure that is expended in total system friction losses to provide the necessary mass flow rates and heat transfer for the 500 MW reactor case shown. At equal reactor outputs, carbon dioxide is the most preferred gas thermodynamically.

Heat Transfer

Since the external heat source for the turbine compressor cycle is the reactor and this same gas is used to cool the reactor as well as absorb heat for turbine work, a basis for comparing the effectiveness of various potential coolants as heat transfer mediums can be made on the proportionate amount of pumping work (parasitic losses) required per unit of heat transferred from the reactor. Such a comparison can only be made for the same reactor output, tube length, and flow area for each gas (1, 12).

A graph showing the comparative relationship of pumping power loss per unit of heat transferred versus reactor outlet temperature is shown on Figure V-3. The order of preference for the gases, with regard to heat transfer, is carbon dioxide, helium, nitrogen, carbon monoxide and argon.

At the same flow areas and mass rates, pumping losses will be higher for the lower density gases, but since a comparison of each gas for pumping losses must be made on the basis of equal reactor rating or heat absorbed; mass rates, because of the different specific heats and densities, will never be equal. Pumping power losses are a cube function of the mass rate and on the basis of equal heat pick-up, power losses, in the reactor, will be proportional to an inverse function of the cube of the specific heat and inverse square of the density. In comparing different gases, the ratio of their specific heats will have a greater effect on pumping power losses than will the ratio of their densities.

Piping outside of the reactor may be sized so that the pressure drops are very nearly the same. This may also be done, with a much lesser degree of freedom, through the cycle heat exchanger equipment, but attempting to balance pressure drops across the reactor for the different gases for the same reactor output is impractical. The net effect of pumping losses through all of the cycle equipment on plant thermal efficiency is illustrated on Figure V-2.

Equipment Size and Cost

The equipment sizes for different gases are affected by the system temperatures, pressures and mass flow rates required for a given plant output. Since one adverse physical property of a gas may be offset by another beneficial property no exact statement can be made about comparative equipment sizes without considering the complete cycle and the chosen condition extremes for a given plant rating.

For the compressor equipment, if inlet volumes, pressures and temperature conditions are made the same, and peripheral speeds are equivalent, one can generalize and say that for a comparison of a given compression, the gas with the higher density or molecular weight will require less work than a gas of lower density. Since size, cost and complexity of equipment are proportional to the amount of work required from a piece of machinery, the lower the density of the gas the greater will be the cost and size of associated equipment. Gases with high k (c_p/c_v) ratios require higher wheel speeds than gases with lower k values to obtain the same degree of compression and as a result the equipment cost will be higher. This would imply that rotating equipment for helium would be a great deal larger than say for nitrogen; however this difference can be decreased, and practically, by increasing He shaft speeds.

Only a few manufacturers are capable of producing closed cycle gas turbine-compressor power plant sets in the large KW sizes. Their experience is relatively small and limited as to the types of gases that have been utilized and conclusive weight figures on gas turbine plants have not yet been developed. However, tentative estimates have been made for marine plants operating in the 1200° F range, on the basis of weight and horsepower requirements. The turbines are anticipated at two to three pounds per turbine horsepower, compressors are more complex but a range of two to six pounds/comp. HP appears reasonable, regenerators will average one to two lbs/sq. ft. of surface. Piping, insulation, intercoolers and auxiliaries are anticipated at two pounds per turbine horsepower. It must be understood that this method is very rough but it will give an indication of comparative plant sizes for comparing different gases as established by their respective work ratios (net work/turbine work). The following table lists the gases being considered in order of increasing plant size in terms of approximate equipment weight per KW output (exclusive of reactor, generator or drive). (5)

TABLE VI

PLANT EQUIPMENT WEIGHT PER KW OUTPUT

Gas	Lbs/KW
N_2	40
CO	40
CO_2	43
He	46

Cost and Availability of Gases (13)

Carbon dioxide, carbon monoxide, hydrogen and nitrogen are readily available at reasonable cost in almost any geographical location. Helium, on the other hand, is a more costly gas and is largely restricted to the continental United States. Argon and neon are both obtained from the liquefaction of air; hence their cost is directly related to power cost.

TABLE VII

COST AND AVAILABILITY OF GASES
(Standard Temperature and Pressure)

Gas	Cost - $/Ft^3 -	Availability
He	0.015 (FOB Amarillo, Texas)	U. S. (Italy and USSR)
A	0.074 (FOB Richland, Wash.)	0.93 v/o of air*
Ne	42.50 (FOB Kennewick, Wash.)	0.0018 v/o of air*
CO_2	0.003 (FOB Kennewick, Wash.)	World wide
CO	0.24 (FOB N. J.)	World wide
H_2	0.10 (FOB Kennewick, Wash.)	World Wide
N_2	0.08 (FOB Kennewick, Wash.)	78.06 v/o of air*

*Obtained by fractional distillation of liquid air.

Design and Operational Problems

With gas, a major problem of design and in later operation is that of making and maintaining seals and in particular dynamic seals on rotating or sliding equipment. The complexity of the design and cost of equipment will, in general, be higher for a low density gas (He as compared to N_2) since rotating shaft and peripheral wheel speeds are usually higher for the low density gases. As speed increases, equipment stresses increase and lubrication and sealing become more difficult. The rate of equipment failure or lost time because of equipment repair is proportional to the complexity of the equipment design.

sealing of helium in a reactor turbine plant will be more difficult than for the other gases considered; however, it is a misconception to assume that system leakage rates with helium will be prohibitive to plant operating costs. Helium is used in large quantities at HAPO and at Oak Ridge. Experience has shown that the reduction of system leakage is more a problem of determining the origin of the leak rather than correcting and stopping the leak. Discussion of this problem with personnel at the Amarillo, Texas office of the Bureau of Mines confirms this experience and opinion. It is apparent then that to combat a high system leakage, provisions may have to be made to incorporate leak detection equipment in the initial design of plant equipment at points of expected critical seal service. By proper plant design with this criteria in mind, the leak detection facilities need not be elaborate nor should they contribute significantly to plant capital costs. Provisions could also be made to bonnet such seals and return leakage gas to the plant decontamination facilities.

The gases listed in order of decreasing density or increasing order of expected difficulty are carbon dioxide, nitrogen, carbon monoxide, argon and helium.

ACKNOWLEDGEMENT

The discussion on fuel element limits was provided by R. G. Post, Engineering Operation, Fuels Preparation Department.

Development of curves shown on Figure V-2 was made by N. F. Fifer, Reactor Modification Design.

REFERENCES

1. AECD - 3646 - "The Reactor Handbook" - Volume 2.

2. IDO 28500, October 3, 1957 (Secret).

3. Woodley, R. E. - "The Promotion of Chemical Reaction by Pile Radiation - Final Report", HW-40142 - November 22, 1955, Unclassified.

4. Woodley, R. E. - HW-52267, August 21, 1957, (Secret).

5. Sawyer, R. T. - "The Modern Gas Turbine", Prentice Hall, Inc., 1947.

6. Robinson, S. T. - "Influence of Working - Fluid Characteristics on the Design of the Closed Cycle Gas Turbine" - ASME paper No. 57-GTP-13.

7. National Bureau of Standards Circular 564 - "Tables of Thermal Properties of Gases".

8. Quinn, E. L. - "Carbon Dioxide", Reinhold Publishing Corp., 1945.

9. Griswold, J. - "Fuels, Combustion and Furnaces", McGraw-Hill Book Co., 1946.

10. Meisels, G. G. - "Radiation Chemistry of Methane" - The Journal of Physical Chemistry - November, 1957.

11. Harteck, P., "Decomposition of Carbon Dioxide by Ionizing Radiation" - The Journal of Chemical Physics, May, June, 1957.

12. Monn - 383 - "Summary Report on Design and Development of High Temperature Gas-Cooled Power Pile" - Confidential - September 15, 1947.

13. Post, R. G. - letter - November 27, 1957, "Chemical Considerations in Selecting a Coolant for a Gas Cooled Reactor".

14. "Nuclear Engineering", November, 1957, page 483.

15. Wade, G. E. - Letter - "Notes on CO_2 and Graphite from Talk with D. N. Curtis, 11-12-57".

DIRECT CYCLE GAS TURBINE - REACTOR PLANT

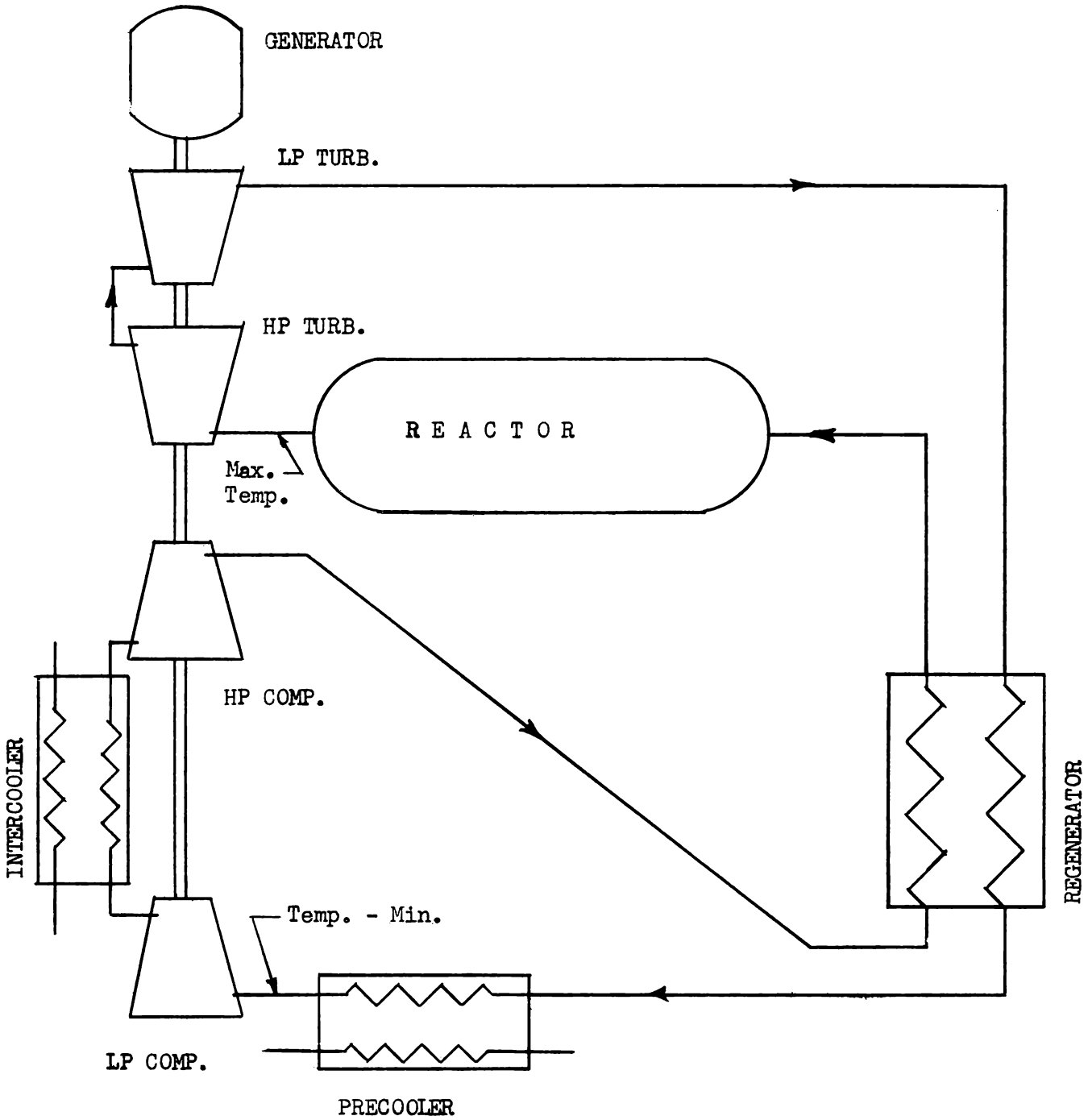

System conditions for curves on Figure V-2.

Turbine Efficiency = 88%. Compressor Efficiency = 85%.
Regenerator Effectiveness = 91%. Parasitic Losses = η_p.
Minimum Temperature = 100° F.

PLANT THERMAL EFFICIENCIES OF He, N_2, & CO_2

VERSUS

MAXIMUM CYCLE TEMPERATURE

BASED ON EQUAL REACTOR OUTPUTS

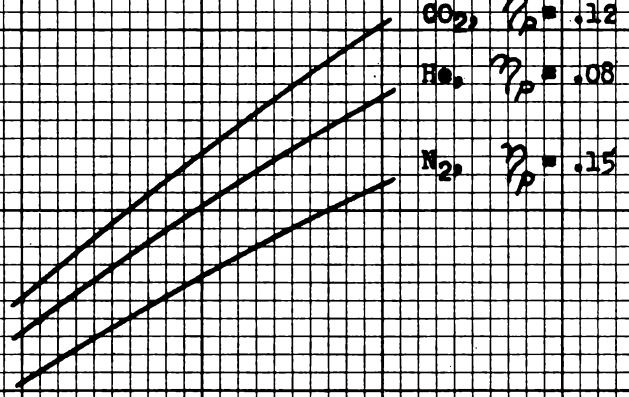

PLANT THERMAL EFFICIENCY, η_{TH}.

40
30
20
10

REACTOR CONDITIONS

Power Level — 500 MW
Reactor ΔT — 500° F
Sp. Tube Power — 25 KW/FT
Lattice — 8 In.
$\eta_p = \Delta P/PMAX$

RATIO OF POWER PLANT INVESTMENT

He — 1.00
N_2 — 1.00
CO_2 — 1.03

1000 1200 1400

MAXIMUM CYCLE TEMPERATURE, °F

FIGURE M-2

2-6-58

PUMPING POWER LOSS PER UNIT OF HEAT TRANSFERRED COMPARED TO CARBON DIOXIDE

VERSUS

REACTOR OUTLET TEMPERATURE

Reactor Dimensions Constant
Reactor Output Constant
Gas Pressure - 600 psia

Ref.: Reactor Handbook
Vol. 2 page 477-(2)

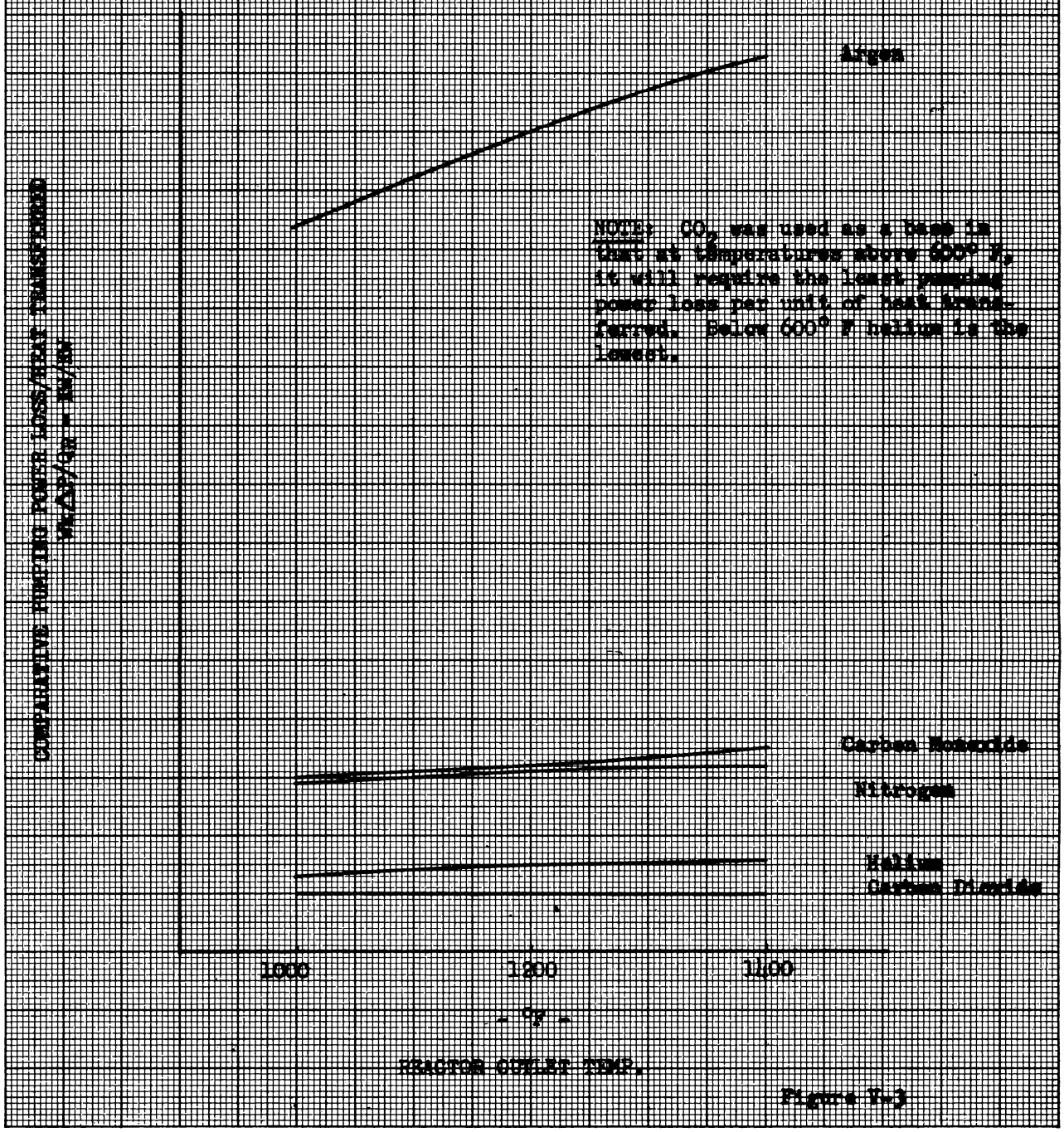

NOTE: CO_2 was used as a base in that at temperatures above 600° F, it will require the least pumping power loss per unit of heat transferred. Below 600° F helium is the lowest.

Figure V-3

SECTION VI

REACTOR CORE ARRANGEMENT AND VESSEL STUDIES

by

E. R. Rudock
Process Design Operation
IRRADIATION PROCESSING DEPARTMENT

REACTOR CORE ARRANGEMENT AND VESSEL STUDIES

INTRODUCTION

To prepare cost estimates for the reactor and pressure vessel that could be used in the parametric reactor and power plant studies, preliminary design of a reactor arrangement was necessary. This report is to discuss the arrangement that was used for developing the reactor equipment costs. At this phase of study, reactor concept can be visualized only in general terms of physical arrangement and size. However, direction of intent of future studies that could develop into the detail phase can be outlined on the basis of engineering feasibility, previous construction and known material limitations.

DISCUSSION

The determination of a reactor case or cases and power plant that presents minimum power costs is dependent on the plant operating conditions which will (1) establish equipment sizes, (2) shape general equipment costs, including the reactor, and (3) effect general plant yearly operating costs.

Because of the extremely large number of reactor cases involved in this study (ten different reactor and system parameters were each varied over a range of investigation), reactor dimension ratios that were considered as having a minor effect on plant optimization were chosen, wherever possible, and used throughout the study for all other parametric cases. These dimension ratios enabled the prediction of reactor size and subsequent pressure vessel studies without being delayed by the exhaustive, time consuming reactor physics studies.

In all cases a fuel column length of twice the face dimension of a square faced active graphite core was used. This face dimension converted to an equivalent cylindrical core diameter was set equal to the ratio of fuel column length divided by the square root of "Pi". A further discussion of this ratio and associated reactor physics is carried in the main body of this report.

REACTOR CORE ARRANGEMENT

The core arrangement and other associated structures within the reactor vessel outlined below are, in general, approximations of a proposed design and would be subject to change by process of optimization during actual detail design.

GENERAL DESCRIPTION

The fuel column and control rods are considered to be oriented on the vertical. The graphite core will be contained in a cylindrical thermal shield. Inlet coolant will enter into a gas plenum and annulus between the thermal shield and pressure vessel walls. The gas will pass the length of the core in this annulus before discharging into an inlet

fuel channel plenum. The gas will then flow through the fuel channel into a discharge plenum. The discharged gas will leave the reactor vessel from exit transport pipes to the turbomachinery or heat exchange equipment.

CORE AND REFLECTOR

The use of a graphite moderator and reflector for the reactor was established as a part of the basic criteria of the study. In brief, this choice is based on HAPO experience with this material as a moderator and the abundance of available physical property data. In addition to being a satisfactory high temperature moderating material it possesses good thermal conductivity and thermal shock resistance. Although reactor size may be larger with graphite as a moderator as compared to BeO or Zr Hx, for a given thermal rating, this fact was considered as unimportant in lieu of the scarcity of data on these materials, the lower graphite moderator material unit costs, and the land based application. Sufficient experience exists at HAPO to cope with design problems of dimensional instability and stored energy effects resulting from using graphite as a moderator.

Because of the resultant core sizes necessary to produce the 500 MW to 1500 MW power levels covered in this study at 6" and 8" lattice spacings, construction of the core by stacking horizontal layers of machined bars was considered as being more economical with regard to field erection costs, and would effect minimum thermal expansion and better dimensional stability as compared to core erection by a vertical bar design.

The empty fuel or coolant gas flow channel was chosen as a square cross section, a side equal to one-half the lattice. Choosing a fractional even multiple of the lattice will simplify core machining and construction lay up procedures. In addition, the square cross section channel provides greater flexibility in fuel element design, maximum flow area and minimum pressure drop compared to a circular or hexagonal cross-section for any given lattice spacing.

Control rod, fuel and gas flow channel openings would be provided by the design and method of stacking of the graphite blocks. Coring by boring machine tools would be eliminated or at a minimum.

Fuel channels were considered as oriented in the vertical direction to simplify construction of the reactor and to minimize thermal stress support loadings that would otherwise be transferred through the pressure vessel walls by a horizontal fuel channel design. For all cases considered, reflector thicknesses were taken at 30 inches to permit approximations of vessel size.

VESSEL STUDIES

Approximate pressure vessel sizes necessary to house any given reactor were determined, in all cases, by adding to the core radius the following dimensions:

Reflector - 30"

See main body of report.

Thermal Shield - 10"

This is an approximation only but would represent the maximum thickness necessary. Reduction in thickness would result in an increase in the induced pressure vessel wall gamma heat generation and resultant thermal stresses. This reduction in thermal shield thickness would tend to permit an equivalent reduction in vessel inside diameter. Actual permissible decrease is somewhat questionable in that the increase in temperature differential across the vessel wall would reduce the allowable pressure stress, resulting in either a lower permissible operating pressure for a given wall thickness, an increased wall thickness, or a compensating result of the combined changes. This effect will be subject to further study for an opportunity for an optimum balance may exist. The choice of a 10" thermal shield is conservative as to the effects on vessel size and results in an insignificant amount of heat generation in the vessel wall, thereby allowing maximum permissible operating pressures for any given wall thickness and vessel temperature.

Gas Annulus and Insulation - 5"

To permit the use of the less expensive low alloy carbon steels in the construction of the pressure vessel, it is necessary to limit pressure vessel wall temperatures to the region of 650 to 700° F. This in effect dictates the passage of inlet gas as a coolant between the pressure vessel wall and the cylindrical surfaces of the heat generating thermal shield. In the cases where inlet gas is at a temperature over 700° F, a high temperature insulation lining would be added to the inside vessel wall. On reactor cases of high gas flow rates, an increase in annulus size would be required to reduce friction pressure losses. The economics of increased pressure vessel size to accommodate a larger annulus as against pumping losses will be a region of further study.

Pressure Vessel

Due to the choice of a fuel column length to active zone diameter ratio of approximately two, the shape of the pressure vessel was chosen to be cylindrical to minimize vessel costs even though a spherical vessel would permit a slight gain in maximum operating pressure for a given wall thickness. A more detailed comparison of cylindrical versus spherical vessel costs should be made in future study phases.

Vessel inside diameters for a reactor were determined by adding to the core diameter the reflector, thermal shield, gas annulus and insulation dimensions which were outlined and explained above.

The necessary inside diameters to cover the 500 MW to 1500 MW cases investigated ranged from 18 to 37 feet. Since the construction site for the reactor is unknown, the assumption was made that an inland location must be considered. Transportation by railroad of vessels 18 feet in diameter and over is impractical, field construction of all study case vessels would be necessary.

Since power plant efficiencies increase with increasing operating pressures and temperatures, the following criteria was chosen to determine the reactor or pressure vessel maximum operating pressure:

Investigation for wall thicknesses used in previous field constructed ASME stress relieved pressure vessels has shown that a nominal two inches is the maximum so far attempted in the range of 18 ft. diameters; a three inch thick vessel is now under construction in Great Britain (Nuclear Engineering, December 1956, February 1957, March 1957).

Field welded, full thickness, flush, butt-type repair patches have been successfully made in small diameter pressure vessels of nominal wall thickness ranging three to five inches (Petroleum Processing, January 1955).

Consultation with manufacturers of pressure vessel equipment on problems of field construction has borne the opinion that wall thicknesses up to six inches could successfully be field welded, radiographed and stress relieved; however construction contingency costs would be extremely high. Since available study time did not permit a successful completion of an analysis of field construction limitations and resultant cost estimates, a wall thickness of 4.5" was chosen as the maximum that could be confidently considered for field construction in the range of diameters considered.

Using 4.5" as a base thickness and 700° F wall temperature, maximum permissible operating pressures were calculated, for each reactor size, in accordance with ASME Boiler and Pressure Vessel Code, Section I - Power Boilers, P180-C, material SA-212B. By using an internal thermal shield, gamma heat generation in the vessel wall is negligible. Temperature differential across the vessel wall is easily controlled by external vessel insulation. Thickness necessary to limit the temperature differential between two degrees and five degrees is under four inches. Allowable pressure stress values used for the above calculations were based on a five degree temperature differential.

ASME Code Section I - Power Boilers was used instead of Section VIII - Unfired Pressure Vessels in that the reactor vessel will contain a heat source.

Figures VI-1 and VI-2 illustrate graphically the maximum pressure as a function of vessel diameter, power level, specific tube power and lattice spacing.

Vessel Support

The support of the vessel, graphite core and thermal shield would be at the approximate location of the base of the core in the vessel. Graphite and thermal shield loads would be transmitted to and through the vessel wall at this point. Vessel to foundation supports would also pass through the same location. This arrangement appears to allow maximum freedom from restrained thermal expansion of the three components. Support arrangements and induced expansion stresses of vessel and gas transport pipes would of course be thoroughly analyzed in the course of actual design.

Vessel Weight

For vessel weight estimates it was assumed that vessel ends were hemispherical. Vessel openings for fuel charging and control rods were limited to one end only. Several small charging openings rather than one large opening would be used to lessen fabrication costs and probability of seal leakage.

Figure VI-3 is a plot of graphite, thermal shield and pressure vessel weights used in preparing comparative reactor case equipment cost estimates.

Control Rods

Control rods and drives would be enclosed in individual small diameter pressure vessel cylinders that would be flange sealed to the main vessel to minimize the high temperature dynamic seal problems that would otherwise be involved with external drives. Low temperature high pressure gas would be bled from the cycle and into the rod vessels to cool the drives. By proper arrangement of the control rods and fuel charging openings, removal of the rod vessels during normal charging and discharging operations would be unnecessary.

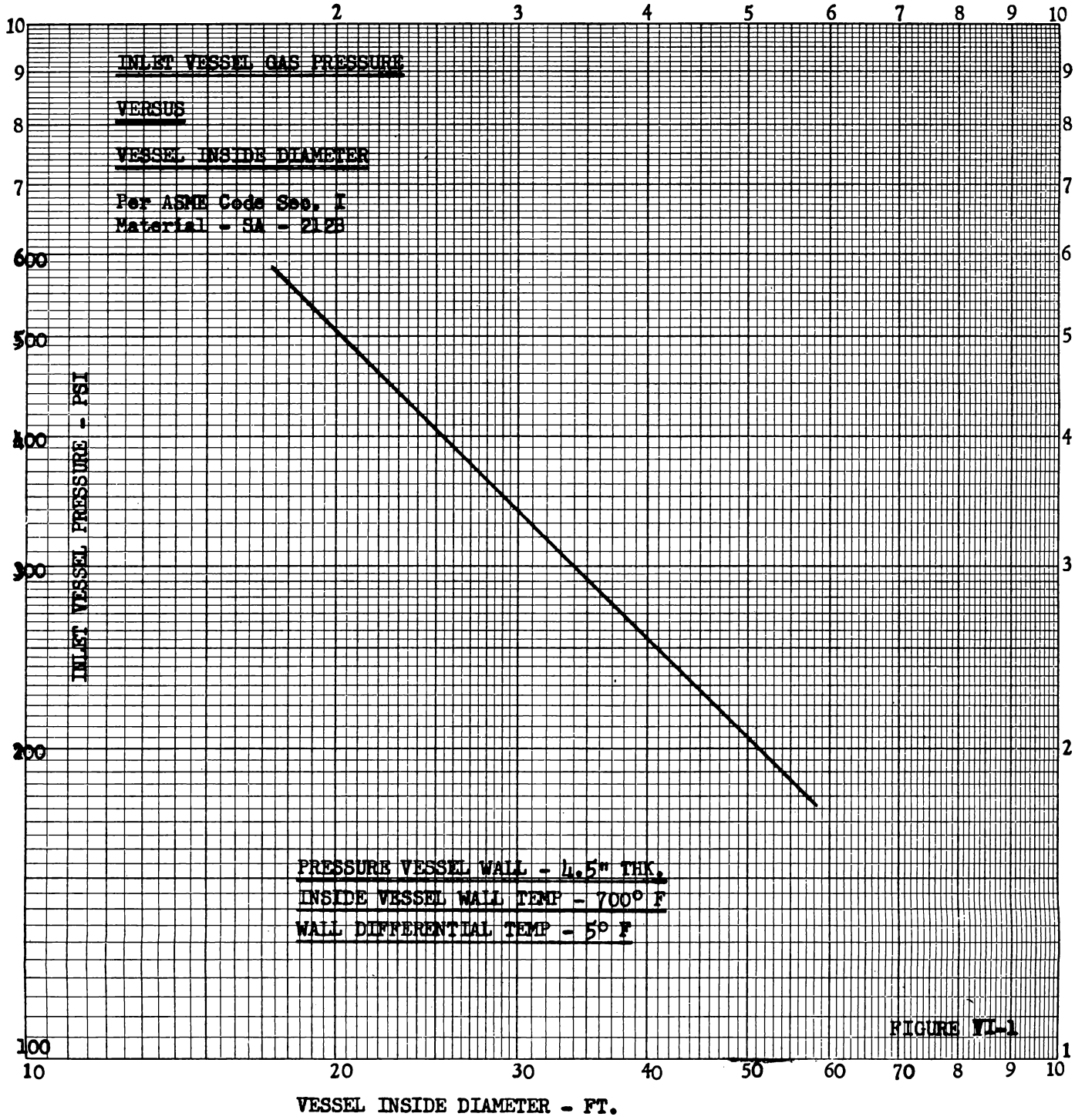
INLET VESSEL GAS PRESSURE
VERSUS
VESSEL INSIDE DIAMETER
For ASME Code Sec. I
Material - SA - 212B
INLET VESSEL PRESSURE - PSI
VESSEL INSIDE DIAMETER - FT.
PRESSURE VESSEL WALL - 4.5" THK.
INSIDE VESSEL WALL TEMP - 700° F
WALL DIFFERENTIAL TEMP - 5° F

FIGURE VI-1

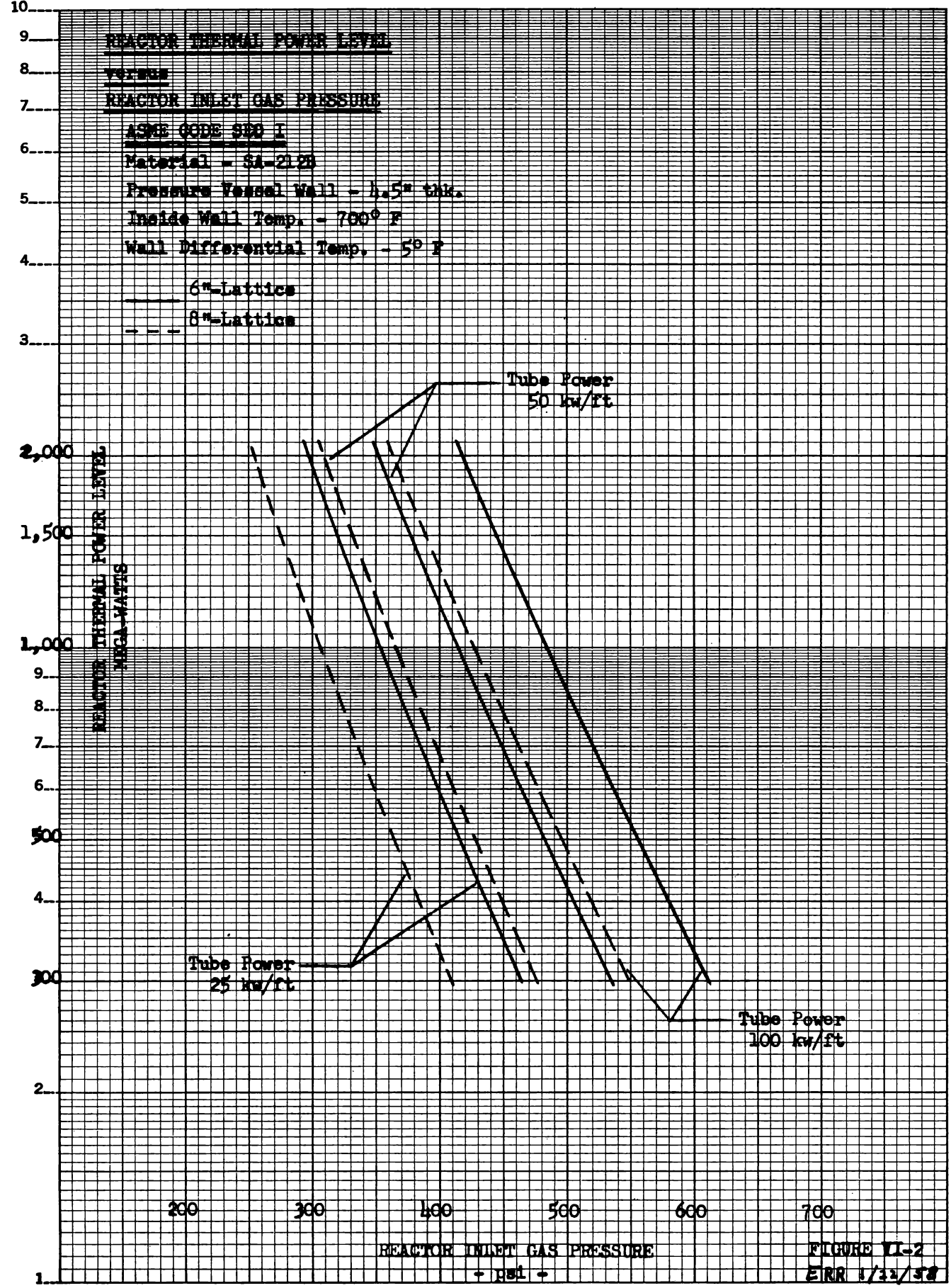

FIGURE VI-2
ERR 1/12/58

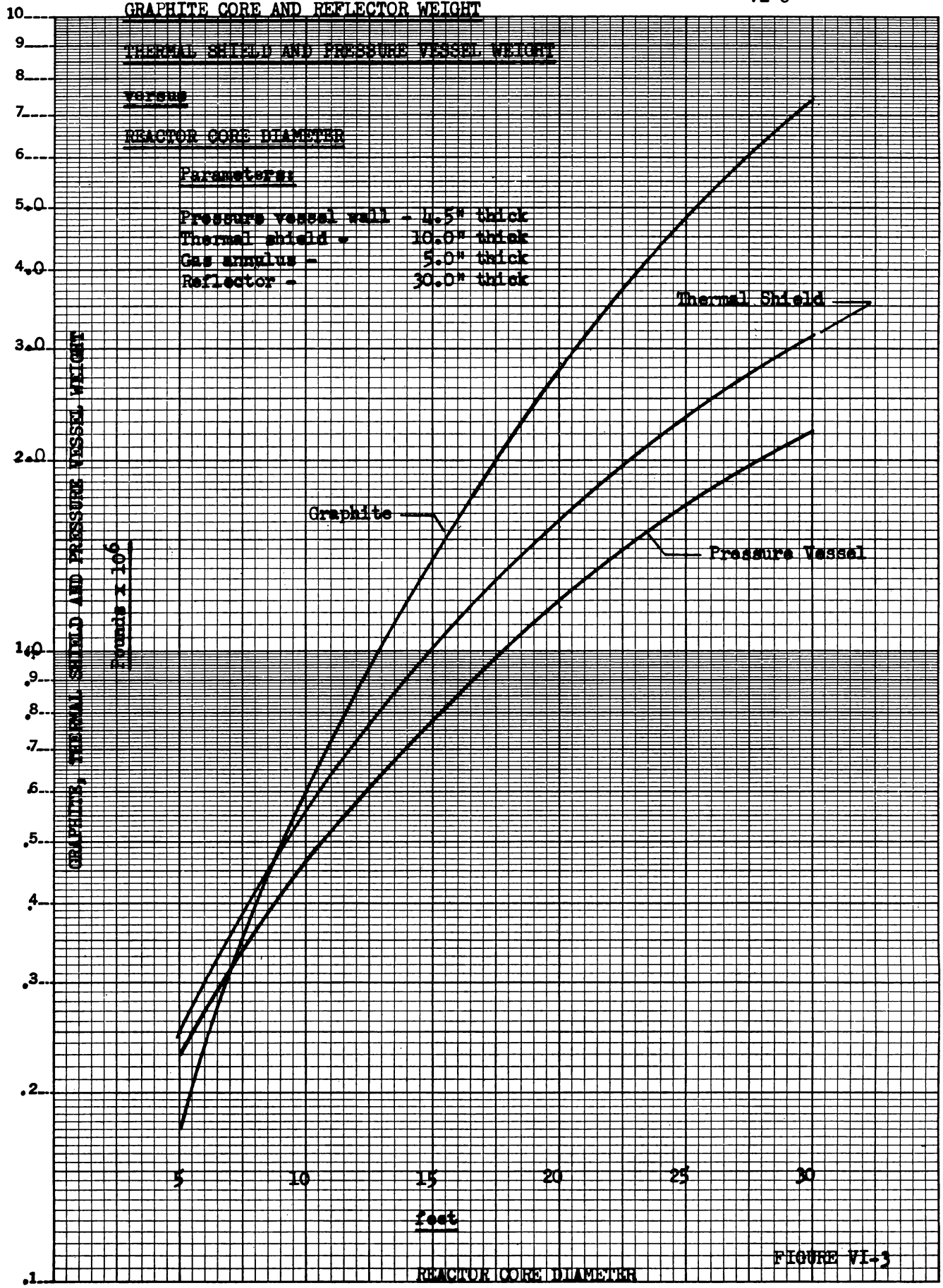
GRAPHITE CORE AND REFLECTOR WEIGHT
THERMAL SHIELD AND PRESSURE VESSEL WEIGHT
versus
REACTOR CORE DIAMETER
Parameters:
Pressure vessel wall - 4.5" thick
Thermal shield - 10.0" thick
Gas annulus - 5.0" thick
Reflector - 30.0" thick
Thermal Shield
Graphite
Pressure Vessel
GRAPHITE, THERMAL SHIELD AND PRESSURE VESSEL WEIGHT
Pounds x 10^6
10
9
8
7
6
5.0
4.0
3.0
2.0
1.0
.9
.8
.7
.6
.5
.4
.3
.2
.1
5
10
15
20
25
30
feet
REACTOR CORE DIAMETER

FIGURE VI-3

SECTION VII

DIRECT CYCLE POWER PLANT STUDIES

by

G. E. Wade
Process Design Operation
IRRADIATION PROCESSING DEPARTMENT

DIRECT CYCLE POWER PLANT STUDIES

INTRODUCTION

Power recovery from a gas cooled reactor can be accomplished by either of two basic cycles. The direct cycle circulates the reactor coolant through the turbo-machinery. In the indirect cycle the reactor coolant transfers heat in a heat exchanger. The secondary fluid, heated in this heat exchanger, is used to drive the turbo-machinery. In either cycle, direct or indirect, the reactor serves as the heat source and the turbo-machinery drives the coolant compressors or blowers as well as the output generator. Figure VII-1 shows the direct cycle that was used throughout Phase I of this study.

With the indirect cycle, steam can be used as the secondary fluid. This simplifies the power plant to the extent that there is a vast store of knowledge about the required equipment. However, maximum temperatures are limited to 1200° F or less. The direct cycle has the advantage of permitting maximum cycle temperatures of 1300° F with possible future rises to 1700° or 1800° F. Because of these temperatures the efficiency of the direct cycle can be higher than the indirect cycle. The two main disadvantages of the direct cycle are (1) the unknown effects of radiation and contamination in the turbo-machinery and heat exchangers, and (2) lack of experience with gas equipment of this size.

Presently available fuel elements (uranium oxide clad with stainless) limit maximum cycle temperatures to 1200° to 1300° F. However, if in the future ceramic elements are developed the maximum cycle temperature could be increased to 1800° F or higher. Therefore, the development of these new elements, with their appreciably lower fuel costs, when combined with the high thermal efficiency of the direct cycle hold promise for lower nuclear power costs.

CONCLUSIONS

The perfect gas laws can be used to calculate cycle efficiencies when helium is the coolant. For other gases the use of a Mollier diagram is mandatory

As would be expected, the cycle thermal efficiency is raised by (1) increasing the cycle maximum temperature, (2) decreasing the cycle minimum temperature, (3) increasing the regenerator effectiveness, and (4) decreasing system pressure losses.

In most cases the reactor ΔT can be increased through wide limits with negligible effects on the thermal efficiency. This increase in reactor ΔT reduces the required mass flow per KW electrical but increases the cycle pressure ratio.

Based on minimum cost per KW electrical the CO_2 plant is best, followed by He and N_2.

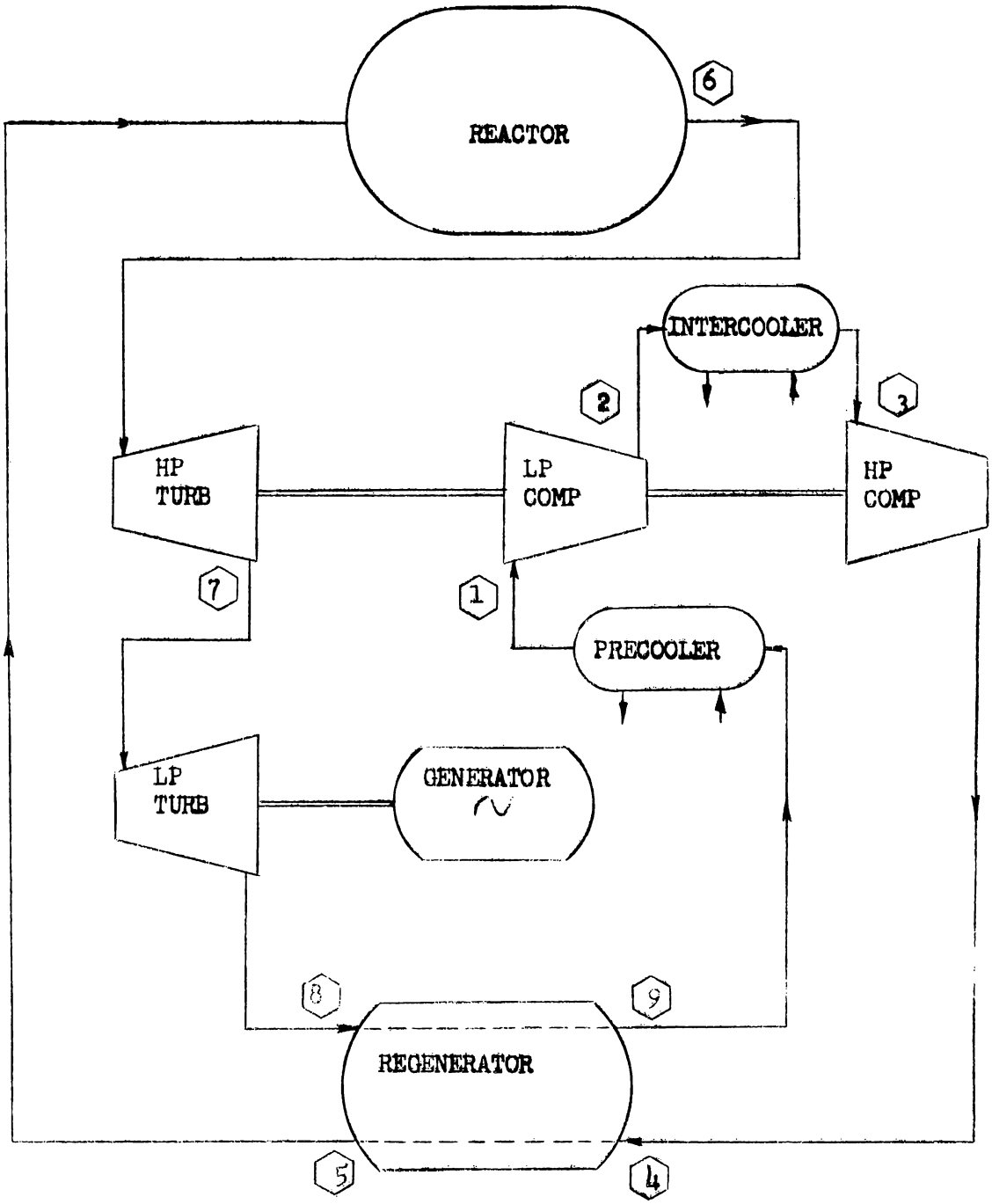
REACTOR
6
INTERCOOLER
2
3
HP
TURB
LP
COMP
HP
COMP
7
1
PRECOOLER
LP
TURB
GENERATOR
8
9
REGENERATOR
5
4

FIGURE VII-1

Helium, although requiring larger volume flows, requires the smallest flow area because it has a high sonic velocity. The piping pressure losses for He will also be lower than for other gases even when He is run through smaller area ducts.

For the reactor and power plant designs considered the cycle efficiency is reduced as specific power and reactor power are increased. However, the point of maximum cycle efficiency does not necessarily give the design for the lowest cost power (mils/kw). The maximum cycle plant efficiency is 36%.

PARAMETERS TO BE STUDIED

The purpose of this study was to examine the feasibility of constructing a graphite moderated gas cooled power producing reactor. Reactor and power recovery plant designs were to be based on a reasonable extrapolation of present data. The study was to include an investigation of the effects of as many design parameters as possible. For the entire study 144 cases were studied with 9 sub-cases for each case. The other 72 cases concerned the indirect cycle and the sub-cases reflected changes in fuel exposure which did not affect the power recovery plant costs. The cases and sub-cases for the direct cycle required cost estimates for 216 power plants.

The parameters for the 216 plants were (1) helium or nitrogen as the coolant; (2) reactor lattice of six and eight inches; (3) specific fuel powers of 25, 50 and 100 kw/ft; (4) coolant Δ T's across the reactor of 400, 500 and 600° F; (5) coolant bulk outlet temperatures of 1200° F and 1400° F; and (6) reactor power levels of 500, 1000 and 1500 MW thermal. A hidden parameter, maximum cycle pressure, was determined by the power level, specific power and lattice as they affected reactor size and therefore the reactor pressure vessel.

Helium was the desired gas for the coolant but nitrogen was studied as an alternate. It was felt that the low cost of nitrogen plus its wider availability might affect its poorer heat transfer and pressure drop considerations.

A range of values for the other parameters was chosen so that by suitable cross plotting minimum costs (mils per KW) could be determined. Parameters two through six affected the cycle efficiency and/or costs by changing pressure losses, maximum cycle pressure or cycle operating temperatures. The parameter values were selected based on previous experience, or on purely arbitrary decisions. For instance the pile power levels represent the range of electrical outputs, 170 to 500 KW, which were considered practical for a base load central station.

Two values of the maximum cycle temperature were necessary to indicate cost trends. This permitted a comparison of the costs of the indirect and direct cycle. It also permitted determination of the crossover point where the direct cycle costs drop below those of the indirect cycle.

The three values of reactorΔT were selected because of the importance of reactor inlet temperature on pressure vessel and piping design and the fuel costs. The temperatures picked do not necessarily represent an optimum thermal efficiency for the case under consideration. This point will be discussed with the calculated results.

During early preliminary studies five gases were considered as possible coolants. These were helium, nitrogen, carbon monoxide, carbon dioxide and argon. Cycle thermal efficiencies for these gases were calculated. The selection of helium and nitrogen for final study is discussed more fully in Section V of this report. The reasons for rejection of other gases are listed below.

The choice of He and N was made after elimination of argon, carbon monoxide, carbon dioxide and hydrogen. Argon was eliminated because of poor heat transfer and nuclear properties. Carbon monoxide was eliminated because of the toxicity effect and also because its calculated efficiencies, flow areas, etc. were so close to those for nitrogen. Carbon dioxide was rejected because it is not compatible with graphite at the temperatures under consideration. Hydrogen had to be dropped because of the potential explosion hazard.

ASSUMPTIONS

The basic cycle shown in Figure VII-1 was used for all gases. This cycle was chosen because it represents a simple straightforward system with minimum complications and reasonable efficiencies. The cycle utilizes the reactor as the heat source. Gas from the reactor passes through the high pressure turbines which in turn drive the compressors. Gas from the high pressure turbine enters the low pressure turbine which drives the electrical generator. A regenerator is used between the low pressure turbine outlet and the high pressure compressor outlet to increase cycle thermal efficiency. The precooler reduces the inlet gas temperature to the compressor. Two stages of compression with intercooling were used.

There are numerous changes that could be made in this cycle to improve thermal efficiency. However, it was felt that these should be investigated during Phase III of the study when there were fewer parameters and more definite cost information. In any case the goal to be attained is the cycle or equipment with the lowest cost per kilowatt of electrical power delivered. Thus all cycles and equipment must be analyzed for capital cost, pressure losses (pumping costs), fuel costs, and maintenance costs to determine the optimum arrangement.

The reactor coolant compressors were divided into four independent sets. This was done to insure continuity of coolant flow in the event that a compressor or drive turbine failed. This division leads to the installation of four independent coolant loops for the reactor. The main disadvantage of this is that four electric generators are required if the loops are to remain independent and piping runs are to be kept to a minimum. In any case it may be possible to locate the generators in a non radiation zone.

Compressor adiabatic efficiencies of 84 to 88% for axial flow gas turbine compressors are quoted in several reports. Test efficiencies as high as 90% have been reported. For this study an efficiency of 85% was used to be on the conservative side.

Higher adiabatic efficiencies are possible with turbines. For this study a value of 88% was selected. While this value is adequate it does not allow for any exhaust losses which amount to approximately three per cent. Future studies will use an over-all adiabatic turbine efficiency of 85%.

Regenerators for the cycle were designed for 91% efficiency. This efficiency (N_R) is defined as the ratio of the temperature change in the hot (low pressure) gas over the temperature difference between the gas entering the hot and cold (low and high pressure) sides of the regenerator and assuming the weight rate of flow and specific heat to be constant:

$$N_R = \frac{(T_8 - T_9)\, Wc_p}{(T_8 - T_4)\, Wc_{p\ min.}}$$

The decision to use this effectiveness was arbitrary. It should be noted that higher regenerator efficiencies increase the cycle thermal efficiency but they also increase the cost of the heat exchanger and pressure drops. The optimum heat exchanger would balance the increased cycle efficiency against increased costs. However, for Phase I of this study there was not sufficient cost information to make the comparison.

Plate fin type surfaces were used in the heat exchanger to calculate system pressure drops. For the low pressure side a 15.08 surface was used and for the high pressure side a 19.86(1). These may not be the optimum surfaces. In fact, a plain tube or fin tube exchanger might be used in the final design. However, the use of these surfaces did permit the calculation of comparative pressure drops for the regenerator, precooler and intercooler and cooling water requirements.

The minimum cycle temperature was picked as 100° F with a maximum cooling water temperature of 70° F. This minimum gas temperature could be lowered and cycle efficiency increased by assuming higher cooler efficiencies. Again this is a question of the effect of the increased cooler cost on the electrical power costs. Now that more data are available the cooler efficiency can be optimized.

Maximum cycle temperatures are limited by the allowable inlet temperature of the turbine. For the present, with standard materials, this limit is 1300° F. This also represents a temperature limit imposed by existing fuel elements.

Cycle thermal efficiencies for all five gases were calculated on the basis of a 15% system pressure loss. This assumes that by making any given piece of equipment (piping, heat exchangers or the reactor) the proper size the pressure losses will equal. This completely disregards

cost as a factor. Assuming equal cost for the equipment (turbines, compressors, piping, heat exchangers and the reactor) was impossible because of the number of cases that needed study and the lack of supporting cost data. Therefore, for the two gases of most interest (He and N_2) efficiencies were calculated at 10, 15 and 20% pressure loss. Final values of efficiency were based on extrapolation between these calculated pressure loss figures.

Helium cycle efficiencies were calculated using the perfect gas laws. Values of 1.25 and 1.66 were used for the specific heat at constant pressure and the ratio of specific heats. Other helium constants were taken from reference (2). A comparison of compressor work as determined on the Mollier diagram in reference (2) and the values calculated using perfect gas relationships indicated essentially no difference.

For the other gases values of c_p, the ratio of specific heats, thermal conductivity, enthalpy, entropy, specific volume, and viscosity were taken from reference (3). This reference had tabulated values for various pressures and temperatures. There was sufficient information to construct Mollier diagrams for CO_2, CO, N_2 and A. These diagrams were used for determining cycle work and efficiency.

Compressor work values for CO_2 calculated from the perfect gas relationships were 10 to 30% higher than for similar calculations using the Mollier diagram. Similar discrepancies existed for the other gases. The differences in the two methods were not as severe for the turbine work. Use of the Mollier diagram raised the cycle thermal efficiency three to six points in every case.

DISCUSSION OF CALCULATIONS

The helium calculations are summed up in Figures VII-2 through VII-7. Figure VII-2 is a plot of cycle thermal efficiency and required helium flow for various cycle compression ratios for three cycle maximum temperatures. Two similar sets of curves can be drawn for pressure loss ratios (Δ /P max) of .10 and .20. The results of these three sets of curves are presented in Figures VII-3 and VII-4. Here the maximum thermal efficiencies and the corresponding flows are plotted as a function of the maximum cycle temperature for the three pressure loss ratios. These figures show the substantial efficiency gains that can be realized by reducing pressure losses.

Figure VII-5 is a plot of the 1860° R maximum temperature line previously shown on Figure VII-2. However, two additional efficiency curves for 100 and 80% regenerator effectiveness have been drawn. The 100% line indicates the gain in efficiency possible with higher regenerator efficiencies. Superimposed on the efficiency curves are the constant reactor ΔT lines. Note that higher ΔT's always require higher compression ratios. However, the higher ΔT's do not necessarily mean

reduced thermal efficiency. Systems with higher reactor Δ T's require less heat exchanger surface, thus reducing pressure losses and equipment costs. Furthermore the lower reactor inlet temperatures may permit higher maximum cycle pressures. These advantages must be balanced against the increased cost of the compressors.

Figures VII-6 and VII-7 are plots similar to Figure VII-5, except the maximum cycle temperatures have been reduced. Figure VII-7 clearly indicates that some reactor Δ T's and regenerator efficiencies are impractical. This trend is indicated at higher cycle temperatures in some of the other gases.

Figures VII-8 through VII-14 are plots of nitrogen flow and cycle efficiencies similar to those just discussed for helium. General trends of the curves are the same as before. For equal pressure loss ratios the thermal efficiencies are higher.

Figures VII-15, VII-16 and VII-17 are basic plots of thermal efficiency and coolant flow for argon, carbon dioxide and carbon monoxide. Data from these curves and Figures VII-2 and VII-9, for maximum efficiency and the corresponding flow, are summarized in Figures VII-18, VII-19 and VII-20. Note that all these figures assume cycle pressure losses of 15%.

Figure VII-18 shows helium to be the least desirable gas from an efficiency standpoint. However, in Figure VII-21 where the gases are compared on an equal equipment power cost basis helium is more desirable than nitrogen but less desirable than CO_2. This results because for equal power costs the pressure drop for N_2 is higher than for He. For CO_2 the higher pressure drops are overbalanced by the increased thermal efficiency. Helium, because of its high specific heat, requires a minimum mass flow as shown in Figure VII-20; however, its lower density requires circulation of a larger volume of gas. Because of its higher sonic velocity helium can be circulated faster, thus the required flow area is less than for most other gases. This is demonstrated by the tabulated flow areas in Table VII-1. If flow areas are compared on the basis of equal pressure drops helium still requires the least area.

System pressure losses for the piping, regenerator, precooler and intercooler were calculated for two maximum cycle temperatures, three reactor ΔT's, and system pressures of 400 and 600 psi for various flow rates. Thus with the reactor ΔT's and maximum cycle pressure calculated for each of 216 cases, it was possible to estimate the plant thermal efficiency and coolant flow per KW of electrical output. The flows for the three sizes of reactors when divided by the coolant flow per KW gave the gross electrical output of the plant.

Figure VII-22 is a plot of net plant efficiency versus reactor size for 1400 and 1200° F maximum outlet temperature, six and eight inch lattice for 600, 500 and 400° F reactor ΔT, using He as the coolant. The general trend is toward lower plant efficiencies as the total power increases. This results because the larger reactors require larger

pressure vessels and this reduces the maximum system pressure. For a given system pressure loss this results in a higher percentage of pressure loss.

The fact that the 500 and 400° F ΔT lines are higher than the 600° F ΔT line can be attributed to the fact that the power plant % ΔP drops as ΔT decreases. This is the opposite of the trend of the reactor % ΔP. For the 1200° F case the change in the power plant overbalances the reactor effect. The opposite is true in the 1400° F case.

Figure VII-23 shows plant efficiency for He as a function of specific fuel power, lattice, maximum cycle temperature, and reactor power for a reactor ΔT of 600° F. In all cases the plant efficiency decreases as specific power, reactor ΔT, and reactor power increase.

Figures VII-24 and VII-25 are plots of the cycle thermal efficiency for the three pressure loss ratios for helium. Superimposed on these curves are the constant reactor ΔT lines which are in turn subdivided into spaces representing a one per cent change in ΔP. Figure VII-24 (1400° F maximum temperature) indicates that for equal % ΔP's the 500° ΔT line is the line of maximum efficiency.

The required mass flow rate lines and the corresponding constant ΔT lines are also shown on Figure VII-24. The mass flow for a specific system ΔP, when divided into the total reactor flow, gives the plant gross electrical output. The mass flow lines were not included, for reasons of clarity, on similar plots for 1200° F helium and nitrogen at 1400 and 1200° F.

Figure VII-26 shows plant efficiency for nitrogen as a function of reactor ΔT, specific power, maximum temperature, lattice and reactor power level. These curves indicate that same reactor ΔT gives the maximum cycle efficiency. Other plots of the N_2 data could not be constructed because a large number of cases could not be worked. These cases were impossible because of excessively high ΔP's across the reactor or in the 1200° F maximum case because 600° ΔT was not practical.

Figures VII-27 and VII-28 are plots of the nitrogen cycle efficiency for three pressure loss ratios. Again the constant reactor ΔT lines have been superimposed. Note that for the 1200° F case 600° F ΔT is not possible.

A note of caution is in order when using curves VII-22, VII-23 and VII-28. The cycle, curve or point indicating the highest cycle efficiency is not necessarily the optimum point. As has been mentioned previously the optimum point is the one which gives power for the lowest cost (mils/kw). On the other hand, the maximum efficiency points on curves VII-24, VII-25, VII-27 and VII-28 are very close to the lowest cost power point as determined by reactor ΔT.

The cycle thermal efficiency curves for all gases were calculated for a maximum cycle pressure of 40 atmospheres (588 psia). Recalculation of the thermal efficiency and mass flow at 400 psia resulted in only a small change (about one per cent) in these values. Therefore, the 40 atmosphere values were used for all calculations of the cycle plant efficiencies in Figures VII-22, 23, and 26. This simplifying assumption was made to reduce the work involved as there were thirteen pressures, ranging from 556 to 276 psia, in the 216 direct cycle cases that were studied.

TABLE VII-1

COMPARATIVE FLOW AREAS
FOR INDIVIDUAL GASES

Gas	Tmax °F	PR	Area*	Reactor Outlet	LP Turb Outlet	Comp Inlet	Comp Outlet	HP Reg. Outlet
He	1400°	2.5	.0715	1.00	2.03	1.27	.562	.789
	1200	2.5	.0956	1.00	2.03	1.34	.596	.792
	1000	2.5	.147	1.00	2.02	1.43	.632	.818
N_2	1400	4	.122	1.00	3.21	1.99	.560	.786
	1200	4	.158	1.00	3.10	1.87	.579	.778
	1000	3	.243	1.00	2.84	1.94	.621	.806
CO	1400	4	.124	1.00	3.18	1.96	.618	.788
	1200	3	.1875	1.00	2.45	1.54	.554	.800
	1000	3	.259	1.00	2.37	1.63	.594	.807
CO_2	1400	5	.108	1.00	4.17	2.44	.509	.815
	1200	5	.133	1.00	4.10	2.58	.539	.804
	1000	4	.199	1.00	3.35	2.06	.608	.804
A	1400	3	.195	1.00	2.37	1.51	.564	.780
	1200	3	.258	1.00	2.32	1.60	.596	.778
	1000	2.5	.418	1.00	2.00	1.41	.603	.830

η_c = .85
η_t = .88
η_p = .15
η_r = .91

T_{min} = 100° F
Mach = 0.1
P_{max} = 40 Atm

* Actual reactor outlet flow area (ft^2/MW electrical)

---

1. W. M. Kays; A. L. London. Compact Heat Exchangers, The National Press - 1955. Table 13.

2. Thermodynamic Properties of Helium at High Pressures and Temperatures. S. W. Akin, General Electric Company., Schenectady Works, NP-124. May 1947.

3. Tables of Thermal Properties of Gases - U. S. Department of Commerce - National Bureau of Standards. Circular 564, November 1, 1955.

1-3-58
1-21-58

HELIUM

THERMAL EFFICIENCY VS COMPRESSION RATIO
HELIUM FLOW VS COMPRESSION RATIO

TEMP	MINIMUM	960 °R
η_c	COMPRESSOR	.85
η_t	TURBINE	.88
η_R	REGENERATOR	.91
P	MAXIMUM	90 ATM
γ_p	$\Delta P / P_{MAX}$	.15

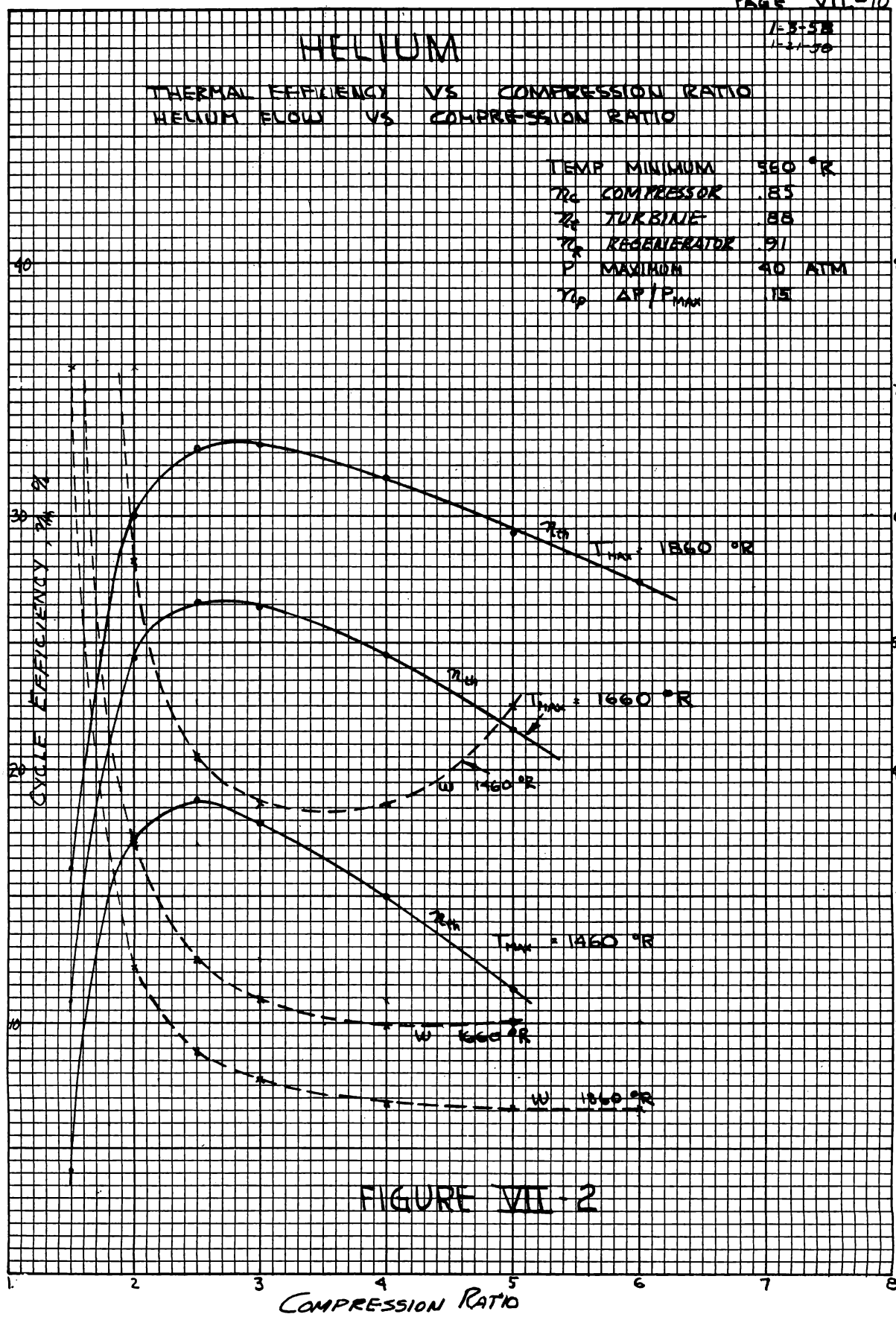

FIGURE VII-2

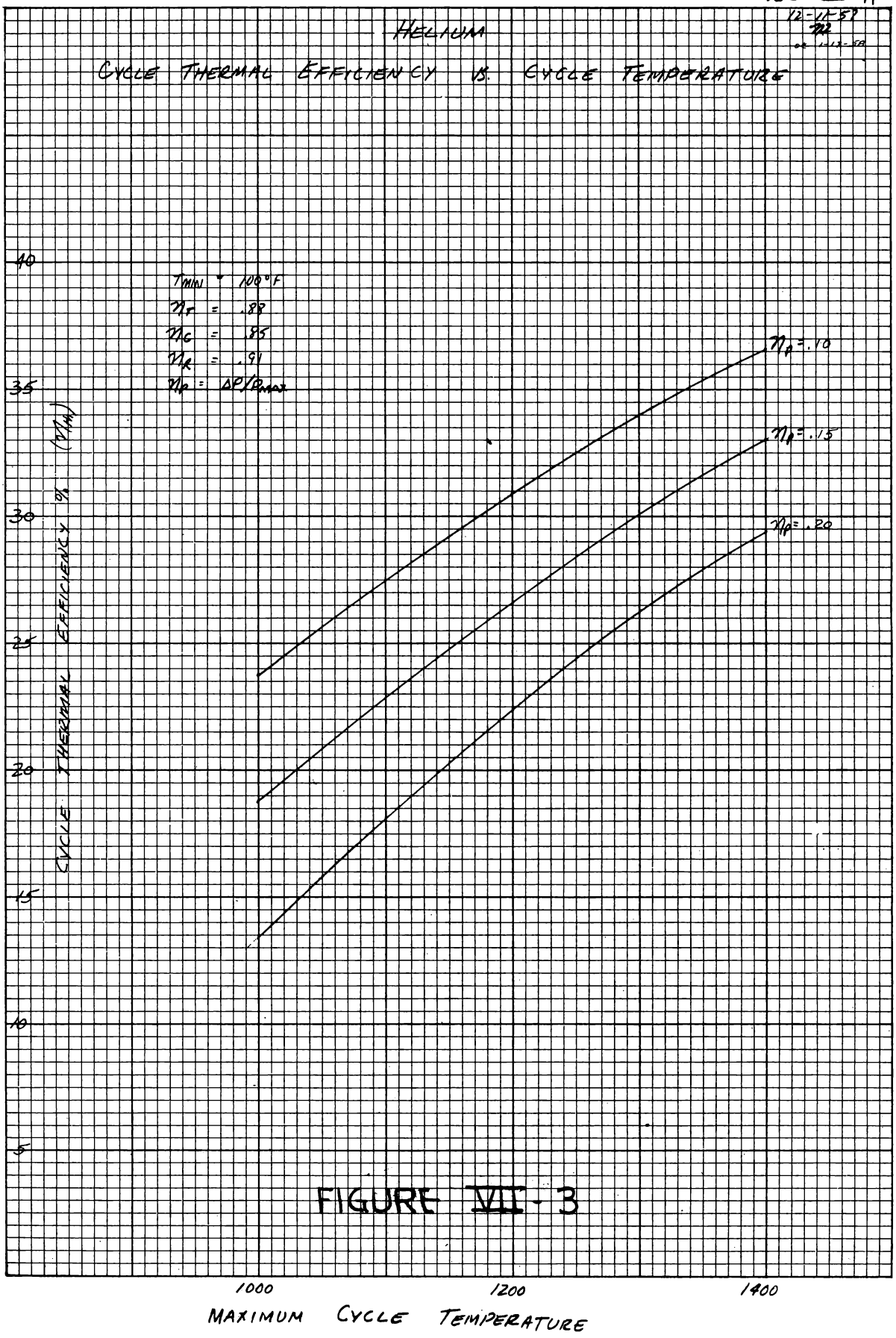
HELIUM
CYCLE THERMAL EFFICIENCY VS. CYCLE TEMPERATURE
12-11-59
T_{MIN} = 100°F
η_T = .88
η_C = .85
η_R = .91
η_P = $\Delta P/P_{max}$
η_P = .10
η_P = .15
η_P = .20
CYCLE THERMAL EFFICIENCY % (η/η')
40
35
30
25
20
15
10
5
1000
1200
1400
MAXIMUM CYCLE TEMPERATURE

FIGURE VII - 3

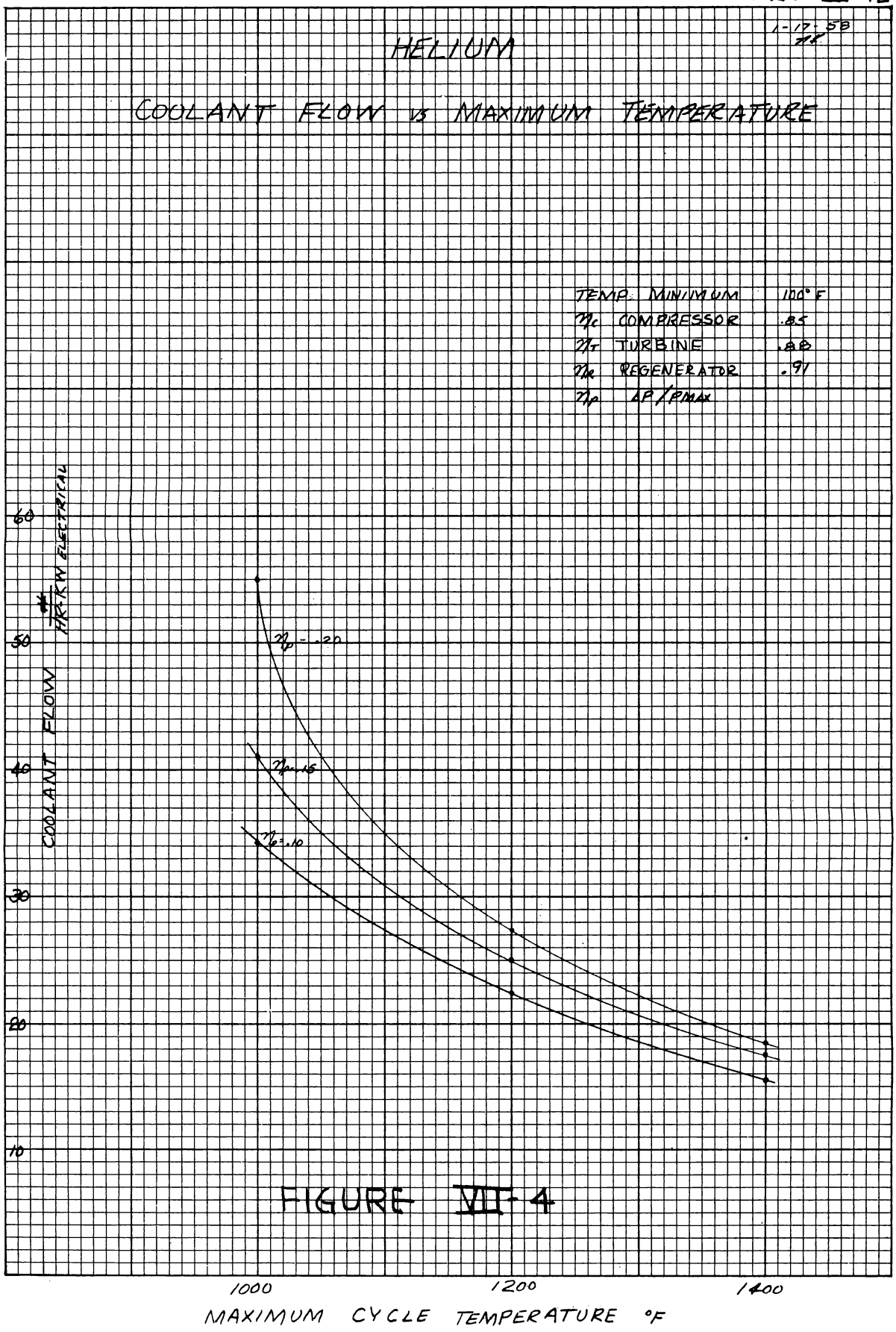
HELIUM
COOLANT FLOW vs MAXIMUM TEMPERATURE
TEMP. MINIMUM 100° F
η_c COMPRESSOR .85
η_T TURBINE .88
η_R REGENERATOR .91
η_p $\Delta P / P_{MAX}$
η_p = .20
η_p = .15
η_p = .10
COOLANT FLOW #/HR-KW ELECTRICAL
GAS FLOW #/HR-KW ELECTRICAL
60
50
40
30
20
10
1000
1200
1400
MAXIMUM CYCLE TEMPERATURE °F

FIGURE III-4

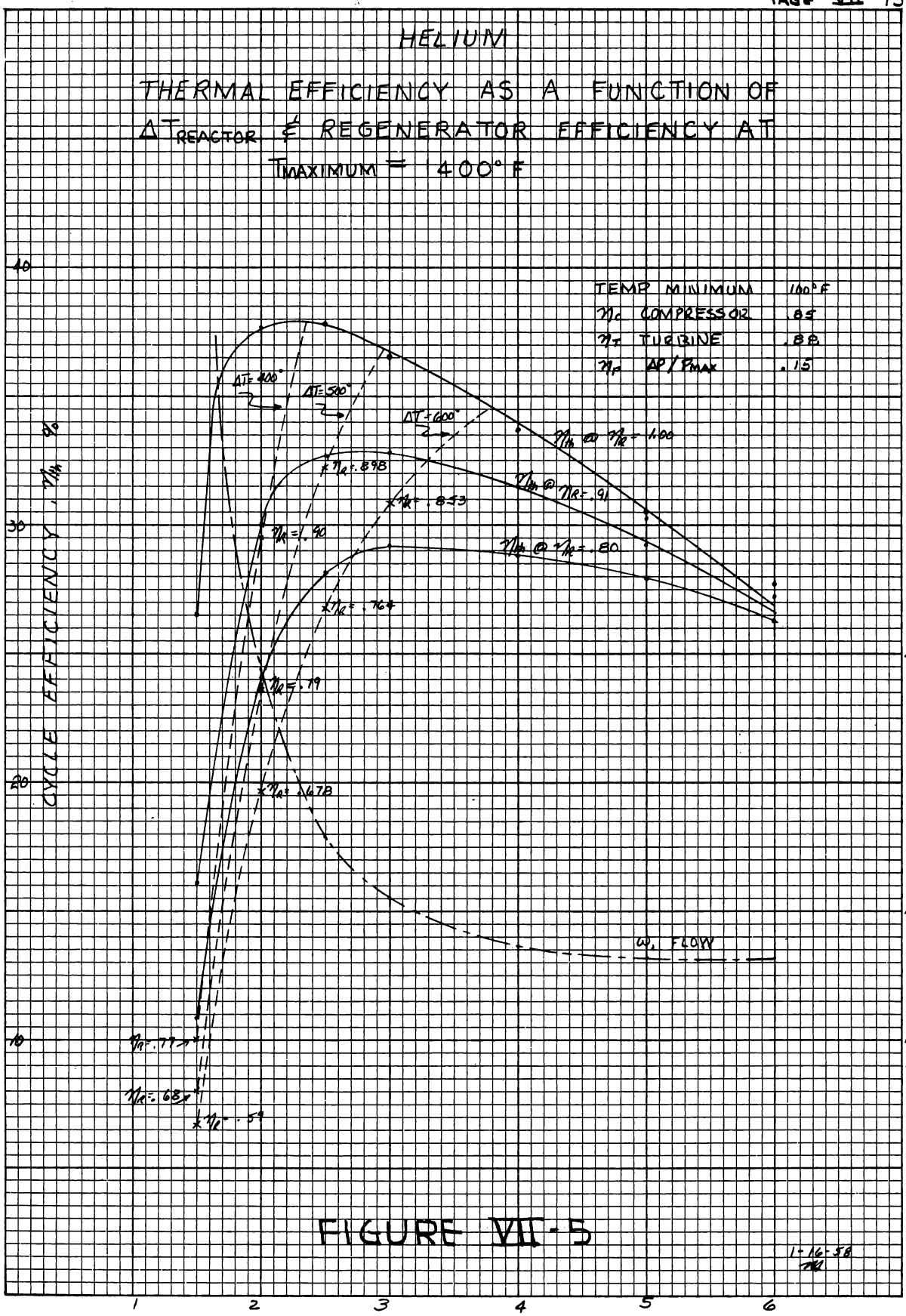
HELIUM
THERMAL EFFICIENCY AS A FUNCTION OF
ΔT REACTOR & REGENERATOR EFFICIENCY AT
T MAXIMUM = 1400° F
TEMP MINIMUM 100° F
η c COMPRESSOR .85
η T TURBINE .88
η P ΔP/P MAX .15
ΔT=400°
ΔT=500°
ΔT=600°
η th @ η R = 1.00
η th @ η R = .91
η th @ η R = .80
η R = .90
η R = .79
η R = .68
η R = .59
ω, FLOW
CYCLE EFFICIENCY η th %
CYCLE EFFICIENCY η th
HELIUM FLOW # / HR-KW ELECTRICAL
COMPRESSION RATIO
40
30
20
10
25
15
5
1
2
3
4
5
6
1-16-58

FIGURE VII-5

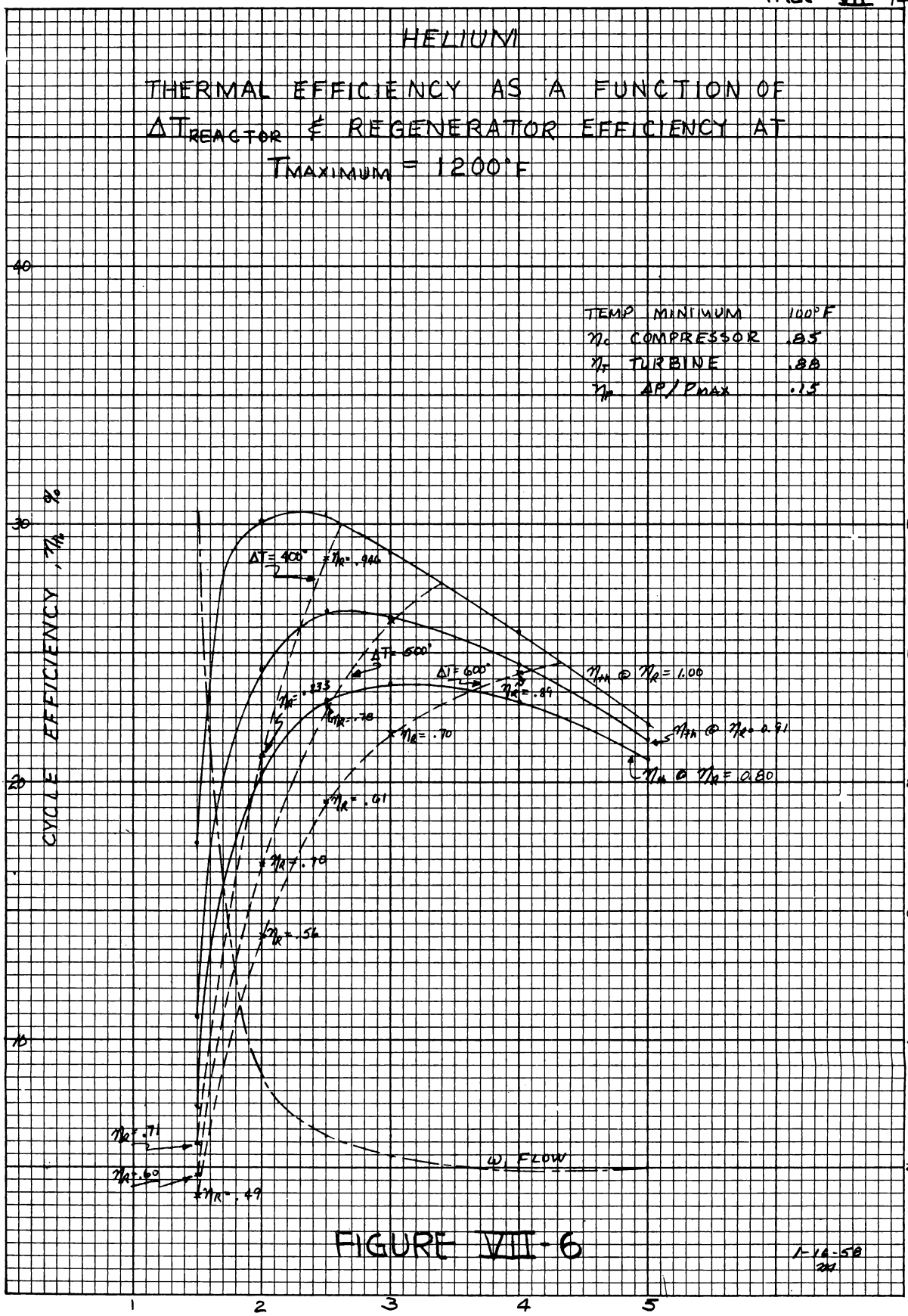

FIGURE VII-6

1-16-58

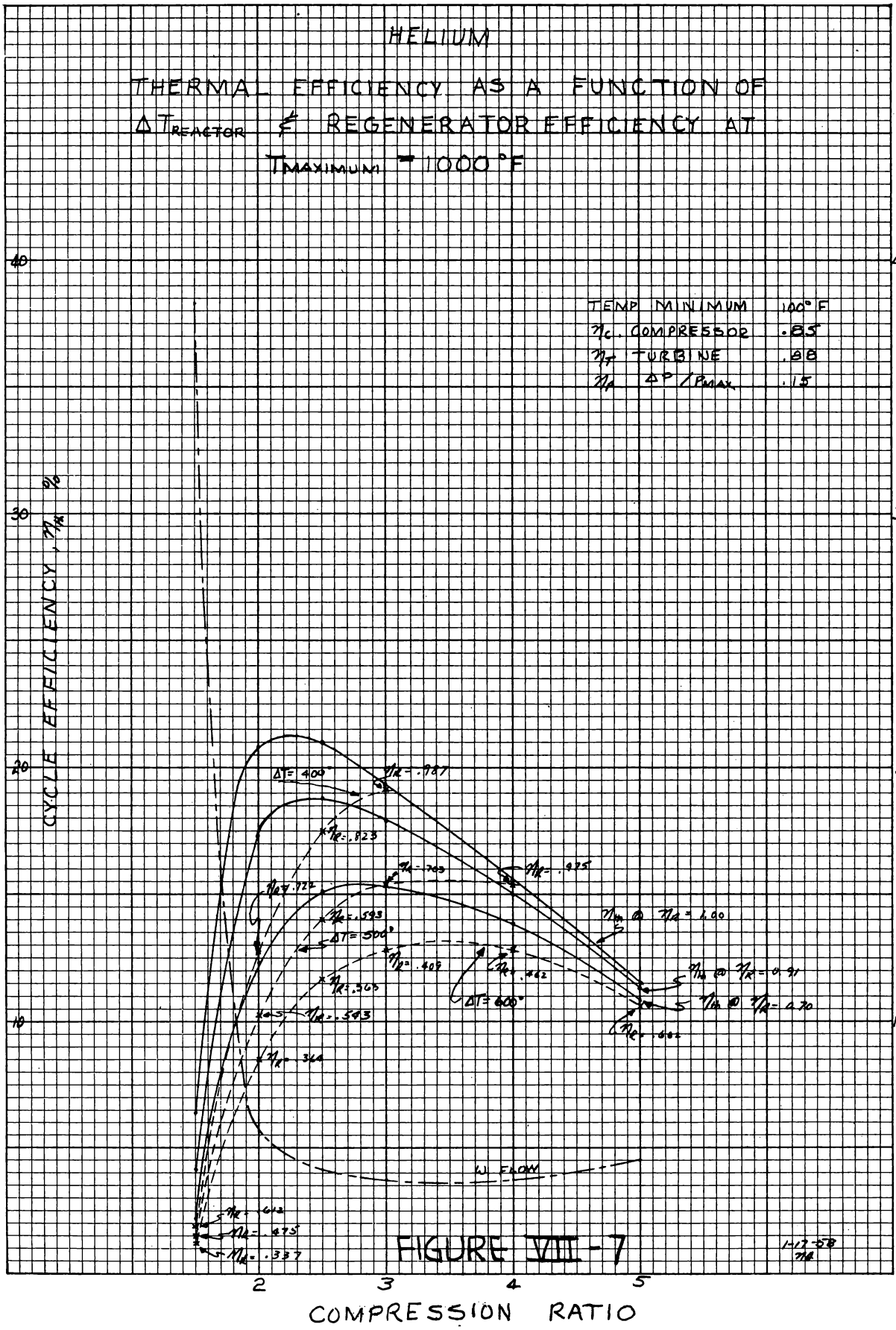

FIGURE VII-7

1-17-58

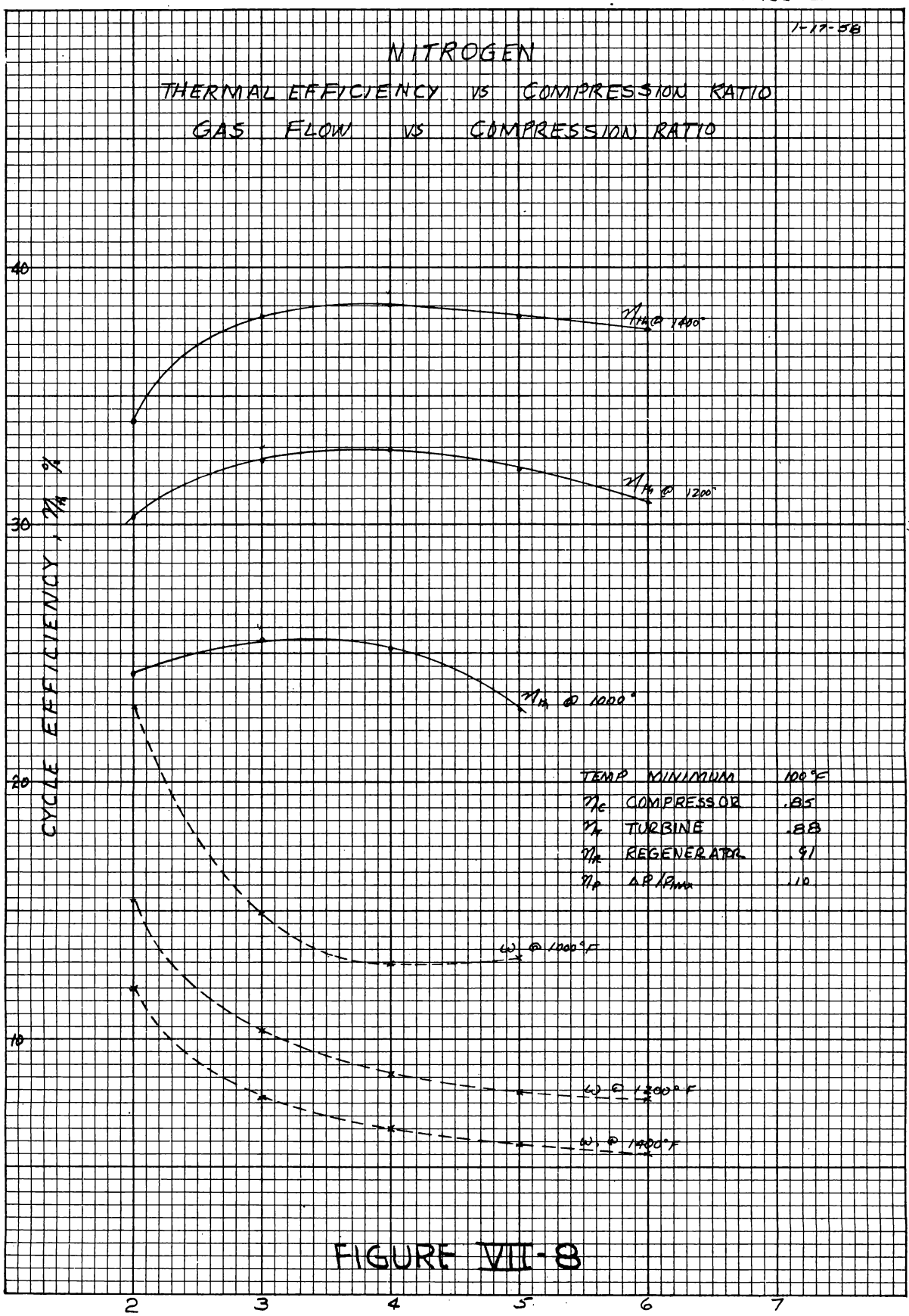
1-17-58
NITROGEN
THERMAL EFFICIENCY VS COMPRESSION RATIO
GAS FLOW VS COMPRESSION RATIO
CYCLE EFFICIENCY, η_{th} %
η_{th} @ 1400°
η_{th} @ 1200°
η_{th} @ 1000°
TEMP MINIMUM 100°F
η_c COMPRESSOR .85
η_t TURBINE .88
η_R REGENERATOR .91
η_p $\Delta P/P_{max}$ .110
W @ 1000°F
W @ 1200°F
W @ 1400°F
40
30
20
10
300
200
100
2
3
4
5
6
7
COMPRESSION RATIO
NITROGEN FLOW, W, # / HR-KW ELECTRICAL
CYCLE EFFICIENCY, η_{th} %

FIGURE VII-8

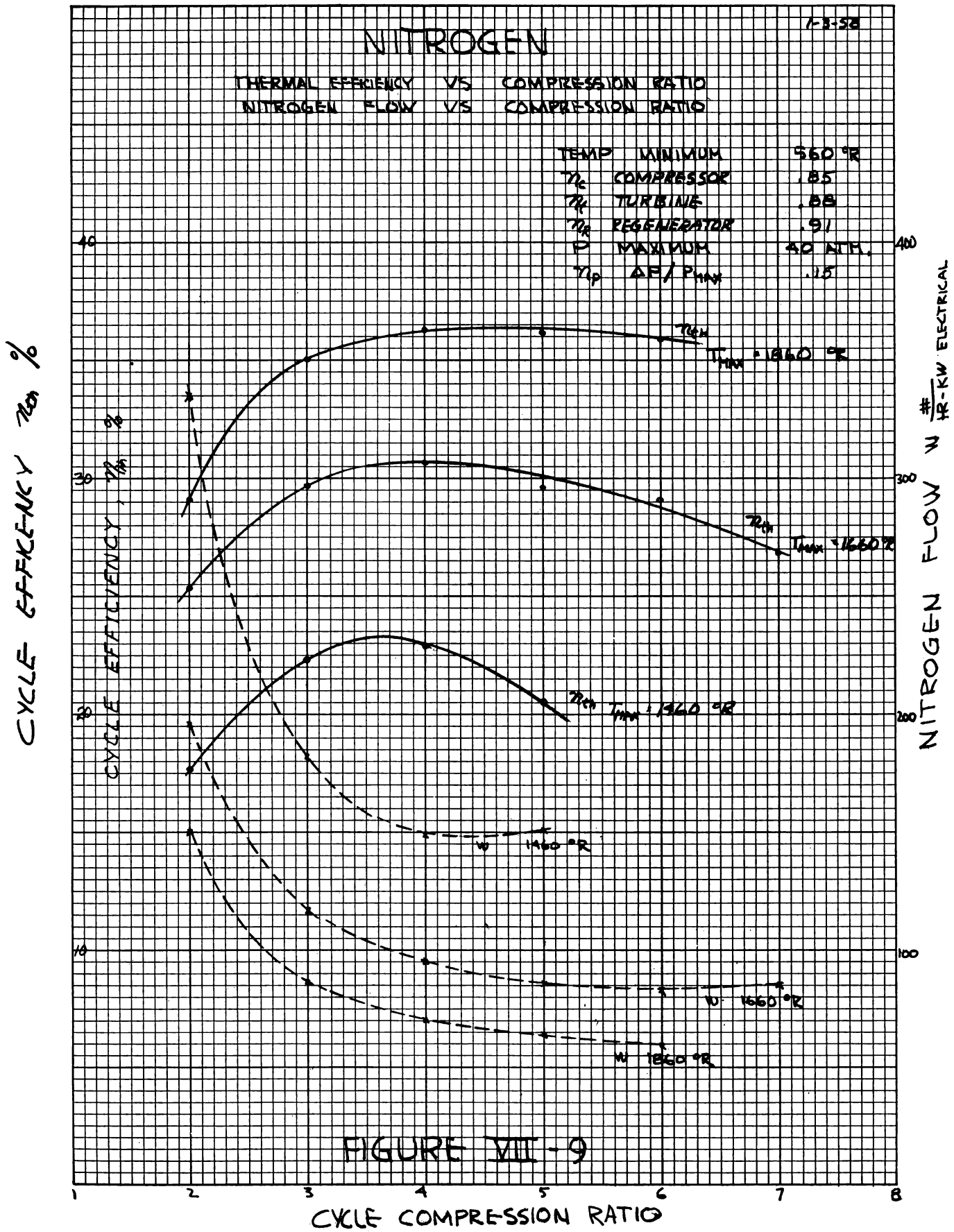
NITROGEN
1-3-58
THERMAL EFFICIENCY VS COMPRESSION RATIO
NITROGEN FLOW VS COMPRESSION RATIO
TEMP MINIMUM 560 °R
η_c COMPRESSOR .85
η_t TURBINE .88
η_R REGENERATOR .91
P MAXIMUM 40 ATM.
η_p $\Delta P / P_{MAX}$ .15
η_{th}
T_{MAX} = 1860 °R
η_{th}
T_{MAX} = 1660 °R
η_{th} T_{MAX} = 1460 °R
W 1460 °R
W 1660 °R
W 1860 °R
CYCLE EFFICIENCY η_{th} %
NITROGEN FLOW W $\frac{\#}{HR\text{-}KW}$ ELECTRICAL
CYCLE COMPRESSION RATIO
40
30
20
10
400
300
200
100
1
2
3
4
5
6
7
8

FIGURE VII-9

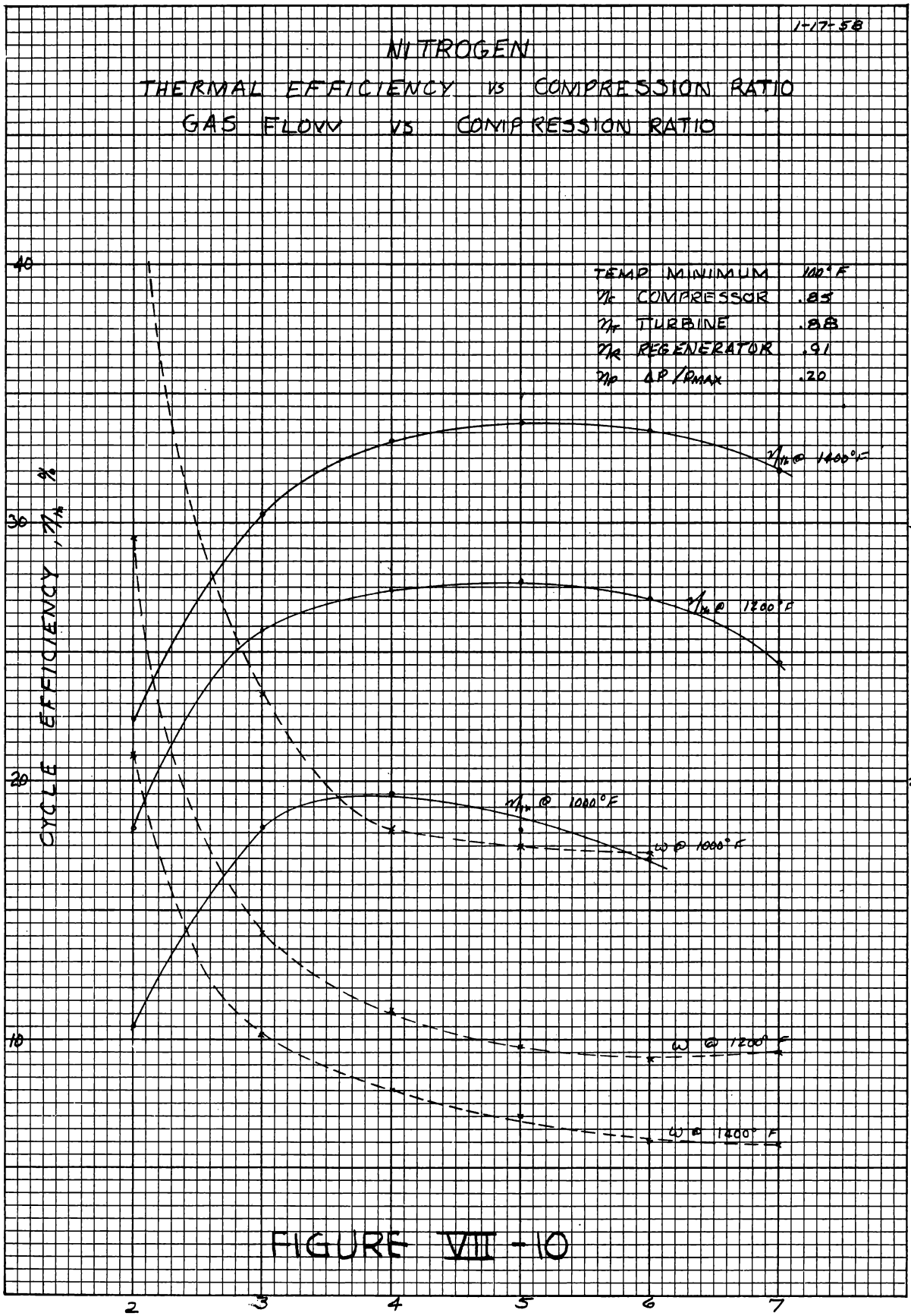

FIGURE VII-10

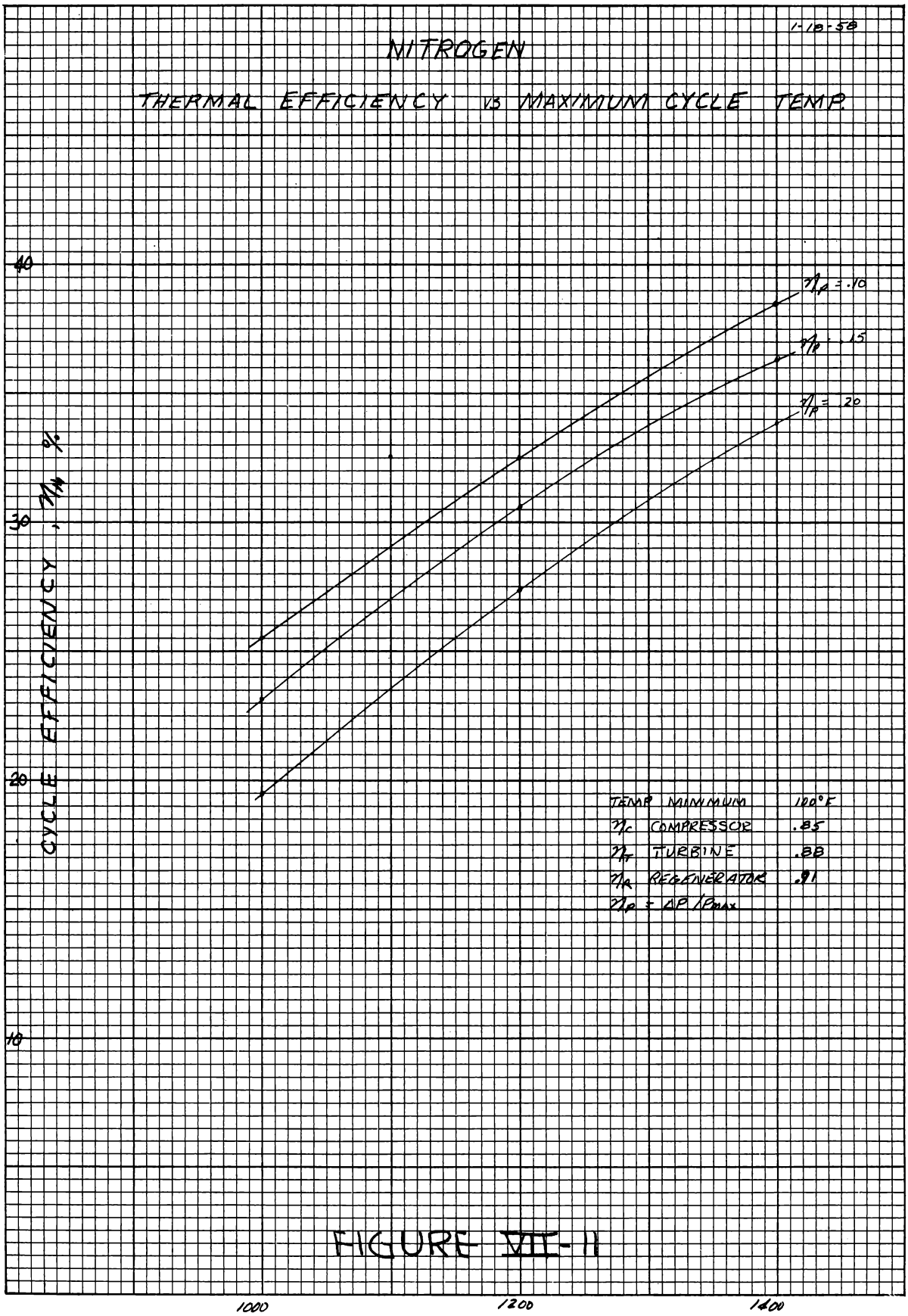

FIGURE VII-11

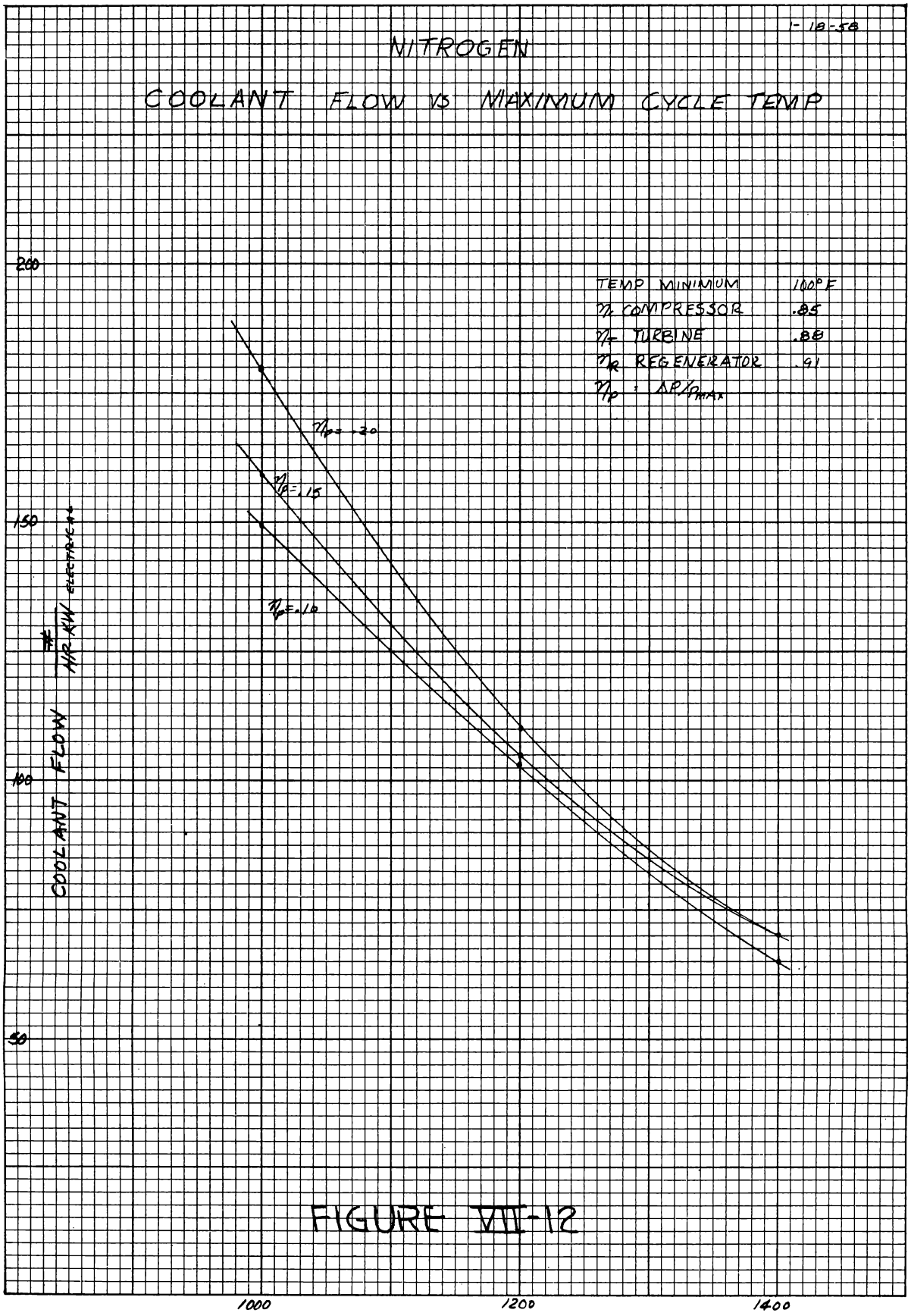

FIGURE VII-12

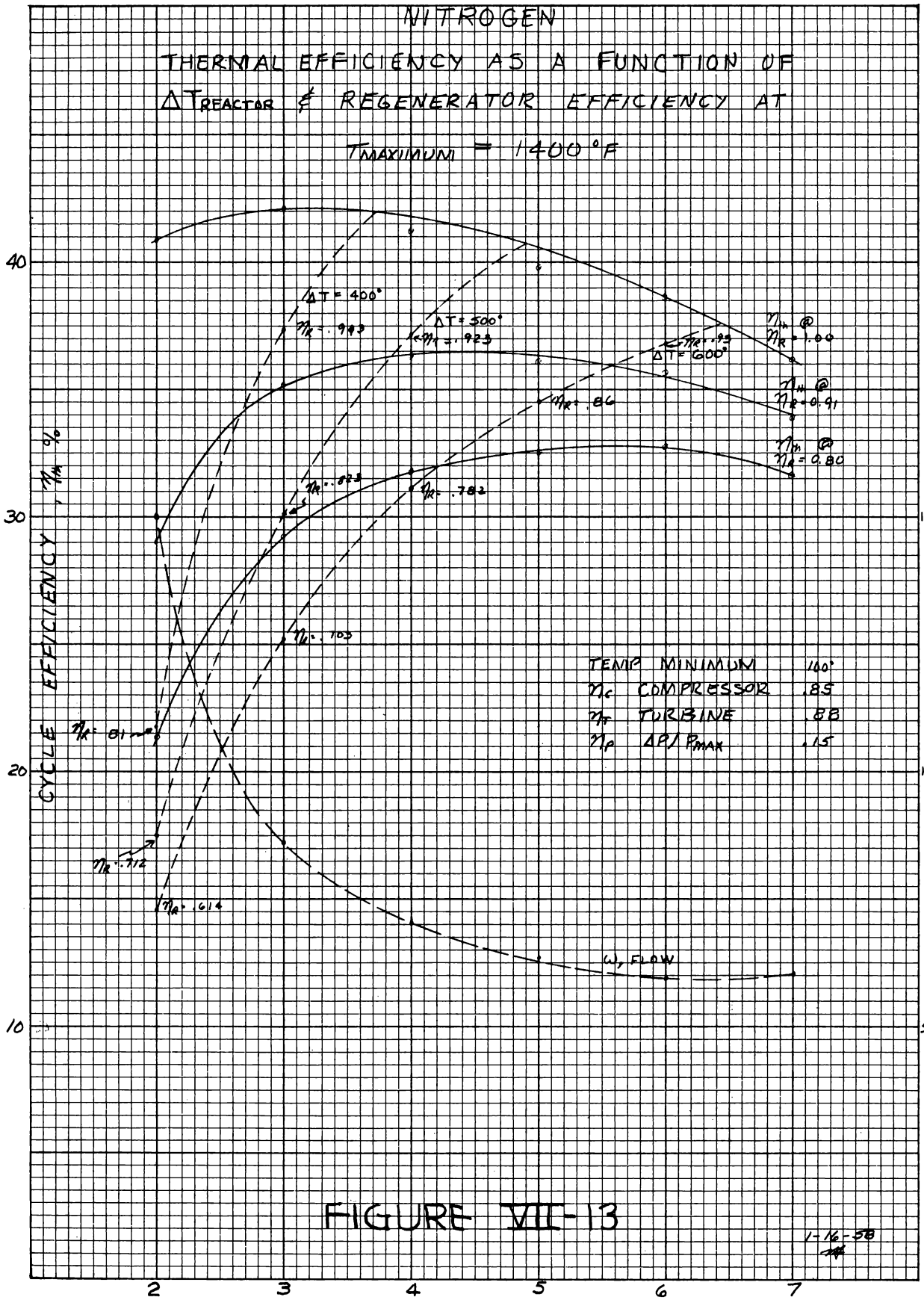

FIGURE VII-13

1-16-58

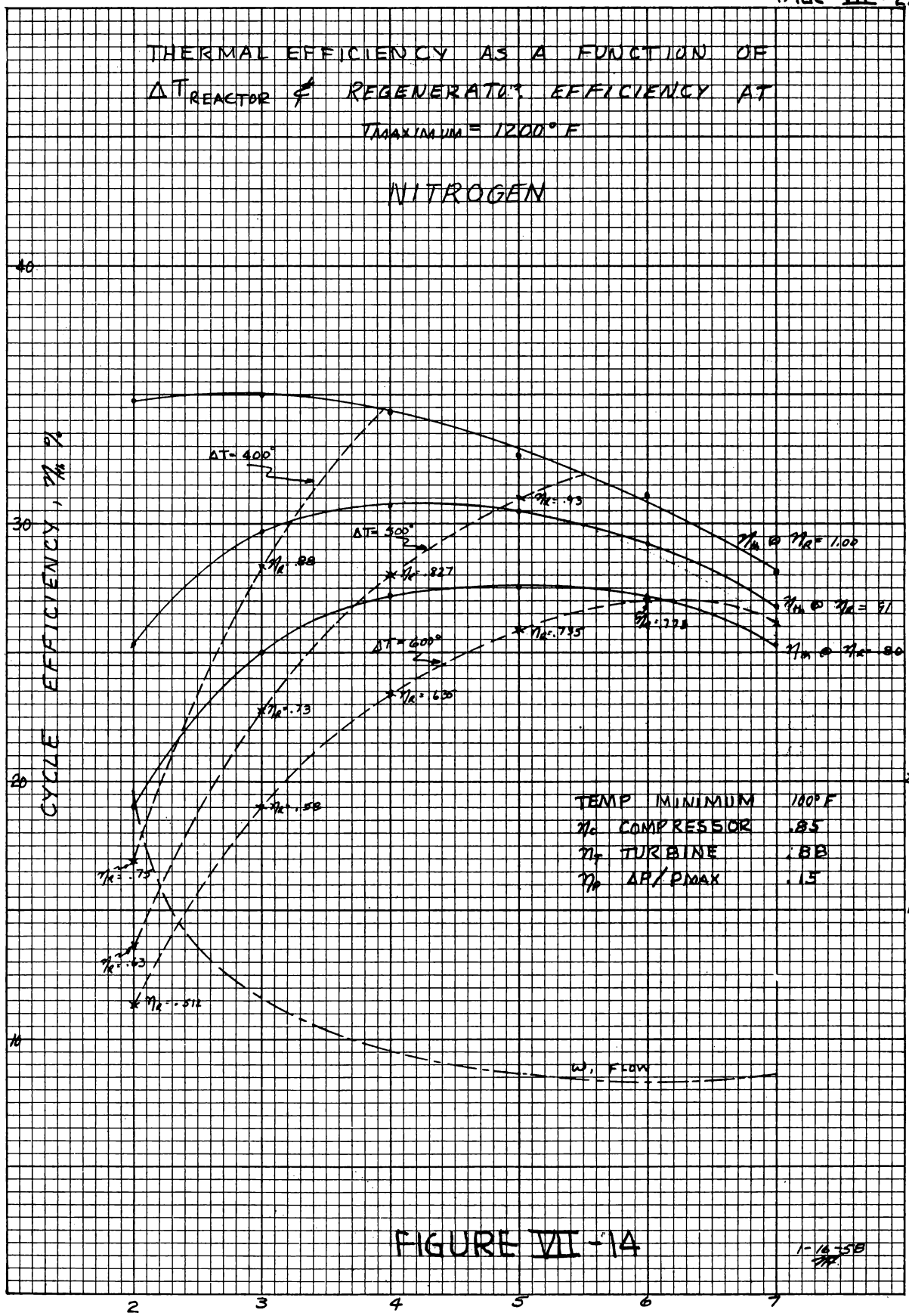

FIGURE VII-14

1-16-58

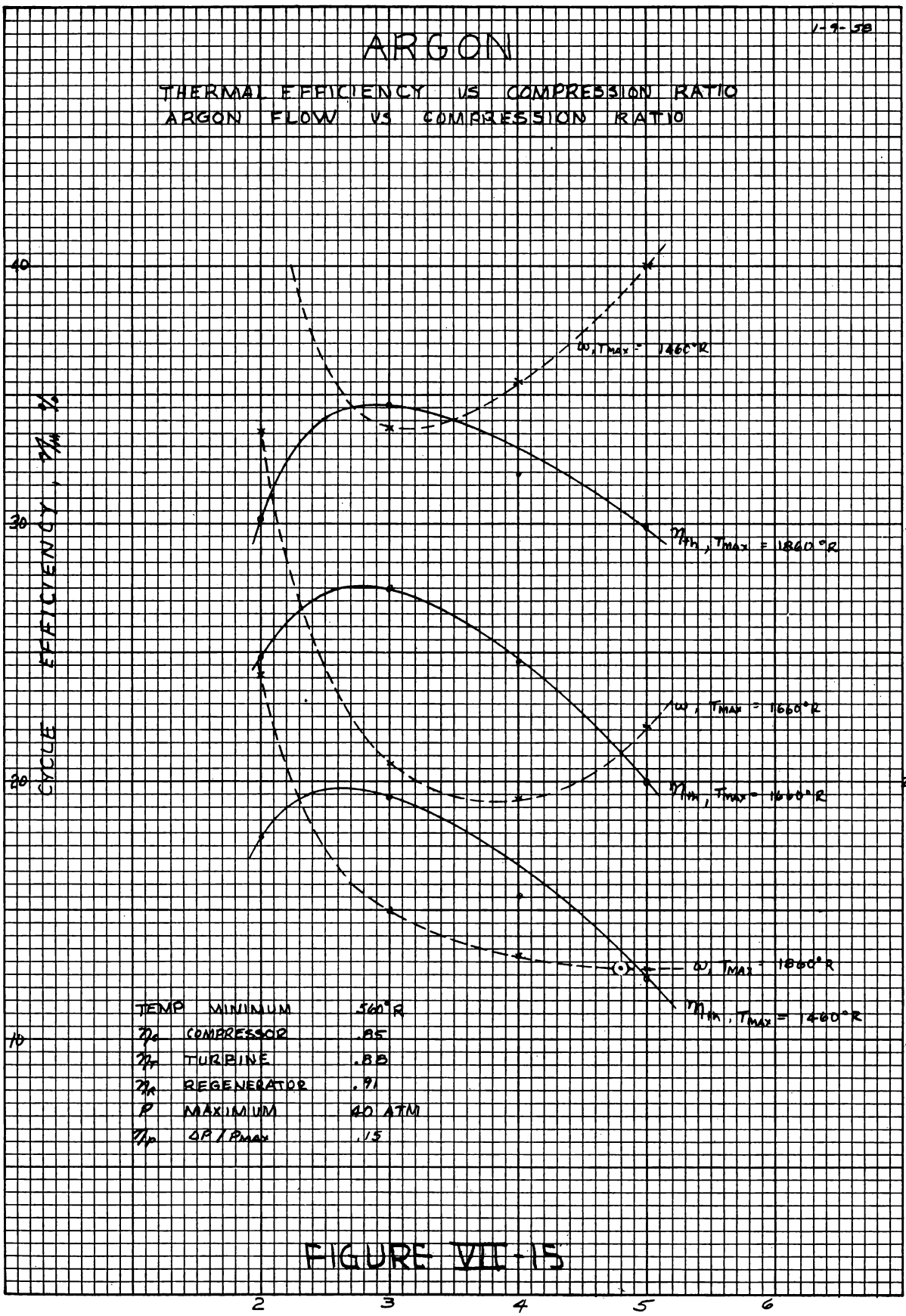

FIGURE VII-15

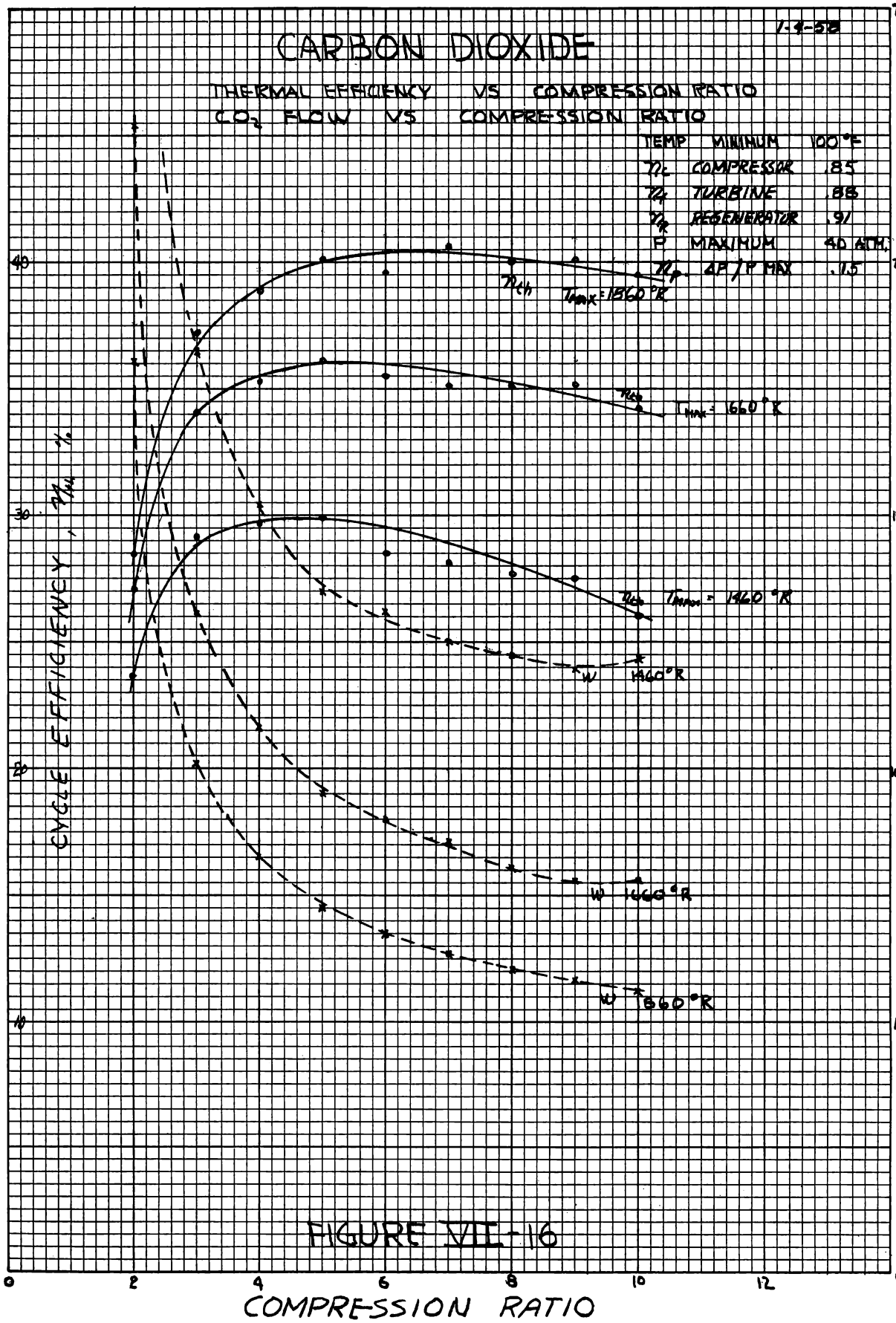

FIGURE VII-16

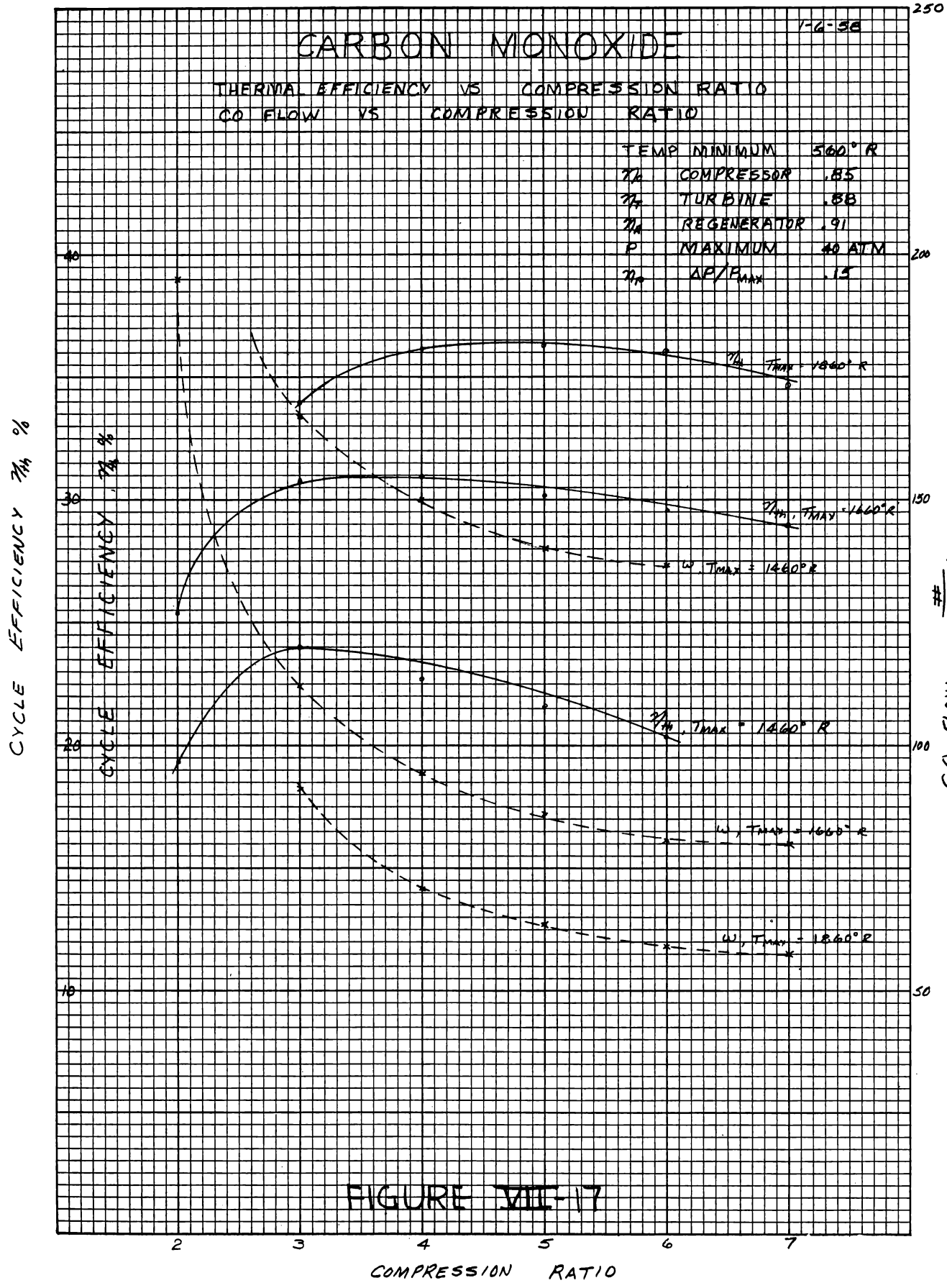

FIGURE VII-17

1-9-58

CYCLE THERMAL EFFICIENCY VS MAXIMUM CYCLE TEMPERATURE

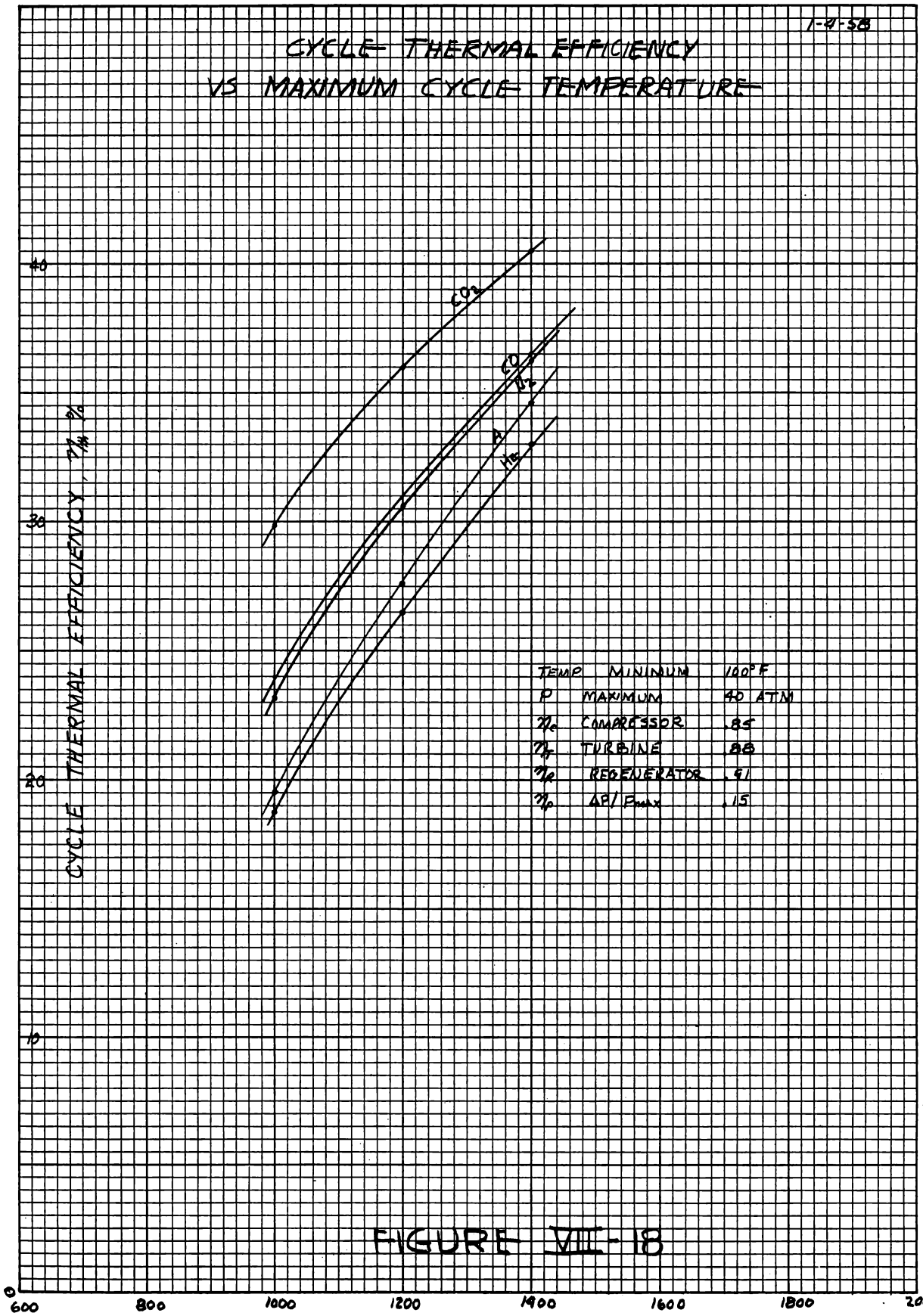

FIGURE VII-18

1-10-58

VOLUME FLOW RATE
VS MAXIMUM CYCLE TEMPERATURE

TEMP	MINIMUM	100°F
P	MAXIMUM	40 ATM
η_c	COMPRESSOR	.85
η_T	TURBINE	.88
η_R	REGENERATOR	.91
η_P	$\Delta P/P_{max}$	.15

GAS FLOW RATE - SCFM / $KW_{ELECTRICAL}$

COOLANT FLOW RATE - SCFM / $KW_{ELECTRICAL}$

70
60
50
40
30
20
10

H_2
A
CO
N_2
CO_2

800 1000 1200 1400 1600 1800

MAXIMUM CYCLE TEMPERATURE - °F

FIGURE VIII-19

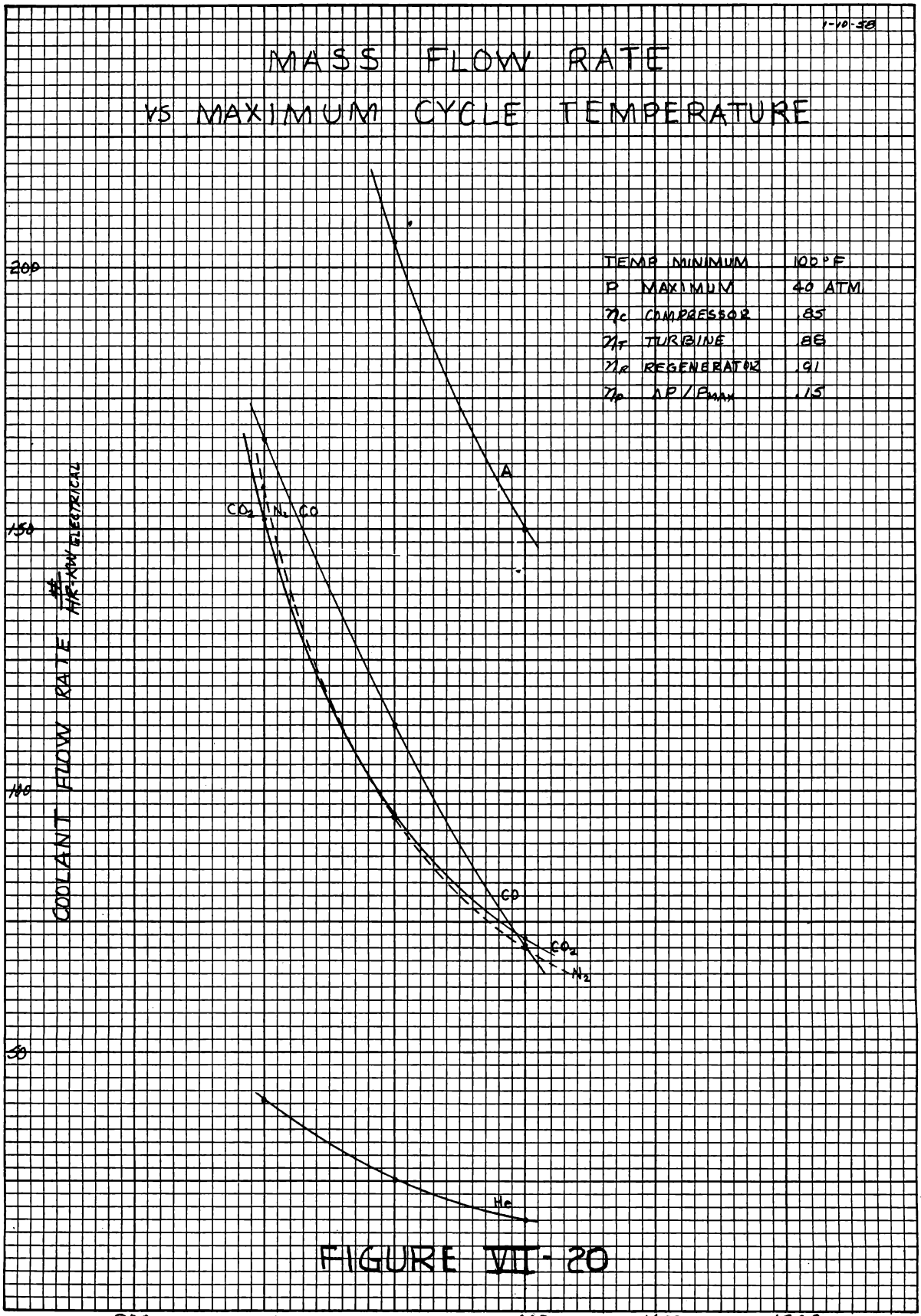

FIGURE VII - 20

For Figure VII-21

see Figure V-2, Page V-17

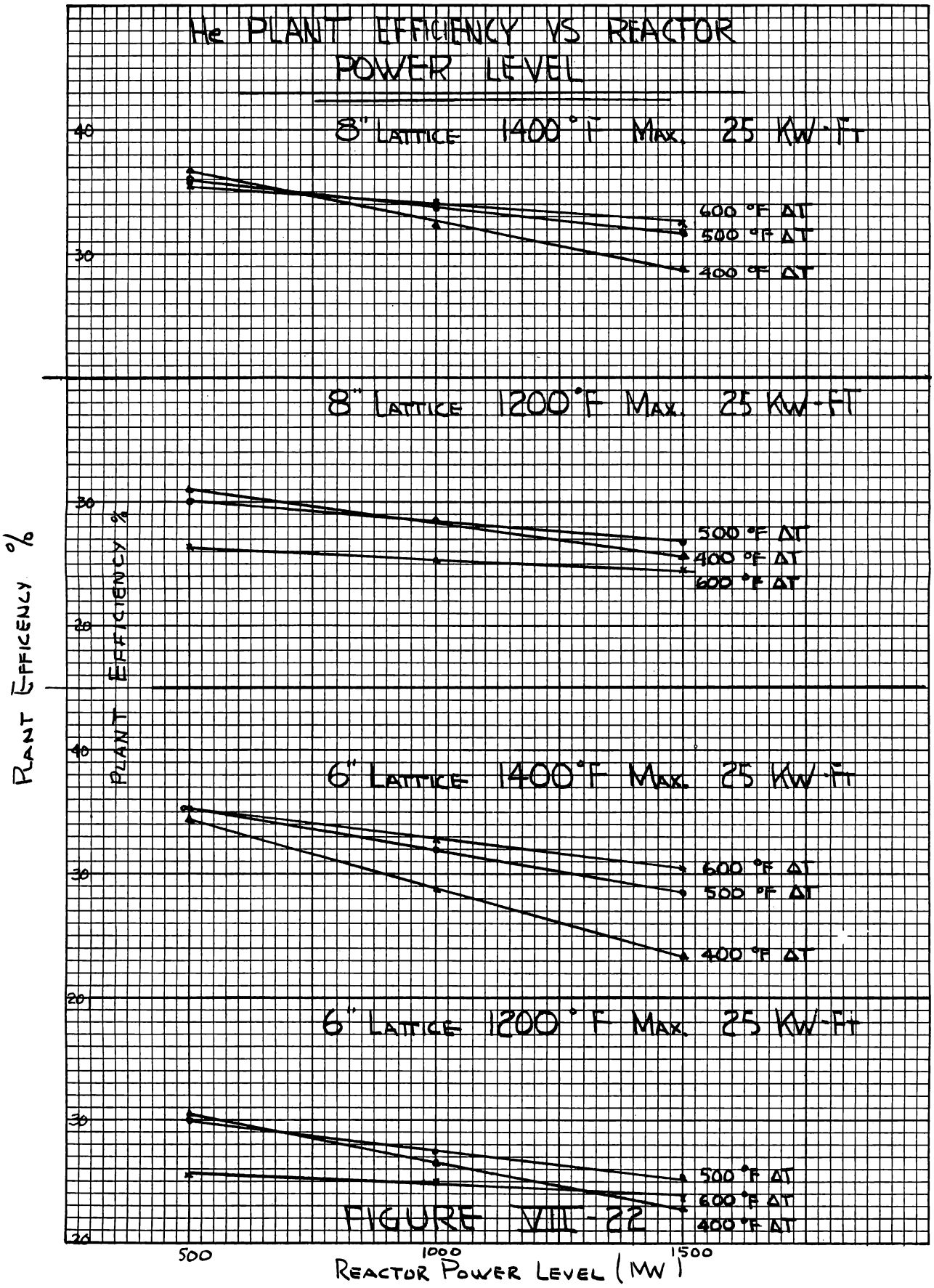

FIGURE VIII-22

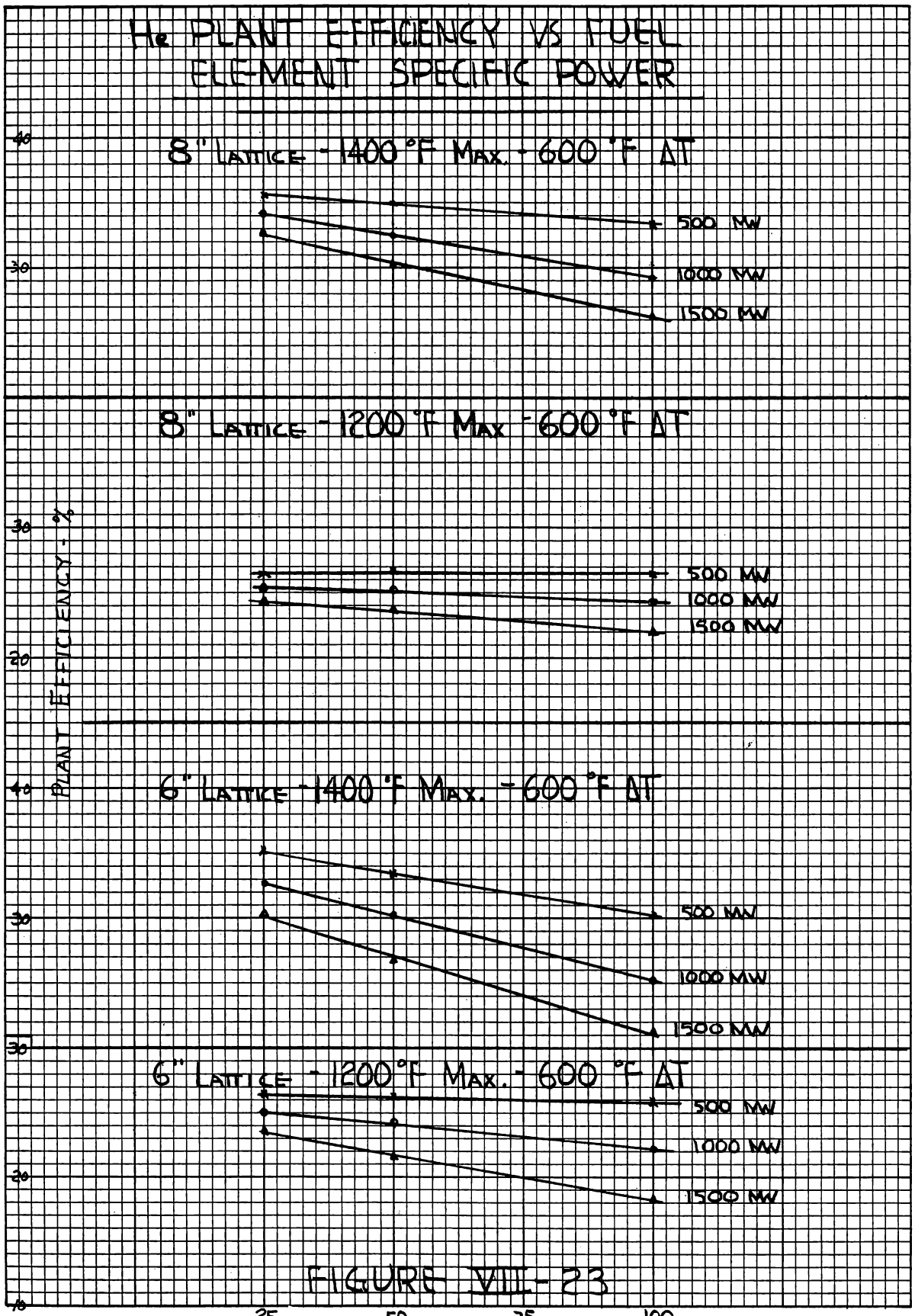

FIGURE VIII-23

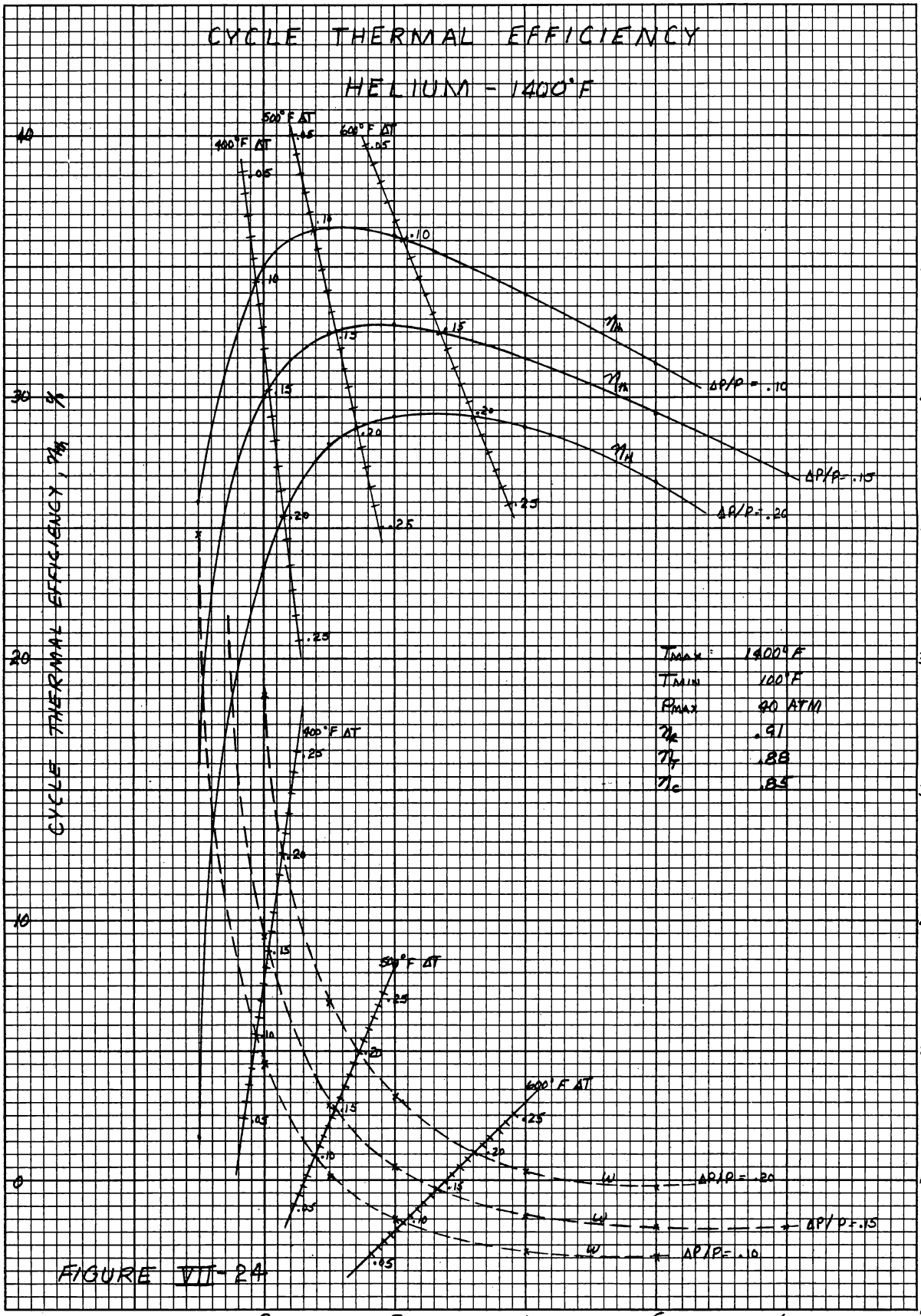

FIGURE VII-24

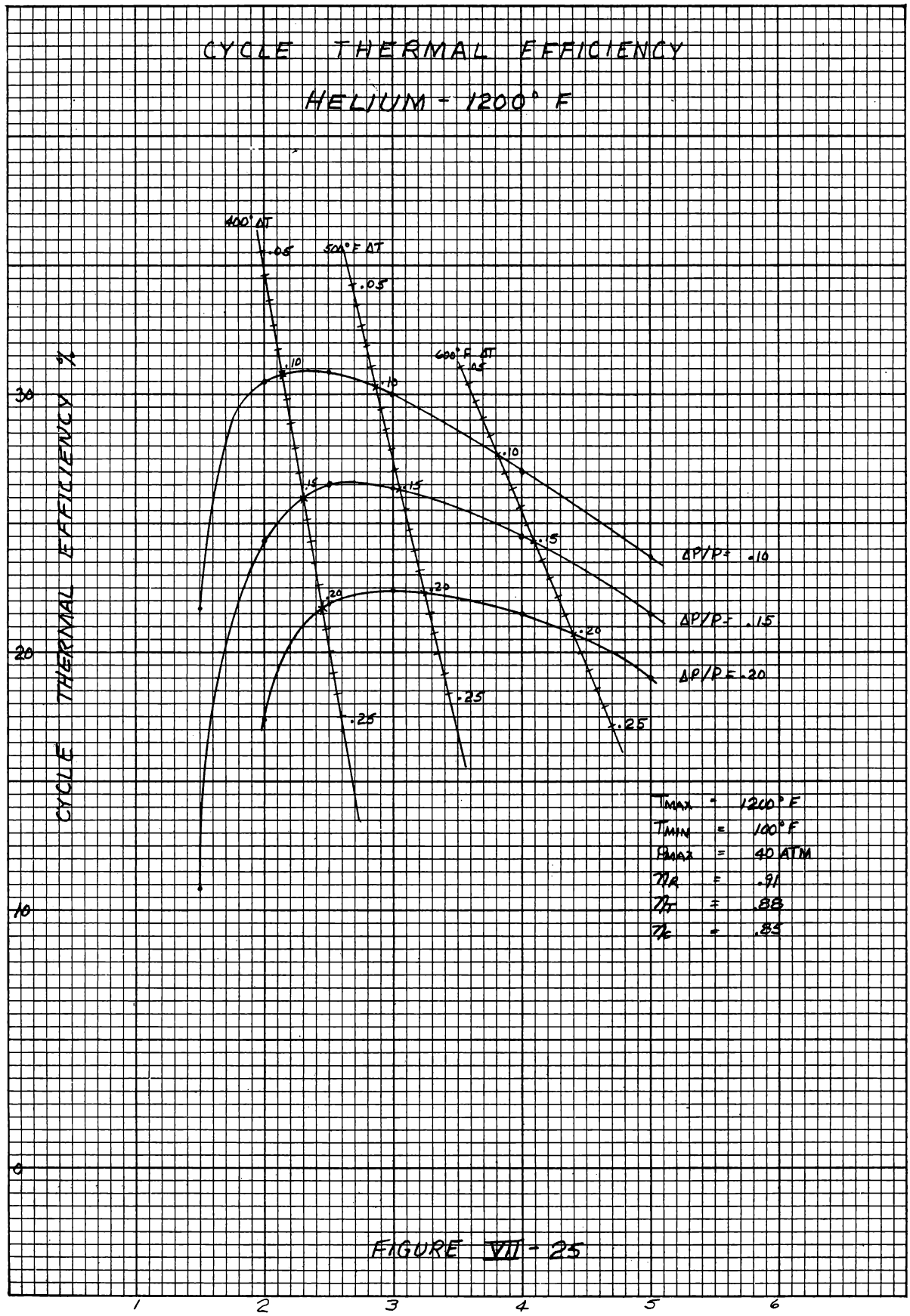

FIGURE VII - 25

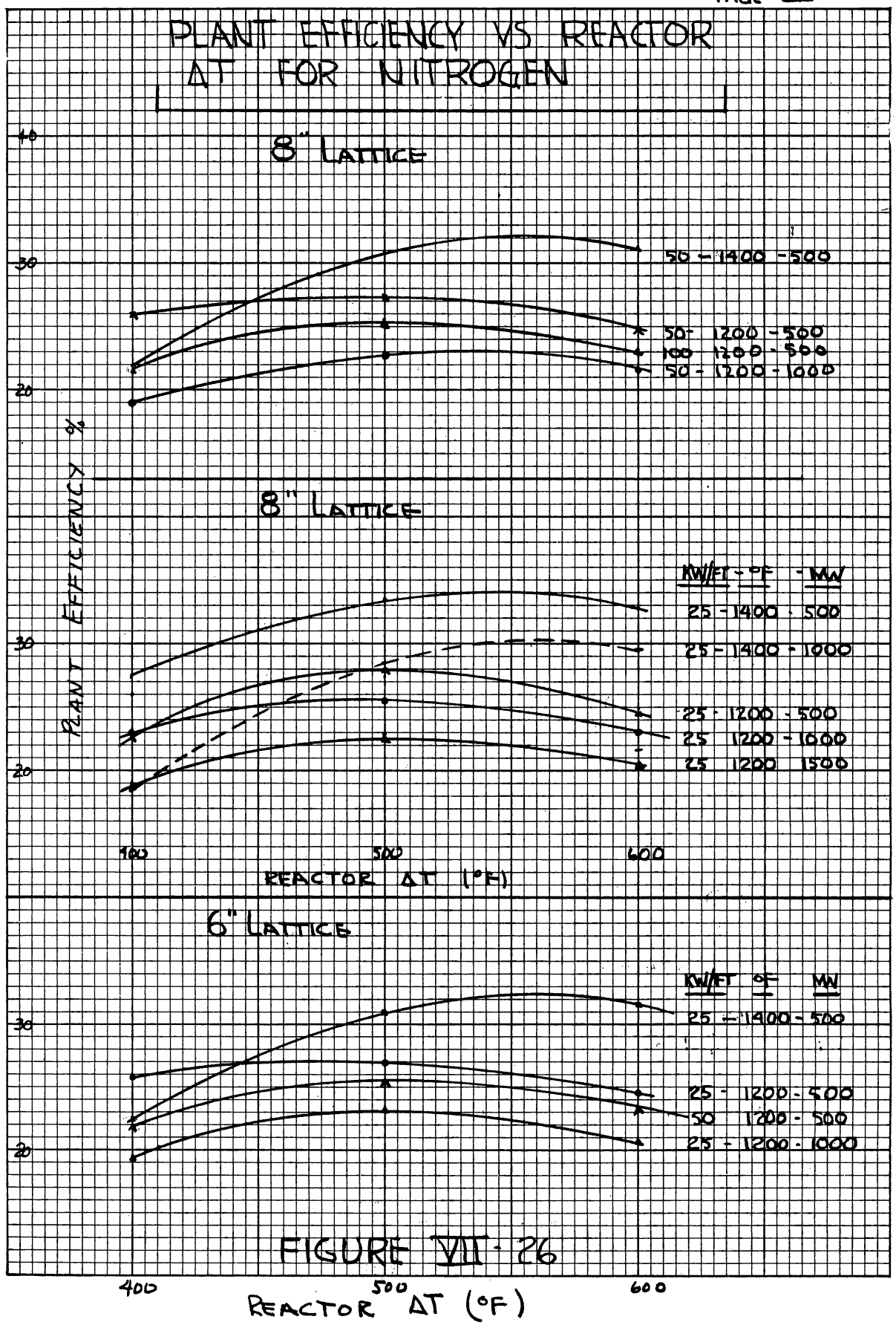

FIGURE VII-26

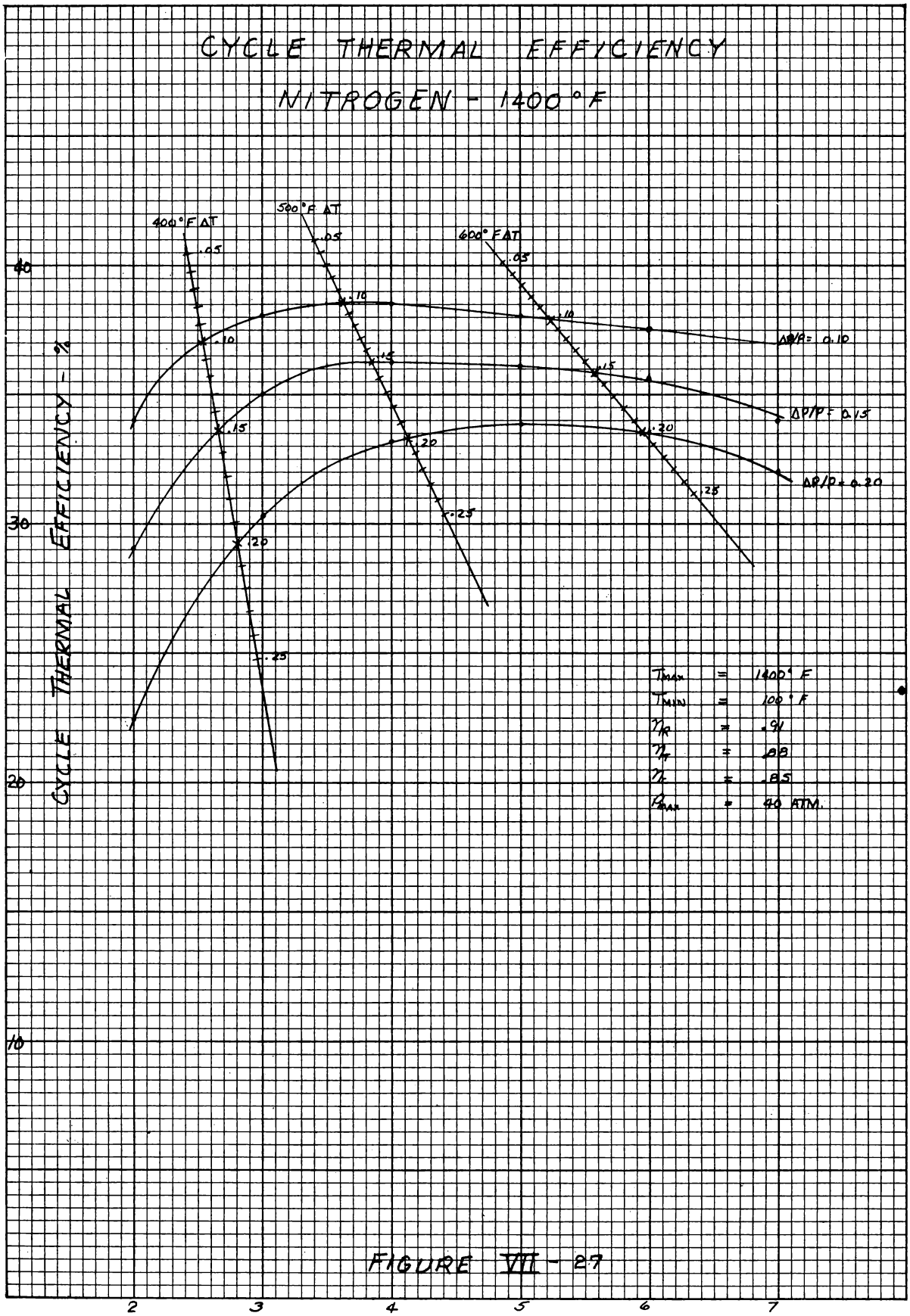

FIGURE VII - 27

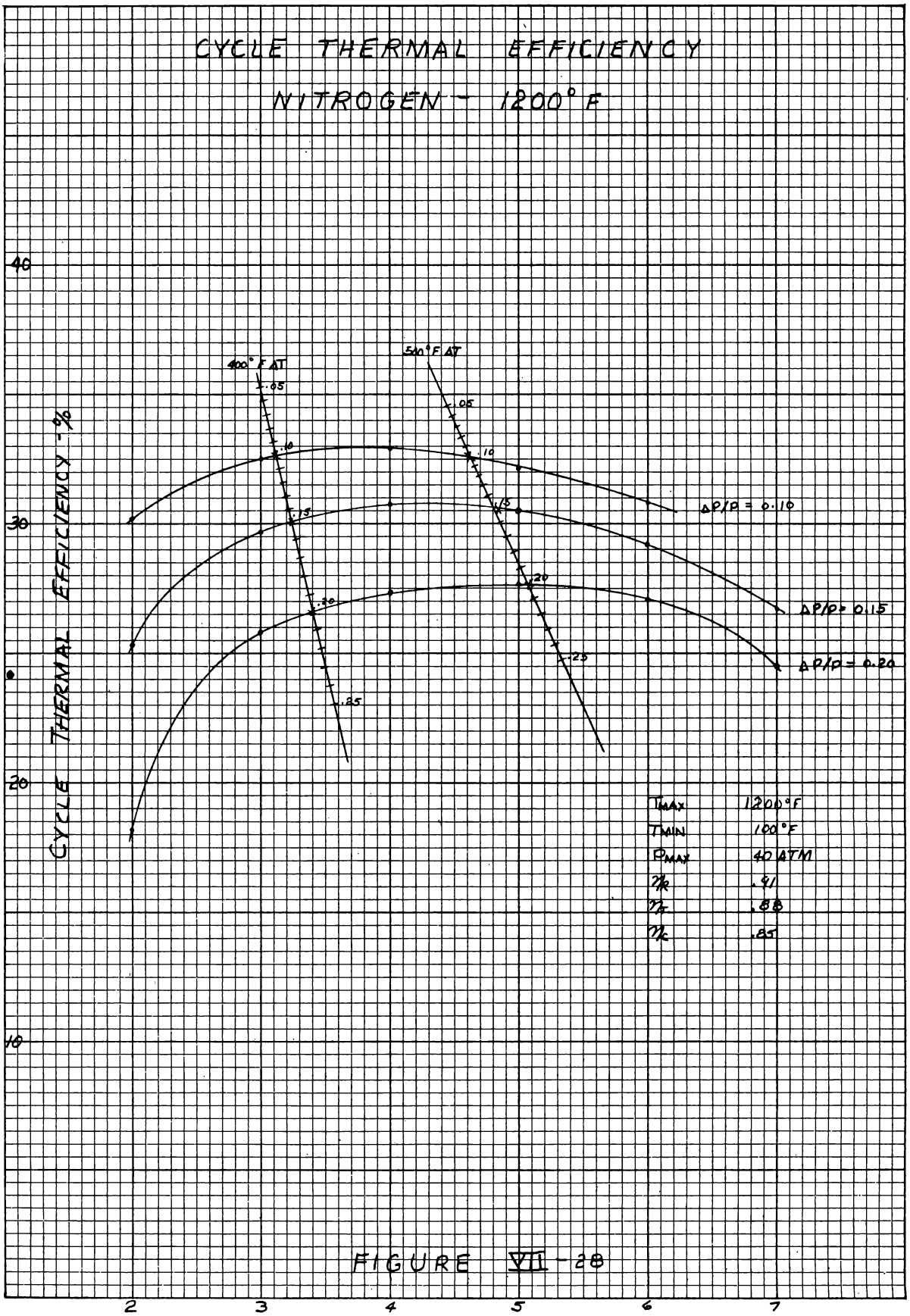

FIGURE VII-28

CYCLE THERMAL EFFICIENCY - %

SECTION VIII

INDIRECT POWER RECOVERY CYCLE STUDY

by

E. L. Etheridge
Process Design Operation
IRRADIATION PROCESSING DEPARTMENT

INDIRECT POWER RECOVERY CYCLE STUDY

INTRODUCTION

As an alternative method of power generation for the gas cooled reactor concept, indirect or steam power cycles were examined. The indirect cycle consists of two separate loops, the reactor primary loop and the secondary or steam loop. The heat energy generated in the reactor is transferred by means of heat exchangers to the steam power cycle. The main advantages of the indirect cycle over the direct power cycle are: (1) Higher plant efficiencies can be obtained at lower coolant temperatures; and (2) Radiation contamination is confined to the reactor and the primary loop, whereas the entire direct gas cycle can be considered to be radioactively contaminated.

For the purposes of economic comparison with the direct gas cycles, steam power cycles were calculated for cases with reactor gas outlet temperatures from 600° F to 1200° F with most emphasis placed on the 1000 and 1200° F cases with reactor ΔT's of 600, 500 and 400° F. The indirect cycle (Figure VIII-1) was considered to consist of the heat exchangers and gas blower equipment and the primary loop piping in the reactor primary loop and the steam power equipment in the secondary loop. This report is a review of the effects of the various reactor parameters upon the steam power generation cycles. The economic evaluation of these parameters will be considered in Section X of this document.

SUMMARY AND CONCLUSIONS

A preliminary power reactor study was made to determine the effects of various gas cooled reactor parameters upon an indirect power cycle or steam power cycle. It was found that the reactor parameters: temperature, ΔT, and specific tube power significantly affect the net plant output due principally to the primary gas coolant pumping power requirements. Therefore, the gas pumping power requirements must be minimized in order to economically produce low cost electrical power with an indirect power cycle. In order to achieve this low gas pumping power requirement, the study results indicate that, for the cases considered, the reactor should be designed for a ΔT of 600° F or greater, a specific tube power of 25 KW per foot or less, and with a maximum reactor outlet temperature of 1200° F.

Superheated steam power plants can be easily adapted to a gas cooled reactor for the production of saleable power; however, extensive development work would be required for the design of heat exchangers and gas blowers.

REACTOR PRIMARY LOOP DESCRIPTION

Heat Exchangers

With the exception of the reactor, the heat exchange equipment comprises the largest single capital cost item in a gas cooled reactor-steam power plant system. In order to obtain low cost power it is

necessary that the heat exchangers be designed for maximum performance per unit of cost. The selection of the type of heat exchange equipment for the indirect cycle case is also influenced by the requirement for a minimum gas pressure loss, reasonable sizes of equipment, and ease of fabrication. For this study, the shell and tube type of exchanger was chosen with the reactor gas coolant on the shell side and the water and/or steam on the tube side. The number of heat exchangers was set at four for the 500 MW reactor cases with the heat exchanger units being doubled and trebled for the 1000 and 1500 MW reactor cases.

Equipment Arrangement

Figure VIII-2 shows a schematic diagram of a heat exchange unit. Reactor gas enters at the top and passes through the superheater, evaporator and preheater sections, respectively, under crossflow conditions. The feedwater enters the preheater section at the base of the heat exchanger and is heated to within 50° F of the saturated steam temperature. The water then enters the evaporator section where 80 per cent evaporation occurs. The steam and water mixture is separated in the steam drum with the saturated steam fed into the superheater section. The steam is superheated to within 50° F of the incoming reactor gas temperature.

The preheater and evaporator sections are made up of multiple pass transverse finned one-inch O.D. tubes spaced on an equilateral tube pitch of 2.125 inches. Each tube is brought out through the shell wall to be connected to a common header. With this method of flow manifolding, single tubes can be isolated without entering the heat exchanger vessel.

The superheater section is arranged in a similar manner as the preheater and evaporator sections, consisting of multiple pass bare two-inch boiler tubes spaced on an equilateral tube pitch of 2½ inches.

The heat exchanger shell is insulated on the inside to permit the use of carbon steel for wall material by reducing the temperature gradient through the wall. To prevent gross contamination of the insulation material a thin metal shell is added on the inside surface of the insulation material. Manholes are provided for inspection of the tubes and vessel interior.

Film Coefficients

Heat transfer data used in calculating gas film coefficients to transverse extended area tubes for the study cases were obtained from Kern's "Process Heat Transfer"[1]. These data have been substantiated by commercial use at moderate pressures and temperatures.

To establish the range of magnitude of the film coefficients under the varying gas conditions, several heat exchanger cases were calculated. It was found after including a scale resistance of 0.001 on the water side that the over-all heat transfer coefficient, U, was practically constant for all study cases. Therefore, the values of U used for all cases are listed below:

	Helium	Nitrogen
Preheater	350 BTU/hr, ft^2, ^oF	290 BTU/hr, ft^2 ^oF
Evaporator	320 " " "	250 " " "
Superheater	45 " " "	30 " " "

Pressure Drop

The gas pressure drop through the heat exchanger was held to less than 10 psi by varying the shell diameter and length. The average pressure drop was about 7.5 psi on the gas side. Individual pressure drops per section are as follows:

Superheater Section	1.0 psi
Evaporator	3.5 psi
Preheater	1.5 psi
Inlet and Exit Losses	1.5 psi
TOTAL	7.5 psi

Gas Blowers

Axial flow compressors coupled with flywheels and variable speed drives were selected to circulate the gas coolant through the primary loop. An over-all efficiency of 80 per cent was assumed to determine power requirements for the compressors. Temperature rise of the gas in the compressor stage was ignored because in the favorable reactor cases the rise was insignificant while in the other reactor cases, the cases were eliminated by their excessive operating power demands. The maximum primary loop pressure drop of the most favorable reactor cases was approximately 20 psi. A considerable number of reactor cases have higher pressure drops which would undoubtedly require multiple stage compressors with interstage gas coolers. However, the power requirements for these cases were calculated by the single stage compressor method as the power requirements were only used to establish comparative trends in the study.

Primary Piping

The primary loop piping sizes were based on a pressure drop of one psi per 100 feet. In the cases of 1200° F reactor outlet temperatures, internally insulated pipe was selected in order to reduce the wall temperatures and consequently the wall thickness.

The internal insulation is held in place by a perforated, light weight pipe. The wall thicknesses were based on type 304 stainless steel for the double wall pipe and 1% or Cr ½% Mo steel for the rest of the primary loop.

STEAM POWER PLANT DESCRIPTION

With the high reactor coolant temperatures available, it is apparent that conventional steam power plant equipment (superheated steam compared to saturated steam usually provided by water cooled power reactors) is easily adaptable for power recovery systems. The equipment considered in this study was taken as standard equipment currently available.

Steam Cycle (2)

For this preliminary reactor parametric study, the actual steam cycle and heat rate cases were not developed in detail but approximations were used. For all cases, the steam cycle was calculated at 80% Rankine efficiency. Turbine pressures were established from the reactor coolant inlet temperatures, allowing sufficient heat to reheat the feedwater to within 50° F of the saturated steam temperatures. Turbine steam pressures of 1200 psia were arbitrarily set as the maximum pressure although some reactor cases with 1200° F outlet temperature would permit the utilization of higher steam pressures. Regenerative feedwater heating was not considered in this study. Turbine exhaust conditions were set at one and one-half inches Hg absolute pressure. When a recommended study reactor design case is selected, then a detailed optimization study of the steam cycle will be made if the indirect cycle plant system is chosen for the study.

Considering the number of variables present in this study the use of a Rankine efficiency of 80 percent will provide a reasonable electrical output for the various study cases.

Turbine-Generator Equipment

A detailed selection of the turbine was not made since at the steam pressure, temperature and size ranges under investigation, the installed cost of turbine-generator equipment may be assumed to be relatively constant per kilowatt capacity. For this study, one turbine-generator set was considered adequate for the 500 MW(th) reactor cases, two sets for the 1000 MW(th) cases, and three for the 1500 MW(th) study cases. In the detailed design study it may be found to be more advantageous to use smaller rated turbine-generator sets to provide better plant balance and stability.

Condenser Cooling Water Requirements

Cooling water temperatures vary according to geographical location. For the purposes of this study, Columbia River water temperatures were used with a maximum inlet temperature of 60° F and an allowable temperature rise of 22° F. Pumping head requirements were assumed to be 70 feet of water.

Plant Auxiliary Equipment

Plant auxiliary equipment were included, commensurate with modern steam power plant practices.

INDIRECT CYCLE ANALYSIS

Although the gross steam cycle efficiency increased with increasing reactor outlet temperatures, Figure VIII-3, the plant net power output of the cases was adversely affected by the variation in the plant operating power requirements. The influence of the reactor parameters, temperature, pressure, specific power, and reactor dimensions is illustrated in Figures VIII-4, 5, 6, 7, 8, and 9. It will be noted that there is considerable variation among the various cases due to the effect of the parameters considered.

The major plant operating power demand is the power for operation of the gas blowers or compressors circulating the gas coolant through the primary loop. Since gas is the reactor coolant, the required pumping power is much more sensitive to temperature and pressure effect than a liquid coolant. Operation of the gas blowers or compressors is greatly affected by the reactor ΔT and the specific tube power. The reactor ΔT determines the reactor mass flow rate and the specific volume of the gas to be pumped.

The reactor coolant mass flow rate at a reactor ΔT of 400° F is one and one-half times larger than the flow rate for the same reactor power level with a ΔT of 600° F. The reactor inlet temperature will, at a constant outlet gas temperature, be 200° F higher for a 400° F ΔT case than for a 600° F ΔT. The inlet specific volume of the 400° F ΔT reactor case as compared to a 600° F ΔT case is simply the ratio of the absolute temperatures times the inlet specific volume of the 600° F ΔT with constant gas pressure.

For a clearer explanation, a numerical example between comparative cases with reactor outlet temperatures of 1000° F and ΔT's of 400 and 600° F is shown below:

$$Q = \Delta T_1 \times C_p \times W_1 = \Delta T_2 \times C_p \times W_2 \qquad (1)$$

$$= 400\, W_1 = 600\, W_2 \qquad (2)$$

$$W_1 = \frac{600}{400} W_2 = 1.5\, W_2 \qquad (3)$$

where Q = Reactor heat generated, Btu/hr
W = Gas mass flow rate, #/hr
C_p = Specific heat, Btu/#/°F
ΔT = Temperature difference across the reactor, °F

$$v_1 = \frac{\gamma_1 RT_1}{p} \qquad (4)$$

$$v_2 = \frac{\gamma_2 RT_2}{p}$$

Assuming γ and p constant which can be considered true for the range of temperature under investigation

$$v_1 = \frac{T_1}{T_2} v_2 = \frac{1060}{860} v_2 = 1.23\ v_2 \qquad (5)$$

The volumetric flow rate is $V = w\ v$ (6)

then, the comparative volumetric flow between a 400° F ΔT and 600° F ΔT is

$$V_1 = 1.23 \times 1.5\ V_2 = 1.85\ V_2 \qquad (7)$$

where v = Specific volume, $ft^3/lb.$
R = Gas constant, ft/°R
T_1 = Temperature, °R
P = Pressure, $\#/ft^2$
γ = Gas compressibility factor
V = Volumetric flow rate, ft^3/hr

The power equation for gas blowers is

$$P = K\ pV\left(\frac{k}{k-1}\right)\left[\left(\frac{P_2}{P_1}\right)^{\frac{k-1}{k}} - 1\right] \qquad (8)$$

where P = Power ft-lbs/unit time
K = Constant
p = Pressure, $\#/ft^2$
V = Volumetric flow rate, ft^3/unit time
k = Ratio of specific heats $\frac{c_p}{c_v}$

From the above it is shown that a 1.85 ratio of blower power is required for a 400° F ΔT case as compared with a 600° F ΔT case, assuming a constant system pressure.

In the reactor cases studied, the pressure loss through the fuel channel varied directly as the specific tube power, i.e., higher specific tube powers required higher gas flow rates and thus produced larger gas pressure drops in the fuel channel. (See Section IV of the report). In the majority of the study cases, the pressure loss through the reactor constituted between 50 and 95 per cent of the total pressure loss of the primary system. Consequently, specific tube powers of 25 kw/ft yielded the highest net electrical output capacity because of the lower gas blower power requirements.

Another effect which must be considered is the composition of the gas coolant. In this study, helium and nitrogen were compared. In general, the pumping requirements of helium as compared to nitrogen are approximately a factor of four greater per pound of gas for identical pressure ratios. Since approximately four times the nitrogen mass flow rate is required to remove equal amounts of heat the pumping power requirement of the two gases is nearly equal. The film coefficients for nitrogen were found to be lower than those for helium even with larger mass flow

rates which adversely affect the performance of nitrogen when compared to helium.

In considering the above effects simultaneously it was found that for the indirect cycle cases studied a 600° F ΔT and a specific tube power of 25 KW per foot reactor produced the largest net output plant. For the 500 MW(th) reactor cases approximately the same net power was produced using nitrogen as with helium as the coolant, but the nitrogen cycle net power output fell off rapidly as the reactor size (MW capacity) was increased due to larger gas pressure losses through the reactor. The 200° F increase in temperature of the 1200° F reactor outlet temperature cases did not produce the anticipated net power increase over the 1000° F reactor outlet cases which is normally expected in fossil fuel steam plants. This would indicate that a larger reactor ΔT than 600° F for the 1200° F reactor outlet temperature cases would produce increased plant efficiencies.

DEVELOPMENT

In the design of gas heat exchangers, the large variety of heat transfer extended surfaces available makes the selection difficult. In this study, an adaption of the British Calder Hall extended tube exchanger design was used. Insufficient time was available to effectively compare the different types extended surface heat exchangers which are now commercially produced. Considerable design and development work on large gas heat exchangers will have to be done before it will be possible to establish an extended surface area heat exchanger design which will yield maximum performance at minimum capital cost. However, this refinement would not alter the relative power costs appreciably.

Another area requiring extensive development is the large circulating gas blowers. The turbomachinery industry in the United States does not yet have any significant experience in the design of gas blowers at the proposed pressures and temperatures of gas-cooled reactor designs. It should be expected that considerable development work would be necessary, before initial manufacture of the blowers, which would increase the cost of the initial units by a significant amount.

REFERENCES

(1) Kern, D. Q., "Process Heat Transfer", McGraw-Hill Book Company, 1950.

(2) Salisbury, J. K., "Steam Turbines and their Cycles", John Wiley and Sons, 1950.

DESIGN DATA

Outlined below are the design data developed for a typical indirect cycle case:

1. Reactor and Primary Loop

	GAS COOLANT	
	He	N_2
Reactor size, MW (th)	500	500
Reactor outlet temperature, °F	1000	1000
Reactor ΔT, °F	600	600
Reactor tube power, kw/ft	25	25
Lattice size, inches	6	6
Reactor mass flow, #/hr	2.28×10^6	10.8×10^6
Total loop pressure drop, psi	9.8	19.2
Reactor pressure drop, psi	3.5	12.6
Heat exchanger pressure drop, psi	4.3	4.6
Piping pressure drop, psi	2.0	2.0
Primary loop piping, outlet, I.D. in.	26.0	31.5
Primary loop piping, inlet, I.D. in.	23.0	28.8

2. Gas Pumping Equipment

Number of blowers	4	4
Mass flow rate, #/hr	5.71×10^5	2.70×10^6
Gas pressure, psia	415	410
Pressure ratio P_2/P_1	1.024	1.047
Gas temperature, °F	400	400
Drive power/blower, HP	2900	3600

3. Heat Exchanger

Number of heat exchangers	4	4
Shell diameter, feet	10	12
Vessel height, feet	56.6	54.0
Shell wall thickness, inches	1.8	2.1
Shell material	Carbon Steel	Carbon Steel
Gas flow/exchanger, #/hr	5.71×10^5	5.71×10^5
Preheater Section		
Mass flow/sq ft, #/hr/ft^2	2.66×10^4	8.64×10^5
U design, BTU/hr/ft^2/°F	350	290
Heat transfer area, ft^2 (tube inside surface area)	2125	2570
Tube, O.D., inches	1	1
Annular fin height, inches	3/8	3/8
Fins/inch	8	8
Tube gauge, BWG	12	12
Fin efficiency	.36	.36
Tube and fin material	Carbon Steel	Carbon Steel
Tube pitch	Triangular	Triangular
Tube ℄ to ℄, inches	2-1/8	2-1/8
Number of tubes	77	95
Number of passes	29	24
Effective height, feet	6.3	7.5
Gas temperature, inlet, °F	520	520
Gas temperature, outlet, °F	400	400
Feedwater temperature, inlet, °F	92	92
Feedwater temperature, outlet, °F	467	467

	He	N_2
3. Heat Exchanger (Cont'd)		
Evaporator Section		
Mass flow/sq ft, #/hr/ft^2	2.66 x 10^4	8.64 x 10^5
U_{design}, BTU/hr/ft^2/°F	320	250
Heat transfer area, ft^2 (tube inside surface area)	4,555	5,830
Tube O.D., inches	1	1
Annular fin height, inches	3/8	3/8
Fins/inch	8	8
Tube gauge, BWG	12	12
Fin efficiency	.36	.36
Tube and fin material	Carbon Steel	Carbon Steel
Tube pitch	Triangular	Triangular
Tube ℄ to ℄, inches	2-1/8	2-1/8
Number of tubes	77	95
Number of passes	42	36
Effective height, feet	12.8	11.0
Gas temperature, inlet, °F	858	858
Gas temperature, outlet, °F	520	520
Steam temperature, inlet, °F	400	400
Steam temperature, outlet, °F	467	467
Superheater Section		
Mass flow/ft^2, #/hr/ft^2	1.20 x 10^4	3.78 x 10^4
U_{design}, BTU/hr/ft^2/°F	45	30
Heat transfer area, ft^2 (tube inside surface area)	13,850	22,775
Tube O.D., inches	2	2
Tube gauge, BWG	14	14
Tube material	Carbon Steel	Carbon Steel
Tube pitch	Triangular	Triangular
Tube ℄ to ℄, inches	2-1/2	2-1/2
Number of tubes	65	79
Number of passes	64	65
Effective height, ft	23.5	23.8
Gas temperature, inlet, °F	1000	1000
Gas temperature, outlet, °F	858	858
Steam temperature, inlet, °F	467	467
Steam temperature, outlet, °F	950	950

4. Steam Power Plant	Same for both gas coolants
Steam flow #/hr	1.23 x 10^6
Steam pressure, psia	500
Steam temperature, °F	950
Degrees, superheat, °F	488
Turbine exhaust pressure, in.Hg. abs.	1½
Turbine exhaust temperature, °F	92
Gross electrical output, MW	153.5
Cycle efficiency, per cent	30.7
Condenser surface area, ft^2	107,600

4. Steam Power Plant (Continued) — Same for both gas coolants

U_{design}, BTU/hr/ft^2/°F	600
Cooling water flow, gpm	110,900
Cooling water head, feet of water	70
Cooling water pumps, BHP	2310
Cooling water pumps, power, KW	2250
Feed water pumps, power, KW	870

5. Plant Power Output

	Gas Coolant	
	He	N_2
Gross electrical output, MW	153.5	153.5
Reactor and auxiliary use, MW	1.5	1.5
Feedwater pumping power, MW	.9	.9
Cooling water pumping power, MW	2.3	2.3
Gas blower power, MW	11.5	14.3
Net electrical output, MW	137.3	134.5
Plant efficiency, percent	27.5	26.9

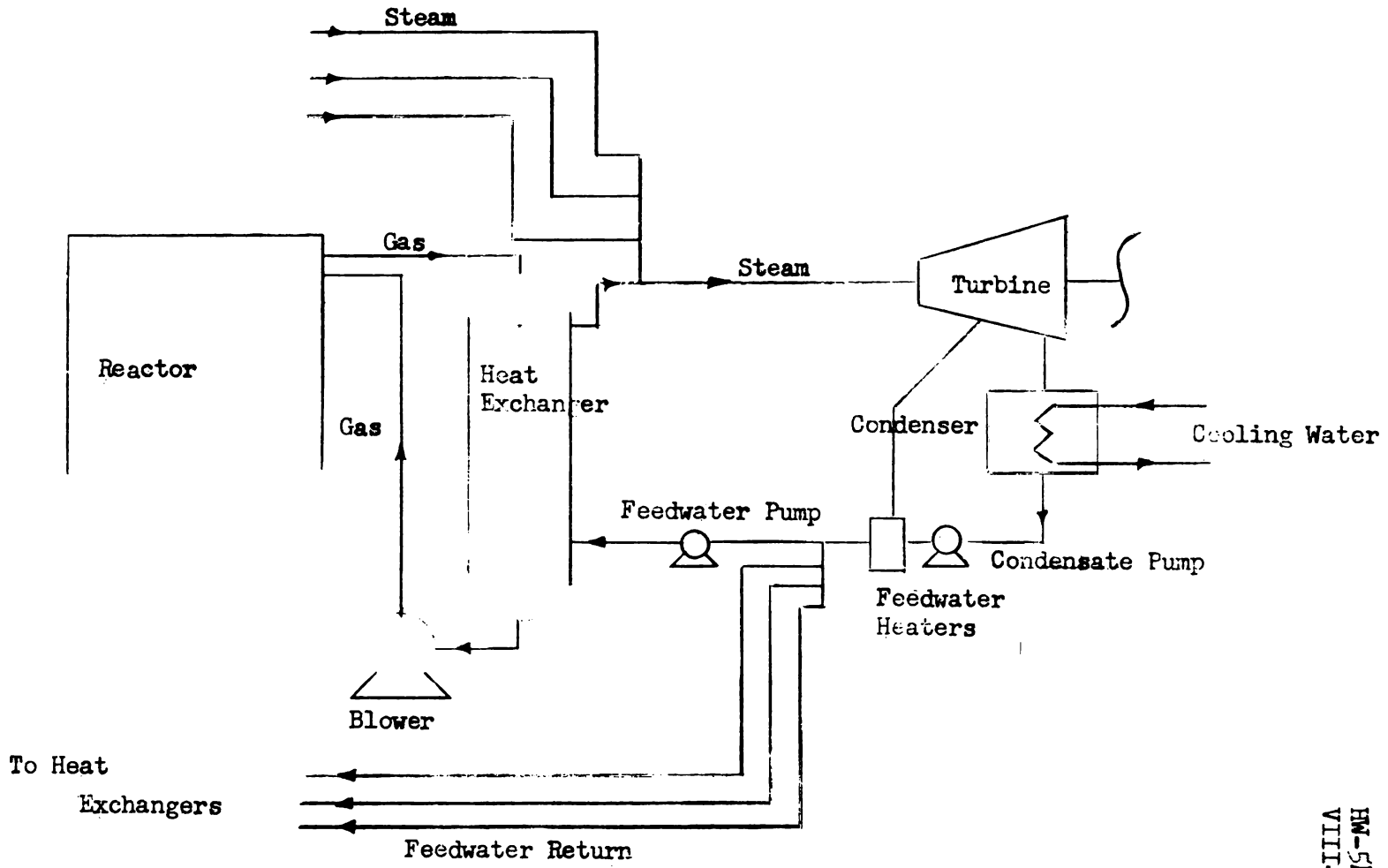

FIGURE VIII-1

SIMPLIFIED FLOW DIAGRAM OF INDIRECT POWER CYCLE FOR
500 MW REACTOR CASE (ONE OF FOUR HEAT EXCHANGERS SHOWN)

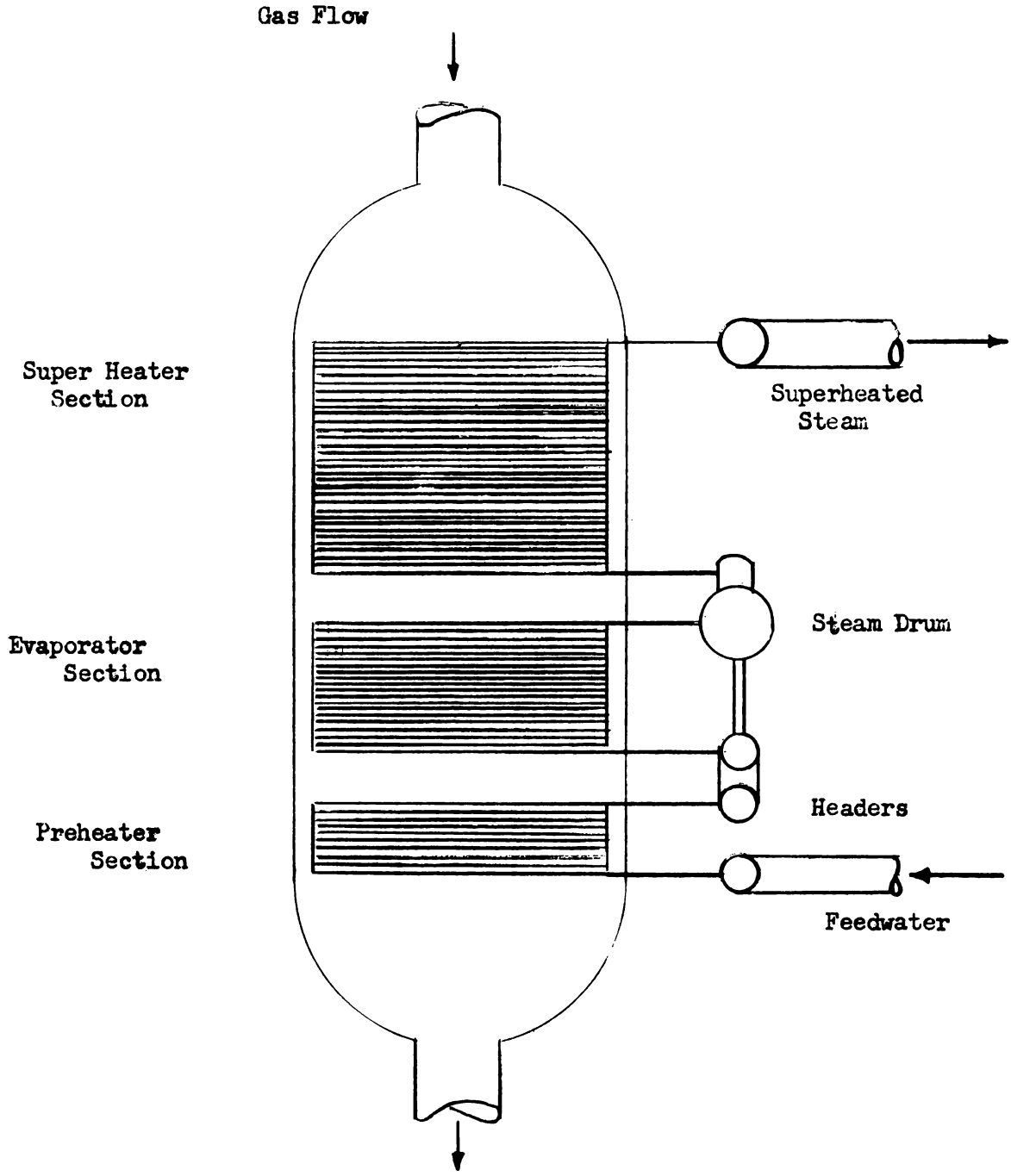

FIGURE VIII-2

SCHEMATIC DRAWING OF HEAT EXCHANGER UNIT

FIGURE VIII-3

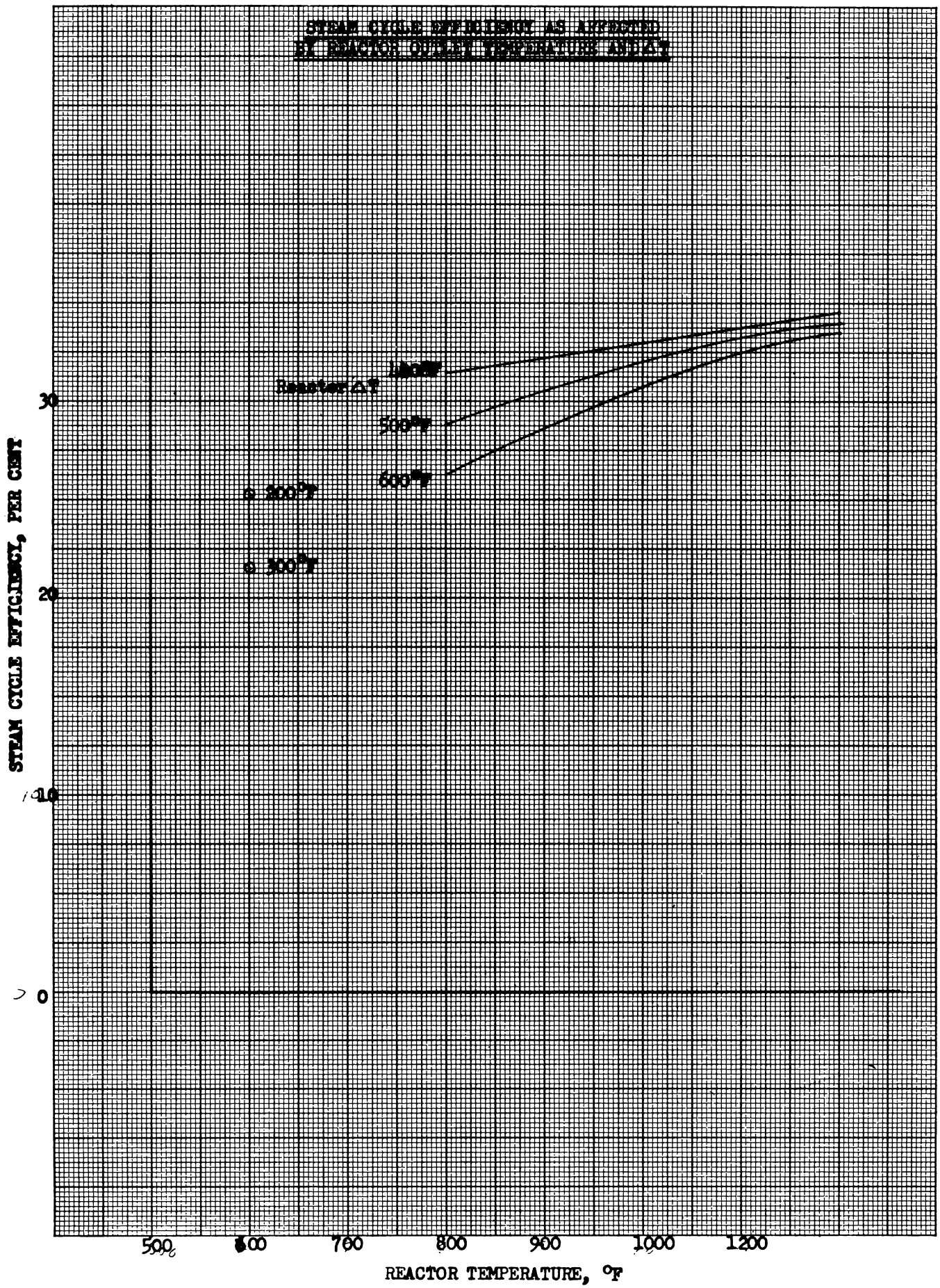

FIGURE VIII-4 INDIRECT CYCLE POWER PRODUCTION
REACTOR CONDITIONS - 1000° F-ΔT 500° F

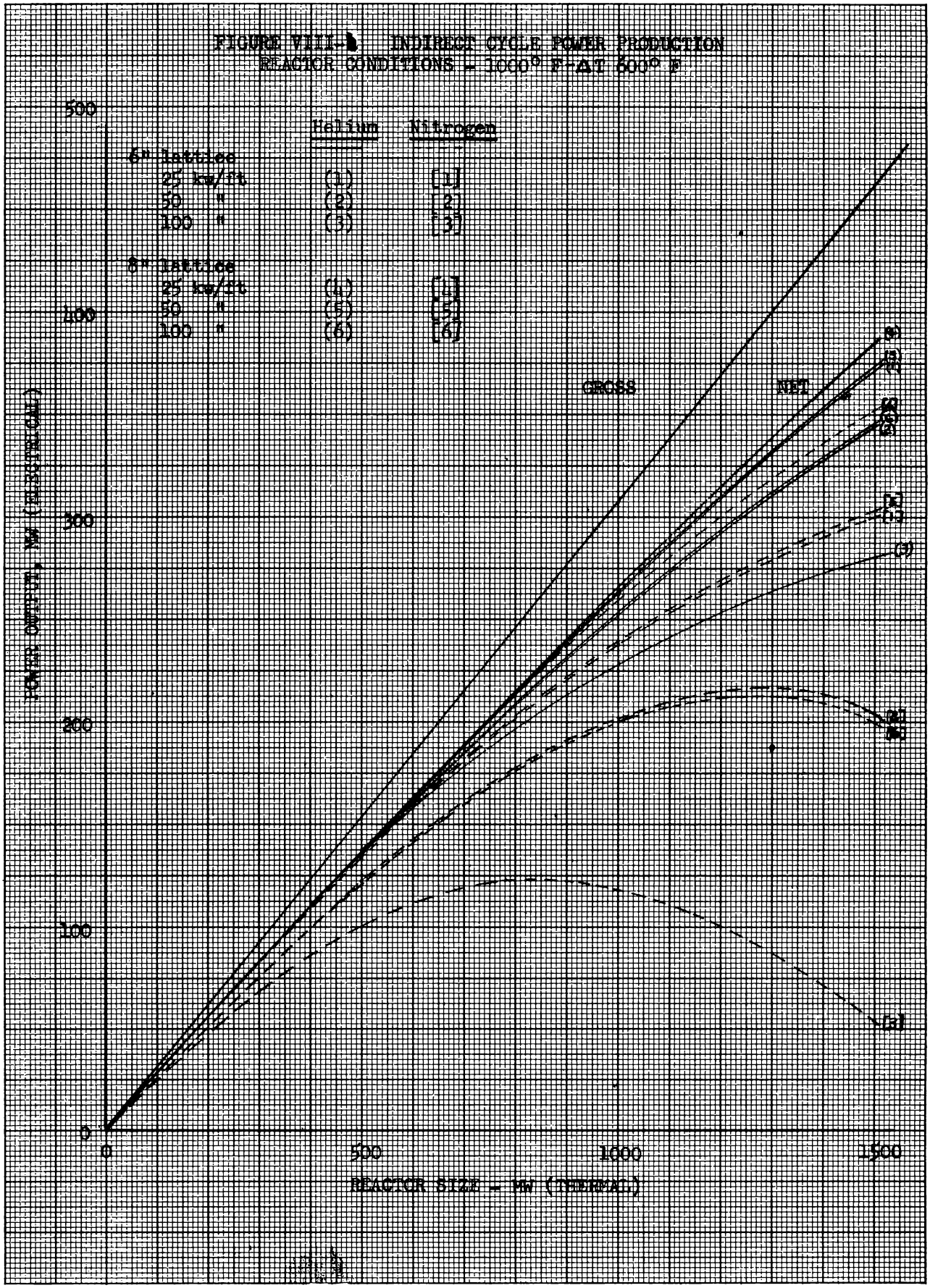

FIGURE VIII-5 INDIRECT CYCLE POWER PRODUCTION
REACTOR CONDITIONS - 1000° F - ΔT 500° F

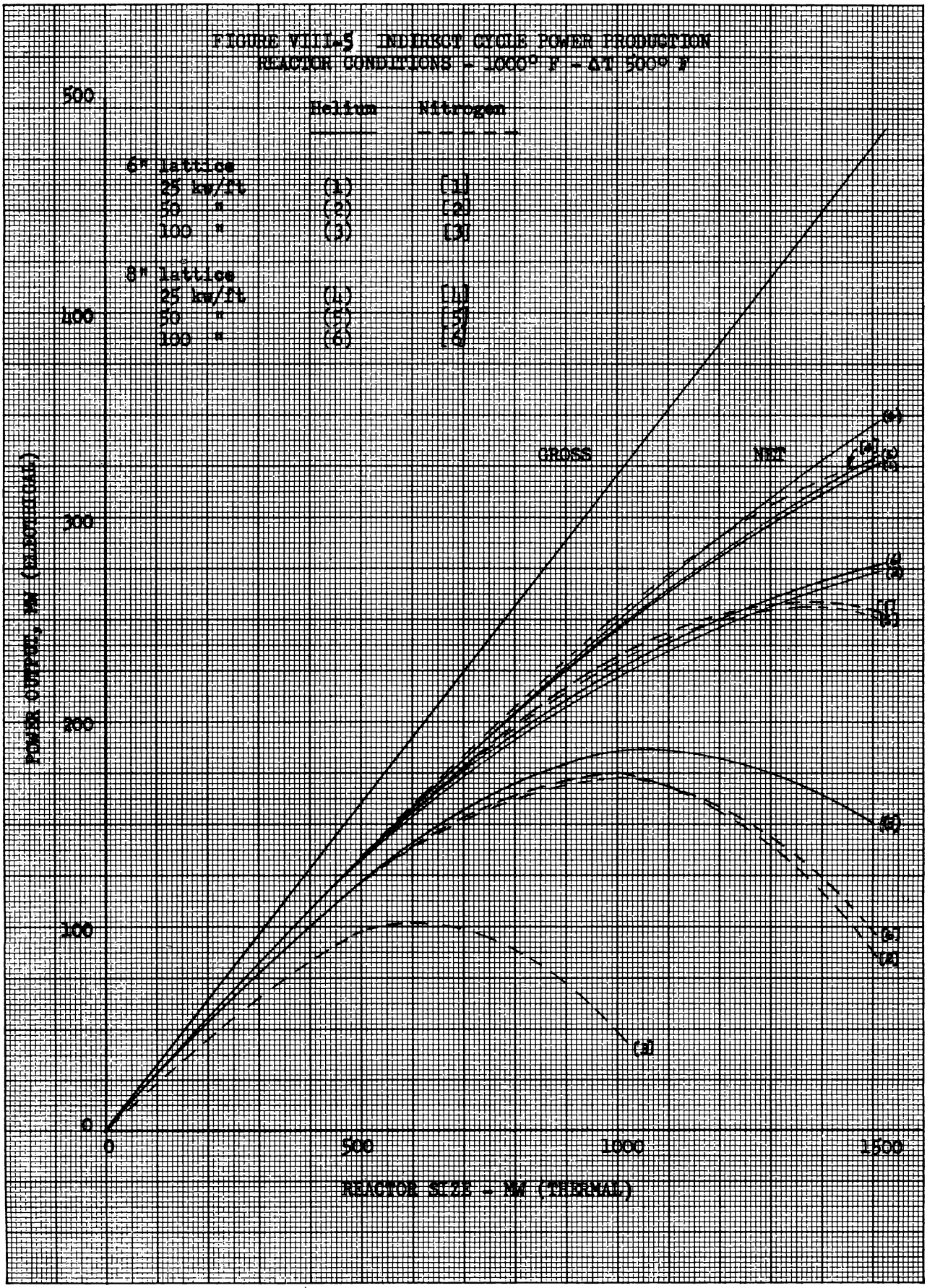

FIGURE VIII-6 INDIRECT CYCLE POWER PRODUCTION
REACTOR CONDITIONS - 1000° F - Δ T 400° F

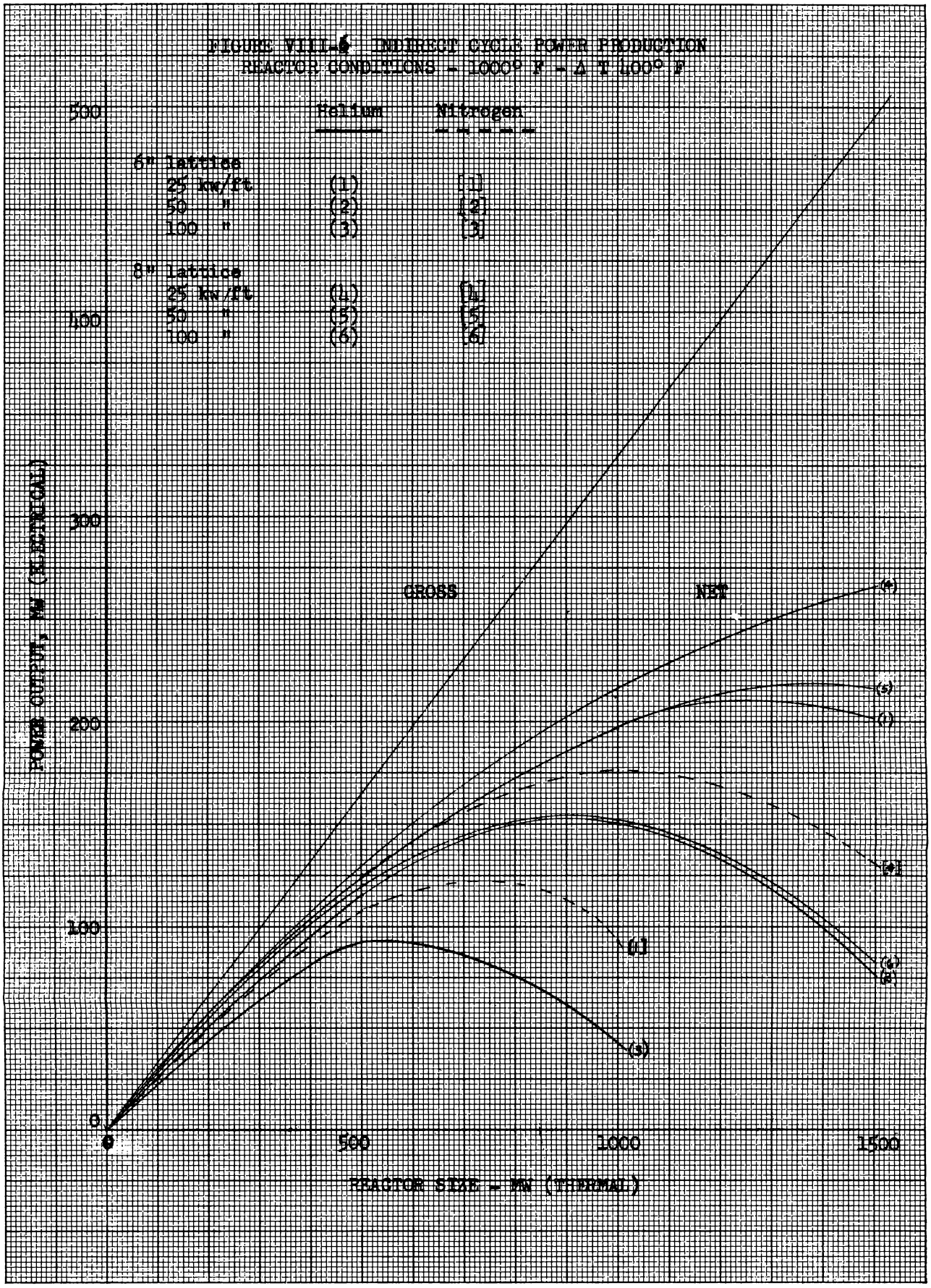

FIGURE VIII-3 INDIRECT CYCLE POWER PRODUCTION
REACTOR CONDITIONS - 1200° F - Δ T 600° F

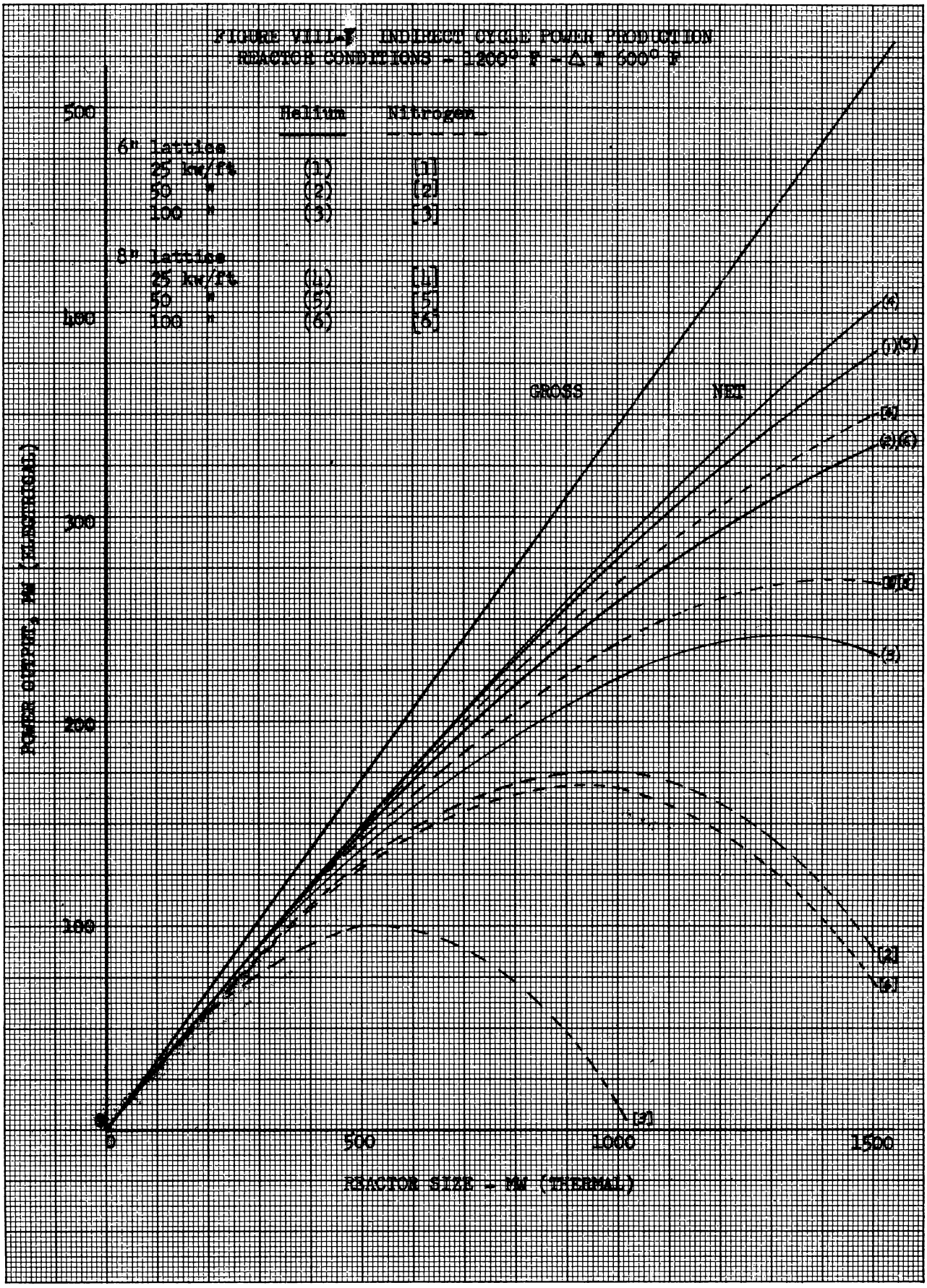

FIGURE VIII-8 INDIRECT CYCLE POWER PRODUCTION
REACTOR CONDITIONS - 1200° F - Δ T 500° F

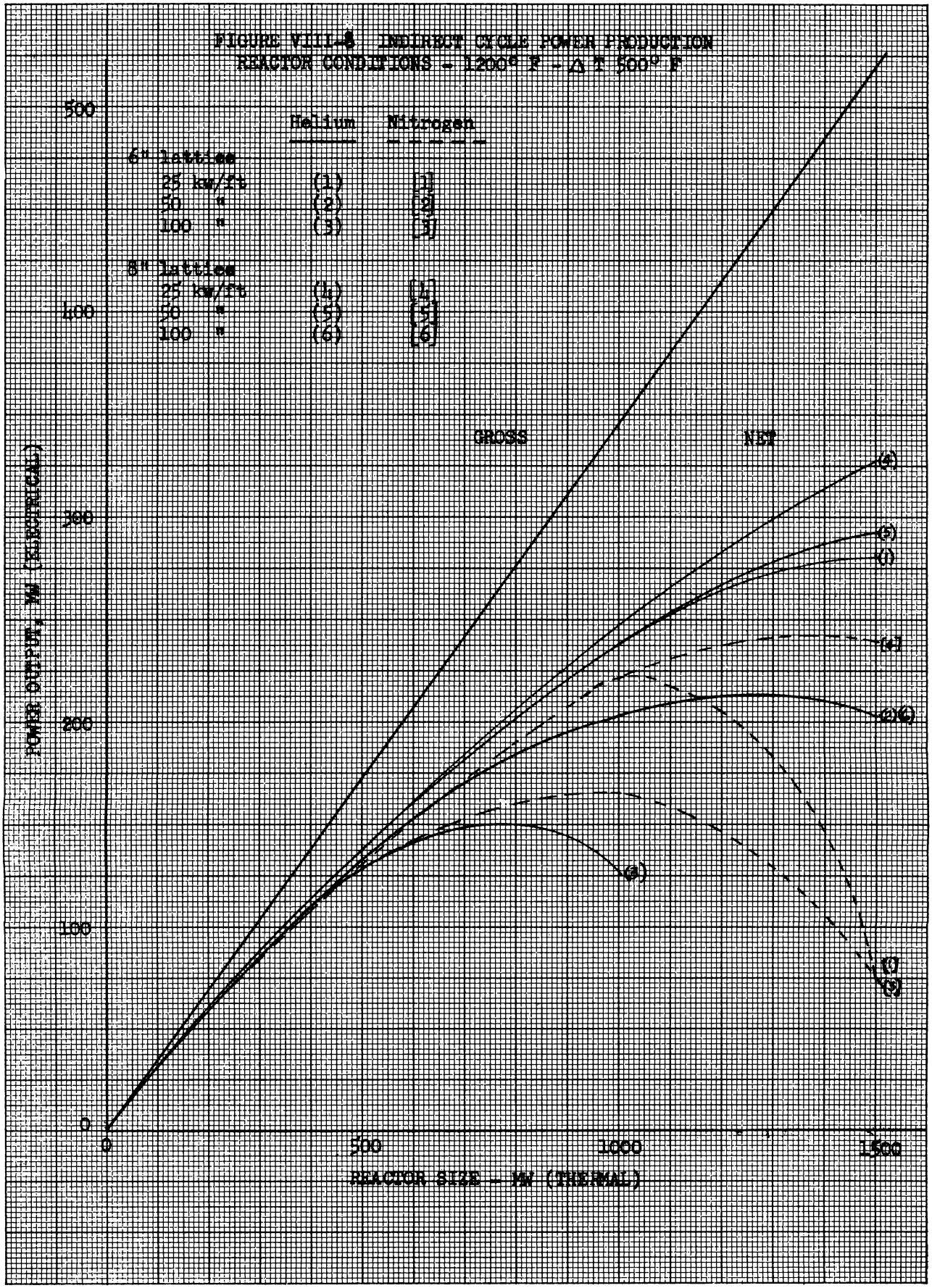

FIGURE VIII-9 INDIRECT CYCLE POWER PRODUCTION
REACTOR CONDITIONS - 1200° F - ΔT 400° F

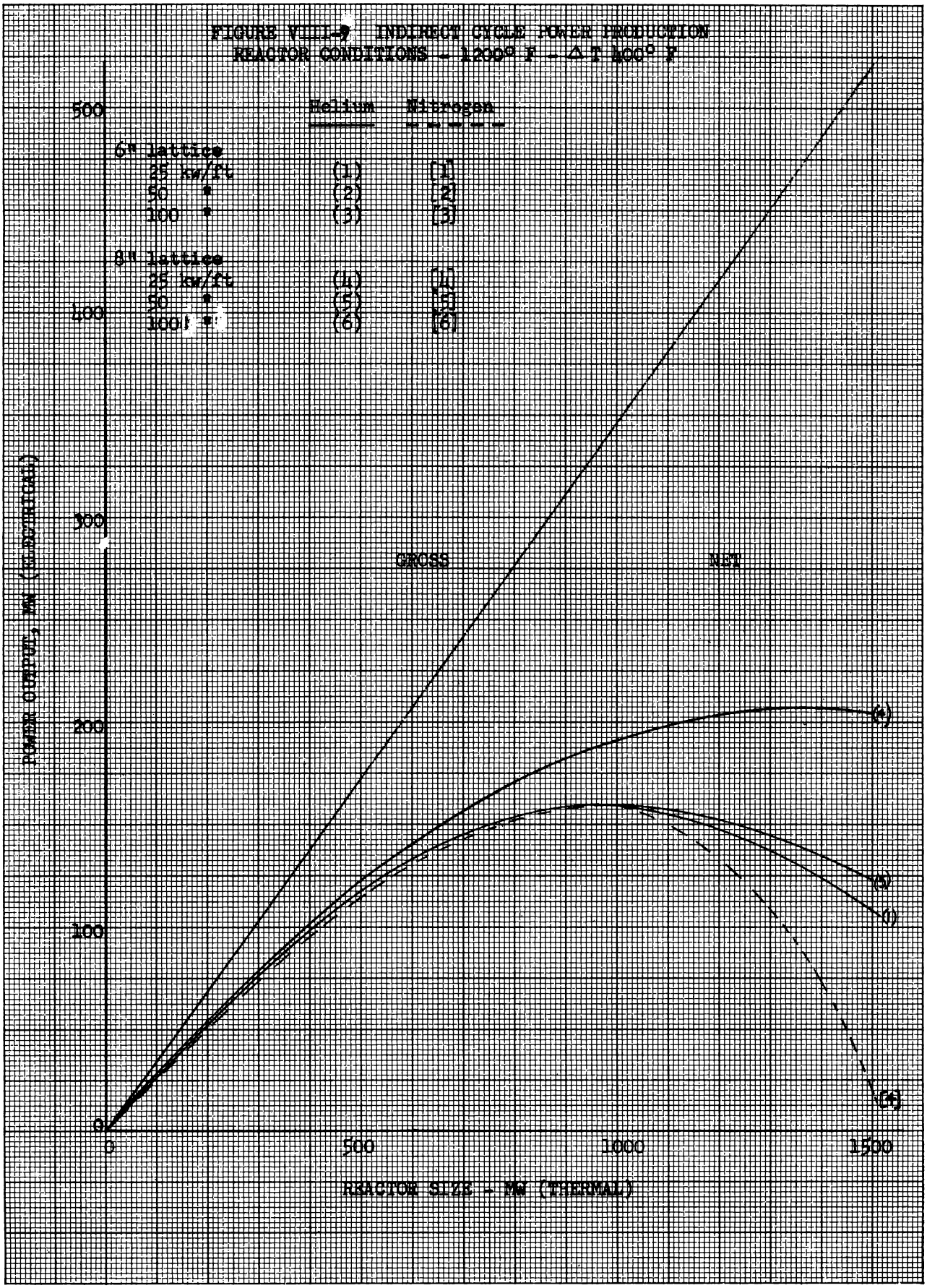

SECTION IX

FUEL CYCLE COST STUDIES

by

E. R. Astley
Reactor Design Analysis Operation
Process Design Operation
IRRADIATION PROCESSING DEPARTMENT

FUEL CYCLE COST STUDIES

INTRODUCTION

One of the annual charges which enters into the calculation of net electrical power costs is the net charge attributed directly to the uranium fuel. Of considerable importance in these costs is the operating enrichment level and production of plutonium in the reactor. Both of these quantities are functions of the degree of undermoderation of the lattice, or in other words, the ratio of the volume of graphite to volume of fuel in the reactor. The following fuel study was made to determine the effect on net electrical power costs due to changing the ratio of the volume of graphite to volume of fuel.

SUMMARY

The following analysis has shown that the contribution to net power costs attributable to the fuel become minimum at the ratio (volume of graphite to volume of UO_2) of 19:1 for the six-inch lattice reactor cases. The actual detailed breakdown of the individual components comprising the net fuel costs are listed in Tables 1, 2, and 3. Figure 1 is a graphical plot of the net fuel cost data given in the above listed tables.

COST BASES FOR FUEL CYCLE STUDIES

1. U-235 Burnout Charge

As the reactor operates, it is of course depleting the U-235 content of the fuel. The annual charge for the burnup of the fuel ($/lb-U) is the value of the uranium fuel as loaded into the reactor minus the value of the fuel delivered to the separations plant times the annual throughput of uranium fuel (lb/year). The uranium values were taken from the "Schedules of Base Charges for Materials Sold or Leased by AEC for use in Private Atomic Energy Development and Base Prices which the AEC will pay for Certain Products from Private Reactors". It was issued by Induatrial Liaison Branch, Division of Reactor Development, USAEC, Washington 25, D. C.

2. Fabrication Costs

The cost of fabricating a swaged UO_2 stainless steel jacketed fuel element is at the present time only a best guess since quantity production of this item has not been attempted. Figure 2 shows the estimated net cost in $/lb-$UO_2$ of starting from UF_6 and proceeding to the clad fuel element. Included in these costs is a fixed $2/lb-$UO_2$ for the $UF_6 \longrightarrow UO_2$ step. The minimum and maximum shown on the curve bracket the estimated costs of swaging stainless steel clad UO_2. The maximum curve was used in the fuel studies for the GCRS. The total annual fabricating charge will be the total uranium oxide throughput in lb/year times the cost of fabrication in $/lb-$UO_2$.

3. Conversion and Separation Costs

The estimated fuel reprocessing costs for the various gas cooled reactor alternates are contained in detail in a letter[1], L. L. Zahn to H. W. Heacock. Although the details of arriving at these costs cannot be described here, the results appear as Table IV. The costs quoted cover chemical separations processing, plutonium reduction to buttons, and uranium conversion to the UO_3 state. The further conversion cost for processing uranium from UO_3 to UF_6 was chosen as a constant $0.56/lb-U for all cases. The net annual charge per year is the product of the $/lb-U times the annual throughput of uranium per year.

4. Inventory Charges

A. The inpile inventory of uranium was charged off at a rate of 4 percent per year on the initial enrichment value of the uranium for each pound of uranium inpile.

B. Additional inventory was considered in the form of the uranium tied up in separations and storage for charging. Although the separations storage is actually at a lower enrichment level than the charging storage, all of this inventory was assessed at the rate of 4 percent of the initial enrichment value. It was considered that there was an average of six months uranium throughput at all times in storage.

The annual cost is six months throughput ($/year) times the initial enrichment value ($/lb) times 4 percent.

5. Annual Interest on Capitalized Fabrication Costs of Initial Inventory

A. The fabrication costs must be capitalized at an annual rate of 15 percent of the total fabrication costs for the initial uranium loading.

B. The fabrication costs for the six months throughput storage of uranium must also be capitalized at an annual rate of 15 percent of the total six months annual fabricating charges.

6. Plutonium Credit

An annual credit was given to the net fuel costs at the rate of $12/ g of plutonium made per year regardless of its Pu-240 content.

DISCUSSION

Examination of the fuel cost bases show that there are six basic parameters that determine these costs. These parameters with their dependent variables listed below are:

(1) HW-54638, January 21, 1958, SECRET.

1. Operating Enrichment Level

   a. Xenon poisoning
   b. Reactor size
   c. Volume of stainless steel in core
   d. Fuel rod geometry configuration
   e. Fuel rod radius
   f. Ratio of number of graphite to uranium atoms in lattice
   g. Neutron temperature
   h. Type and pressure of gas coolant
   i. Type of fuel
   j. Coolant temperature
   k. Reactor Δt
   l. Flattening ratio
   m. Orificing efficiency
   n. Exposure period

2. Grams of U-235 Destroyed Per Year

   a. Operating enrichment level
   b. Resonance escape probability
   c. Exposure period
   d. Time operating efficiency

3. Grams of Pu-239 Destroyed Per Year

   a. Operating enrichment level
   b. Resonance escape probability
   c. Exposure period
   d. Time operating efficiency

4. Fabrication Costs

   a. Manufacturing method
   b. Type of fuel
   c. Type of cladding
   d. Rod diameter

5. Reactor Inventory

   a. Ratio of number of atoms of graphite to uranium in a cell
   b. Specific power
   c. Power level
   d. Lattice dimension

6. Reactor Uranium Throughput

   a. Power level
   b. Exposure period
   c. Time operating efficiency

The above list shows that one variable occurs directly or indirectly in five out of the six parameters; namely, the ratio (Ng/Nu) of the number of graphite to uranium atoms in a given lattice cell. To carry this variable along in the over-all study would multiply the already large number of necessary cases by a factor of 3 or 4. It was hoped that a preliminary examination of the effect of this ratio on net power costs might lead to the selection of a single ratio for the rest of the study. From previous studies accomplished in the past few years, it has been noted that there are no large significant differences in enrichment requirements for small changes in lattice size. Consequently, three helium cooled, six-inch lattice reactor cases were picked for a detailed study which had the following characteristics.

1. 500 thermal megawatts - 100 KW/Ft.

2. 1000 thermal megawatts - 50 KW/Ft.

3. 1500 thermal megawatts - 25 KW/Ft.

All of these reactors were considered to be fueled with a stainless steel clad UO_2 cluster. The number of rods necessary to supply the specific power was chosen by the method described in detail in the Addendum, Section IV. A detailed breakdown of the individual costs appear in Tables 1, 2, and 3. Yearly electrical energy was computed on the basis of an 80 percent time operating efficiency. Pumping power, which was a function of Ng/Nu was determined by the pressure, temperature, reactor Δt and reactor pressure drop, was also accounted for in the yearly electrical energy. Effects on gas turbine efficiency are described in detail in the Addendum, Section VII.

The net fuel costs as a function of Ng/Nu, outlet temperature and reactor Δt are plotted as Figure 1. In all the reactor cases considered, the fuel costs flattened out in the neighborhood of Ng/Nu = 75. The variation in minimums for these widely different reactor cases was considered small enough that the rest of the study could precede using the one value of Ng/Nu = 75. This atomic ratio corresponds to a volume of graphite to volume of UO_2 ratio equal to 19 in the case of six-inch lattice and 20 in the case of the eight-inch lattice.

IX Table 1.

21.6 Ft. File
25 KW/Ft.
1500 MW Thermal

DIRECT CYCLE - HELIUM - 6 INCH LATTICE
5000 MWD/T

Mg Thk	T_o	Reactor Δt	SS Area	Radius of Canned Fuel - (in)	No. of Fuel Rods	U Feed Enrichment Requirements (w/o)	5000 MWD/T Push Enrichment (w/o) Content	Feed U-235 ($/lb-U) Value	Push U-235 ($/lb-U) Value	Value U-235 Burnup ($/lb-U)	Fab. Cost ($/lb-$UO_2$)	Conversion & Separation ($/lb-U)	Pu Content (kg/Ton-U)	ΔP (Across Reactor)	(Efficiency) η	U-235 Burnup Thru-put Cost ($ x 10^{-6}/Yr.)	Conversion & Separation Cost ($/Yr. x 10^{-6})	Pu Credit ($/Yr. x 10^{-6})	Fab. Cost ($/Yr. x 10^{-6})	U-235 Thru-put Inventory Charge	U-235 Inpile Inventory Charge	SS Thru-put Inventory Charge	SS Inpile Inventory Charge	Net Fuel Costs ($/Yr. x 10^{-6})	Yearly x 10^{-9} Elec. Energy (KW/Hrs)	Net Fuel Costs (Mills/KWH)
60	1000°F	400	.5966	.373	4	1.118	.659	41.60	15.20	26.4	9.20	7.56	3.09	15.1	21.2	4.63	1.325	3.25	1.83	.146	.825	.137	.777	6.420	2.089	3.073
		500	.5966	.373	4	1.118	.659	41.60	15.20	26.4	9.20	7.56	3.09	9.4	18.1	4.63	1.325	3.25	1.83	.146	.825	.137	.777	6.420	1.779	3.609
		600	.5966	.373	4	1.118	.659	41.60	15.20	26.4	9.20	7.56	3.09	6.4	7.5	4.63	1.325	3.25	1.83	.146	.825	.137	.777	6.420	0.721	8.904
	1200°F	400	.6601	.335	5	1.139	.667	42.90	15.60	27.3	9.40	7.56	3.08	18.2	30.3	4.78	1.325	3.24	1.87	.150	.851	.140	.793	6.669	2.998	2.224
		500	.7329	.306	6	1.160	.685	44.30	16.60	27.7	9.50	7.56	3.07	11.8	30.25	4.85	1.325	3.23	1.89	.155	.879	.142	.802	6.813	3.018	2.257
		600	.7927	.284	7	1.177	.700	45.40	17.35	28.15	9.70	7.56	3.06	8.3	27.45	4.93	1.325	3.22	1.93	.150	.901	.145	.819	6.989	2.713	2.576
	1400°F	400	1.321	.177	19	1.335	.837	55.50	24.90	30.60	11.40	7.56	3.01	29.7	33.5	5.36	1.325	3.16	2.27	.194	1.101	.170	.962	8.222	3.317	2.479
		500	1.553	.152	26	1.406	.902	60.00	28.60	31.40	12.30	7.56	3.00	20.7	36.0	5.50	1.325	3.15	2.45	.210	1.190	.183	1.038	8.746	3.315	2.638
		600	1.865	.129	37	1.500	.988	66.20	33.70	32.50	13.30	7.56	2.99	16.0	36.2	5.69	1.325	3.14	2.64	.232	1.313	.198	1.123	9.380	3.587	2.615
80	1000°F	400	.5177	.324	4	1.009	.554	34.95	10.00	24.95	9.50	7.56	2.82	12.3	21.9	4.37	1.325	2.96	1.89	.122	.519	.142	.600	6.008	2.159	2.783
		500	.5177	.324	4	1.009	.554	34.95	10.00	24.95	9.50	7.56	2.82	7.8	18.3	4.37	1.325	2.96	1.89	.122	.519	.142	.600	6.008	1.799	3.340
		600	.5799	.291	5	1.030	.571	36.20	10.55	25.65	9.65	7.56	2.81	5.4	7.75	4.49	1.325	2.95	1.92	.127	.537	.144	.609	6.202	0.746	8.314
	1200°F	400	.636	.267	6	1.078	.586	37.30	11.55	25.75	9.80	7.56	2.80	15.3	30.75	4.51	1.325	2.94	1.95	.131	.554	.146	.619	6.295	3.043	2.069
		500	.737	.232	8	1.078	.611	39.10	12.70	26.4	10.30	7.56	2.78	10.2	30.6	4.63	1.325	2.92	2.05	.137	.580	.154	.650	6.606	3.028	2.182
		600	.783	.220	9	1.092	.620	40.00	13.15	26.85	10.45	7.56	2.78	7.1	27.6	4.70	1.325	2.92	2.08	.140	.594	.156	.660	6.735	2.728	2.469
	1400°F	400	1.35	.133	26	1.265	.764	50.97	20.80	30.17	13.20	7.56	2.70	25.7	33.75	5.29	1.325	2.84	2.62	.179	.756	.197	.833	8.360	3.342	2.501
		500	1.60	.115	36	1.338	.826	55.70	24.30	31.4	14.00	7.56	2.67	18.0	36.5	5.50	1.325	2.81	2.78	.195	.827	.209	.884	8.910	3.617	2.463
		600	1.92	.098	51	1.437	.909	61.70	29.05	32.65	14.70	7.56	2.64	14.0	36.5	5.72	1.325	2.77	2.92	.216	.916	.219	.928	9.474	3.617	2.619
120	1000°F	400	.475	.240	5	.998	.526	34.30	8.75	25.55	10.10	7.56	2.51	10.3	22.4	4.48	1.325	2.64	2.01	.120	.341	.151	.427	6.214	2.209	2.813
		500	.522	.220	6	1.017	.542	35.40	9.45	25.95	10.45	7.56	2.49	6.7	18.45	4.55	1.325	2.62	2.08	.124	.352	.156	.442	6.409	1.814	3.533
		600	.605	.191	8	1.050	.569	37.40	10.72	26.68	11.00	7.56	2.47	4.8	8.0	4.67	1.325	2.60	2.19	.131	.372	.164	.465	6.717	0.771	8.712
	1200°F	400	.642	.181	9	1.063	.579	38.20	11.18	27.02	11.25	7.56	2.46	13.3	31.4	4.73	1.325	2.59	2.24	.134	.380	.168	.476	6.863	3.108	2.208
		500	.745	.158	12	1.109	.618	41.00	13.06	27.94	12.05	7.56	2.44	8.8	30.8	4.90	1.325	2.56	2.40	.144	.407	.180	.509	7.305	3.048	2.397
		600	.807	.147	14	1.120	.638	41.70	14.10	27.60	12.50	7.56	2.42	6.2	27.7	4.84	1.325	2.54	2.49	.146	.444	.186	.528	7.389	2.738	2.699
	1400°F	400	1.40	.091	40	1.363	.833	57.30	24.60	32.70	15.00	7.56	2.30	22.7	33.75	5.73	1.325	2.42	2.98	.201	.569	.224	.634	9.243	3.342	2.766
		500	1.65	.079	55	1.460	.921	63.50	29.70	33.80	16.05	7.56	2.25	16.0	36.8	5.92	1.325	2.36	3.19	.223	.631	.239	.678	9.846	3.647	2.700
		600	1.97	.069	76	1.580	1.032	71.55	36.30	35.25	16.70	7.56	2.20	12.4	36.72	6.18	1.325	2.31	3.32	.251	.711	.249	.706	10.432	3.639	2.867
160	1000°F	400	.491	.178	7	1.058	.552	37.90	9.95	27.95	11.30	7.56	2.28	9.9	22.5	4.90	1.325	2.40	2.25	.133	.282	.168	.358	7.016	2.219	3.162
		500	.526	.167	8	1.073	.579	38.80	11.20	27.60	11.70	7.56	2.26	6.3	18.5	4.94	1.325	2.38	2.33	.136	.289	.174	.370	7.184	1.819	3.949
		600	.590	.151	10	1.108	.608	41.00	12.55	28.45	12.20	7.56	2.24	4.4	8.1	4.98	1.325	2.35	2.43	.144	.305	.182	.386	7.402	0.781	9.478
	1200°F	400	.648	.138	12	1.137	.631	42.80	13.70	29.10	12.95	7.56	2.23	12.6	31.55	5.10	1.325	2.34	2.57	.150	.318	.193	.410	7.726	3.123	2.474
		500	.753	.121	16	1.190	.674	46.20	16.00	30.20	13.70	7.56	2.20	8.4	30.9	5.29	1.325	2.31	2.72	.162	.344	.204	.434	8.169	3.058	2.671
		600	.801	.115	18	1.215	.696	47.80	17.15	30.65	13.95	7.56	2.18	5.8	27.75	5.37	1.325	2.29	2.77	.167	.356	.208	.442	8.348	2.743	3.043
	1400°F	400	1.40	.072	52	1.508	.954	66.70	31.60	35.10	16.60	7.56	2.04	22.0	33.75	6.15	1.325	2.14	3.30	.234	.496	.248	.525	10.138	3.342	3.034
		500	1.65	.063	70	1.627	1.064	74.70	38.30	36.40	17.15	7.56	1.98	15.3	36.85	6.38	1.325	2.08	3.41	.262	.556	.256	.543	10.652	3.692	2.917
		600	1.97	.055	97	1.777	1.207	84.90	47.25	37.65	17.70	7.56	1.92	17.8	36.8	6.60	1.325	2.02	3.52	.297	.632	.264	.560	11.178	3.647	3.065

15 Ft. Pile
50 KW/Ft.
1000 MW Thermal

IX. Table 2.

DIRECT CYCLE - HELIUM - 6 INCH LATTICE
5000 MWD/T

Ng / Nu	t°	Reactor Δt	SS Area	U Feed Enrichment Requirements (w/o)	5000 MWD/T Push Enrichment (w/o) Content	Feed ($/lb-U) U-235 Value	Push ($/lb-U) U-235 Value	Value U-235 Burnup ($/lb-U)	Fab. Cost ($/lb-$UO_2$)	Conversion & Separation ($/lb-U)	Pu Content (kg/Ton-U)	Radius of Canned Fuel - (in)	No. of Fuel Rods	ΔP (Across Reactor)	η (Efficiency)	U-235 Burnup Thru-put Cost ($ x 10^{-6}/Yr.)	Conversion & Separation Cost ($ x 10^{-6}/Yr.)	Pu Credit - ($/Yr. x 10^{-6})	Fab. Cost ($/Yr. x 10^{-6})	U-235 Inpile Inventory Charge	U-235 Thru-put Inventory Charge	SS Thru-put Inventory Charge	SS Inpile Inventory Charge	Yearly x 10^{-9} Elec. Energy (MW/Hrs.)	Net Fuel Costs ($/Yr. x 10^{-6})	Net Fuel Costs (Mills/KWH)
60	1000°F	400	.7927	1.213	.734	47.65	19.20	28.45	9.70	8.36	3.05	.2844	7	19.3	20.45	3.32	.98	2.135	1.285	.314	.111	.0963	.272	1.341	4.24	3.162
		500	.7927	1.213	.734	47.65	19.20	28.45	9.70	8.36	3.05	.2844	7	12.1	17.70	3.32	.98	2.135	1.285	.314	.111	.0963	.272	1.157	4.24	3.665
		600	.7927	1.213	.734	47.65	19.20	28.45	9.70	8.36	3.05	.2844	7	8.3	7.20	3.32	.98	2.135	1.285	.314	.111	.0963	.272	0.458	4.24	9.258
	1200°F	400	.9009	1.247	.764	49.80	20.80	29.00	10.00	8.36	3.04	.2520	9	23.6	29.2	3.39	.98	2.130	1.323	.329	.116	.0993	.281	1.923	4.39	2.293
		500	.9982	1.279	.792	51.90	22.30	29.60	10.30	8.36	3.03	.2289	11	15.6	29.5	3.46	.98	2.120	1.363	.343	.121	.102	.289	1.943	4.54	2.33
		600	1.0872	1.306	.816	53.60	23.70	29.90	10.60	8.36	3.02	.2114	13	11.1	27.15	3.49	.98	2.118	1.403	.354	.125	.105	.297	1.787	4.64	2.597
	1400°F	400	1.865	1.552	1.033	69.60	36.40	33.20	13.20	8.36	2.97	.1294	37	41.7	30.55	3.88	.98	2.080	1.748	.460	.163	.131	.370	2.013	5.65	2.807
		500	2.205	1.659	1.127	76.90	42.20	34.70	14.20	8.36	2.95	.1117	51	29.8	34.23	4.05	.98	2.068	1.880	.507	.177	.141	.398	2.258	6.07	2.688
		600	2.662	1.808	1.261	87.00	50.70	36.30	15.00	8.36	2.92	.0950	73	23.8	35.01	4.24	.98	2.045	1.988	.574	.203	.149	.421	2.352	6.51	2.768
80	1000°F	400	.6884	1.073	.605	38.80	12.40	26.40	10.00	8.36	2.78	.2476	7	15.6	21.20	3.08	.98	1.947	1.323	.192	.0907	.0993	.209	1.390	4.03	2.899
		500	.7369	1.090	.618	39.90	13.10	26.80	10.30	8.36	2.77	.2323	8	10.1	18.0	3.13	.98	1.940	1.363	.197	.0933	.102	.215	1.177	4.14	3.517
		600	.7827	1.102	.628	40.60	13.55	27.05	10.40	8.36	2.76	.2196	9	7.1	7.45	3.16	.98	1.933	1.378	.201	.0950	.103	.217	0.475	4.20	8.842
	1200°F	400	.907	1.14	.658	42.95	15.10	27.85	11.0	8.36	2.75	.1915	12	20.4	29.9	3.25	.98	1.925	1.46	.213	.100	.109	.230	1.970	4.42	2.244
		500	1.017	1.172	.685	45.02	16.55	28.47	11.5	8.36	2.74	.1723	15	13.5	29.85	3.33	.98	1.920	1.52	.223	.105	.114	.240	1.966	4.59	2.335
		600	1.118	1.205	.713	47.15	18.05	29.10	12.1	8.36	2.73	.1582	18	9.7	27.3	3.40	.98	1.910	1.60	.233	.110	.120	.253	1.797	4.79	2.666
	1400°F	400	1.923	1.453	.927	63.10	30.08	33.02	14.8	8.36	2.62	.0980	51	36.5	32.33	3.86	.98	1.84	1.96	.312	.147	.147	.309	2.132	5.88	2.758
		500	2.273	1.567	1.029	70.65	36.18	34.47	15.7	8.36	2.58	.0852	70	26.2	34.92	4.03	.98	1.81	2.08	.350	.165	.156	.328	2.304	6.28	2.726
		600	2.751	1.705	1.153	80.50	43.8	36.70	16.3	8.36	2.53	.0729	100	21.0	35.37	4.28	.98	1.77	2.16	.398	.188	.162	.341	2.334	6.74	2.888
120	1000°F	400	.6782	1.098	.609	40.35	12.60	27.75	11.50	8.36	2.43	.1723	10	13.5	21.7	3.24	.98	1.703	1.523	.133	.0943	.114	.162	1.424	4.54	3.188
		500	.7450	1.130	.636	42.35	14.00	28.35	12.10	8.36	2.41	.1582	12	8.8	18.25	3.31	.98	1.688	1.603	.140	.0989	.120	.171	1.194	4.73	3.961
		600	.8068	1.155	.657	43.90	15.05	28.85	12.50	8.36	2.40	.1472	14	6.2	7.70	3.37	.98	1.682	1.655	.145	.103	.124	.176	0.492	4.87	9.898
	1200°F	400	.9192	1.198	.694	46.70	17.05	29.65	13.2	8.36	2.37	.131	18	17.8	30.55	3.47	.98	1.66	1.75	.155	.109	.131	.186	2.013	5.12	2.543
		500	1.044	1.248	.736	49.88	19.30	30.58	13.9	8.36	2.35	.117	23	11.9	30.28	3.57	.98	1.65	1.84	.165	.117	.138	.196	1.995	5.36	2.687
		600	1.114	1.275	.759	51.60	20.55	31.05	14.2	8.36	2.33	.1107	26	8.4	27.50	3.63	.98	1.63	1.88	.171	.121	.141	.200	1.810	5.49	3.033
	1400°F	400	1.968	1.610	1.058	73.60	37.95	35.65	16.6	8.36	2.19	.0689	76	32.3	33.12	4.16	.98	1.53	2.20	.244	.172	.165	.234	2.184	6.63	3.036
		500	2.332	1.755	1.191	83.45	46.30	37.15	17.3	8.36	2.13	.0603	104	23.2	35.53	4.34	.98	1.49	2.39	.276	.195	.172	.244	2.345	7.11	3.032
		600	2.788	1.933	1.356	96.00	56.82	39.18	17.8	8.36	2.06	.0528	144	18.5	35.78	4.58	.98	1.44	2.36	.318	.224	.177	.251	2.361	7.45	3.155
160	1000°F	400	.6760	1.180	.668	45.50	15.65	29.85	13.2	8.36	2.19	.1333	13	12.6	22.0	3.49	.98	1.534	1.749	.151	.106	.131	.141	1.444	5.21	3.608
		500	.7531	1.215	.697	57.80	17.20	30.60	13.7	8.36	2.17	.1212	16	8.3	18.3	3.57	.98	1.520	1.813	.158	.112	.136	.145	1.197	5.39	4.503
		600	.8239	1.250	.727	50.00	18.80	31.20	14.2	8.36	2.15	.1120	19	5.9	7.80	3.64	.98	1.508	1.880	.166	.117	.141	.151	0.498	5.57	11.185
	1200°F	400	.931	1.300	.770	53.25	21.12	32.13	14.7	8.36	2.12	.1008	24	16.8	30.80	3.75	.98	1.49	1.95	.132	.124	.146	.156	2.030	5.75	2.833
		500	1.029	1.348	.812	56.30	23.50	32.80	15.2	8.36	2.10	.0926	29	11.1	30.40	3.83	.98	1.47	2.02	.140	.132	.151	.161	2.003	5.94	2.966
		600	1.137	1.400	.858	59.65	26.10	33.55	15.7	8.36	2.07	.0852	35	7.95	27.5	3.92	.98	1.45	2.08	.149	.139	.156	.167	1.810	6.14	3.392
	1400°F	400	1.973	1.800	1.225	86.50	48.40	38.10	17.7	8.36	1.90	.0551	97	30.4	33.38	4.45	.98	1.33	2.35	.215	.202	.176	.188	2.201	7.23	3.285
		500	2.328	1.977	1.391	98.50	59.05	39.85	18.3	8.36	1.84	.0488	131	21.8	35.11	4.65	.98	1.29	2.42	.246	.231	.182	.194	2.361	7.61	3.223
		600	2.791	2.200	1.602	114.50	73.02	41.48	19.2	8.71	1.77	.0430	181	17.4	36.00	4.84	1.02	1.24	2.54	.285	.268	.191	.204	2.355	8.11	3.444

9.4 Ft. File
100 KW/Ft.
500 MW Thermal

DIRECT CYCLE - HELIUM - 6 INCH LATTICE
5000 MWD/T

IX. Table 3.

Mg/Ml	t-°F	Reactor Δt	SS Area	Radius of Canned Fuel - (in)	No. of Fuel Rods	U Feed Enrichment (w/o) Requirements	5000 MWD/T Push Enrichment (w/o) Content	Feed U-235 ($/lb-U) Value	Push U-235 ($/lb-U) Value	Value U-235 Burnup ($/lb-U)	Fab. Cost ($/lb-$UO_2$)	Conversion & Separation ($/lb-U)	Pu Content (Kg/Ton-U)	ΔP (Across Reactor)	η (Efficiency)	U-235 Burnup Thru-put Cost ($ x 10^{-6}/Yr.)	Conversion & Separation Cost ($/Yr. x 10^{-6})	Pu Credit ($/Yr. x 10^{-6})	Fab. Cost ($/Yr. x 10^{-6})	U-235 Thru-put Inventory Charge	U-235 Inpile Inventory Charge	SS Thru-put Inventory Charge	SS Inpile Inventory Charge	Net Fuel Costs ($/Yr. x 10^{-6})	Yearly x 10^{-9} Elec. Energy (KW/Hrs.)	Net Fuel Costs (Mills/KWH)
60	1000°F	400	1.129	.204	14	1.495	.978	65.80	33.08	32.72	10.70	9.06	2.98	20.4	19.8	1.91	0.53	1.044	0.709	.0769	.108	.0532	.0747	2.42	0.650	3.723
		500	1.129	.204	14	1.495	.978	65.80	33.08	32.72	10.70	9.06	2.98	12.9	17.45	1.91	0.53	1.044	0.709	.0769	.108	.0532	.0747	2.42	0.572	4.231
		600	1.129	.204	14	1.495	.978	65.80	33.08	32.72	10.70	9.06	2.98	8.8	6.90	1.91	0.53	1.044	0.709	.0769	.108	.0532	.0747	2.42	0.221	10.950
	1200°F	400	1.321	.177	19	1.568	1.044	70.70	37.10	33.60	11.35	9.06	2.96	5.5	28.4	1.96	0.53	1.037	0.752	.0826	.116	.0564	.0792	2.54	0.936	2.714
		500	1.458	.161	23	1.618	1.089	74.10	39.80	34.30	11.90	9.06	2.94	17.0	29.1	2.00	0.53	1.030	0.788	.0865	.122	.0591	.0830	2.64	0.960	2.750
		600	1.584	.150	27	1.668	1.134	77.50	42.60	34.90	12.30	9.06	2.92	12.2	26.8	2.04	0.53	1.023	0.815	.0905	.127	.0611	.0858	2.73	0.883	3.092
	1400°F	400	2.775	.0917	79	2.140	1.571	110.0	70.90	39.10	15.40	9.06	2.72	49.4	26.3	2.28	0.53	0.953	1.020	.128	.180	.0765	.107	3.37	0.867	3.887
		500	3.341	.0786	112	2.375	1.794	126.5	86.10	40.40	15.70	9.06	2.63	36.9	37.80	2.36	0.53	0.922	1.040	.148	.207	.0780	.110	3.55	1.083	3.278
		600	4.087	.0669	163	2.715	2.119	150.0	108.50	41.50	16.80	9.06	2.50	30.8	33.2	2.42	0.53	0.876	1.113	.175	.246	.0835	.117	3.81	1.096	3.476
80	1000°F	400	0.982	.178	14	1.350	.837	56.45	24.90	31.55	11.30	9.06	2.67	16.4	20.8	1.84	0.53	0.936	0.749	.0659	.0700	.0561	.0596	2.43	0.683	3.558
		500	1.085	.162	17	1.395	.877	59.35	27.00	32.35	11.80	9.06	2.66	10.9	17.8	1.89	0.53	0.932	0.782	.0693	.0736	.0586	.0622	2.53	0.584	4.332
		600	1.180	.151	20	1.440	.917	62.25	29.50	32.75	12.30	9.06	2.64	7.7	7.1	1.91	0.53	0.925	0.815	.0727	.0772	.0611	.0649	2.61	0.227	11.498
	1200°F	400	1.352	.133	26	1.514	.983	67.05	33.35	33.70	13.20	9.06	2.62	22.3	29.15	1.97	0.53	0.918	0.875	.0783	.0831	.0656	.0696	2.75	0.961	2.862
		500	1.482	.123	31	1.572	1.035	71.00	36.50	34.50	13.70	9.06	2.60	14.8	29.5	2.01	0.53	0.911	0.908	.0829	.0880	.0681	.0723	2.85	0.982	2.902
		600	1.625	.113	37	1.632	1.089	75.10	39.80	35.30	14.20	9.06	2.58	10.7	27.15	2.06	0.53	0.904	0.941	.0877	.0931	.0705	.0749	2.95	0.904	3.263
	1400°F	400	2.867	.0705	108	2.190	1.609	113.5	73.50	40.00	16.60	9.06	2.41	43.6	29.5	2.34	0.53	0.814	1.100	.133	.141	.0825	.0875	3.57	0.973	3.669
		500	3.425	.0613	150	2.440	1.846	131.0	89.90	41.10	17.30	9.06	2.34	32.3	33.6	2.40	0.53	0.820	1.146	.153	.162	.0859	.0912	3.75	1.110	3.378
		600	4.193	.0527	217	2.820	2.210	157.0	115.0	42.00	17.90	9.06	2.24	27.0	34.1	2.45	0.53	0.785	1.186	.183	.195	.0889	.0944	3.94	1.126	3.499
120	1000°F	400	0.996	.122	21	1.388	0.859	58.90	26.15	32.75	13.65	9.06	2.28	14.6	21.1	1.91	0.53	0.799	0.904	.0688	.0485	.0678	.0475	2.78	0.693	4.012
		500	1.114	.111	26	1.440	0.904	62.25	28.70	33.55	14.20	9.06	2.26	9.7	17.9	1.96	0.53	0.792	0.941	.0727	.0513	.0705	.0494	2.88	0.587	4.906
		600	1.200	.104	30	1.480	0.940	64.85	30.80	34.05	14.60	9.06	2.24	6.8	7.45	1.99	0.53	0.785	0.967	.0757	.0534	.0725	.0508	2.95	0.239	12.343
	1200°F	400	1.360	.0933	38	1.552	1.005	69.60	34.70	34.90	15.20	9.06	2.22	19.9	29.8	2.04	0.53	0.778	1.007	.0813	.0574	.0755	.0529	3.07	0.983	3.123
		500	1.522	.0849	47	1.625	1.100	74.60	40.50	34.10	15.70	9.06	2.19	13.3	29.87	1.99	0.53	0.767	1.040	.0871	.0615	.0780	.0546	3.07	0.985	3.117
		600	1.670	.0786	56	1.695	1.136	79.35	42.70	36.65	16.20	9.06	2.17	9.6	27.25	2.14	0.53	0.760	1.073	.0927	.0654	.0805	.0564	3.28	0.898	3.653
	1400°F	400	2.915	.0511	156	2.265	1.669	119.0	77.60	41.40	17.80	9.06	1.98	40.2	30.9	2.42	0.53	0.694	1.179	.139	.0981	.0884	.0619	3.82	1.020	3.745
		500	3.477	.0451	214	2.520	1.912	137.0	94.20	42.80	18.70	9.06	1.90	29.5	34.23	2.50	0.53	0.666	1.239	.160	.113	.0929	.0651	4.03	1.131	3.563
		600	4.236	.0395	303	2.880	2.256	162.0	118.30	43.70	20.00	9.06	1.79	24.4	34.6	2.55	0.53	0.627	1.325	.189	.133	.0994	.0696	4.27	1.143	3.736
160	1000°F	400	0.991	.0956	27	1.488	0.939	65.40	30.75	34.65	15.00	9.06	2.03	13.7	21.5	2.02	0.53	0.711	0.994	.0764	.0670	.0745	.0396	3.09	0.707	4.371
		500	1.102	.0874	33	1.542	0.988	68.95	33.70	35.25	15.50	9.06	2.01	9.0	18.1	2.06	0.53	0.704	1.027	.0805	.0706	.0770	.0409	3.18	0.594	5.354
		600	1.204	.0811	39	1.598	1.039	72.80	36.75	36.05	16.00	9.06	1.99	6.4	7.5	2.11	0.53	0.697	1.060	.0850	.0745	.0795	.0422	3.28	0.241	13.610
	1200°F	400	1.375	.0729	50	1.688	1.122	78.90	41.80	37.10	16.50	9.06	1.95	18.8	30.1	2.17	0.53	0.683	1.093	.0922	.0808	.0820	.0436	3.41	0.993	3.434
		500	1.531	.0669	61	1.769	1.197	84.40	46.70	37.70	16.80	9.06	1.93	12.5	30.0	2.20	0.53	0.676	1.113	.0986	.0846	.0835	.0444	3.48	0.990	3.515
		600	1.675	.0624	72	1.848	1.271	89.90	51.40	38.50	17.10	9.06	1.90	9.0	27.3	2.25	0.53	0.666	1.133	.105	.0921	.0850	.0451	3.57	0.900	3.967
	1400°F	400	2.903	.0419	194	2.487	1.875	134.0	91.50	42.50	19.80	9.06	1.69	37.7	30.4	2.48	0.53	0.592	1.312	.157	.137	.0984	.0523	4.17	1.003	4.158
		500	3.470	.0373	265	2.778	2.154	154.5	111.00	43.50	—	9.06	1.60	27.7	34.6	2.54	0.53	0.561	—	.180	.158	--	—	--	--	
		600	4.222	.0331	371	3.000	2.361	170.0	126.00	44.00	—	9.06	1.48	23.0	34.85	2.57	0.53	0.519	—	.199	.174	--	—	--	—	

UNCLASSIFIED
UNCLASSIFIED

Net Fuel Costs

6" Lattice
1000° F
Pile Size = 21.6 Ft.
25 Kw/Ft
1500 MW Thermal
5000 MWD/T

6" Lattice
1000° F
Pile Size = 15.0 Ft.
50 Kw/Ft
1,000 MW Thermal
5000 MWD/T

6" Lattice
1000° F
Pile Size = 9.8 Ft.
100 Kw/Ft
500 MW Thermal
5000 MWD/T

6" Lattice
1200° F
Pile Size = 21.6 Ft.
25 Kw/Ft
1500 MW Thermal
5000 MWD/T

6" Lattice
1200° F
Pile Size = 15.0 Ft.
50 Kw/Ft
1000 MW Thermal
5,000 MWD/T

6" Lattice
1200° F
Pile Size = 9.8 Ft.
100 Kw/Ft
500 MW Thermal
5000 MWD/T

6" Lattice
1400° F
Pile Size = 21.6 Ft.
25 Kw/Ft
1,500 MW Thermal
5000 MWD/T

6" Lattice
1400° F
Pile Size = 15.0 Ft.
50 Kw/Ft
10,000 MW Thermal
5000 MWD/T

6" Lattice
1,200° F.
Pile Size = 9.8 Ft.
100 Kw/Ft.
500 MW Thermal
5000 MWD/T

IX Figure 1

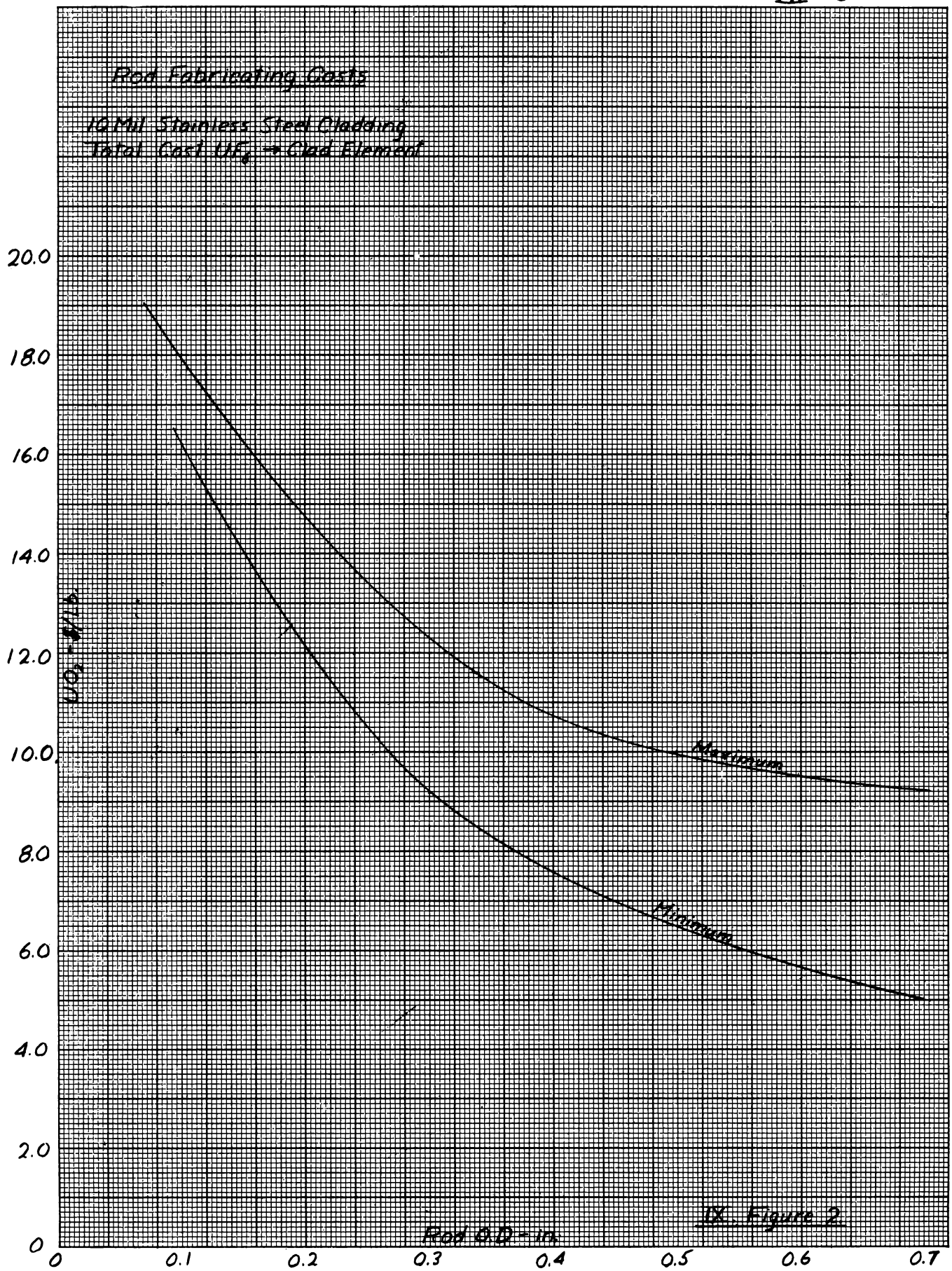
Rod Fabricating Costs
10 Mil Stainless Steel Cladding
Total Cost UF_6 → Clad Element
$/Kg U
20.0
18.0
16.0
14.0
12.0
10.0
8.0
6.0
4.0
2.0
0
0
0.1
0.2
0.3
0.4
0.5
0.6
0.7
Rod O.D. - in.
Maximum
Minimum

IX Figure 2

SECTION X

COST EVALUATION AND CASE SELECTION

by

R. C. Walker
Process Design Operation
IRRADIATION PROCESSING DEPARTMENT

and

D. F. Watson
Process Design Operation
IRRADIATION PROCESSING DEPARTMENT

COST EVALUATION AND CASE SELECTION

INTRODUCTION

The ultimate answer in any study which is evaluating an electrical power-producing system, whether it be coal-fired, hydroelectric, or nuclear, must inevitably be reduced to net power cost. This is the figure which establishes the minimum amount which must be charged for each kilowatt-hour of saleable power in order to maintain the plant on a profitable basis.

Another consideration of primary importance to any investor who is considering the installation of a power station is the amount of capital investment required for each kilowatt of saleable power as well as the size of the power block attainable.

In both regards, these study results indicate that the gas-cooled reactor concept appears to be competitive with most "power-only" reactors which have been proposed for construction in the United States. Moreover, the results of this preliminary study indicate that large power blocks, up to 400 MW (e), may possibly be obtained at a net power cost of less than 10 mils/kwh and for an initial investment of less than $300/kw. While these figures may seem somewhat low, an attempt was made to avoid optimistic unit costs, the greatest element of question lying in the direct cycle equipment costs, pressure vessel costs and, as most other studies have admitted, fuel element fabrication costs. However, further study of a single concept including development of basic arrangement drawings and contact with manufacturers of equipment for which more specific sizing has been determined will aid in verifying these estimates. It is significant to note that even if the total capital investment estimates were increased by 30 - 40%, the resulting power costs for many cases will still lie within the range of 10-14 mills/kwh. Of course, this is not presently considered as serious competition to hydroelectric and fossil-fired plants but it is certainly ample evidence that the gas-cooled reactor concept, although somewhat more space consuming than some of the other basic reactor types, indicates enough potential to justify considerable additional study and more refined development of system components.

CONCLUSIONS AND RECOMMENDATIONS

On the basis of the parameters which were established for this study, net power costs have been derived for over 1000 various combinations. These have been plotted (Figures X-1 to X-8, inclusive) in a manner which shows at a glance the effect on net power costs of coolant temperature, specific tube power, lattice size, power level, goal exposure, coolant and type of heat recovery cycle. In these figures, net power cost in mils/kwh is shown on the ordinate as a function of reactor ΔT in ^{o}F on the abscissa. Due to space limitations the various curves have been identified by integers which have the following values:

Number	Bulk Outlet Gas Temp. - °F	Specific Tube Power*-kw/ft
1	1,400	25
2	1,400	50
3	1,400	100
4	1,200	25
5	1,200	50
6	1,200	100
7	1,000	25
8	1,000	50
9	1,000	100

*Specific tube power is defined as the average power generation in the maximum performance tube.

Representative cases for each basic type of heat recovery cycle have been plotted in Figures X-9 and X-10 which delineate the estimated range of capital investment required per saleable power unit as a function of the net quantity of saleable power. These latter two figures also show the latest capital cost estimates for other major nuclear power projects as well as a curve which shows the theoretical relationship between these two factors.

From examination of this data, there are several conclusions which are immediately evident:

1. For any given combination of power level, exposure, specific tube power, coolant and lattice size, the optimum indirect cycle cases show slightly lower power costs than the direct cycle counterparts. This is primarily due to capital cost differences, although fuel costs are somewhat higher in the more efficient direct cycle cases as a result of the higher gas temperatures.

2. Net power costs for operation with a helium coolant are consistently and significantly lower. This, of course, is directly related to the much higher reactor pressure drop with nitrogen and it can be reasoned that enlargement of the process channel would improve the nitrogen case. However, increased flow area would also be an advantage for helium and it appears that the advantage would remain with helium although the difference in cost may become less.

3. In general, it can be shown that higher power levels result in lower net power costs; however, the difference in these costs between operation at 1000 MW (th) and 1500 MW (th) is very slight and, in some instances, the trend shows a reversal within this range.

4. Optimum goal exposure appears to be approximately midway between 5000 and 10,000 MWD/T for the 6" lattice while it would probably optimize closer to 10,000 MWD/T for the 8" lattice.

5. There is a strong incentive to extend gas temperatures as high as possible for the direct cycle; however, with stainless clad elements,

1500° F is about limiting and, in addition, gas turbine manufacturers are currently recommending an upper limit of 1300° F for continuous operation of their equipment. With the indirect cycle, there is not much incentive for going above 1200° F since in some cases net power costs are even lower at 1000° F.

6. In general, power costs increase with specific tube powers of 25 kw/ft and higher. This again is due to the increased pumping power required for the higher gas flows. This particular parameter will require reoptimization for any particular concept which is selected for further study, but it should optimize within the range of 15 - 30 kw/ft.

7. Power costs for the 8" lattice are consistently lower than for the 6" lattice. This, also, relates back to pressure drop since a larger process channel area was used in the 8" lattice cases. Due to the comparatively small difference resulting from changing lattices, it would seem that more gain in net power output may be made through enlarging the channel area for any given lattice size. Of course, the 8" lattice provides more flexibility for this type of adjustment and it seems reasonable that even larger lattices may reduce power costs even further, although not proportionally.

8. The indirect cycle cases, especially at high power levels, are extremely sensitive to reactor ΔT while the direct cycle cases are relatively unaffected by nominal differences in ΔT, particularly at the lower (and more optimum) specific tube powers.

9. Enrichment requirements for the various cases studied ran as high as three per cent. However, for the cases showing the lowest net power costs, enrichment did not exceed 1.6% for the direct cycle and 1.3% for the indirect cycle. For the recommended direct cycle case of 1000 MW (th) and 5000 MWD/T, enrichment should not exceed 1.25%.

On the basis of this comparison, in addition to other considerations which will be discussed more fully in the following section, it has been concluded that further study should reasonably be directed toward development of the following basic concept:

1. Direct cycle heat recovery.

2. Helium coolant.

3. Thermal power level of 1000 MW which will provide approximately 300 MW (e) of firm power at an estimated 10-14 mills/kwh and for a capital investment of approximately $300 - $350/kw (net).

4. Goal exposure for reference design of 5000 MWD/T with calculations included to show the effect of increasing exposure to at least 10,000 MWD/T if fuel element integrity is not limiting.

5. Bulk outlet temperature of 1300° F with further optimization to be made of reactor ΔT.

6. Further optimization of specific tube power in the range of 15 - 30 kw/ft.

7. Lattice spacing of 8" with investigation of effects of varying process channel cross-sectional area.

DISCUSSION OF RECOMMENDATIONS

In addition to the purely economic considerations in determining the basic reactor concept, there are several other factors which have influenced the ultimate recommendations and which should be clearly understood.

1. Inasmuch as the estimated net power costs for the indirect and direct cycles do not differ significantly (1-2 mills/kwh for comparable cases) and since ORNL is currently conducting a gas-cooled reactor study which incorporates the indirect cycle, it could seem much more beneficial to the over-all gas-cooled reactor program for additional study to be made utilizing the direct cycle heat recovery process. Further incentive for this choice lies in the fact that steam cycle equipment costs are well known and relatively stable whereas direct cycle equipment is still in the embryo stage and there should logically be much more latitude for capital cost reduction as technological advances permit.

2. As has been more fully covered in another portion of this document, helium appears to have a substantial advantage over other candidate gases in all respects -- the one possible exception being containment. However, talks with personnel at the government-operated helium wells have partially dispelled much of the previous apprehension in this regard. Moreover, with an annual capital charge of 15%, it is obvious that there is an inherent justification for investing nearly seven million dollars of capital to avoid an addition one million dollars of annual operating costs. Stated differently, this means that an initial expense is justified of the order of one million dollars for each five million cubic feet per year reduction in helium leakage. This type of economic leverage should be quite effective in controlling undesirable and unnecessary gas leakage.

3. Because of the negligible reduction in net power cost realized by increasing the reactor operating level from 1000 - 1500 MW, it seems more prudent to conduct initial studies in this field at the lower level since there is considerable probability that as advances are attained in fuel element technology, higher power levels may be realized by increasing the specific tube power which would have no effect on reactor size.

4. The data presently available for pile physics calculations at the high exposures are much less reliable than those at 5000 MWD/T. Therefore, since the calculated difference in net power cost resulting from extending exposures from 5000 to 10,000 MWD/T, even in the most optimistic case, amounts to less than $\frac{1}{2}$ mill/ kwh it seems more reasonable to accept an upper limit of 5000 MWD/T for any reference design with the goal of extending exposures as more exact data becomes available.

5. As stated previously, an upper limit of 1300° F has been selected upon recommendations of gas turbine manufacturers.

6. Inasmuch as power costs are much more sensitive to cross-sectional flow area than to lattice size, it seems that an 8" lattice should be selected for a reference design since this choice allows slightly more flexibility in channel enlargement than a 6" lattice. It could be reasoned that a 10" or 12" lattice would provide even greater flexibility; however, an increasingly larger lattice also requires an increasingly larger pressure vessel for the same power level. For a given pressure vessel wall thickness, this would be accompanied by a lower allowable system pressure which would result in lower cycle efficiencies. Therefore, until large thick-walled pressure vessel fabrication techniques are developed beyond the point where they now stand, it does not seem prudent to base an entire reactor concept on the supposition that such development will be immediately forthcoming.

COST EVALUATION

Net power costs for nuclear plants are composed of three basic components: fuel cyclic costs, annual charge on capital investment, and plant operating and maintenance costs. In general it has been determined through this study that each of these factors contributes to the net power cost in widely varying degrees, but for most of the more reasonable combinations of system parameters the breakdown is approximately 18 to 38% for fuel cyclic costs, 55 to 70% for annual charge on capital investment, and 7 to 17% for operating and maintenance costs.

Due to the extremely large number of cases that have been calculated in the course of this study, only a few of the more reasonable cases have been selected for presentation in a detailed form. These cases have been selected since they tend to illustrate the over-all effects on net power cost as a result of varying the more critical parameters. Case No. 1 (Figure X-11) is presented for three different exposures and three different power levels and is representative of the trend to lower net power costs as exposures and thermal power levels are increased. Other cases are only shown (Figure X-12) for an exposure of 5000 MWD/T at a thermal power level of 1000 MW.

Following is a list of the cases presented in Figures X-11 to X-13 inclusive, which will aid in relating the effect of specific changes in process conditions to the net power cost.

Case No.	Heat Cycle	Coolant	Lattice (Inches)	Specific Power (kw/ft)	Bulk Outlet Temp.(F)	Reactor ΔT (F)
1	Direct	Helium	8	25	1400	500
2	Direct	Helium	8	100	1400	500
3	Direct	Helium	8	100	1400	400
4	Direct	Helium	8	25	1200	500
5	Direct	Helium	6	100	1400	500
6	Direct	Nitrogen	8	25	1400	500
7	Indirect	Helium	8	25	1200	500
8	Indirect	Helium	8	25	1200	600
9	Indirect	Helium	8	100	1200	500
10	Indirect	Nitrogen	8	25	1200	500

BASIS FOR COST ESTIMATE

Fuel Costs

Fuel cyclic costs are based on an optimized graphite-to-uranium ratio of 75 (atom-to-atom ratio) and are reported in detail in Section IX of this report. In brief, U^{235} prices are taken from the standard AEC price schedule, plutonium is credited at $12/gm. and inventory charges are based on the pile loading plus six months throughput.

From the tabulation presented herein it can be seen that these net fuel costs are a strong function of outlet temperature and that, in general, extended exposures result in lower net costs since the decreased throughput charges are more than compensating for the increased enrichment requirements.

Operating and Maintenance Costs

These costs are essentially unaffected by changes in process conditions such as temperatures, pressures, tube powers, etc.; however, past experience shows a fairly reliable correlation of these costs as a function of reactor power level. Due to the relatively minor effect of these costs on net power costs at power levels of 1000 MW and over, this method was therefore used for establishing these costs in this study.

Capital Costs

Annual charge or capital investment was taken at 15% per year which is a fairly standard rate for comparison studies of this type.

Where possible, unit costs for capital expenditures were derived from past HAPO construction experience which were escalated to allow for time differences. In cases where no related experience was obtainable (e.g. pressure vessel, direct cycle turbomachinery, high temperature piping and valves, etc.) cost estimates were obtained from equipment manufacturers and/or other nuclear sites.

In instances where total cost was not significantly affected by slight changes in process parameters (e.g. fuel charging and handling equipment, building services, site costs, etc.) constant values were used throughout the study.

It is recognized that many of these figures may necessarily be altered when further estimates are initiated on a single reactor concept. However, at a thermal power rating of 1000 MW and a cycle efficiency of 30%, net power costs will only change by approximately 0.07 mills/kwh for each one million dollars of capital expenditure. This indicates that a more precise evaluation based on sufficient basic arrangement drawings as well as equipment costs based on more exact sizing will still show net power costs to fall within the range of 10-14 mills/kwh.

FIGURE X-1

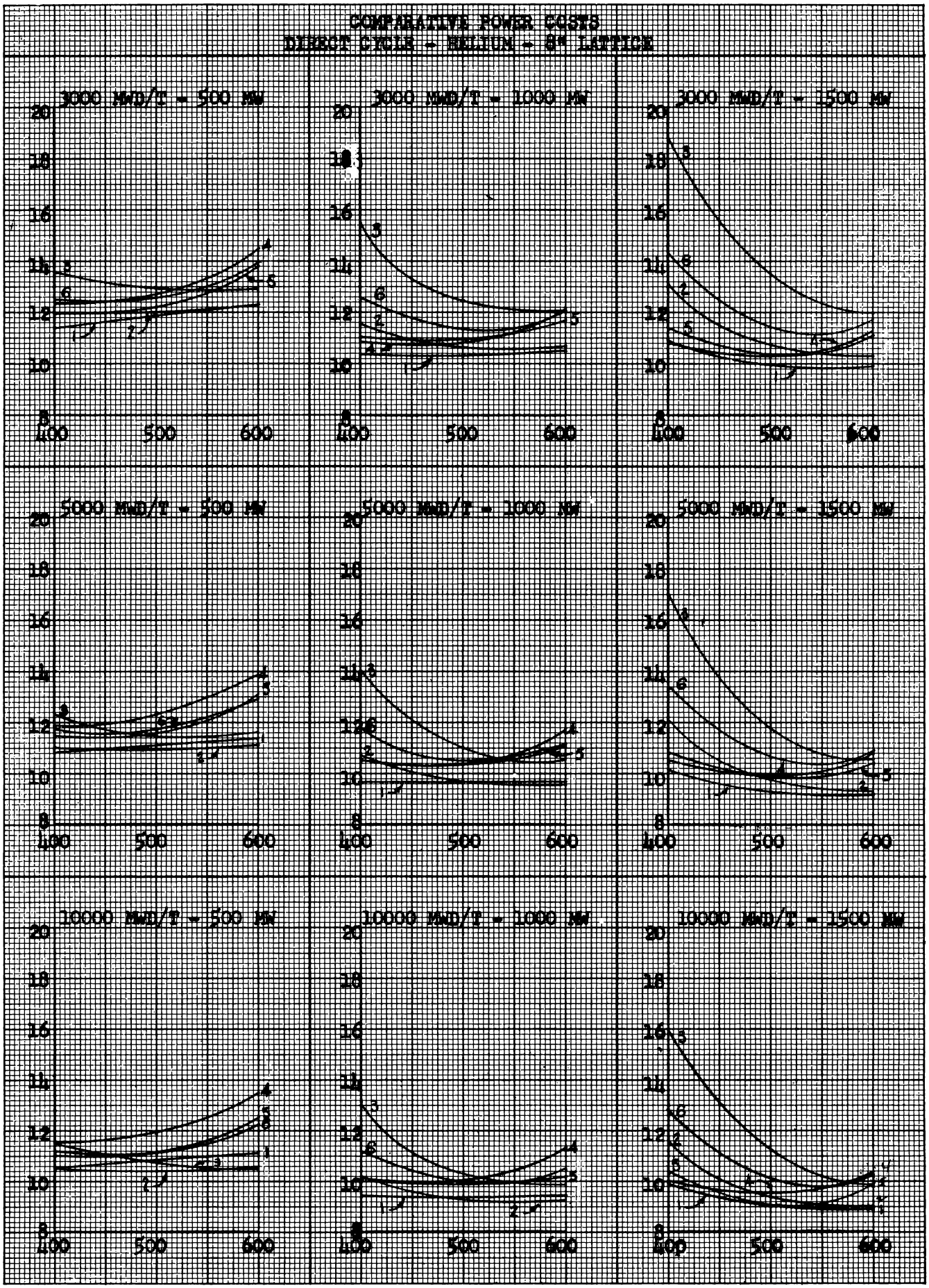
COMPARATIVE POWER COSTS
DIRECT CYCLE - HELIUM - 8" LATTICE
3000 MWD/T - 500 MW
3000 MWD/T - 1000 MW
3000 MWD/T - 1500 MW
5000 MWD/T - 500 MW
5000 MWD/T - 1000 MW
5000 MWD/T - 1500 MW
10000 MWD/T - 500 MW
10000 MWD/T - 1000 MW
10000 MWD/T - 1500 MW
20
18
16
14
12
10
8
400
500
600

FIGURE X-2

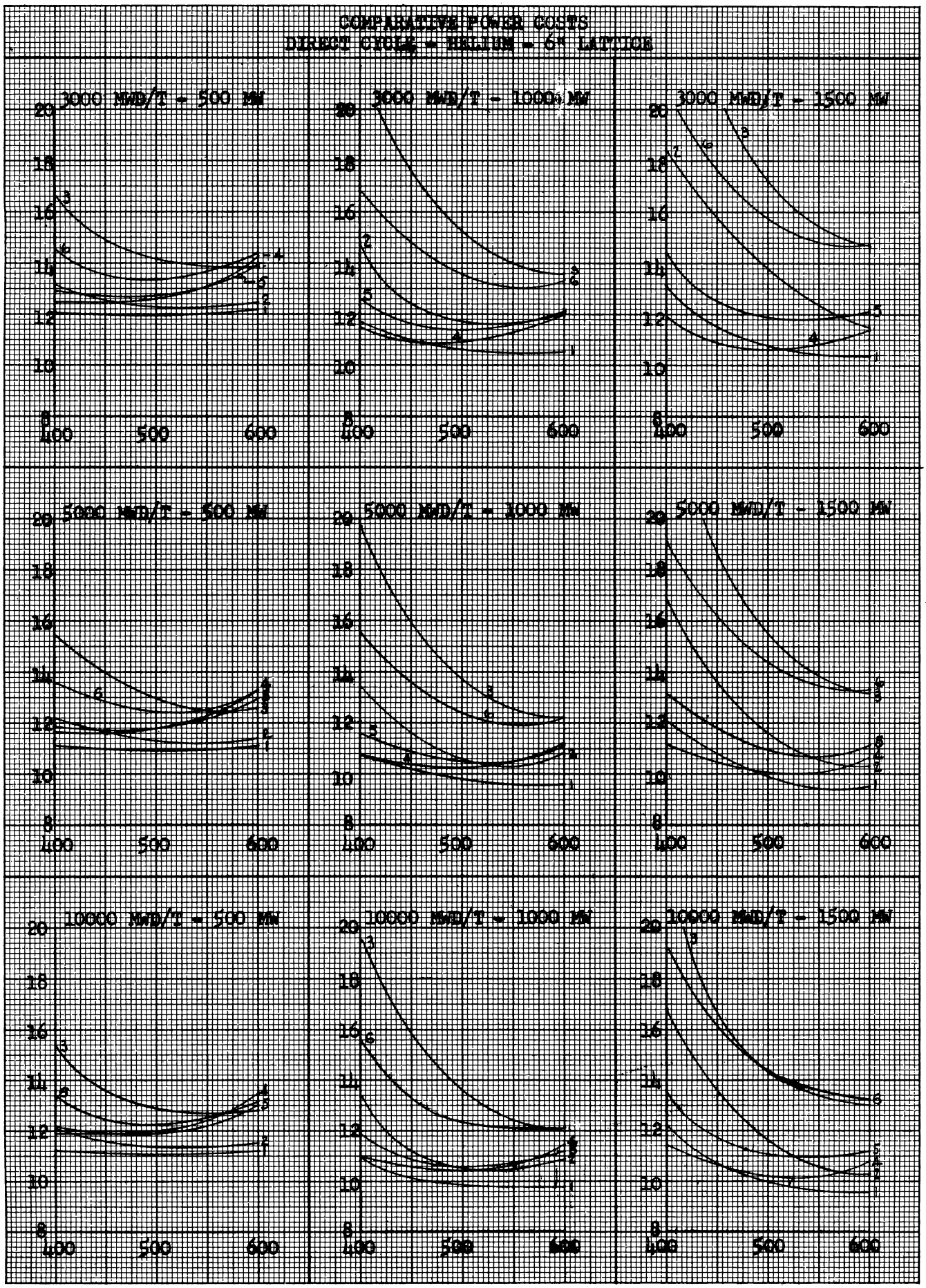
COMPARATIVE POWER COSTS
DIRECT CYCLE - HELIUM - 6" LATTICE
3000 MWD/T - 500 MW
3000 MWD/T - 1000 MW
3000 MWD/T - 1500 MW
5000 MWD/T - 500 MW
5000 MWD/T - 1000 MW
5000 MWD/T - 1500 MW
10000 MWD/T - 500 MW
10000 MWD/T - 1000 MW
10000 MWD/T - 1500 MW
20
18
16
14
12
10
8
400
500
600

FIGURE X-3

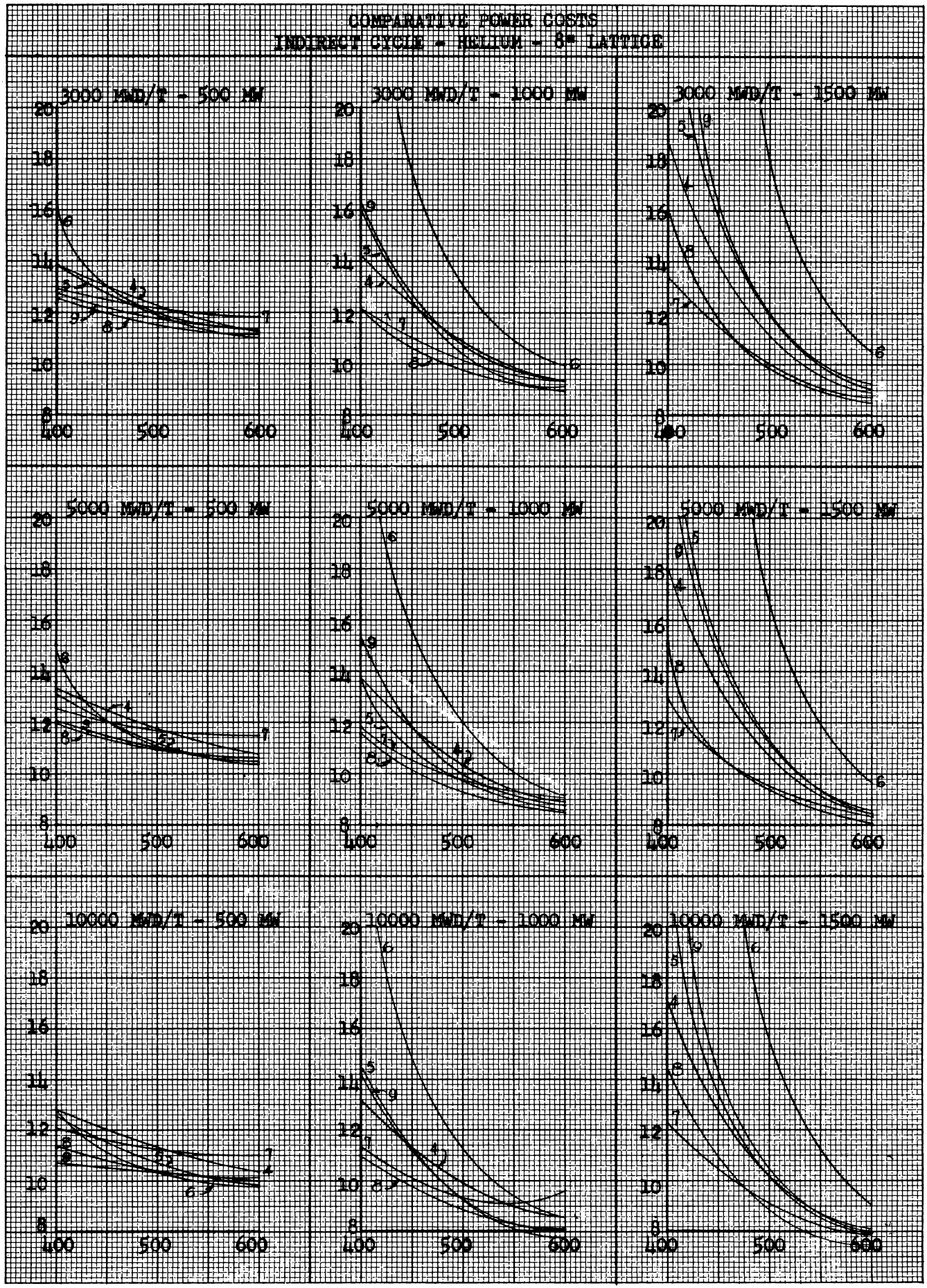
COMPARATIVE POWER COSTS
INDIRECT CYCLE - HELIUM - 8" LATTICE
3000 MWD/T - 500 MW
3000 MWD/T - 1000 MW
3000 MWD/T - 1500 MW
5000 MWD/T - 500 MW
5000 MWD/T - 1000 MW
5000 MWD/T - 1500 MW
10000 MWD/T - 500 MW
10000 MWD/T - 1000 MW
10000 MWD/T - 1500 MW
20
18
16
14
12
10
8
400
500
600

FIGURE X-5

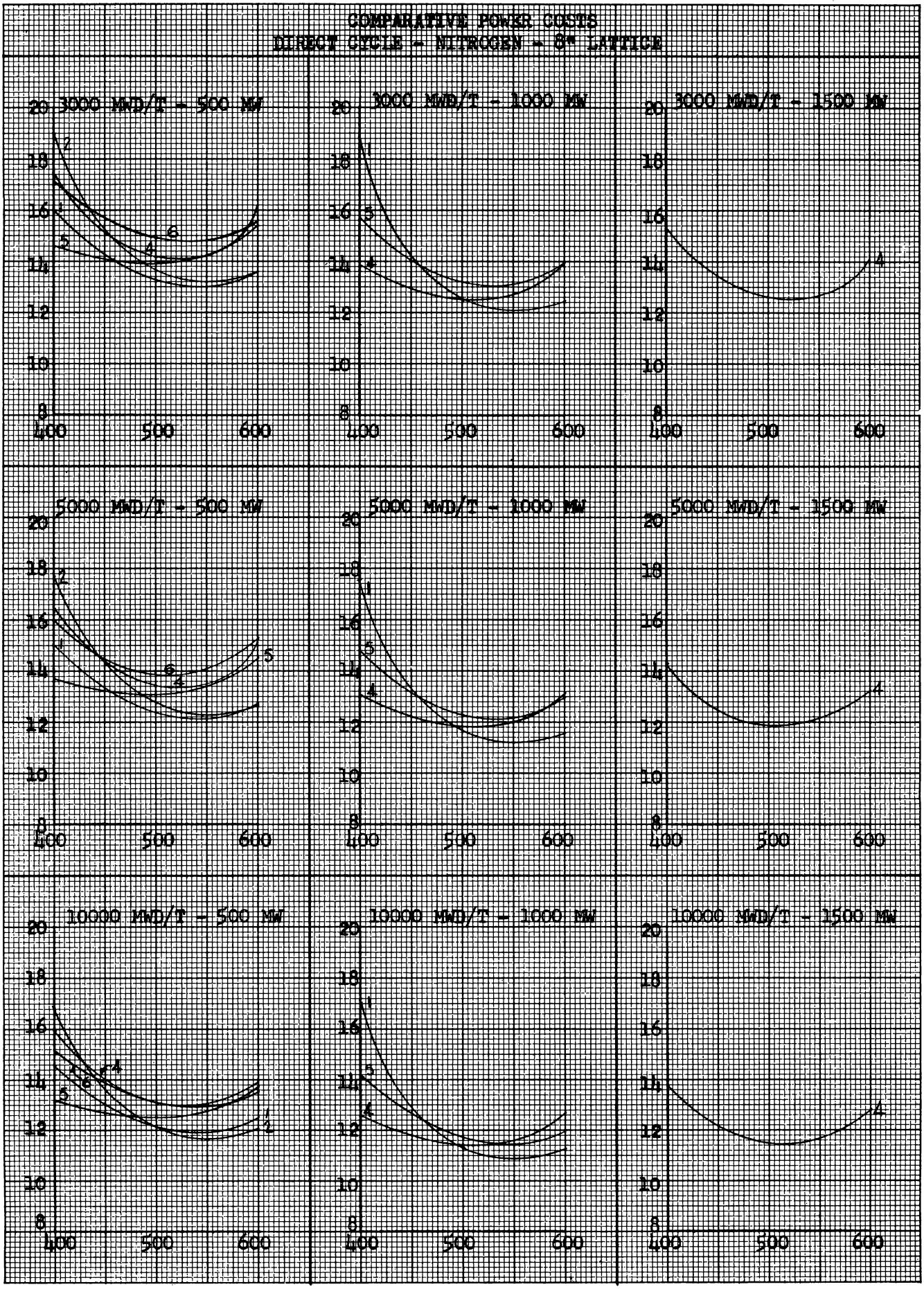
COMPARATIVE POWER COSTS
DIRECT CYCLE - NITROGEN - 8" LATTICE
3000 MWD/T - 500 MW
3000 MWD/T - 1000 MW
3000 MWD/T - 1500 MW
5000 MWD/T - 500 MW
5000 MWD/T - 1000 MW
5000 MWD/T - 1500 MW
10000 MWD/T - 500 MW
10000 MWD/T - 1000 MW
10000 MWD/T - 1500 MW
20
18
16
14
12
10
8
400
500
600

FIGURE X-6

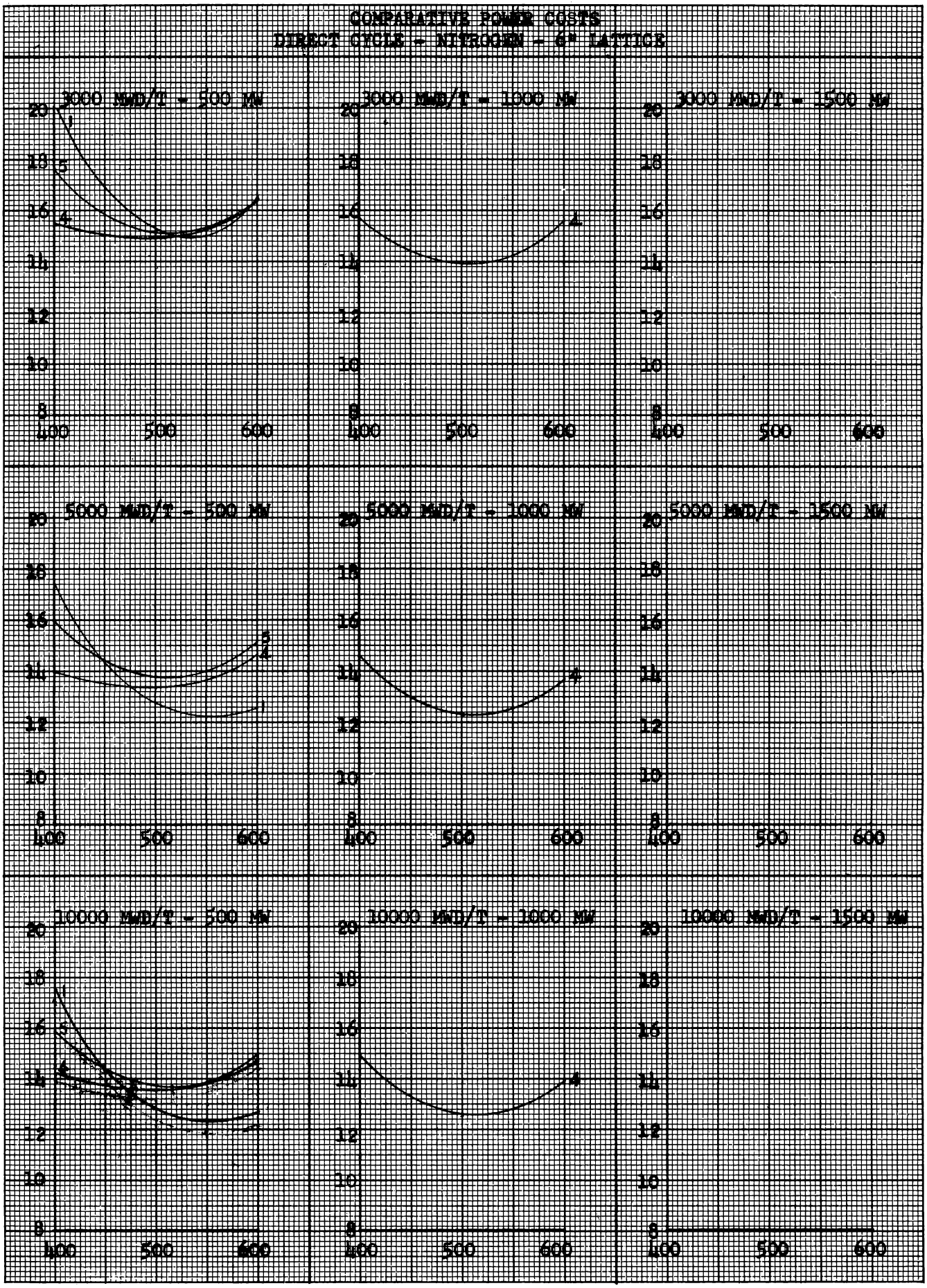
COMPARATIVE POWER COSTS
DIRECT CYCLE - NITROGEN - 6" LATTICE
3000 MWD/T - 500 MW
3000 MWD/T - 1000 MW
3000 MWD/T - 1500 MW
5000 MWD/T - 500 MW
5000 MWD/T - 1000 MW
5000 MWD/T - 1500 MW
10000 MWD/T - 500 MW
10000 MWD/T - 1000 MW
10000 MWD/T - 1500 MW
20
18
16
14
12
10
8
400
500
600

FIGURE X-7

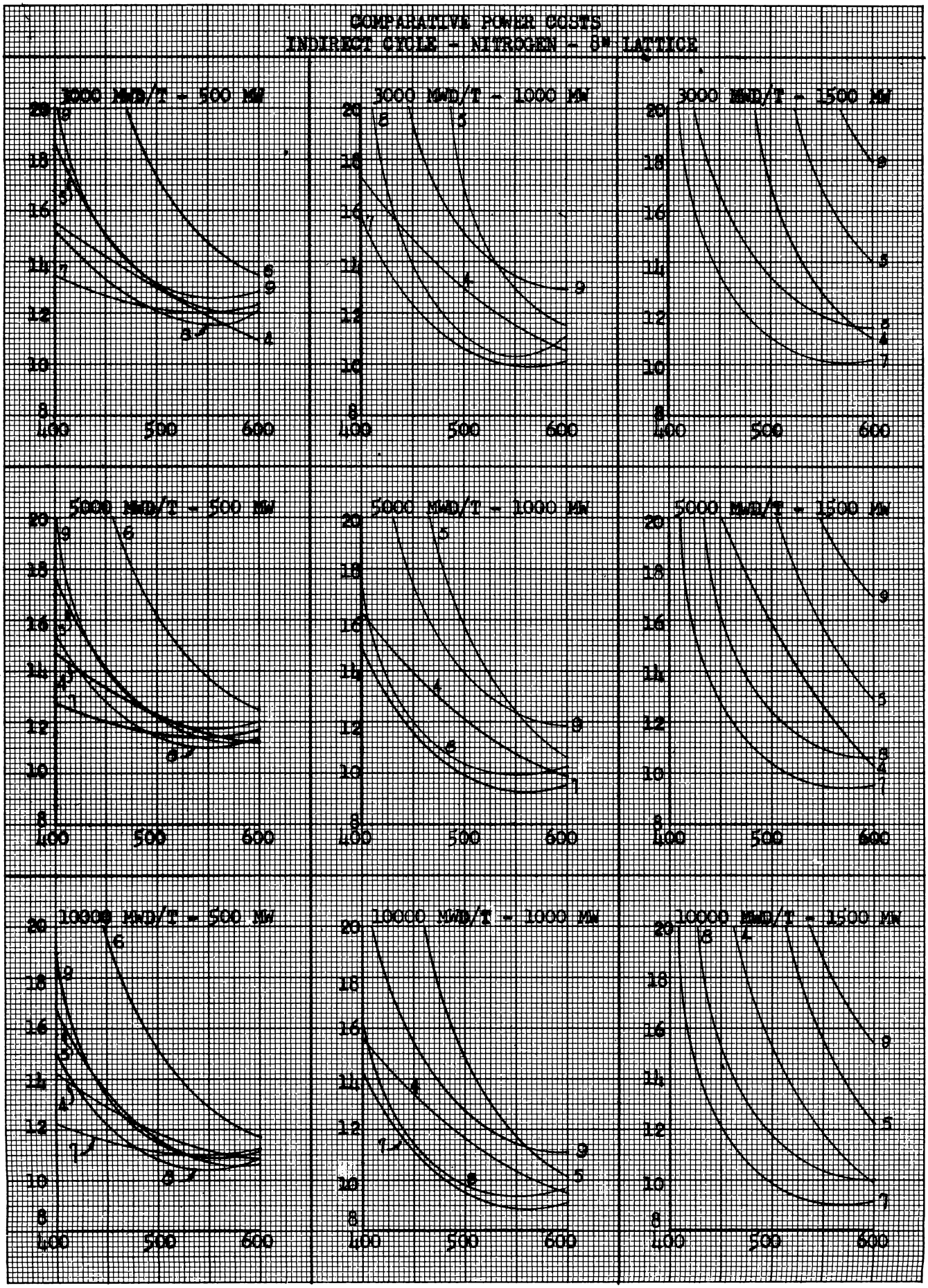
COMPARATIVE POWER COSTS
INDIRECT CYCLE - NITROGEN - 8" LATTICE
3000 MWD/T - 500 MW
3000 MWD/T - 1000 MW
3000 MWD/T - 1500 MW
5000 MWD/T - 500 MW
5000 MWD/T - 1000 MW
5000 MWD/T - 1500 MW
10000 MWD/T - 500 MW
10000 MWD/T - 1000 MW
10000 MWD/T - 1500 MW
8
10
12
14
16
18
20
400
500
600

FIGURE X-4

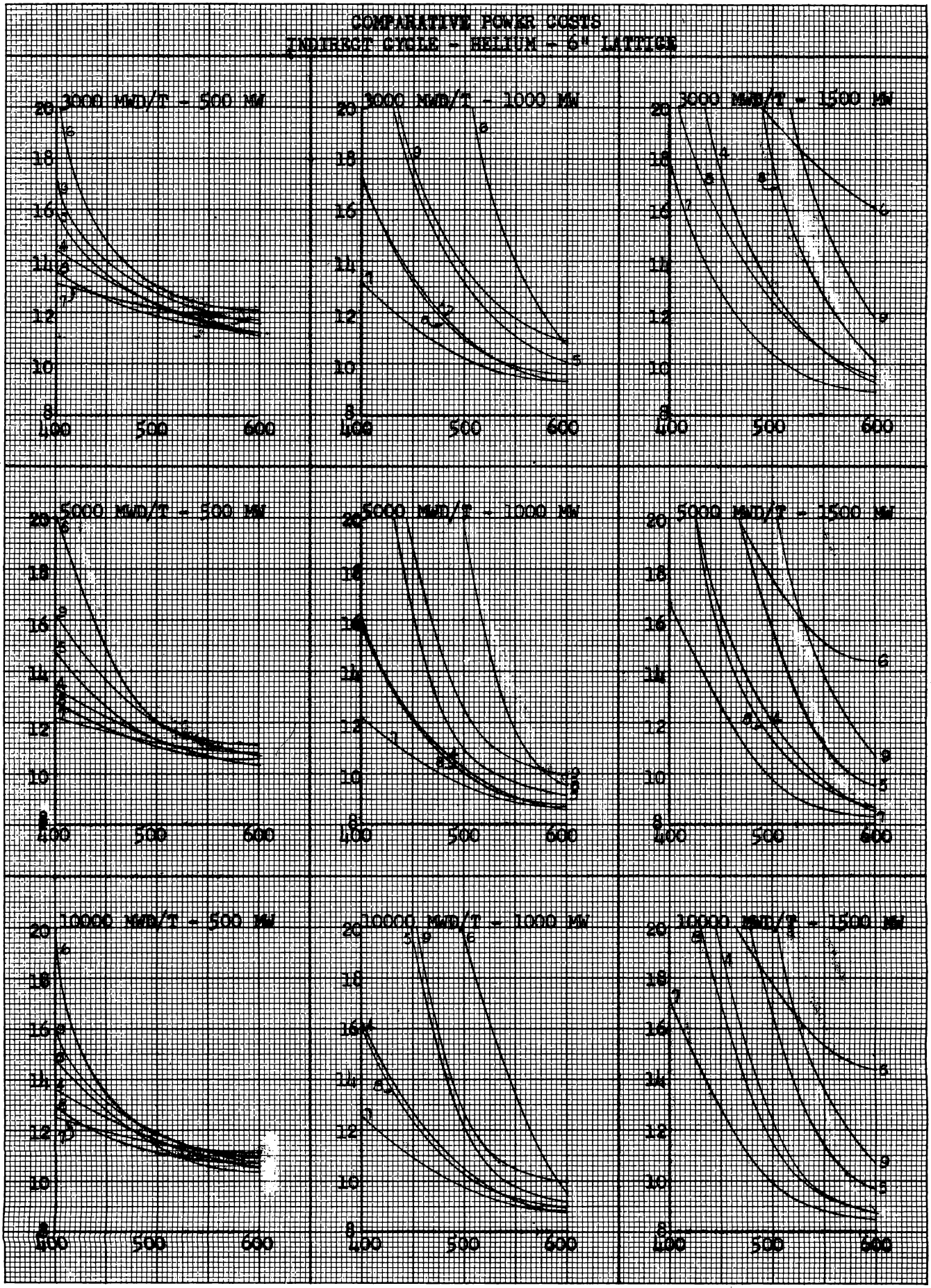
COMPARATIVE POWER COSTS
INDIRECT CYCLE - HELIUM - 6" LATTICE
3000 MWD/T - 500 MW
3000 MWD/T - 1000 MW
3000 MWD/T - 1500 MW
5000 MWD/T - 500 MW
5000 MWD/T - 1000 MW
5000 MWD/T - 1500 MW
10000 MWD/T - 500 MW
10000 MWD/T - 1000 MW
10000 MWD/T - 1500 MW
20
18
16
14
12
10
8
400
500
600

FIGURE X-8

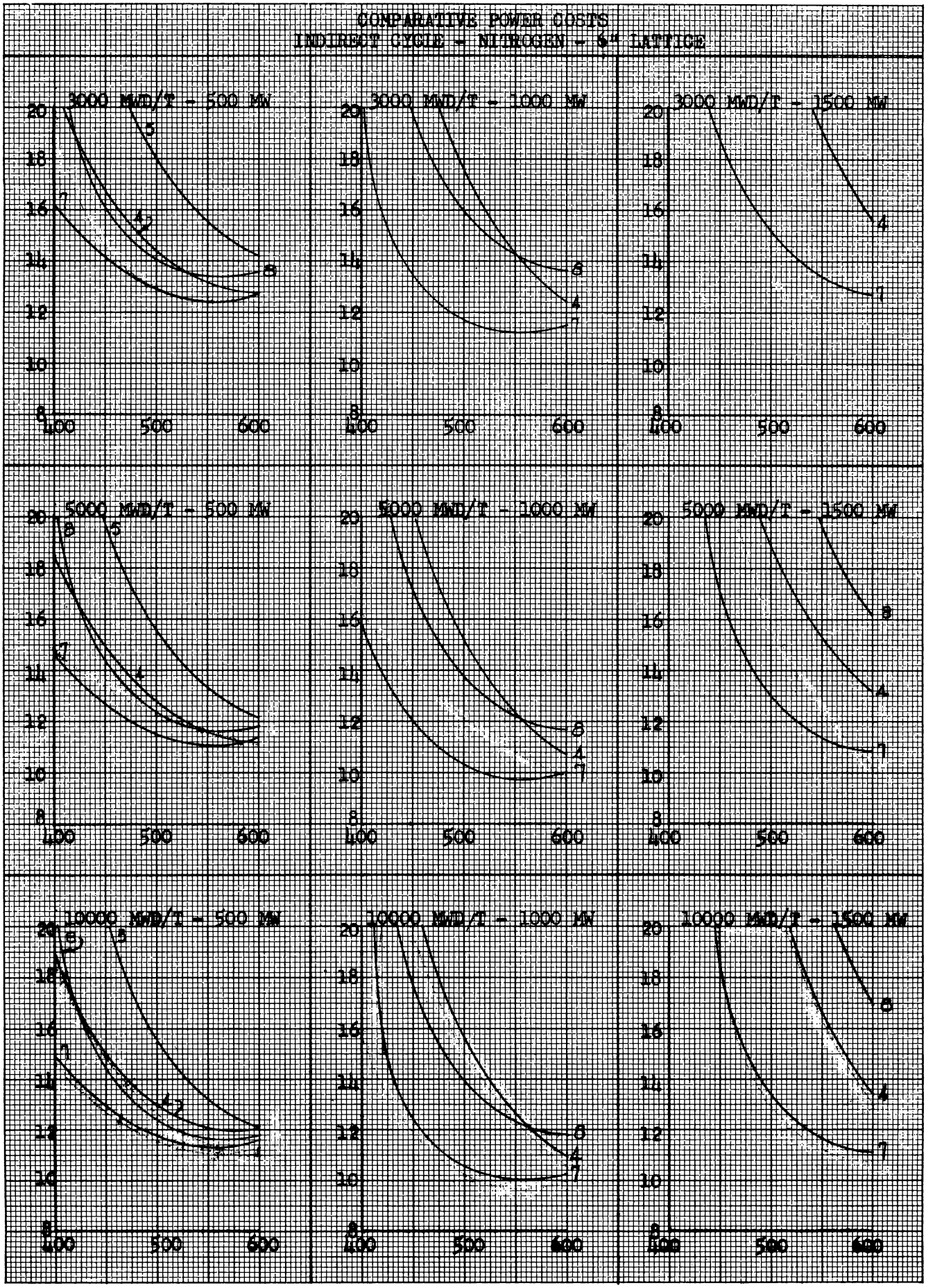
COMPARATIVE POWER COSTS
INDIRECT CYCLE - NITROGEN - 6" LATTICE
3000 MWD/T - 500 MW
3000 MWD/T - 1000 MW
3000 MWD/T - 1500 MW
5000 MWD/T - 500 MW
5000 MWD/T - 1000 MW
5000 MWD/T - 1500 MW
10000 MWD/T - 500 MW
10000 MWD/T - 1000 MW
10000 MWD/T - 1500 MW
20
18
16
14
12
10
8
400
500
600

FIGURE X-9

COMPARATIVE CAPITAL INVESTMENT PER SALEABLE POWER UNIT
FOR REPRESENTATIVE DIRECT CYCLE, HELIUM COOLED CASES

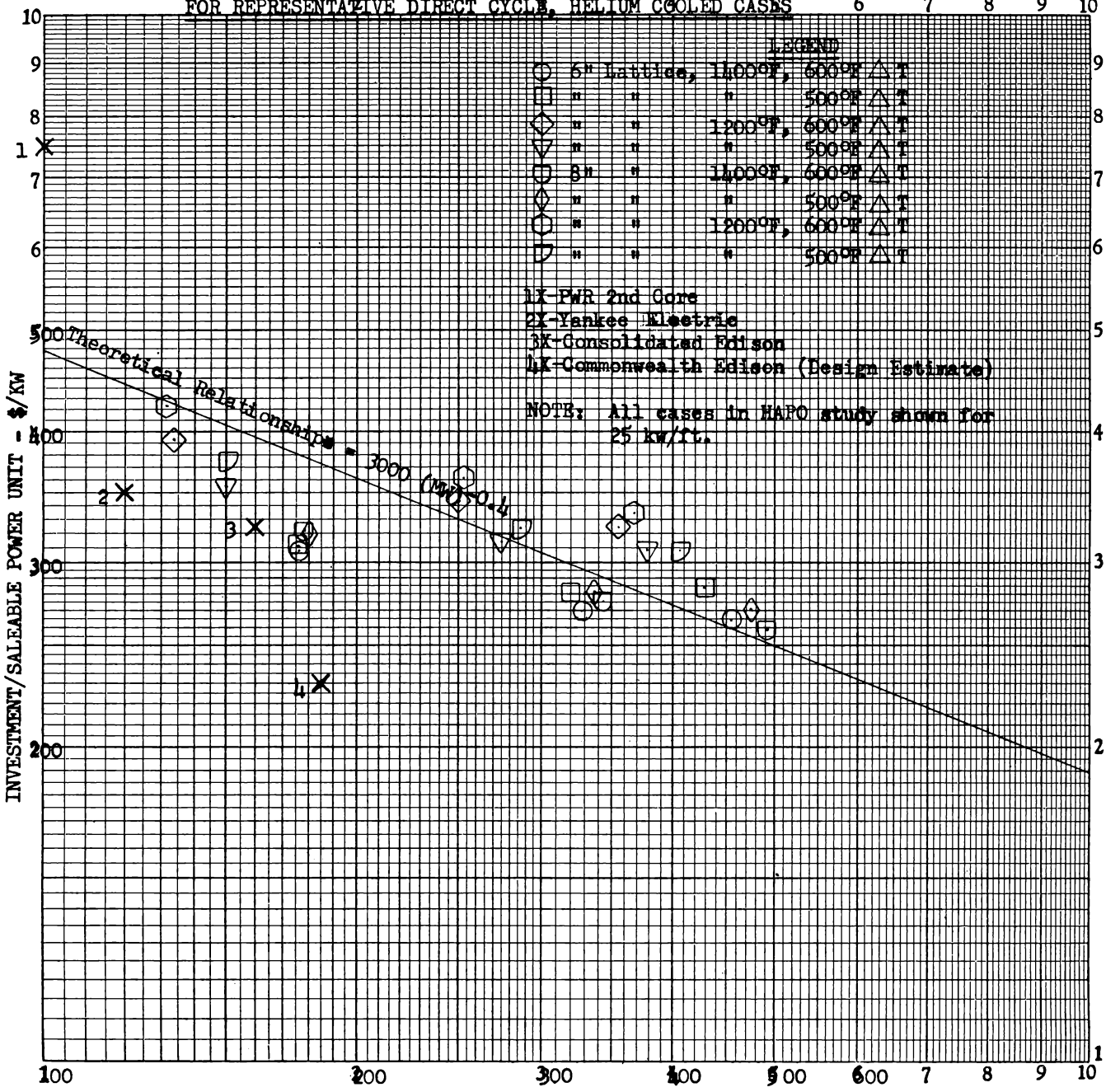

*Theoretical relationship and data for other than HAPO from chart prepared by W. K. Davis and presented at the Atomic Industrial Forum, October, 1957.

FIGURE X-10
COMPARATIVE CAPITAL INVESTMENT PER SALEABLE POWER UNIT
FOR REPRESENTATIVE INDIRECT CYCLE, HELIUM COOLED CASES

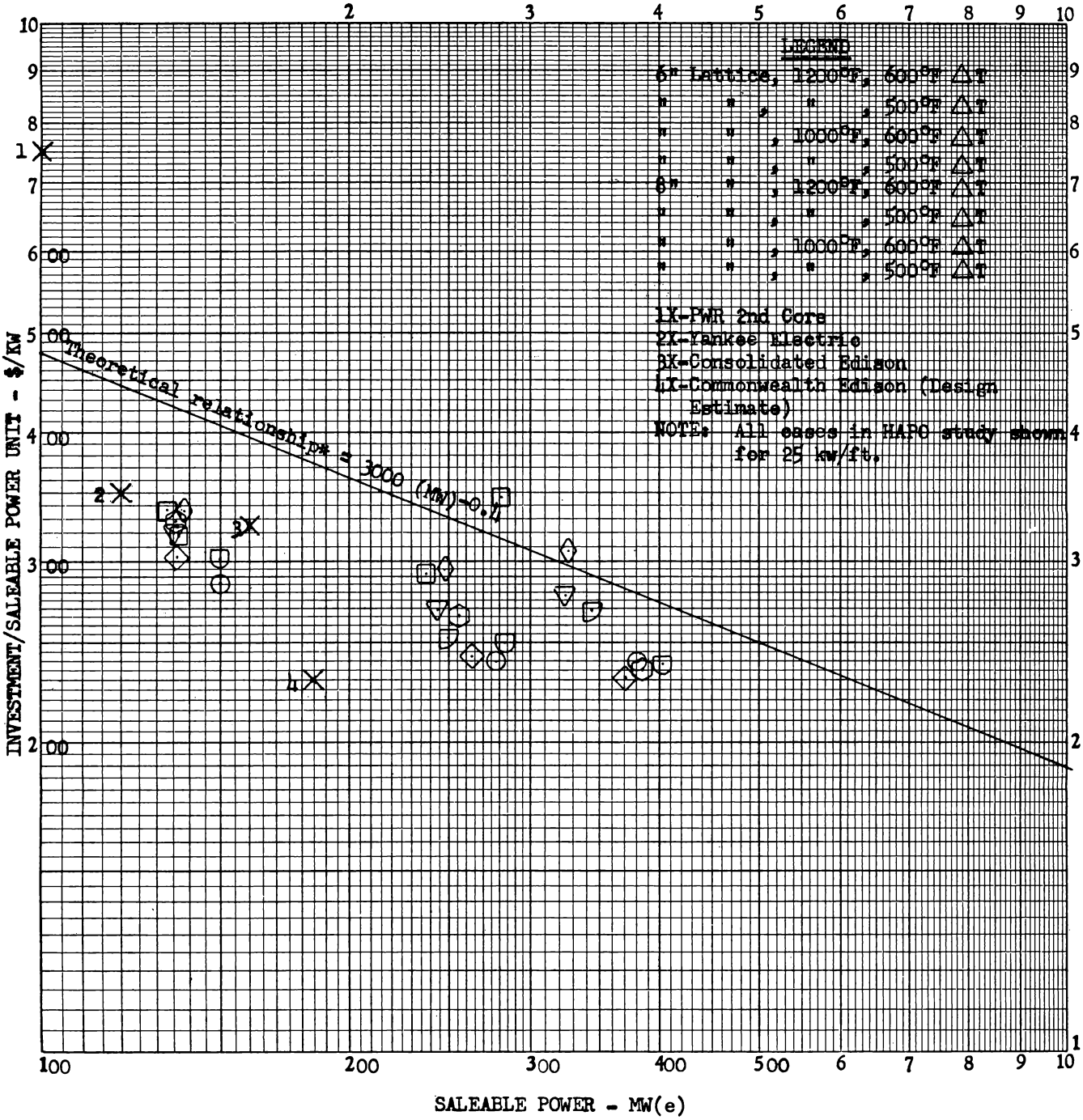

*Theoretical relationship and data for other than HAPO from chart prepared by W. K. Davis and presented at the Atomic Industrial Forum, October, 1957.

FIGURE X-11

SUMMARY OF ESTIMATED COSTS FOR REPRESENTATIVE DIRECT CYCLE, HELIUM COOLED REACTOR*

ITEM	UNITS	2000			5000			10,000		
GOAL EXPOSURE	MWD/T									
REACTOR POWER LEVEL	MW	500	1000	1500	500	1000	1500	500	1000	1500
BURNUP COST	$/yr x 10^6	1.951	3.744	5.592	1.831	3.451	5.098	1.727	3.291	4.783
FUEL FABRICATION COST	"	1.523	2.848	4.106	.914	1.708	2.463	.457	.854	1.231
SEPARATIONS & CONVERSION COST	"	.778	1.377	1.869	.529	.976	1.325	.294	.571	.811
U^{235} INVENTORY CHARGE	"	.517	.912	1.324	.557	.995	1.432	.780	1.414	2.014
S/S INVENTORY CHARGE	"	.668	1.281	1.889	.623	1.232	1.682	.589	1.100	1.590
PLUTONIUM CREDIT	"	1.051	2.161	3.259	.908	1.836	2.775	.685	1.375	2.066
NET ANNUAL FUEL COST	"	4.386	8.001	11.521	3.546	6.526	9.225	3.162	5.855	8.363
ANNUAL OPERATING & MAINTENANCE	"	1.89	2.12	2.34	1.89	2.12	2.34	1.89	2.12	2.34
TOTAL CAPITAL INVESTMENT	"	57.534	94.920	128.71	57.534	94.920	128.71	57.534	94.920	128.71
ANNUAL CAPITAL CHARGE	"	8.630	14.238	19.307	8.630	14.238	19.307	8.630	14.238	19.307
TOTAL ANNUAL COST	"	14.906	24.359	33.168	14.066	22.884	30.872	13.682	22.213	30.010
GROSS ELECTRICAL POWER**	MW(e)	182	341	479	182	341	479	182	341	479
SALEABLE POWER	MW(e)	180	338	475	180	338	475	180	338	475
NET POWER COST	Mills/kwh	11.817	10.284	9.964	11.151	9.662	9.275	10.847	9.378	9.016
GROSS CAPITAL INVESTMENT/ SALEABLE POWER UNIT	$/KW	320	281	271	320	281	271	320	281	271

* This summary is for Case #1 which is described in more detail on page X-6 of this section.

** For the direct cycle cases, gross power differs from saleable power only by the amount of power required for miscellaneous services since the compressor is on a common shaft with the turbine. For the indirect cycle cases, pumping power is also subtracted from gross power.

FIGURE X-12

SUMMARY OF ESTIMATED COSTS FOR REPRESENTATIVE CASES*

ITEM	UNITS	CASE NUMBER 1	2	3	4	5	6	7	8	9	10
BURNUP COST	$/yr x 10^6	3.451	4.129	3.989	2.902	4.520	3.743	2.902	2.978	3.393	3.060
FUEL FABRICATION	"	1.708	2.105	1.999	1.271	2.190	1.907	1.271	1.298	1.509	1.350
SEPARATIONS & CONVERSION	"	.976	.976	.976	.976	0.980	.976	.976	.976	.976	.976
U^{235} INVENTORY CHARGE	"	.995	.505	.451	.707	0.475	1.153	.707	.730	.313	.767
S/S INVENTORY CHARGE	"	1.232	.472	.448	.866	0.350	1.299	.866	.884	.338	.920
PLUTONIUM CREDIT	"	1.836	1.738	1.766	1.913	1.800	1.801	1.913	1.906	1.850	1.892
NET ANNUAL FUEL COST	"	6.526	6.449	6.097	4.809	6.715	7.277	4.809	4.960	4.679	5.181
NET ANNUAL OPERATING COSTS	"	2.120	2.120	2.120	2.120	2.120	2.120	2.120	2.120	2.120	2.120
TOTAL CAPITAL INVESTMENT	"	94.920	85.449	89.399	92.220	86.121	92.742	73.226	71.101	67.986	76.262
ANNUAL CAPITAL CHARGE	"	14.238	12.817	13.410	13.833	12.918	13.911	10.984	10.665	10.198	11.439
TOTAL ANNUAL COST	"	22.884	21.386	21.627	20.762	21.753	23.308	17.913	17.745	16.997	18.740
GROSS ELECTRICAL POWER **	MW(e)	341	280	224	289	229	288	346	346	346	346
SALEABLE POWER	MW(e)	338	277	221	286	226	285	248	284	202	221
NET POWER COST(15+17)	Mills/kwh	9.662	11.017	13.965	10.359	13.735	11.671	10.307	8.916	12.007	12.101
GROSS CAPITAL INVESTMENT/ SALEABLE POWER UNIT	$/KW	281	308	405	322	381	325	295	250	337	345

* All cases shown at 1000 MW (thermal) and 5000 MWD/T.
Refer to page X-6 of this section for description of cases.

** For the direct cycle cases, gross power differs from saleable power only by the amount of power required for miscellaneous services since the compressor is on a common shaft with the turbine. For the indirect cycle cases, pumping power is also subtracted from gross power.

FIGURE X-13

SUMMARY OF ESTIMATED CAPITAL COST FOR REPRESENTATIVE CASES*

ITEM	CASE NUMBER 1	2	3	4	5	6	7	8	9	10
REACTOR CORE, VESSEL, ETC.	11.200	5.000	5.000	11.200	3.750	11.200	11.200	11.200	5.000	11.200
GAS MAKE UP, PURIFICATION, SAMPLING	1.000	1.000	1.000	1.000	1.000	1.000	1.000	1.000	1.000	1.000
GAS PIPING	3.340	3.340	4.160	2.240	3.340	2.970	1.672	1.547	1.672	1.942
EMERGENCY COOLING	.150	.150	.150	.150	.150	.150	.150	.150	.150	.150
FANS, FILTERS, STACK	.300	.300	.300	.300	.300	.300	.275	.275	.275	.275
GAS BLOWERS	---	---	---	---	---	---	3.970	2.350	6.020	5.165
REACTOR, POWER & ADMIN. BLDG.	5.520	5.520	5.520	5.520	5.520	5.520	6.233	6.233	6.233	6.233
TURBINES, COMPRESSORS, GENERATORS	36.800	34.400	34.400	36.800	33.200	36.800	12.100	12.100	12.100	12.100
HEAT EXCHANGERS	---	---	---	---	---	---	1.443	1.580	1.851	2.147
CONDENSERS	---	---	---	---	---	---	1.972	1.972	1.972	1.972
CONDENSATE PUMPS, HEATERS, WATER TREATMENT	---	---	---	---	---	---	.566	.566	.566	.566
PUMP HOUSE AND PUMPS	.315	.315	.346	.335	.315	.305	1.837	1.837	1.837	1.837
PIPING (STEAM & WATER)	.110	.110	.121	.117	.110	.099	1.230	1.230	1.230	1.230
STAND BY ELECTRICAL	.645	3.150	5.460	.360	6.640	.066	.180	.180	.180	.180
SWITCHGEAR	3.750	3.080	2.460	3.180	2.520	3.170	3.806	3.806	3.806	3.806
REACTOR CONTROL & INST.	1.650	1.650	1.650	1.650	1.650	1.650	1.650	1.650	1.650	1.650
POWER CONTROL & INST.	.340	.340	.340	.340	.340	.340	.340	.340	.340	.340
CHARGING & FUEL HANDLING	1.750	1.750	1.750	1.750	1.750	1.750	1.750	1.750	1.750	1.750
SITE COST, INCLUDING ROADS, RAILROADS	.930	.930	.930	.930	.930	.930	.930	.930	.930	.930
SUB TOTAL	67.800	61.035	63.587	65.872	61.515	66.244	52.304	50.696	48.562	54.472
TOTAL (INCLUDES 40% FOR DESIGN, CONTINGENCY, OVERHEAD AND PROFIT)	94.920	85.449	89.399	92.220	86.121	92.742	73.226	70.974	67.987	76.262

* Refer to page X-6 of this section for description of cases

NOTE: All figures are given in $ x 10^6

* U. S. GOVERNMENT PRINTING OFFICE : 1958 O—470381